

**SYNTHESIS, CHARACTERIZATION AND
FLUORESCENCE PROPERTIES OF SELECTED
PYRAZINE DERIVATIVES**

HASNA NADIAH BINTI JOHARI

**FACULTY OF SCIENCE
UNIVERSITY OF MALAYA
KUALA LUMPUR**

2015

**SYNTHESIS, CHARACTERIZATION AND
FLUORESCENCE PROPERTIES OF SELECTED
PYRAZINE DERIVATIVES**

HASNA NADIAH BINTI JOHARI

**DISSERTATION SUBMITTED IN FULFILMENT OF
THE REQUIREMENTS FOR THE DEGREE OF MASTER
OF SCIENCE**

**FACULTY OF SCIENCE
UNIVERSITY OF MALAYA
KUALA LUMPUR**

2015

UNIVERSITI MALAYA

ORIGINAL LITERARY WORK DECLARATION

Name of Candidate: **HASNA NADIAH BINTI JOHARI**

I/C/Passport No: **881121-11-5422**

Registration/Matric No.: **SGR110041**

Name of Degree: **MASTER OF SCIENCE**

Title of Project Paper/Research Report/Dissertation/Thesis ("this Work"):

**"SYNTHESIS, CHARACTERIZATION AND FLUORESCENCE PROPERTIES OF
SELECTED PYRAZINE DERIVATIVES"**

Field of Study: **ORGANIC CHEMICAL SYNTHESIS**

I do solemnly and sincerely declare that:

- (1) I am the sole author/writer of this Work,
- (2) This Work is original,
- (3) Any use of any work in which copyright exists was done by way of fair dealing and for permitted purposes and any excerpt or extract from, or reference to or reproduction of any copyright work has been disclosed expressly and sufficiently and the title of the Work and its authorship have been acknowledged in this Work,
- (4) I do not have any actual knowledge nor do I ought reasonably to know that the making of this work constitutes an infringement of any copyright work,
- (5) I hereby assign all and every rights in the copyright to this Work to the University of Malaya ("UM"), who henceforth shall be owner of the copyright in this Work and that any reproduction or use in any form or by any means whatsoever is prohibited without the written consent of UM having been first had and obtained,
- (6) I am fully aware that if in the course of making this Work I have infringed any copyright whether intentionally or otherwise, I may be subject to legal action or any other action as may be determined by UM.

(Candidate Signature)

Date: **25 MEI 2015**

Subscribed and solemnly declared before,

Witness's Signature

Date: **25 MEI 2015**

Name **PROFESSOR DR ZANARIAH ABDULLAH**

Designation

ABSTRACT

Phenoxypyrazine (44), 2-*o*-methylphenoxypyrazine (46), 2-*m*-methylphenoxypyrazine (48), 2-*p*-methylphenoxypyrazine (50) and 2-*N*-piperidinopyrazine (56) were obtained after the reaction between 2-chloropyrazine (42) with phenol (43), *o*-cresol (45), *m*-cresol (47), *p*-cresol (49) and piperidine (55) respectively. 5-Phenoxypyrazine-2-carboxylic acid methyl ester (58), 5-*m*-tolylloxypyrazine-2-carboxylic acid methyl ester (59), 5-(-3-nitrophenoxy)pyrazine-2-carboxylic acid methyl ester (61) on the other hand, were obtained after the reaction between 2-chloropyrazine-5-carboxylic acid methyl ester (57) with phenol (43), 3-methylphenol (47), and 3-nitrophenol (60) respectively. While, 2,5-dimethyl-3-phenoxypyrazine (63) were prepared by reacting 3-chloro-2,5-dimethyl pyrazine (62) with phenol (43). Naphthalenyloxy pyrazine derivatives, 2-naphthalen-1-yloxypyrazine (52), and 2-naphthalen-2-yloxypyrazine (54) were prepared by reacting 2-chloropyrazine (42) with 1-naphtol (51) and 2-naphtol (53) respectively. The structures of these compounds were confirmed using ¹H NMR, ¹³CNMR, GC-MS and IR spectra. The fluorescence properties were recorded using Luminescence Spectrophotometer.

Fluorescence characteristic of phenoxy pyrazine derivatives studied showed fluorescence intensity varies with concentration. Compound (46), (50) and (63) showed fluorescence quenched in the presence of oxygen. Besides, compound (44) and (61) showed higher fluorescence intensity in alkaline condition. Furthermore, compound (46), (50) and (63) exhibit highest emission in nonpolar solvents and drastic fall in fluorescence emission in polar aprotic solvents. Highest fluorescence intensity were observed by phenoxy pyrazine derivatives with electron donating group nature, and substituent at *ortho* and *para* position in benzene ring whereas, naphthalenyloxy pyrazine derivatives with linear and rigid structure showed highest fluorescence intensity.

ABSTRAK

Fenoksipirazina (**44**), 2-*o*-metilfenoksipirazina (**46**), 2-*m*-metilfenoksipirazina (**48**), 2-*p*-metilfenoksipirazina (**50**), and 2-*N*-piperidinopirazina (**56**) diperolehi selepas tindak balas antara 2-kloropirazina (**42**) dengan fenol (**43**), *o*-kresol (**45**), *m*-kresol (**47**), *p*-kresol (**49**) dan piperidina (**55**) masing-masing. 5-Fenoksipirazina-2-karboksilik asid metil ester (**58**), 5-*m*-toliloksipirazina-2-karboksilik asid metil ester (**59**), 5-(3-nitrofenoksi)pirazina-2-karboksilik asid metil ester (**61**) diperolehi selepas tindak balas antara 2-kloropirazina-5-karboksilik asid metil ester (**57**) dengan fenol (**43**), 3-metilfenol (**47**), dan 3-nitrofenol (**60**) masing-masing. Sementara, 2,5-dimetil-3-fenoksipirazina (**63**) disediakan dengan tindak balas antara 3-kloro-2,5-dimetil pirazina (**62**) dengan fenol (**43**). Selain itu, terbitan naftalenyloksi pirazina, 2-naftalena-1-iloksipirazina (**52**), dan 2-naftalena-2-iloksipirazina (**54**) disediakan dengan tindak balas 2-kloropirazina dengan 1-naftol (**51**) dan 2-naftol (**53**) masing-masing. Struktur semua sebatian ditentukan dengan menggunakan spektroskopi ^1H NMR, ^{13}C NMR, GC-MS dan infra-merah. Ciri pendafluoran telah direkod menggunakan Spektrometer Pendafluoran.

Ciri pendafluoran terbitan fenoksi pirazina yang dikaji menunjukkan keamatan pendafluoran berkadar dengan kepekatan sebatian. Sebatian (**46**), (**50**) dan (**63**) menunjukkan sifat pendafluor dilindap dengan kehadiran oksigen. Selain itu, sebatian (**44**) dan (**61**) menunjukkan keamatan pendafluoran yang tertinggi dalam keadaan beralkali. Sebatian (**46**), (**50**) dan (**63**) pula mempamerkan perlepasan pendafluor tertinggi dalam pelarut kurang berkutub dan keamatan pendafluoran menurun dalam pelarut protik berkutub. Keamatan pendafluoran yang tinggi diperhatikan oleh terbitan fenoksi pirazina dengan kumpulan penderma elektron dan kumpulan berfungsi pada kedudukan *orto* dan *para* dalam gelang benzena, manakala terbitan naptalenaoksi

pirazina dengan struktur yang linear dan tegar memberi keamanan pendafluor yang tertinggi.

ACKNOWLEDGEMENTS

First of all, I am profoundly grateful to Allah, the most merciful and most forgiving. It was He who gave me strength to complete this task.

I want to acknowledge and express my deep gratitude to my supervisor Professor Dr. Zanariah Abdullah for influencing and directing my efforts, and for all her support, patience and feedback over the whole duration of this research.

All staff members of Chemistry Department and University Malaya for their help and support through the years.

University of Malaya UMRG grant (RG 027/ 09 AFR) and PPP grant (PV 081/ 2012 A) for their financial assistance throughout the entire course.

In addition, I want to thank the many friends that I made during years at University of Malaya, especially blue lab members for the incredible support and motivation that I received from them throughout the years. I want to thank Dr. Hairul Anuar Tajuddin, for his encouraging, comments and financial assistance.

Finally, I am grateful to my beloved parents and siblings for their unconditional loved, strength and inspiration. Without them, I could not have persued my dreams.

TABLE OF CONTENTS

| | |
|---|--------------|
| Abstract..... | iii |
| Abstrak..... | iv |
| Acknowledgements..... | vi |
| Table of Contents | vii |
| List of Figures..... | xi |
| List of Tables | xiv |
| List of Schemes | xvi |
| List of Symbols and Abbreviations..... | xviii |

CHAPTER 1: SYNTHESIS AND REACTIVITY OF PYRAZINE AND NAPHTHALENE.....1

| | |
|--|----|
| 1.1 Introduction of pyrazine | 1 |
| 1.1.1 Reactivity of Pyrazine | 3 |
| 1.1.2 Synthesis of pyrazine derivatives | 6 |
| 1.1.2.1 Self condensation of a α -amino carbonyl compounds..... | 7 |
| 1.1.2.2 Condensation of 1,2-diamino ethane and related..... | 8 |
| compounds with α diketones | |
| 1.1.2.3 Wolff and Marburg method..... | 8 |
| 1.2 Introduction of naphthalene | 9 |
| 1.2.1 Synthesis of naphthalenyl derivatives | 11 |
| 1.2.1.1 Haworth synthesis..... | 11 |
| 1.2.1.2 Formation of naphthalene through Diels-Alder reaction..... | 12 |
| 1.2.1.3 Preparation of naphthalene from..... | 12 |
| (α,β - dibromobutyl)benzene | |
| 1.2.2 Reactivity of naphthalene | 13 |

| | |
|---|-----------|
| 1.2.2.1 Oxidation | 13 |
| 1.2.2.2 Reduction..... | 14 |
| 1.2.2.3 Halogenation..... | 15 |
| 1.2.2.4 Sulfonation of naphthalene..... | 16 |
| CHAPTER 2: FLUORESCENCE SPECTROSCOPY | 18 |
| 2.0 Introduction to fluorescence | 18 |
| 2.1 Theory of fluorescence | 19 |
| 2.2 Factors that effects the fluorescence | 23 |
| 2.2.1 Effects of molecular structure to fluorescence | 23 |
| 2.2.2 Environmental effect | 24 |
| 2.2.2.1 Influence of the solvent | 24 |
| 2.2.2.2 Influence of pH | 27 |
| 2.2.2.3 Influence of concentration | 30 |
| 2.3 Instrumentation of fluorescence spectroscopy..... | 31 |
| 2.3.1 Light sources | 32 |
| 2.3.2 Monochromator | 34 |
| 2.3.3 Sample holder..... | 35 |
| 2.3.4 Cuvette..... | 38 |
| 2.3.5 Detector | 40 |
| 2.4 Objectives of the project..... | 42 |
| CHAPTER 3: RESULTS AND DISCUSSION | 43 |
| 3.1 Synthesis of the compounds studied..... | 43 |
| 3.2 Synthesis of phenoxypyrazines..... | 46 |
| 3.2.1 Reaction of 2-chloropyrazines with various phenol derivatives | 46 |
| 3.2.3 Reaction of 2-chloropyrazine with piperidine..... | 52 |

| | | |
|--|--|-----------|
| 3.2.4 | Reaction of 2-chloropyrazine-5-carboxylic acid methyl ester with phenol derivatives | 54 |
| 3.2.5 | Reaction of 3-chloro-2,5-dimethylpyrazine with phenol | 57 |
| 3.3 | Fluorescence characteristics of synthesized compounds | 58 |
| CHAPTER 4: CONCLUSION | | 80 |
| CHAPTER 5: EXPERIMENTAL DETAILS | | 83 |
| 5.0 | General procedures | 83 |
| 5.1 | Preparation of pyrazine and naphthalene derivatives | 84 |
| 5.1.1 | Pyrazine derivatives | 84 |
| 5.1.1.1 | Preparation of phenoxypyrazine (50) | 84 |
| 5.1.1.2 | Preparation of 2- <i>o</i> -methylphenoxypyrazine (52) | 85 |
| 5.1.1.3 | Preparation of 2-(<i>m</i> -methyl)phenoxypyrazine (54) | 86 |
| 5.1.1.4 | Preparation of 2- <i>p</i> -methylphenoxypyrazine (56) | 87 |
| 5.1.1.5 | Preparation of 5-phenoxypyrazine-2-carboxylic acid methyl ester (65) | 88 |
| 5.1.1.6 | Preparation of 5- <i>m</i> -tolylloxypyrazine-2-carboxylic acid methyl ester (66) | 89 |
| 5.1.1.7 | Preparation of 5-(-3-nitrophenoxy)pyrazine-2-carboxylic acid methyl ester (67) | 90 |
| 5.1.1.8 | Preparation of 2,5-dimethyl-3 phenoxypyrazine (69) | 91 |
| 5.1.1.9 | Preparation of 2- <i>N</i> -piperidinopyrazine (62) | 92 |
| 5.1.2 | Naphthalene derivatives | 93 |
| 5.1.2.1 | Preparation of 2-naphthalen-1-ylloxypyrazine (58) | 93 |
| 5.1.2.2 | Preparation of 2-naphthalen-2-ylloxypyrazine (60) | 94 |
| 5.2 | Fluorescence measurements | 95 |

| | | |
|------------------------------|--|------------|
| 5.2.1 | Fluorescence Measurement of pyrazine derivatives..... | 95 |
| References | | 99 |
| List of Publication | | 108 |
| Conference Proceeding | | 109 |
| Appendices | | |
| Appendix 1 | : ¹ H NMR, ¹³ C NMR, IR, GCMS Spectra for all compounds prepared | |
| Appendix 2 | : Publication | |

LIST OF FIGURES

| | Page |
|--|------|
| Figure 1.1: Bond lengths and ring angles in pyrazine (1) | 2 |
| Figure 1.2: Resonance hybrid of pyrazine ring | 2 |
| Figure 1.3: Reactivity of halodiazines | 4 |
| Figure 1.4: The bond lengths of naphthalene (21) | 10 |
| Figure 1.5: Resonance hybrid of naphthalene (21) | 13 |
| Figure 1.6: Steric hindrance in naphthalene-1-sulfonic acid (40) and naphthalene-2-sulfonic acid (41) | 17 |
| Figure 2.1: Schematic representation of an energy diagram (Jablonski diagram) | 21 |
| Figure 2.2: Stokes fluorescence diagram | 22 |
| Figure 2.3: Schematic representation of equilibrium and Franck-Condon (F-C) electronic states | 26 |
| Figure 2.4: Fluorimeter schematic | 32 |
| Figure 2.5: Spectral output of a continuous xenon arc lamp and a xenon flash lamp | 33 |
| Figure 2.6: Output wavelength distribution of a xenon arc | 33 |
| Figure 2.7: A typical monochromator elements | 34 |
| Figure 2.8: Image of plane grating and concave grating | 35 |
| Figure 2.9: 180° excitation beam geometry | 36 |
| Figure 2.10: 90° excitation beam geometry | 37 |
| Figure 2.11: Front-face excitation beam geometry | 37 |
| Figure 2.12: Graph of absorbance spectra of water in different cuvettes | 38 |

| | | |
|--------------|--|----|
| Figure 2.13: | The structure of cuvette that shows different path length in different orientation | 39 |
| Figure 2.14: | Schematic diagram of PMT | 41 |
| Figure 3.1: | Reactions of 2-chloropyrazine (48) with phenol derivatives, naphthols and piperidine. | 44 |
| Figure 3.2: | Reaction of 5-chloropyrazine-2-carboxylic acid methyl ester (63) with phenol derivatives | 45 |
| Figure 3.3: | Reaction of 3-chloro-2,5-dimethylpyrazine (68) with phenol (49) | 45 |
| Figure 3.4: | ORTEP diagram of 5-phenoxy pyrazine-2-carboxylic acid methyl ester (65) | 57 |
| Figure 3.5: | Fluorescence intensity of 2-phenoxy pyrazine (50), 2- <i>o</i> -tolylloxypyrazine (52), 2- <i>N</i> -piperidinopyrazine (62) and 2,5-dimethyl-3-phenoxy pyrazine (69) with three different concentrations in ethyl acetate | 60 |
| Figure 3.6: | Fluorescence intensity of 2-phenoxy pyrazine (50), 2- <i>o</i> -tolylloxypyrazine (52), 2- <i>N</i> -piperidinopyrazine (62) and 2,5-dimethyl-3-phenoxy pyrazine (69) with three different concentrations in acetonitrile | 60 |
| Figure 3.7: | Fluorescence spectra of 2, 5-dimethyl-3-phenoxy pyrazine (69) taken at different time frame in acetonitrile (concentration: 3.8314×10^{-4} M) | 62 |
| Figure 3.8: | Fluorescence spectra of 2- <i>o</i> -tolylloxypyrazine (52) at different time frame in acetonitrile (concentration: 3.8314×10^{-4} M) | 62 |
| Figure 3.9: | Fluorescence spectra of 2- <i>p</i> -tolylloxypyrazine (46) at different time frame in acetonitrile (concentration: 3.8314×10^{-4} M) | 63 |
| Figure 3.10: | Fluorescence spectra of 2-phenoxy pyrazine (50) in various pH (concentration: 3.8314×10^{-5} M) | 65 |

| | | |
|--------------|--|----|
| Figure 3.11: | Fluorescence spectra of 5-(3-nitrophenoxy)pyrazine-2-carboxylic acid methyl ester (67) in various pH (concentration: 3.8314×10^{-5} M) | 65 |
| Figure 3.12: | The electron transfer mechanism of (50) to the phenoxy ring | 65 |
| Figure 3.13: | The electron transfer mechanism of 5-(3-nitrophenoxy)pyrazine-2-carboxylic acid methyl ester (67) to the phenoxy ring | 66 |
| Figure 3.14: | Fluorescence intensity of (52), (56) and (69) in various solvents in 3.8314×10^{-4} M. | 67 |
| Figure 3.15: | Formation of hydrogen bonded complexes of compound (52), (56), and (69) in ethanol. | 68 |
| Figure 3.16: | Fluorescence spectra of compound (50), (58), and (60) in acetonitrile at 3.8314×10^{-6} M | 70 |
| Figure 3.17: | Fluorescence spectra of compound (65), (66), and (67) in hexane in 3.8314×10^{-4} M | 73 |
| Figure 3.18: | Fluorescence spectra of compound (65), (66), and (67) in tetrahydrofuran in 3.8314×10^{-4} M | 73 |
| Figure 3.19: | Fluorescence spectra of compound (50), (65), and (69) in hexane at 3.8314×10^{-4} M | 76 |
| Figure 3.20: | Fluorescence spectra of compound (50), (65), and (69) in tetrahydrofuran at 3.8314×10^{-4} M | 76 |
| Figure 3.21: | Fluorescence characteristic of 2- <i>o</i> -tolylloxypyrazine (52), 2- <i>m</i> -tolylloxypyrazine (54), and 2- <i>p</i> -tolylloxypyrazine (56) in various solvents at concentration 3.8314×10^{-4} M | 78 |
| Figure 3.22: | Resonance mechanism in 2-phenoxy pyrazine (50) | 79 |

LIST OF TABLES

| | Page |
|--|------|
| Table 2.1: pKa and pKa* reading of molecules attach to electron-donating group ^[25] | 28 |
| Table 2.2: pK _a and pK _a * reading of molecules attach to electron-withdrawing group ^[25] | 29 |
| Table 3.1: The crystal system and refinement data of compound (65) | 57 |
| Table 3.2: Fluorescence characteristic of 2-phenoxy pyrazine (50) in various concentrations in ethyl acetate and acetonitrile | 59 |
| Table 3.3: Fluorescence characteristic of 2- <i>o</i> -tolyl oxy pyrazine (52) in different concentrations in ethyl acetate and acetonitrile | 59 |
| Table 3.4: Fluorescence characteristic of 2- <i>N</i> -piperidinopyrazine (62) in different concentrations in ethyl acetate and acetonitrile | 59 |
| Table 3.5: Fluorescence characteristic of 2,5-dimethyl-3-phenoxy pyrazine (69) in different concentrations in ethyl acetate and acetonitrile | 60 |
| Table 3.6: Fluorescence characteristic of compound (52) , (56) , and (69) in acetonitrile in 3.8314x10 ⁻⁴ M | 61 |
| Table 3.7: Fluorescence characteristic of 2-phenoxy pyrazine (50) and 5-(3-nitrophenoxy)pyrazine-2-carboxylic acid methyl ester (67) in various pH (concentration: 3.8314 x10 ⁻⁵ M) | 64 |
| Table 3.8: Fluorescence characteristic of (52) , (56) and (69) in various solvents in 3.8314 x10 ⁻⁴ M. | 66 |
| Table 3.9: Fluorescence characteristic of compounds (50) , (58) , and (60) in acetonitrile at 3.8314x10 ⁻⁵ M | 70 |

| | | |
|-------------|---|----|
| Table 3.10: | Fluorescence characteristic of compound (65) , (66) , and (67) in hexane and tetrahydrofuran in 3.8314×10^{-4} M | 72 |
| Table 3.11: | Fluorescence characteristic of compound (50) , (65) , and (69) in hexane at 3.8314×10^{-4} M | 75 |
| Table 3.12: | Fluorescence characteristic of 2- <i>o</i> -tolylloxypyrazine (52) , 2- <i>m</i> - tolylloxypyrazine (54) , and 2- <i>p</i> -tolylloxypyrazine (56) in various solvents at concentration 3.8314×10^{-4} M | 77 |

LIST OF SCHEMES

| | Page |
|---|------|
| Scheme 1.1: Chlorination process of methyl pyrazine (5) | 3 |
| Scheme 1.2: Bromonation and chlorination of pyrazine (1) | 4 |
| Scheme 1.3: Reaction of 2-halogenopyrazine | 5 |
| Scheme 1.4: Oxidation of quinoxaline (12) and 2,5-dimethylpyrazine (13) | 6 |
| Scheme 1.5: Preparation of pyrazine derivative through self-condensation of 2-amino carbonyl compounds (14) | 7 |
| Scheme 1.6: Synthesis of pyrazine through condensation of diacetyl (16) and 1,2-diamino ethane (17) | 8 |
| Scheme 1.7: Synthesis of two isomeric pyrazine | 8 |
| Scheme 1.8: Synthesis of pyrazine (1) through Wolff and Marburg method | 9 |
| Scheme 1.9: Haworth synthesis reaction to synthesis naphthalene (21) | 11 |
| Scheme 1.10: Formation of naphthalene (21) through Diels Alder reaction | 12 |
| Scheme 1.11: Synthesis of naphthalene (21) from (α,β - dibromo-butyl)-benzene (31) | 12 |
| Scheme 1.12: Oxidation of naphthalene (21) with oxygen and vanadium pentoxide as catalyst | 13 |
| Scheme 1.13: Oxidation of 2-methylnaphthalene (34) with chromic acid and glacial acetic acid | 14 |
| Scheme 1.14: Reduction of naphthalene (21) to 1,4-dihydronaphthalene (35) | 14 |
| Scheme 1.15: Reduction of naphthalene (21) to tetraline (36) | 15 |
| Scheme 1.16: Catalytically reduction of tetralin (36) to decalin (37) | 15 |
| Scheme 1.17: Bromination of naphthalene (21) in aluminium chloride | 15 |
| Scheme 1.18: Bromination of naphthalene (21) in carbon tetrachloride | 16 |

| | | |
|--------------|--|----|
| Scheme 1.19: | Sulfonation of naphthalene (21) at 80 °C | 16 |
| Scheme 1.20: | Sulfonation of naphthalene (21) at 160 °C | 16 |
| Scheme 3.1: | Reaction mechanism of formation of 2-phenoxy pyrazine (50) | 46 |
| Scheme 3.2: | Reaction of 2-chloropyrazine (48) with naphthalene derivatives | 50 |
| Scheme 3.3: | Reaction mechanism of formation of 2-(naphthalene-1-yloxy)pyrazine (58) | 50 |
| Scheme 3.4: | Reaction mechanism of formation of 2-(naphthalene-2-yloxy)pyrazine (60) | 51 |
| Scheme 3.5: | Reaction mechanism of formation of 5-phenoxy pyrazine-2-carboxylic acid methyl ester (65) | 54 |
| Scheme 3.6: | Reaction mechanism of formation of 2, 5-dimethyl-3-phenoxy pyrazine (69) | 57 |

LIST OF SYMBOLS AND ABBREVIATIONS

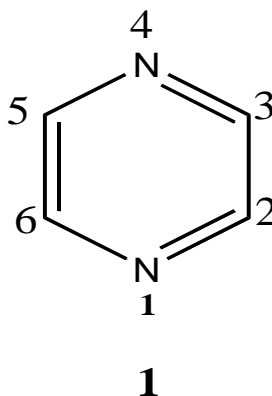
| | | |
|------------------------|---|--|
| CDCl_3 | : | deuterated chloroform |
| CH_3CN | : | acetonitrile |
| d | : | doublet |
| dd | : | doublet of doublets |
| ddd | : | doublet of doublets of doublets |
| Eq | : | equivalent |
| EtOAc | : | ethyl acetate |
| EtOH | : | ethanol |
| IR | : | infrared |
| J | : | coupling constant |
| M | : | mole per litre |
| m | : | multiplet |
| m.p. | : | melting point |
| min | : | minute |
| MW | : | molecular weight |
| NMR | : | nuclear magnetic resonance |
| s | : | singlet |
| t | : | triplet |
| THF | : | tetrahydrofuran |
| TLC | : | thin layer chromatography |
| λ | : | wavelength |
| ν | : | stretching vibration |
| δ | : | chemical shift |
| HBDI | : | <i>p</i> -hydroxybenzylidene-1,2-dimethyl-imidazolin-5-one |

CHAPTER 1: SYNTHESIS AND REACTIVITY OF PYRAZINE AND NAPHTHALENE

1.1 Introduction of pyrazine

Heterocyclic compounds (or heterocycles)-cyclic are compounds in which one or more of the atoms of the ring are heteroatoms. A heteroatom is an atom other than carbon. The name comes from Greek word *heteros*, which means “different”. A variety of atoms, such as Nitrogen, Oxygen, Sulphur, Selenium, Phosphorus, Silicon, Boron and Arsenic, can be incorporated into ring structures. The cyclic part come from Greek word *kyklos*, meaning “circle” of heterocyclic indicates that at least one ring structure is present in such a compound. In general, heterocyclic compounds resemble cyclic organic compounds that incorporate only carbon atom in the rings, but the presence of heteroatoms gives heterocyclic compounds physical and chemical properties that are often quite distinct from those of their all-carbon-ring analogs.

Almost all the compound we know as vitamins, drugs, antibiotics and many other natural products are heterocyclic compounds, as are most hallucinogens^[1]. Modern society is dependent on synthetic heterocycles for use as drugs, pesticides, dyes, and plastics.



This research is focused on pyrazine derivatives or also known as 1,4-diazine. Pyrazine (**1**) is a heterocyclic aromatic organic compound with the chemical formula $C_4H_4N_2$ containing two azomethine nitrogen atoms and 4 carbon atoms. In pyrazines (**1**), the C-N bonds are short when compared with C-C bonds, and their ring angles at the heteroatoms are smaller than at the carbon atoms^[2], as shown in Figure 1.1.

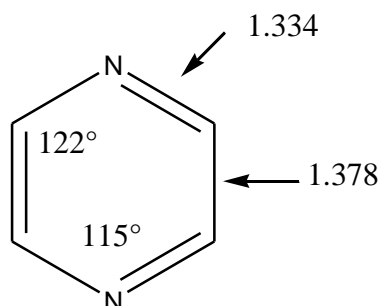


Figure 1.1: Bond lengths and ring angles in pyrazine (1)

Pyrazines (**1**) are aromatic compounds as well as tertiary amines, and their properties closely resemble those of the pyridines. The pyrazines (**1**) nucleus may be considered as resonance hybrid of which two of the contributing forms (**2** and **3**) as shown in Figure 1.2 are analogous to those of benzene. It has already been proved that the electron diffraction photographs for benzene, pyridine, and pyrazine (**1**) are closely similar^[3-5].

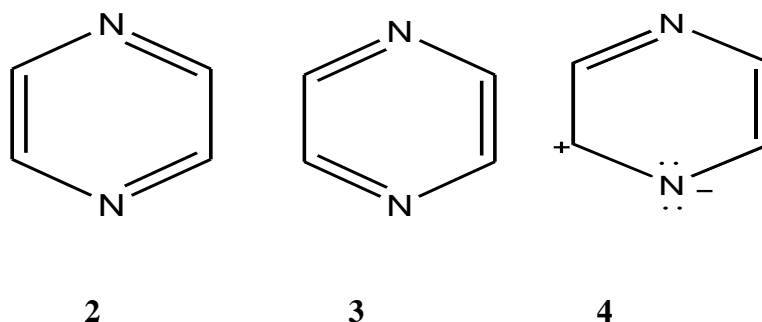


Figure 1.2: Resonance hybrid of pyrazine ring

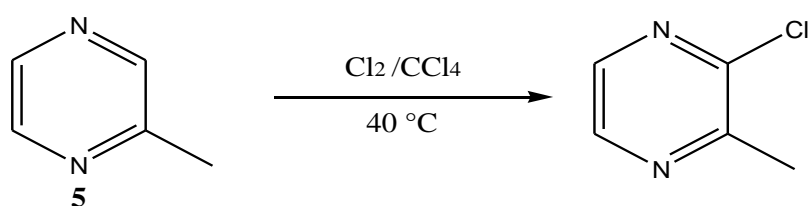
The C-C bond distances in these three compounds as shown in Figure 1.2, have the expected value for 50% double-bond character. The C-N bond distances in pyrazines,

hence, are slightly greater because of the high additional contributions to the resonance by structures such as **4**. The electronegativity of the two nitrogen atoms would be expected to have a definite influence on both the basic and aromatic properties of the pyrazines.

Pyrazine (**1**) is a low melting solid, and most of the lower homologs are liquid at room temperature. In general, pyrazines (**1**) have narcotic odour, sublime readily and may be distilled with steam. The lower members of the series are very soluble in water, and some are miscible in all proportions.

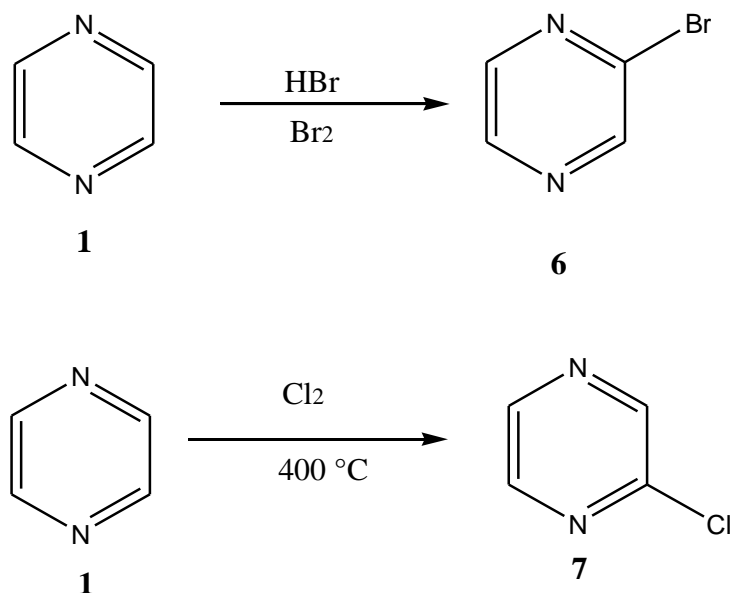
1.1.1 Reactivity of Pyrazine

Pyrazine (**1**) is essentially monobasic substance which has two heteroatoms withdraw electron density from the ring carbons even more than one in pyridine, so, unsubstituted pyrazines (**1**) are even more resistant to electrophilic substitution than in pyridines, hence this strongly electron-poor nature make it able to add nucleophilic reagent easily^[6]. The nitrogen lone pair's availability also reduced, making pyrazine (**1**) less basic. Hence, pyrazine (**1**) is much weaker base than pyridine^[7-9]. This reduction in basicity gave a huge consequence of destabilization of the mono-protonated cations due to inductive withdrawal by second nitrogen atom in the molecule. These two heteroatoms withdraw electron density from the ring even more than in pyridine which has only one nitrogen, so unsubstituted pyrazines (**1**) are even more resistant to electrophilic substitution than in pyridines. However, chlorination of methyl pyrazine (**5**) occurs under mild conditions at C-3^[10] as shown in Scheme 1.1.



Scheme 1.1: Chlorination process of methyl pyrazine (5**)**

2-Bromopyrazine (**6**) is formed when bromine plus hydrogen bromide was strongly heated with pyrazine (**1**). 2-Chloropyrazine (**7**) is formed when pyrazine (**1**) was added to chlorine in 400 °C temperature giving mixtures of 2-chloropyrazine (**7**) and polychloropyrazines, as demonstrated in Scheme 1.2 below^[2].



Scheme 1.2: Bromonation and chlorination of pyrazine (1)

All halodiazines apart from 5-halopyrimidines, react readily with ‘soft’ nucleophiles with substituent

ion reaction with the halide. The reactivity of all halodiazines can be summarised as below in Figure 1.3.

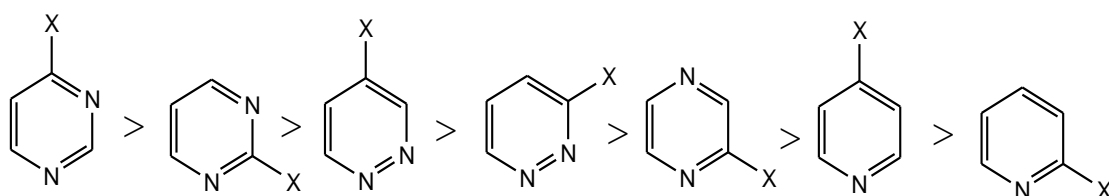
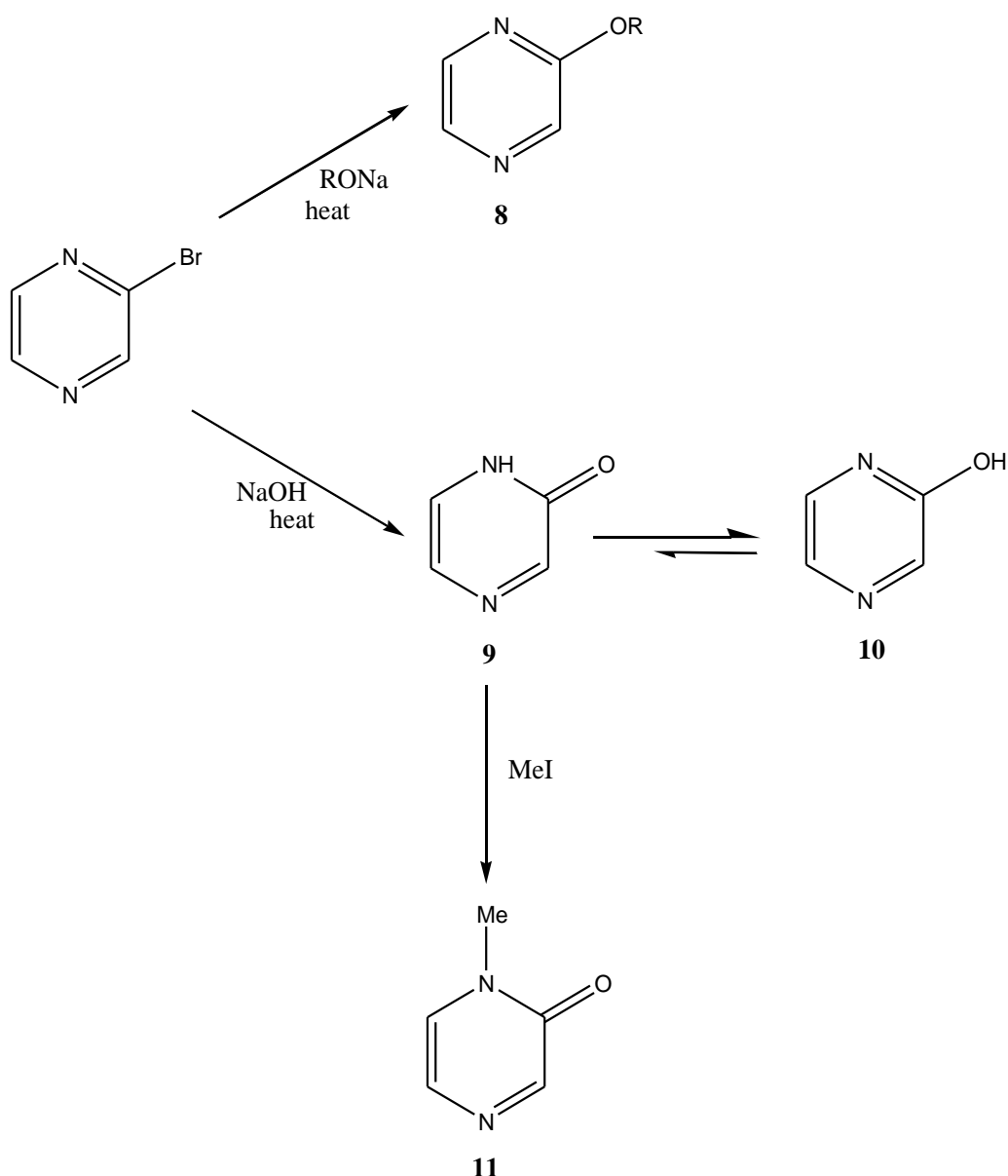


Figure 1.3: Reactivity of halodiazines

The 2-halogenopyrazines are readily converted to 2-alkoxypyrazines (**8**) and 2-pyrazinones (**9**). The dominance of 2-pyrazinone (**9**) over the tautomer 2-

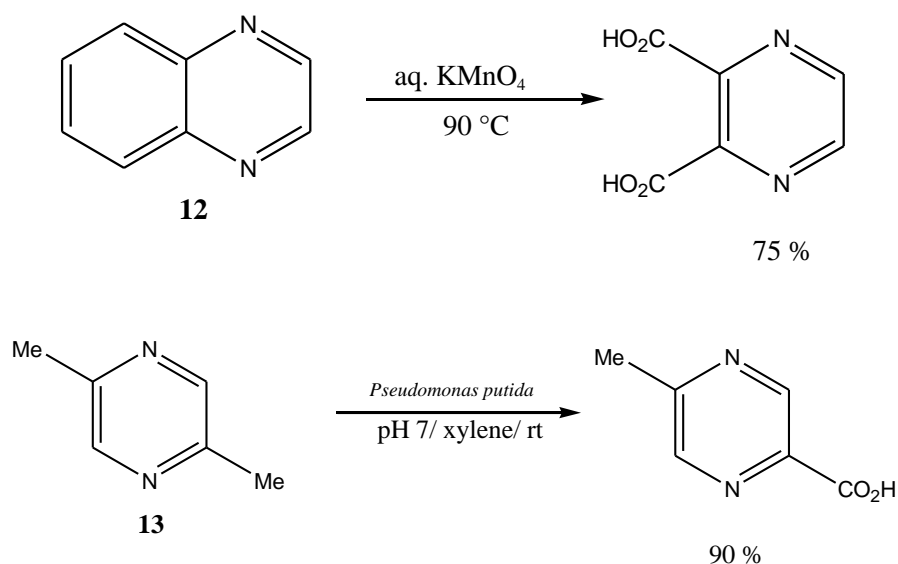
hydroxypyrazine (**10**) has been confirmed by ultraviolet spectra comparison of the ultraviolet spectra of the fixed alkylated derivatives 2-methoxypyrazine ($\lambda_{\text{max}}=292 \text{ m}\mu$) and 1-methyl-2-pyrazinone (**11**) ($\lambda_{\text{max}}=223, 319 \text{ m}\mu$), with the tautomeric mixture of 2-pyrazinone (**9**) and 2-hydroxypyrazine (**10**) which has $\lambda_{\text{max}}=221, 316 \text{ m}\mu$, as demonstrated in Scheme 1.3 below^[2].



Scheme 1.3: Reaction of 2-halogenopyrazine

Although pyrazines (**1**) have lower aromaticity properties, but generally it is resistant towards oxidative attack at ring carbon. However, alkaline oxidizing agent can

reduce pyrazine by initial nucleophilic addition to pyrazine ring. The alkylated pyrazine can be oxidised to carboxylic acid residues can be oxidised to carboxylic acid residues in the presence of an enzyme leaving the heterocyclic ring untouched as shown in Scheme 1.4^[7].



Scheme 1.4: Oxidation of quinoxaline (12) and 2,5-dimethylpyrazine (13)

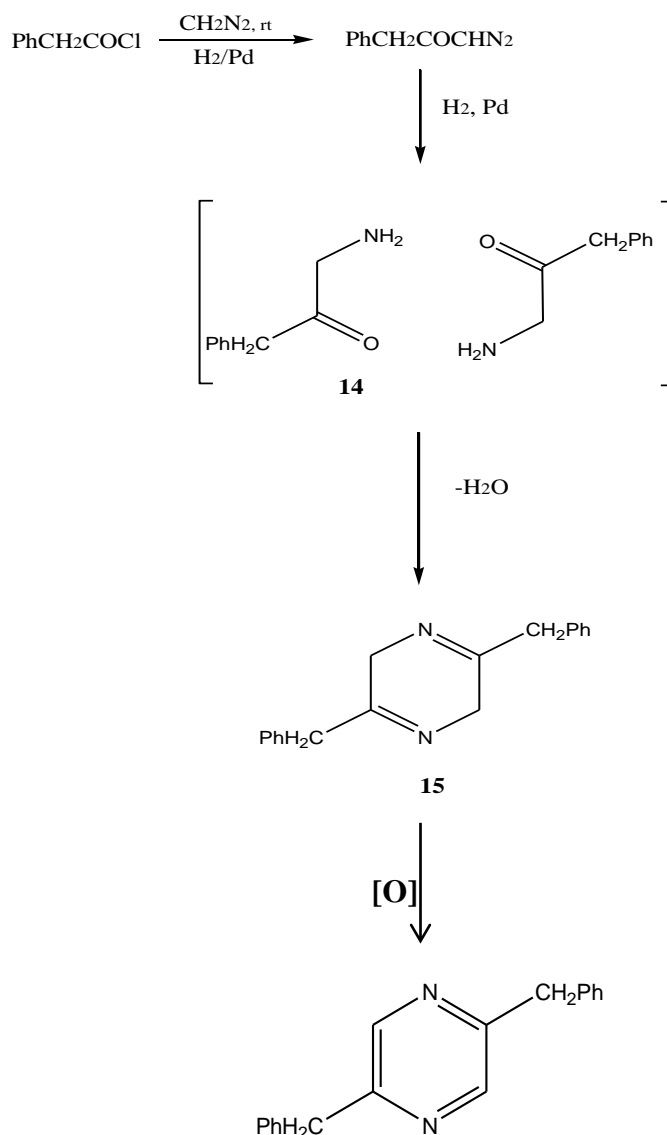
1.1.2 Synthesis of pyrazine derivatives

Pyrazines occur in nature in relatively small quantities. Because of the lack of natural sources of pyrazine and its derivatives, these compounds have been relatively expensive in the past. Earlier, there is no important use developed in the field of pyrazine chemistry. It did not attract research activity, until there were advances in chemotherapy's research. Advances in chemotherapy suggested new application for the less accessible substances, thus renewed interest in pyrazines became evident. Since there were more research and potential of pyrazines been revealed, more economical and new synthetic processes for the synthesis of pyrazines have since been rapidly developed. It is to be expected that the increase in their availability of these compounds

will focus greater attention on their potentialities both in fundamental research and in practical applications^[8].

1.1.2.1 Self condensation of a α -amino carbonyl compounds

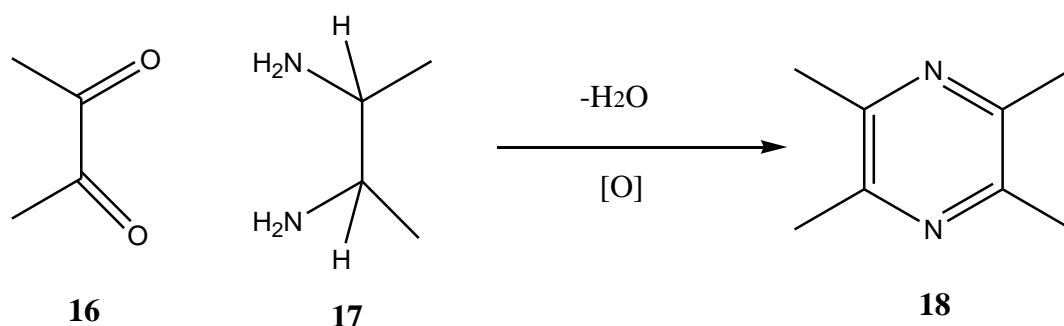
2-Amino carbonyl (**14**) compounds which are most stable at salts condition prepared in situ by reduction of oximio-, diazo-, azido ketones^{[7][10]} or by the Gabriel Method^[2]. Formation of pyrazine from the dihydropyrazine (**15**) requires oxidation, special precaution needed in order to obtain direct pyrazine as reaction occurs very readily, the reaction is shown in Scheme 1.5.



Scheme 1.5: Preparation of pyrazine derivative through self-condensation of 1-amino-3-phenylpropan-2-one (14**)**

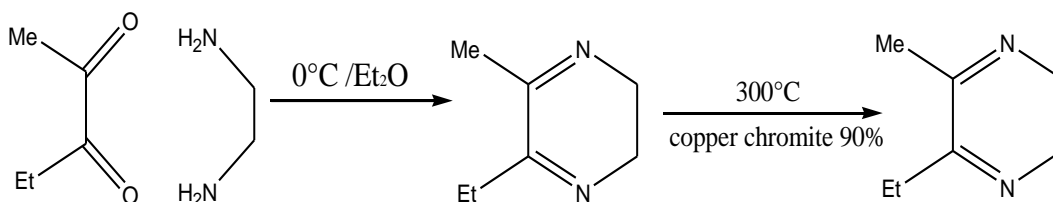
1.1.2.2 Condensation of 1,2-diamino ethane and related compounds with α diketones.

Another general method to synthesis pyrazine ring is condensation of 1,2-dicarbonyl (**16**) and 1,2-diamino (**17**), an oxidation is then required. This method generally one of the best method to synthesis symmetrical pyrazines (**18**), as shown in Scheme 1.6 below.



Scheme 1.6: Synthesis of pyrazine through condensation of diacetyl (16) and 1,2-diamino ethane (17)

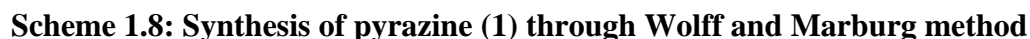
If both diketone and diamine are unsymmetrical, two isomeric pyrazines are produced, as shown in Scheme 1.7^[7].



Scheme 1.7: Synthesis of two isomeric pyrazine

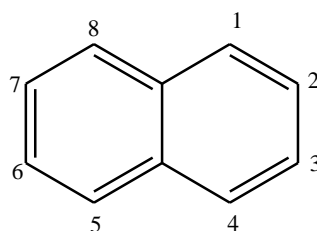
1.1.2.3 Wolff and Marburg method

One of the most efficient method to synthesis pyrazine was that of Wolff and Marburg from acetal of iminodiacetaldehyde (**19**) as shown in Scheme 1.8.



1.2 Introduction of naphthalene

9



(21)

The positions 1 and 2 are also called the α - and β - positions. Different with benzene (26), the bond length in naphthalene (21) are not all equal as illustrated in Figure 1.4.

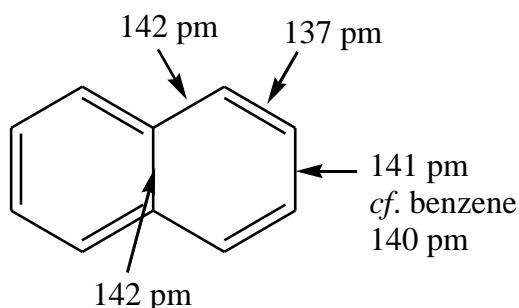


Figure 1.4: The bond lengths of naphthalene (21)

Naphthalene (21) is best known as the main ingredient of traditional mothballs^[11-12]. Scientist discovered that Formosan Subterranean termite (*Coptotermes formosanus*) was the first insect that fumigate their nests with naphthalene (21) and other volatile compounds^[13]. Termites inhibiting many adversaries such as bacteria, nematodes, ants, fungus and invertebrate invaders into their nest. A postdoctoral researcher from Louisiana State University and colleagues, Jian Chen discovered that termites build naphthalene (21) by cementing together masticated wood and soil with their excrement and saliva^[14]. Naphthalene (21) also traced produced by magnolias flowers^[15-16], Annonacea flowers^[17], and forehead of male white-tailed deer (*Odocoileus Virginianus*)^[18].

Naphthalene (21) is mainly used as intermediate to other chemicals. They can be substituted with combinations of strongly electron-donating functional groups and

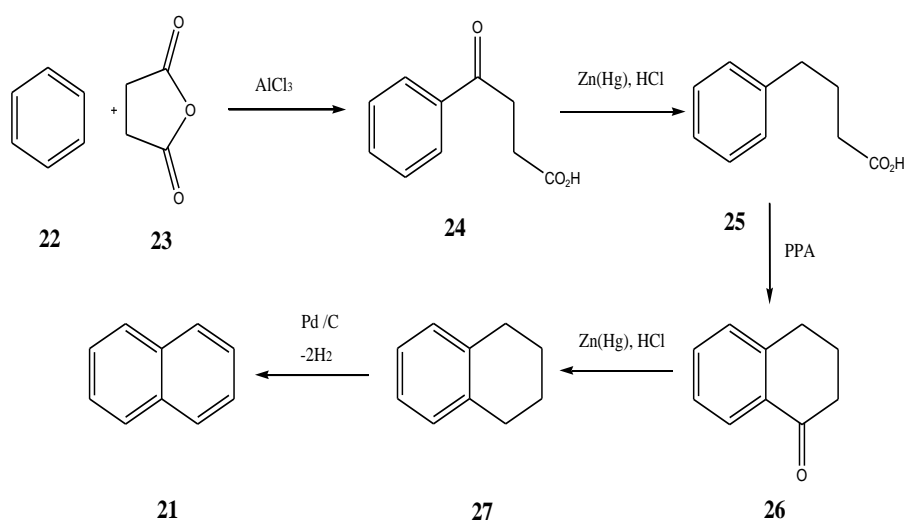
strongly electron withdrawing groups in the process to prepare many synthetic dyes^[19-20].

1.2.1 Synthesis of naphthalenyl derivatives

Naphthalene (**21**) was firstly produced from distillation of coal tar in early 1820, which constitutes the most important starting material for its production. Naphthalene-oil, a tar fraction boiling at 195-230 °C, is cooled and the crude naphthalene is crystallized. Then, by centrifuging or pressing, the oily impurities were removed, and the naphthalene (**21**) is distilled. While in the molten state, it is treated with small quantities of concentrated sulphuric acid and caustic soda solution, and finally followed by further purification by distillation and sublimation^[21]. There are many synthetic routes to synthesis naphthalene (**21**) that have been reported.

1.2.1.1 Haworth synthesis

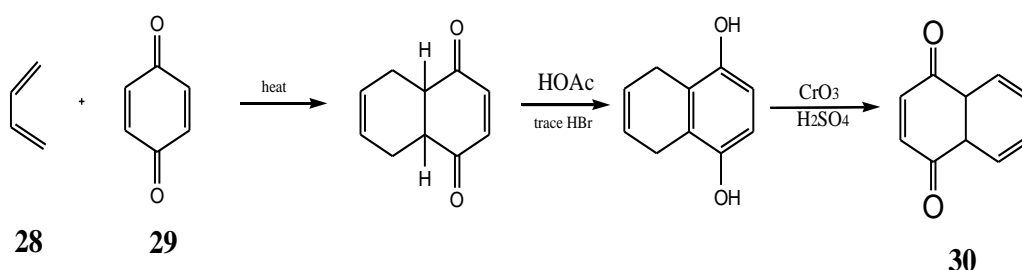
This synthesis got its name from R. D. Harworth from University of Durham. Scheme 1.9 below shows Haworth synthetic approaches to naphthalene (**21**).



Scheme 1.9: Haworth synthesis reaction to synthesis naphthalene (21**)**

In the Harworth synthesis, the reaction started between benzene (**22**) and succinic acid (**23**) to produce 4-oxo-4-phenylbutanoic acid (**24**). Under Friedel-Crafts conditions this acid was then reduced with either amalgamated zinc and HCl or with hydrazine ethane-1,2-diol and potassium hydroxide to 4-phenylbutanoic acid (**25**). Ring closure is achieved by heating in phosphoric acid producing 1-tetralone (**26**). Reduction of the carbonyl group gave 1,2,3,4-tetrahydronaphthalene (tetraline) (**27**). Dehydration through a palladium catalyst of tetraline produced naphthalene (**21**)^[22-23].

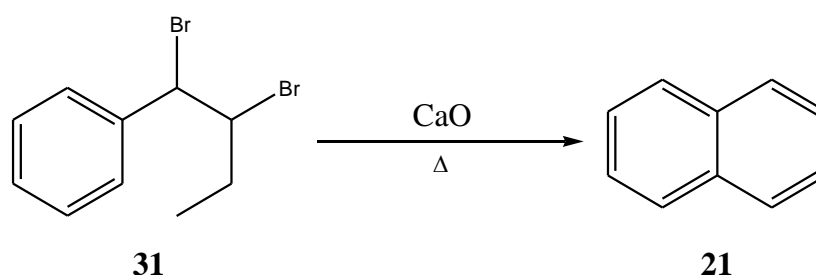
1.2.1.2 Formation of naphthalene (**21**) through Diels-Alder reaction



Scheme 1.10: Formation of naphthalene (21**) through Diels-Alder reaction**

The Diels-Alder reaction between diene (**28**) and *p*-benzoquinone (**29**) produces adducts that may be converted to naphtha-1,4-quinones (**30**) via enolization and oxidation^[22-30].

1.2.1.3 Preparation of naphthalene (**21**) from (α,β - dibromobutyl)benzene (**31**)



Scheme 1.11: Synthesis of naphthalene (21**) from (α,β - dibromobutyl)benzene (**31**)**

(α,β -dibromobutyl)benzene (**31**) were heated with lime to produce naphthalene (**21**)^[22].

1.2.2 Reactivity of naphthalene (**21**)

The term polycyclic aromatic hydrocarbon is usually applied to compounds where the rings are fused together as in the case of naphthalene (**21**). Naphthalene (**21**) is less aromatic than aromatic benzene (**22**), which accounts for its higher reactivity towards electrophilic attack compared with benzene (**22**). The resonance hybrid of naphthalene (**21**) is as shown in Figure 1.5.

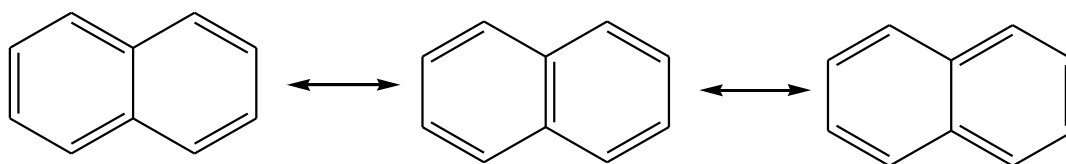
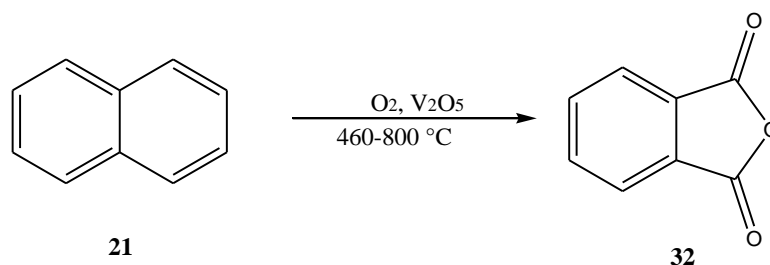


Figure 1.5: Resonance hybrid of naphthalene (21**)**

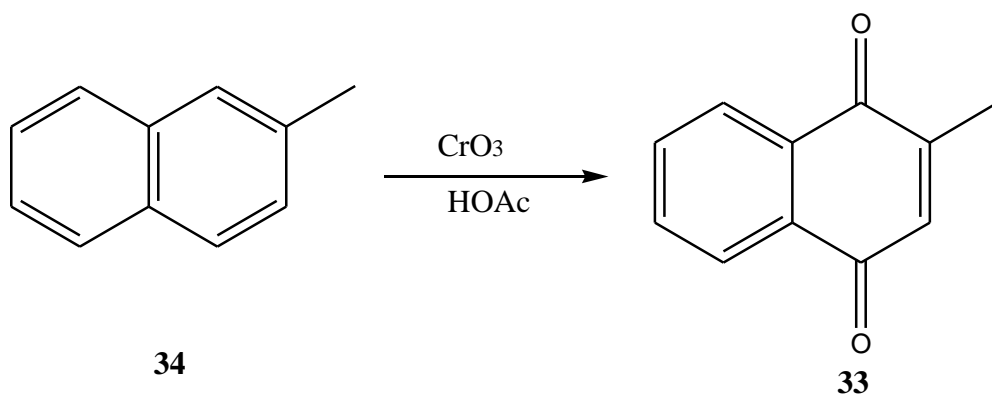
1.2.2.1 Oxidation

Naphthalene (**21**) undergoes oxidation as compared to benzene (**21**). Naphthalene (**21**) will undergoes oxidation to form phthalic acid (**32**) with oxygen and vanadium pentoxide as catalyst. As most of naphthalene (**21**) is obtained from coal tar, and a very high request for phthalic acid (**32**), this reaction become very important in phthalic acid (**32**) production as shown in Scheme 1.12^[22].



Scheme 1.12: Oxidation of naphthalene (21**) with oxygen and vanadium pentoxide as catalyst**

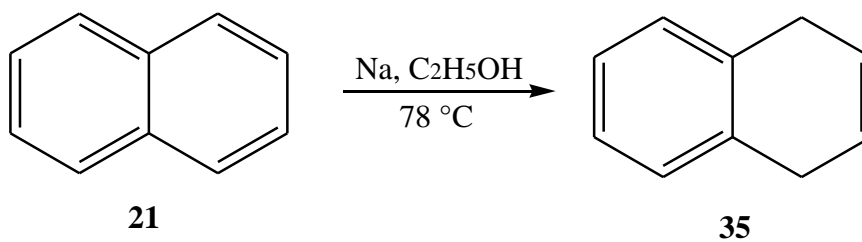
1,4-Napthoquinone (**33**) may be obtained by direct oxidation of 2-methylnaphthalene (**34**) with chromic acid and glacial acetic acid as illustrated in Scheme 1.13^[24].



Scheme 1.13: Oxidation of 2-methylnaphthalene (34**) with chromic acid and glacial acetic acid**

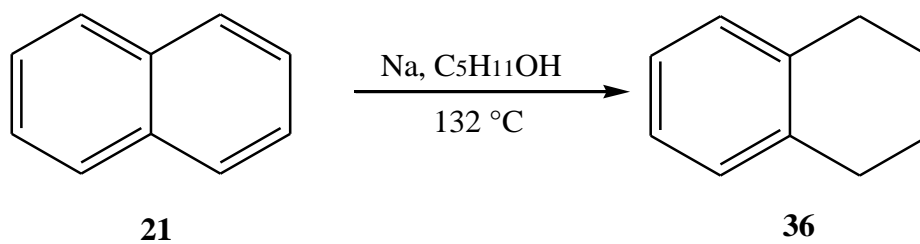
1.2.2.2 Reduction

Naphthalene (**21**) is readily reduced by dissolving metals, e.g. sodium and alcohol. The product of reduction process depends on the reaction condition. 1,4-Dihydronaphthalene (**35**) is produced when naphthalene (**21**) and sodium were boiled in ethanol, as shown in Scheme 1.14^[22].



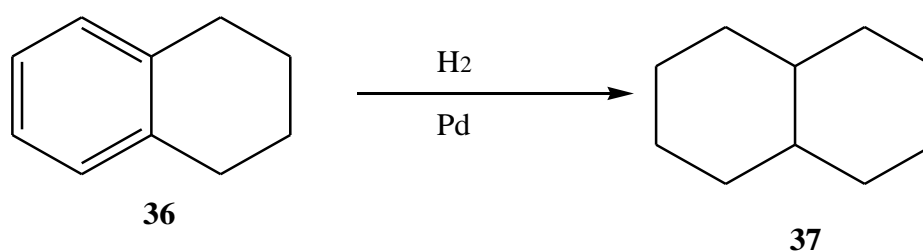
Scheme 1.14: Reduction of naphthalene (21**) to 1,4-dihydronaphthalene (**35**)**

When, naphthalene (**21**) and sodium being refluxed in *isopentyl* alcohol, 1,2,3,4-tetrahydronaphthalene or tetraline (**36**) was produced, this was shown in Scheme 1.15 below.



Scheme 1.15: Reduction of naphthalene (21) to tetralin (36)

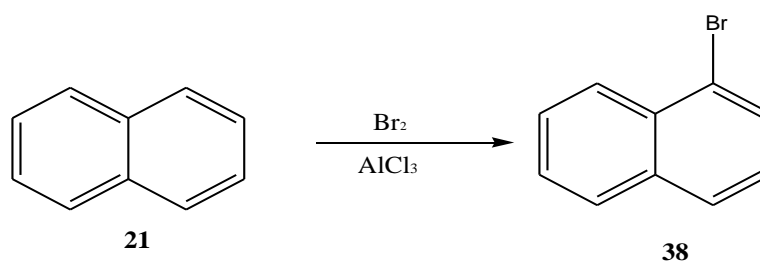
Tetralin (**36**) can be further reduced to decalin (**37**), catalytically as shown in Scheme 1.16^[24].



Scheme 1.16: Catalytic reduction of tetralin (36) to decalin (37)

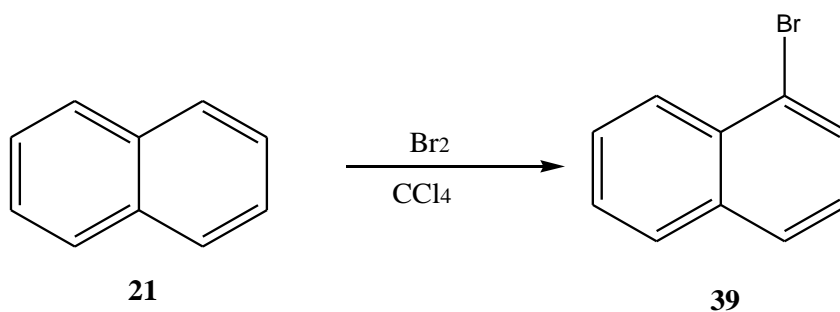
1.2.2.3 Halogenation

Naphthalene (**21**) undergoes bromination in the presence of aluminium chloride to give 99 % yield of 1-bromonaphthalene (**38**) as shown in Scheme 1.17^[23].



Scheme 1.17: Bromination of naphthalene (21) in aluminium chloride

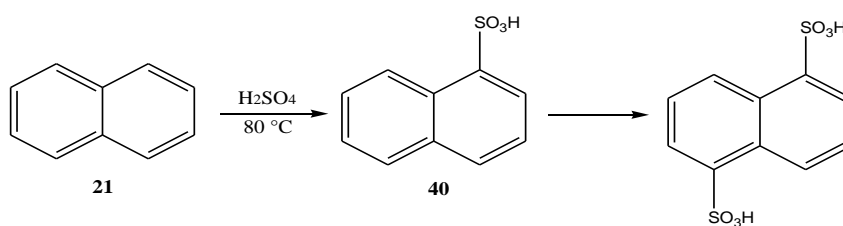
Naphthalene (**21**) also undergoes bromination in carbon tetrachloride results in 75 % yield of 1-bromonaphthaene (α -naphthalene) (**39**) as shown in Scheme 1.18^[22].



Scheme 1.18: Bromination of naphthalene (21) in carbon tetrachloride

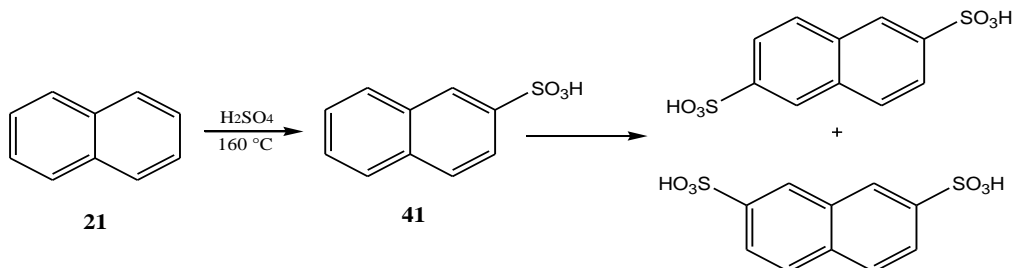
1.2.2.4 Sulfonation of naphthalene

Sulfonation is a reversible and temperature controlled reaction. Sulfonation at $80\text{ }^\circ\text{C}$ in concentrated sulphuric acid gave naphthalene-1-sulfonic acid (40) as shown in Scheme 1.19.



Scheme 1.19: Sulfonation of naphthalene (21) at $80\text{ }^\circ\text{C}$

When the temperature increase to $160\text{ }^\circ\text{C}$, naphthalene-2-sulfonic acid (41) predominates, this was shown in Scheme 1.20 below.



Scheme 1.20: Sulfonation of naphthalene (21) at $160\text{ }^\circ\text{C}$

Naphthalene-2-sulfonic acid (**41**) also formed when naphthalene-1-sulfonic acid (**40**) heated at 160 °C^[22]. The sulfonation of naphthalene easily occurred at C-1, because the reaction at this position involved the formation of more stable carbocation. C-1 position is more reactive compared with C-2 position, but formation of naphthalene-2-sulfonic acid (**41**) is more stable, probably because there is less steric hindrance between the bulky sulfonic acid group and the adjacent *ortho* H atoms (H-1 and H-3) than between the naphthalene-1-sulfonic acid (**40**) and the *peri* H-8 atom as illustrated at Figure 1.6 below^[23].

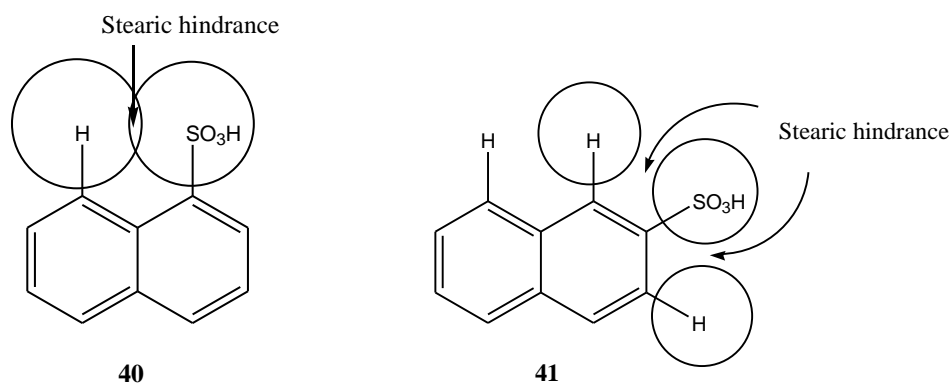


Figure 1.6: Steric hindrance in naphthalene-1-sulfonic acid (40**) and naphthalene-2-sulfonic acid (**41**)**

CHAPTER 2: FLUORESCENCE SPECTROSCOPY

2.0 Introduction to fluorescence

Luminescence is an emission of ultraviolet, visible or infrared photons from an electronically excited species. Luminescence word come from the Latin (lumen=light) was first introduced as *luminescentz* by Eilhardt Wiedemann in 1888. Luminescence is cold light whereas incandescence is hot light. Fluorescence is particular cases of luminescence.

Fluorescence is a chemical substances property when irradiated with light of a short wavelength, some of the light is absorbed and part of the energy from the absorbed light is re-radiated as light, usually to a longer wavelength. The term fluorescence was introduced by Sir George Gabriel Stroke, which was a physicist and professor of mathematics at Cambridge in the middle of nineteenth century. He described the phenomenon of fluorescence in his famous paper on the change of wavelength of light in 1852, as exhibited by fluorspar and uranium glass, materials which he viewed as having the power to convert invisible ultra-violet radiation into radiation of longer wavelengths that are visible^[25].

Furthermore, fluorescence microscopy is a technique of microscopy whereby fluorescent substances are examined. It was a German microscopist Köhler, who invented fluorescence microscopy and best known for the development of a system of illumination. Köhler was experimenting with ultraviolet microscopy, which, because of its shorter wavelength, can give a finer resolution than microscopy with visible light^[26]. In 1941, Coons and co-workers discovered the development of fluorescence antibody technique, and this brought to major factor in extension of fluorescence microscopy uses. As a result, fluorescence microscopes become more readily available, leading to developments in other fields.

Fluorescence spectroscopy and time-resolved fluorescence are considered to be primarily research tools in biochemistry and biophysics. This emphasis has changed, and the use of fluorescence has expanded and become dominant methodology used widely in flow cytometry, medical diagnostic, biotechnology, DNA sequencing, forensics, and generic analysis^[27]. Fluorescence is used by scientist from many disciplines.

2.1 Theory of fluorescence

Fluorophores play as crucial role in fluorescence spectroscopy and imaging as it is a part of a molecule which responsible for the fluorescence. This term was used by R. Meyer in 1897 to describe chemical groups which tended to be associated with fluorescence. Different fluorophores component are able to absorb energy at different specific wavelength and re-emit energy at different but equally specific wavelength. The amount and wavelength of the emitted energy depend on both the fluorophores and the chemical environment of the fluorophore^[28].

Molecules may exist at any one of several energy levels, each associated with a particular arrangement of the electronic orbitals. Electronic state with least energy is known as ground state. At room temperature, under normal condition, most molecules occupy this lowest vibrational level of the ground electronic state. When light from external source such as an incandescent lamp or a laser hit the molecule (generally polyaromatic hydrocarbons or heterocycles) called fluorophore, and energy absorbed is sufficient, the molecules are elevated to produce excited state. The amount of energy which a photon must possess to achieve a particular excited state is equals the energy gap between the ground and excited state. However, not all frequencies of light are capable of being absorbed by molecular electrons. Energy associated with one wavelength of light of frequency ν , was explain by quantum theory with:

$$E = h\nu = \frac{hc}{\lambda}$$

Where E is the energy, h is Planck's constant, 6.625×10^{-27} erg/seconds, c the velocity of light, ν the vibration frequency (second^{-1}), and the λ wavelength. A condition for light of frequency ν to be absorbed by a molecule in its ground state is that the energy difference gap between the ground state and the excited state to which excitation occurs is exactly equal to $h\nu$.

$$E_e - E_g = h\nu$$

Where E_e and E_g are energies of the excited states and ground, respectively. But, if $E_e - E_g$ not equal to $h\nu$, absorption will not occur, and the molecule is said to be transparent to light of frequency ν ^[29]. Absorption process is extremely rapid, taking about $1 \text{ fs} = 10^{-15} \text{ s}$. Excitation can result in the molecule reaching any of the vibrational sub-levels associated with each electronic state. Since the energy is absorbed as discrete quanta, this should result in a series of distinct absorption bands. In the electronically excited state, the excited molecule may be vibrationally excited. The molecule will begin to vibrate with a frequency characteristic of the vibrationally excited state. Excess vibrational energy will be giving up in the form of infrared quanta or in the form of kinetic energy transmitted to other molecules which it collides. Within the lifetime of a few vibrations, which take about 10^{-14} - 10^{-12} s , the molecule will undergo vibrational relaxation, where the molecule will thermally descended to the lowest vibrational level of the electronically excited singlet state.

Kasha's rule state that emission will always occur from the lowest lying electronically excited singlet state $S_{1,V=0}$ ^[28]. Hence, from this point, the molecule may remain in the lowest vibrational level of the lowest excited singlet state for 10^{-10} - 10^{-7} s

followed by emission of visible or ultraviolet fluorescence. This fluorescence emission process was illustrated in Figure 2.1 below. The coloured circles represent the energy state of the fluorophore, where green depicts the normal energy level and red the maximum energy level.

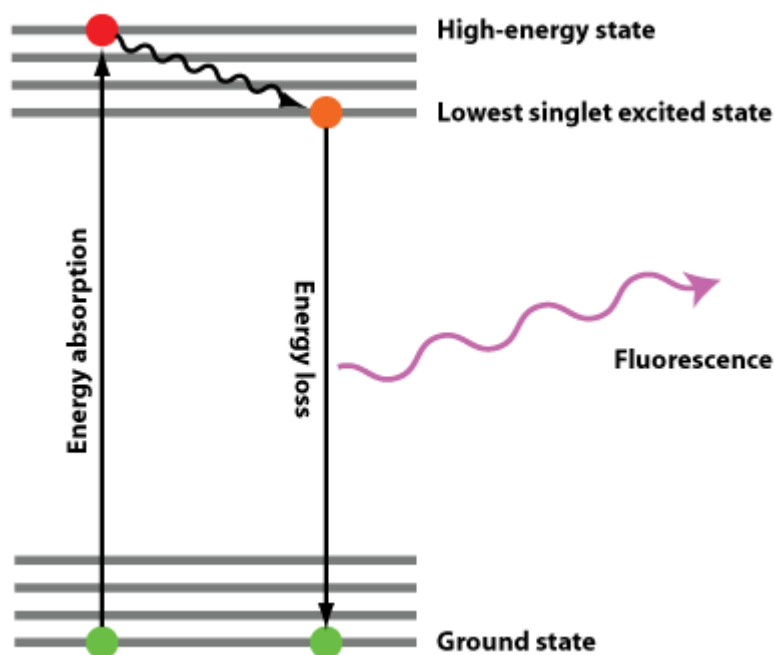


Figure 2.1: Schematic representation of an energy diagram (Jablonski diagram)

However, molecule also can return to ground state with many other de-excitation pathway, for example, internal conversion (i.e direct return to ground state without emission of fluorescence), molecule may move to excited triplet state (intersystem crossing) and then returned to the ground state by emission of photon (phosphorescence), intramolecular charge transfer and conformational change, and interactions in the excited state with other molecules also can compete with de-excitation. All these de-excitation pathways may compete with fluorescence emission if they take place on a time-scale comparable with the lifetime during which the molecules stay in the excited state.

The fluorescence normally observed is called *Stokes fluorescence*, where the re-emission photons are less energetic, and having a longer wavelength, this phenomenon was illustrated in Figure 2.2.

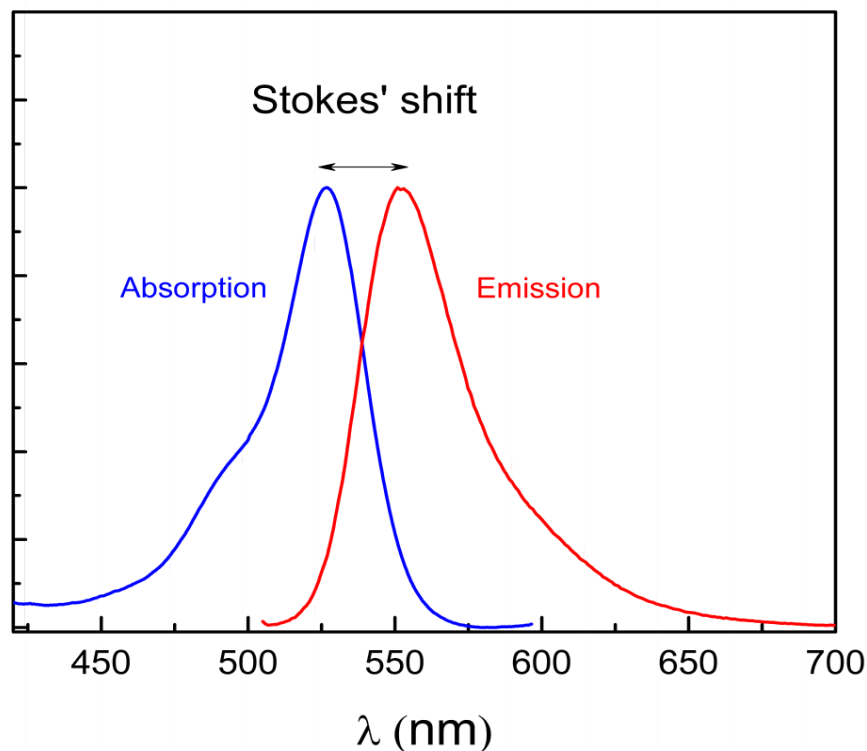


Figure 2.2: Stokes fluorescence diagram

This different in energy occur because, the loss of vibrational excitation energy of a molecule during the excitation/emission cycle, fluorescence cycle always occur at lower energy, such loss of photon energy is often called Stokes Shift^[28].

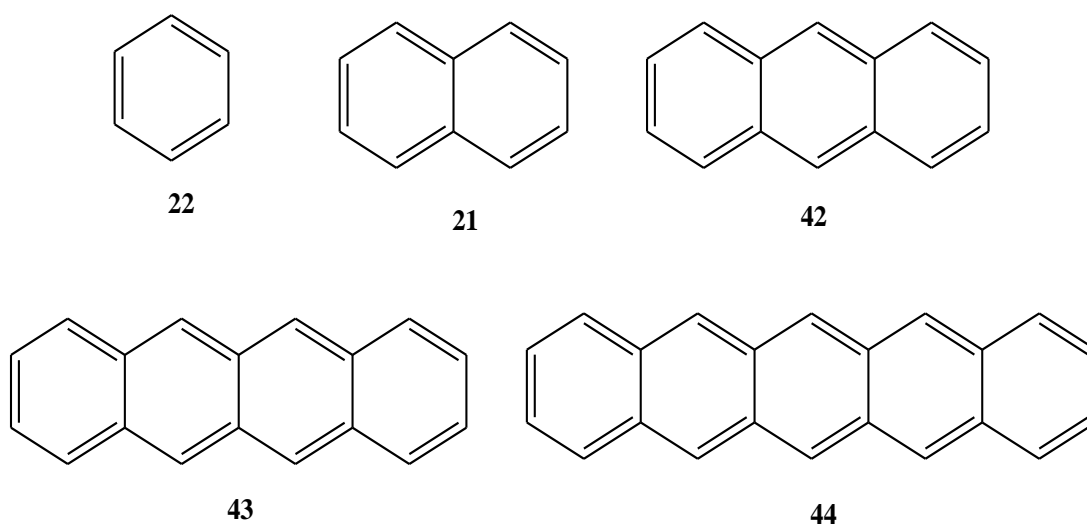
In situation, where emission at shorter wavelengths than that of excitation, it is known as *anti-Stokes fluorescence*. The additional energy at re-emission photons may come from thermal energy or be associated with a molecule with many highly populated vibrational energy levels. Furthermore, when re-emission of photons have the same energy as the absorbed photons, it is called *resonance fluorescence*. This situation never

observed in solution, but occurs in solids and gases and is the basis of atomic fluorescence.

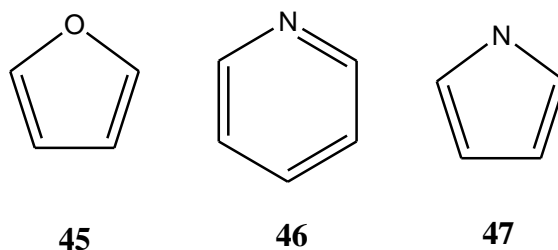
2.2 Factors that effects the fluorescence

2.2.1 Effects of molecular structure to fluorescence

The fluorescence of a molecule is dependent upon the structure and environment of the molecule in which it is situated. Most fluorescent compounds are organic molecules, and some of them are inorganic compounds. Many fluorescent compounds are aromatic. Generally, an increase in the degree of conjugation leads to a shift of the absorption and fluorescence spectra to longer wavelengths and the quantum yield. This is believed, due to the presence of low energy π - π^* transition. This rule is illustrated by the series of linear aromatic hydrocarbons benzene (**22**), naphthalene (**21**) fluoresce in ultraviolet, while anthracene (**42**), naphthacene (**43**) and pentacene (**44**) emit fluorescence in the blue, green, and red respectively.



Although luminescence best observed in compound with π bonds, but some heterocyclic aromatic rings compound do not show fluorescence. This include furan (**45**), pyridine (**46**), and pyrrole (**47**).



The relatively low fluorescence quantum yields in this compound is largely believed to be due to existence of a low lying $n-\pi^*$ transitions. Because of this low lying transition, excited e will rapidly converts to the triplet state and this will prevent fluorescence. The higher the atomic weight of the halogen in aromatic ring, and a subsequent increase in phosphorescence observed. However, by fusing a phenyl ring to any of the above molecules, this can increase the possibility of $\pi-\pi^*$ transitions, thus this can increase the fluorescence quantum efficiency.

Furthermore, most unsubstituted, nonheterocyclic aromatic compounds will show favourable fluorescence quantum yields, substitution to the parent molecule can have a significant effect on fluorescent quantum yield, ϕ_f . As an example, substitution with electron donating groups will induces an increase in the molar absorption and fluorescence spectra^[30-31]. On the other hand, the presence of electron withdrawing groups, will decrease the fluorescence quantum yield, ϕ_f ^{[25][32]}.

2.2.2 Environmental effect

2.2.2.1 Influence of the solvent

Solvents influence electronic spectra primarily through their electrostatic properties. Solvents can interact with solute molecules in number of way, it may be dipole-dipole, dipole-induced dipole, induced dipole-induced dipole or hydrogen bonding, depending upon the structures of solute and solvent.

In solution, solvent molecules surrounding the ground state fluorophore have dipole moments that can interact with the dipole moment of the fluorophore, in order to be the

most stable solvent configuration for the ground state electronic distribution of the solute.

When a molecule absorbs a photon, the light absorption alters the electronic distribution of the solute, thus, the electronic dipole moment of the electronically excited molecule becomes different from that of the molecule in its ground state. As a result, this induces a rearrangement of surrounding solvent molecules.

However, during excitation of a fluorophore, the molecule takes shorter timeframe to excite to a higher electronic energy level than it takes for fluorophore and solvent molecules to re-orient themselves within the solvent-solute interaction environment, as dictated by Frank-Condon principle.

After metastable excited state achieved by fluorophore at first excited singlet state (S_1), excess vibrational energy is rapidly lost to surrounding as the system slowly relaxes through reorientation of fluorophore's solvation envelope until "equilibrium" excited state achieved. Emission from this state, forming Frank Condon ground state. Follow by solvent relaxation, forming the equilibrium ground state. Figure 2.3 illustrates the Franck-Condon principle applied to solvation.

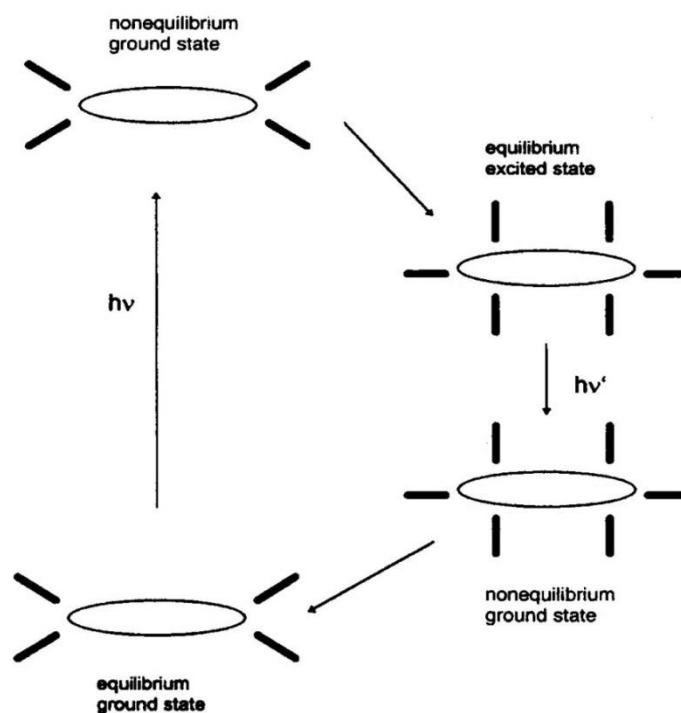


Figure 2.3: Schematic representation of equilibrium and Franck-Condon (F-C) electronic states.

From the diagram, it was shown the solvent was change due to excitation or emission. Solvent and solute molecules in various Franck-Condon states are represented by solid lines and ovals, respectively. If the solvent and solute, either one is polar and another one is nonpolar or if both are nonpolar, in this case, the polarization term that described the solvent-solute interaction is induced dipole-induced dipole or dipole-induced dipole. Thus, no interaction strain occurs, therefore the Franck-Condon and equilibrium states are nearly the same. Furthermore, the frequency shifts in absorption and emission are predicted to be the same.

When the solvent and solute are both polar, the situation in fluorescence is more complicated. If the solute molecules become more polar in the excited state, there will be greater electrostatic stabilization of electronically excited state, relative to the ground state. The solvent relaxation introduces an additional red shift to the Stokes shift of the fluorophore. Hence, fluorescence emission spectra of fluorophores in more polar

solvents tend to show bathochromic shift, this type of behaviour is characteristic of most $\pi - \pi^*$ and intramolecular absorption band.

Absorption transitions of the $n-\pi^*$ type is usually more affected by hydrogen bonding solvents because of the involvement of unshared valence electron pairs and intramolecular charge-transfer transitions.

If a nonbonding pair on a solute molecule is coordinated by a hydrogen atom of the solvent, the hydrogen-bonding interaction lowers the energy of the ground state as well as the n, π^* state of the solute. However, as molecule has two electrons in the nonbonding orbital and only has one at excited state, the stabilization of the ground state is greater. As a result, increasing hydrogen-bond donor bond capacity, higher the energy of $n-\pi^*$ absorptions needed. Therefore, the spectra shift will show hypsochromic shift.

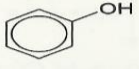
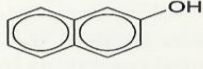
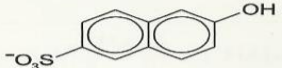
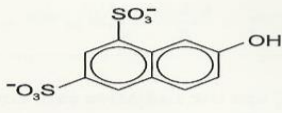
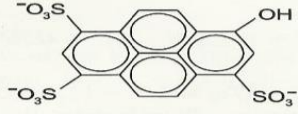

2.2.2.2 Influence of pH

The acidic or basic properties of a molecule that absorbs light are not the same in the ground state and in the excited state. One of the possible causes of this observation is electron distributions of acids and bases in ground state are different than in excited state. As a result, the degree of acidity or basicity may be very different for the same molecule in S_0 and S_1 , as reflected by the respective equilibrium constants pK_a and pK_a^* . Normally, only functional groups which bonded directly to aromatic ring will experience changes in charge distribution sufficient to be able to detect the differences between pK_a and pK_a^* .

In a molecule which have electron-donating groups, excitation from S_0 to S_1 state result in the movement of lone electron pairs transferred to the lowest lying π^* orbitals of the aromatic system. Upon excitation, the electronic charge density at these groups decrease and as a result, a proton may be more readily to lose from or with more

difficulty added to the group in S_1 state than in S_0 . So that, the pK_a^* of this group in excited state, is much lower than the pK_a in the ground state. Table 2.1 shows pK_a^* and pK_a reading of some molecules which attach to electron-donating groups.

Table 2.1: pK_a and pK_a^* reading of molecules attach to electron-donating group^[25]

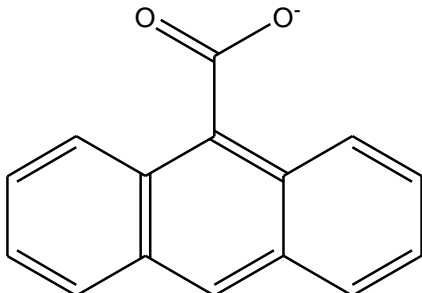
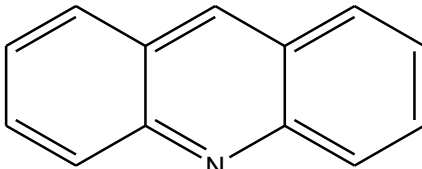
| | | COMPOUND | FORMULA | pK | pK^* |
|-----------------------------|--|---|--|------|--------|
| EXCITED-STATE DEPROTONATION | $\text{ArOH} \xrightarrow{-H^+} \text{ArO}^-$ | phenol |  | 10.6 | 3.6 |
| | | 2-naphthol |  | 9.3 | 2.8 |
| | | 2-naphthol-6-sulfonate |  | 9.12 | 1.66 |
| | | 2-naphthol-6,8-disulfonate |  | 9.3 | <1 |
| | | 8-hydroxypyrene-1,3,6-trisulfonate (pyranine) |  | 7.7 | 1.3 |
| | $\text{ArNH}_2 \xrightarrow{-H^+} \text{ArNH}^-$ | 2-naphthylamine |  | 7.1 | 12.2 |

In molecules containing electron donor groups, excitation will results in the movement of electronic charge away from electron donating group. Hence, for these molecules, characteristic of excitation from the S_0 to the S_1 state, is inhibited by protonation and facilitated by dissociation. This will increase the energy difference between S_0 and S_1 in the conjugate species having the higher state of protonation. Therefore, the longest wavelength absorption and fluorescence bands of these molecules shift to shorter wavelengths upon protonation and to longer wavelengths upon dissociation.

In molecules containing electron-withdrawing group, as excitation may trigger a photo-induced proton transfer, then, the basic character of a proton acceptor group (e. g. heterocyclic nitrogen atom) can be enhanced upon excitation, so that the pK_a^* of this

group in the excited state is much higher than the pK_a in the ground state. These were shown in Table 2.2 below:

Table 2.2: pK_a and pK_a^* reading of molecules attach to electron-withdrawing group^[25]

| Excited-state protonation | Compounds | pK_a | pK_a^* |
|---|--|--------|----------|
| $\text{ArCO}_2^- \xrightarrow{+\text{H}^+} \text{ArCO}_2\text{H}$ |  <p>anthracene-9-carboxylate</p> | 3.7 | 6.9 |
| $\text{ArN} \xrightarrow{+\text{H}^+} \text{ArNH}^+$ |  <p>acridine</p> | 5.5 | 10.6 |

Moreover, in a molecule containing an electron-withdrawing group, excitation will results in the movement of electronic charge to the electron withdrawing group. Consequently, S_1 state will be stabilize to a greater degree than S_0 state by protonation at the electron withdrawing group. Thus, the spectra will shift to the longest wavelength

absorption band and the fluorescence spectrum to longer wavelengths upon protonation and to shorter wavelengths upon dissociation, this is related to the increase in basicity and decrease in acidity upon going from the ground state to the lowest excited singlet state.

2.2.2.3 Influence of concentration

At low concentrations of the fluorophore, concentration is proportional with intensity of fluorescence, as more light is absorbed. However, at very high concentration, the linearity between absorbance and concentration appears to break down. This, phenomenon is known as concentration quenching.

In theory, the intensity of measured fluorescence (I_f) is proportional to the amount of light absorbed by the specimen (I_a), the quantum efficiency of the fluorophore (ϕ), and optical instrumental factors, represented by a constant (r). The intensity of fluorescence can be derived as follows:

$$I_f = rI_a\phi$$

According to the Beer-Lambert exponential law, the amount of light absorbed (I_a) is determined by the amount of light incident on the specimen (I_o) and the extinction coefficient (ϵ ; a constant which expresses the ability of the fluorophore to absorb light), concentration (c) and thickness (d) of the specimen. These are related by the equation:

$$\text{Log } I_a = \epsilon cd \times \log I_o$$

It is convenient to denote I_f / I_o the emission intensity by a symbol, F . Under normal conditions, where the concentration of the fluorophore is not excessive, the exponential relationship can be simplified to:

$$F=2.3 \epsilon cd$$

Theory states that, the emitted fluorescence is directly proportional to the concentration of fluorophore. As fluorescence is not really linearly related to concentration experimentally, thus, if the concentration of the fluorophore is high, the relationship become nonlinear and the closer approximation derived as follow:

$$F=2.3 \epsilon cd(1-1.15 \epsilon cd)$$

Where, F is denoted by the emission intensity, ϵ is constant which express the ability of the fluorophore to absorb light, c is concentration and d is the thickness of the specimen.

There is number of ways high concentration of absorbing or luminescing species may disturb the interpretation of molecular electronic spectra. Some arise from the optical and electronic responses of the spectrophotometric instrumentation, and others were related with solute-solute interaction^[29]. As the concentration of solutions increase, the absorbance may appear invariant with concentration due to low level of transmitted light detected by detector, and the increased importance of random noise in determining the measured signal. However, at well concentration, below the instrumental limits of absorbance measurement, the nonlinearity of absorbance with concentration maybe due to a chemical phenomenon in the ground electronic state.

2.3 Instrumentation of fluorescence spectroscopy

There are three basic items in all fluorescence instruments: a source of light for an example, tungsten-halogen lamp and mercury lamp, a sample holder and a detector. Furthermore, to be of analytical use, the incident radiation wavelength needs to be selectable, and this is provided by a monochromator. In addition, the detector signal also

substantial to have precise manipulation and presentation. Figure 2.4 shows the fluorimeter schematic:

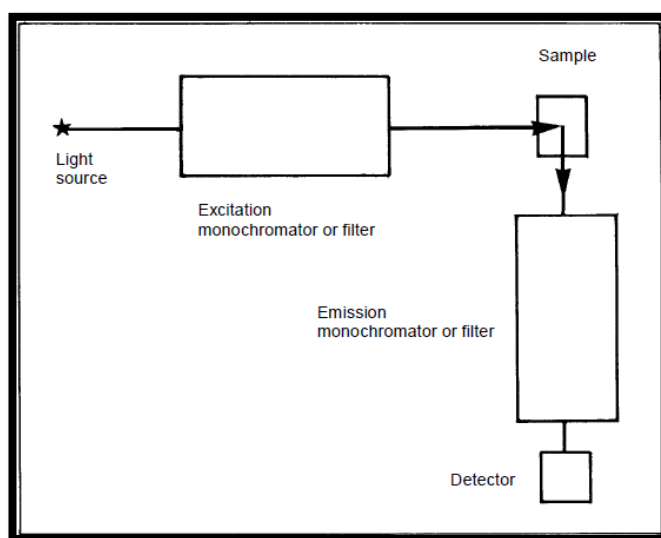


Figure 2.4: Fluorimeter schematic

2.3.1 Light sources

Fluorescence signal is directly proportional to the intensity of the incident light. Therefore, one of the requirements of good spectrofluorometer is a high-power light source. There's several requirements need to be met by a fluorescence excitation light source. These include constant output and ideally a uniform spectral emission.

There are several types of light source available that can be employed in the fluorescence spectrometer such as halogen lamps, xenon lamps, mercury vapour lamps, and tungsten filament lamps^[29].

At present, the most commonly used light source for a steady-state spectrofluorometer is a high-pressure xenon (Xe) arc lamp. These lamps provide a continuous light output from 250 to 700 nm, see Figure 2.5.

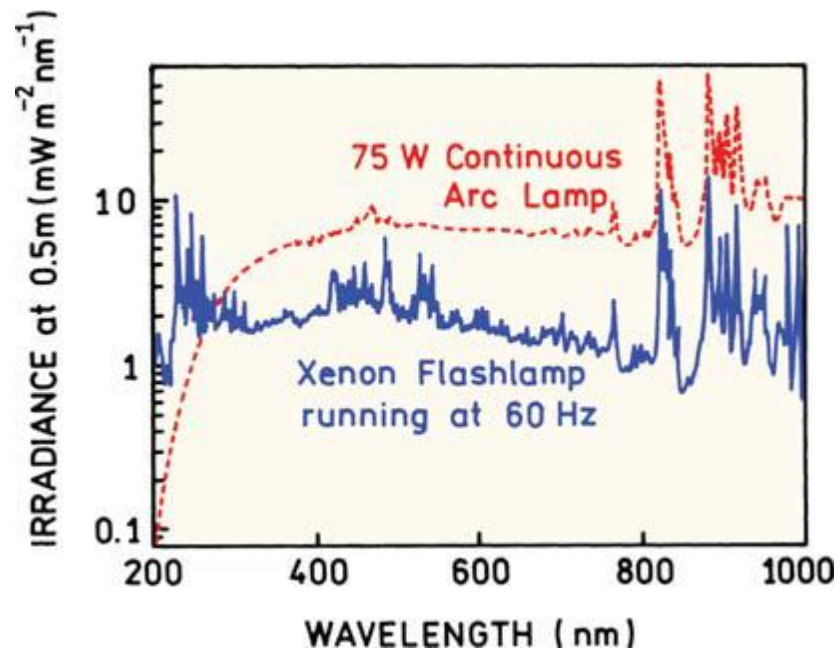


Figure 2.5: Spectral output of a continuous xenon arc lamp and a xenon flash lamp

With a number of sharp lines around 450 nm and above 800 nm that are caused by the excited xenon atoms. The output intensity drops rapidly below 280 nm. These were illustrated in Figure 2.6 below:

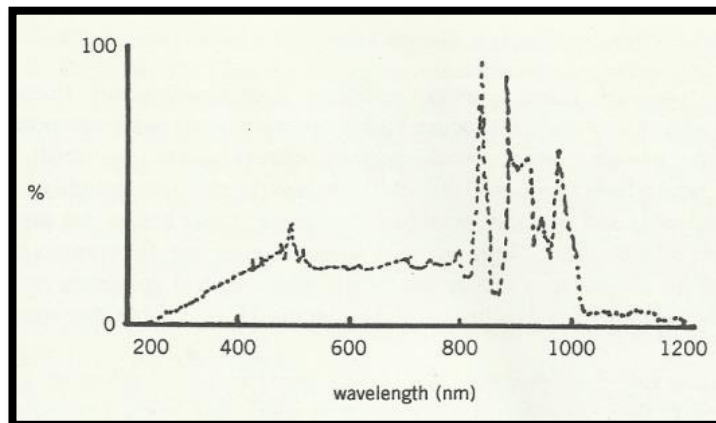


Figure 2.6: Output wavelength distribution of a xenon arc.

Many Xe lamps are classified as being ozone-free, meaning that, no ozone generated at the surrounding air during their operation^[27]. However, a common disadvantage

feature of the xenon arc lamp is the need to trigger the arc at high voltages, followed by operation at high currents.

2.3.2 Monochromator

Monochromation, or production of individual wavelengths from polychromatic or white light source, is usually accomplished by dispersion of light by using prisms or diffraction gratings. In the past, prisms have been widely used. Nowadays, diffraction grating monochromation devices are commonly used rather than prisms in most spectrofluorometer.

A typical monochromator consists of a diffraction grating(dispersing element), slits, and spherical mirrors. Figure 2.7 below shows a typical monochromator design.

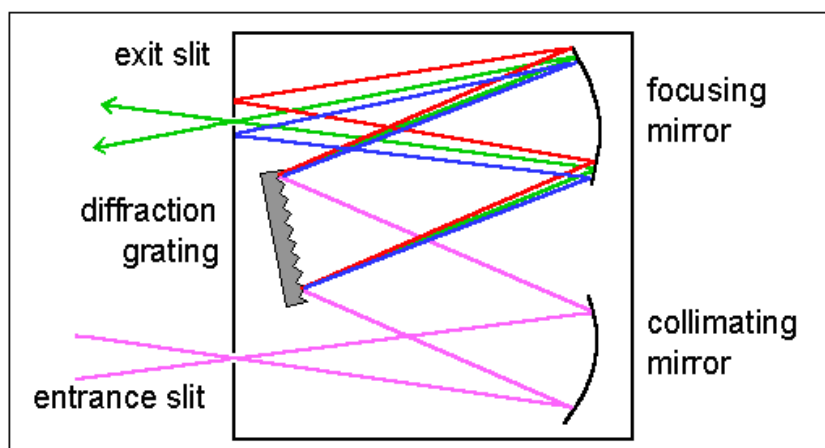


Figure 2.7: A typical monochromator elements.

The performance specifications of monochromator cover dispersion, efficiency, and stray light levels. A typical monochromator will have both an entrance and exit slit. The slit widths are generally variable, light intensity that passes through a monochromator is approximately proportional to the square of the slit width.

There are two types of gratings that a monochromator can have, it is planar grating or concave grating. The differences between planar gratings and concave gratings are, planar gratings are usually produced mechanically while concave gratings are usually produced by holographic and photoresist methods. The image of planar grating and concave was shown in Figure 2.8:

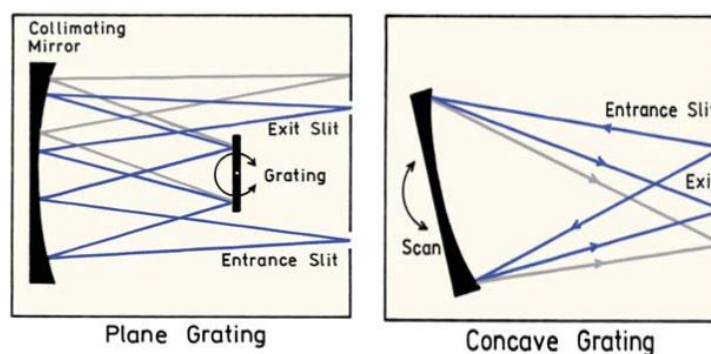


Figure 2.8: Image of plane grating and concave grating

Usually, holographic gratings are usually preferable for fluorescence spectroscopy. This is because, a concave grating can serve as diffraction and focusing element, resulting on one reflecting surfaces, instead of three reflecting surfaces. In addition, concave gratings can have fewer reflecting surfaces, lower stray light and can be more efficient.

In monochromator, the position of slit and mirror remain fixed, but the angle of gratings was rotated in order to get a particular selected wavelength that passed through the monochromator.

2.3.3 Sample holder

The configuration of the sample and the design of the sample holder play an important role in determining the quality of the fluorescence measurement. In fluorescence measurement, one has to cope with a substantial background of the

excitation intensity to avoid from situation where unwanted light being measured along with the fluorescence signal.

In absorption spectroscopy, normally a cuvette is placed at the incident beam. The fluorescence is given off equally in all directions and can be collect in many possible ways. It is possible to use a simple $1 \times 1 \text{ cm}^2$ and a 180° geometry, the arrangement were shown in Figure 2.9 .

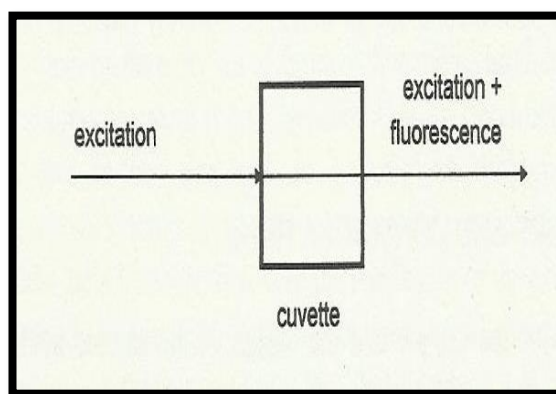


Figure 2.9: 180° excitation beam geometry

However, in this arrangement, the detector not only will detect the fluorescence from the sample but also all the excitation light that has not been absorbed by the sample, in consequence, the measurement will suffer from the high background light. By using 90° geometry, this situation can be avoided. Even so, it is not able to reduce the Tydal, Rayleigh, and Raman scattering. This measuring condition is widely practiced in analytical procedures.

In this arrangement, the fluorescence was measured at the right angle to the incident excitation beam. Often, a mirror is placed at the side facing the excitation beam to enhance the fluorescence. The arrangement is illustrated in the Figure 2.10:

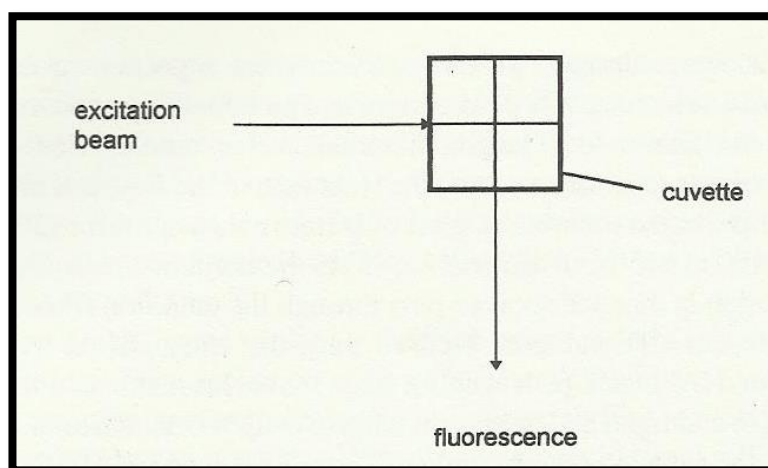


Figure 2.10: 90° excitation beam geometry

In addition, for a highly concentrate samples and those which related to the Tyndall scattering, those problems can be minimized by the use of front-face excitation. Figure 2.11 shows the arrangement of this collector method:

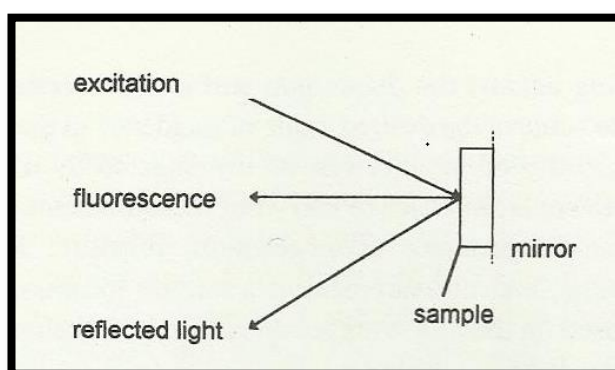


Figure 2.11: Front-face excitation beam geometry

In this case, both the incident radiation beam and the fluorescence emission light are facing sample holder. In some instruments, few collecting method were provided, it depend upon the characteristic of the sample to decide which collector method to be use.

2.3.4 Cuvette

Most of fluorescence assays are carried out in solution. The final measurement being made upon the sample contained in a cuvette or in a flowcell. A cuvette is a small tube of circular, square or rectangular, sealed at one end, made of plastic, glass, quartz, and designed to hold material that will transmit both incident and emitted light. In fluorescence spectroscopy, cuvettes to be used must be clear on all four sides, in order to measure fluorescence at a right angle to the beam path to avoid high background light.

Disposable plastic cuvettes are increasingly popular and often used in fast spectroscopic assays, where speed is more important than high accuracy. Moreover, they do not shatter when dropped and also their inexpensive makes them disposable. However, they tend to have considerable absorbance in the ultraviolet region. Cuvettes with different material have different optical properties. Figure 2.12 below shows absorbance spectra for cuvettes of different composition, where each cuvette contains water:

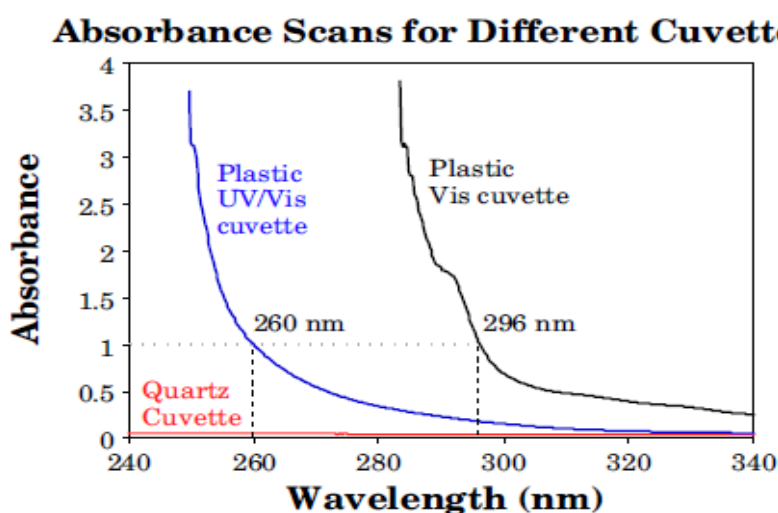


Figure 2.12: Graph of absorbance spectra of water in different cuvettes

From the graph, it is obvious that only the quartz cuvette is useful below about 260 nm. Although quartz cuvettes can have absorbance in the far ultraviolet(below ~250 nm) region, but they are relatively fragile and expensive.

Among the issue with cuvettes is that, some cuvettes do not show same path length in all orientation. In a spectrometer, if a cuvette has a 1 cm path length were inserted into an instrument in a different orientation, the path length would consider shorter than 1 cm, about 0.3 cm. Figure 2.13 illustrated the situation:

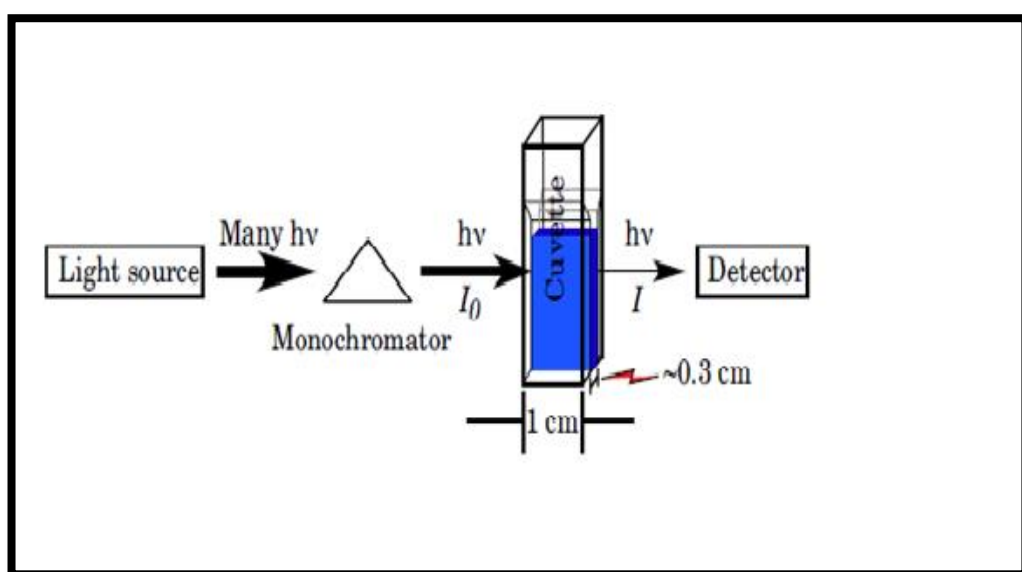


Figure 2.13: The structure of cuvette that shows different path length in different orientation

In a spectrophotometer, if a cuvette has a 1 cm path length was inserted into an instrument in a different orientation, the path length would consider shorter than 1 cm, about 0.3 cm. Since the modern deviation of Beer-Lambert law stated that absorbance is directly proportional to the path length. Where^[33]:

$$A = \epsilon bc$$

Beer's law provides a relationship among absorbance, molar absorptivity (ϵ), path length (b) and molar concentration (c). When the path length decrease, the absorbance will also be smaller than expected for a sample of a given concentration.

In addition, glassware and cells used for fluorimetric analysis also should be carefully cleaned. Preferably by boiling in 50 % nitric acid followed by rinsing it in distilled water in order to avoid any impurities.

2.3.5 Detector

There are several types of detector used in fluorescence spectroscopy. Two types of detector that commonly being use are multichannel and single-channel. Detectors were classified to their type base on their capabilities. The multichannel detectors are able to measure the intensity on the same time also the wavelength, and some even offer the measurement of the spatial differences along the slit's length. On the contrary, the single-channel detectors are capable to make measurements at a single point of the radiant spectrum at a given time. The difference types of detector have both advantage and disadvantage.

One of the most commonly used single-channel detector in fluorescence spectroscopy is the photomultiplier tube detector, or more commonly known as the PMT. A PMT is best regarded as a current source. The current is depends on the light intensity. A PMT, by responding to single photons, and the pulses can be detected as an average signal or counted as individual photons.

A PMT vacuum tube consists of a photocathode and a series of dynodes which are amplification stages in an evacuated glass enclosure. Figure 2.14 below shows the schematic of PMT:

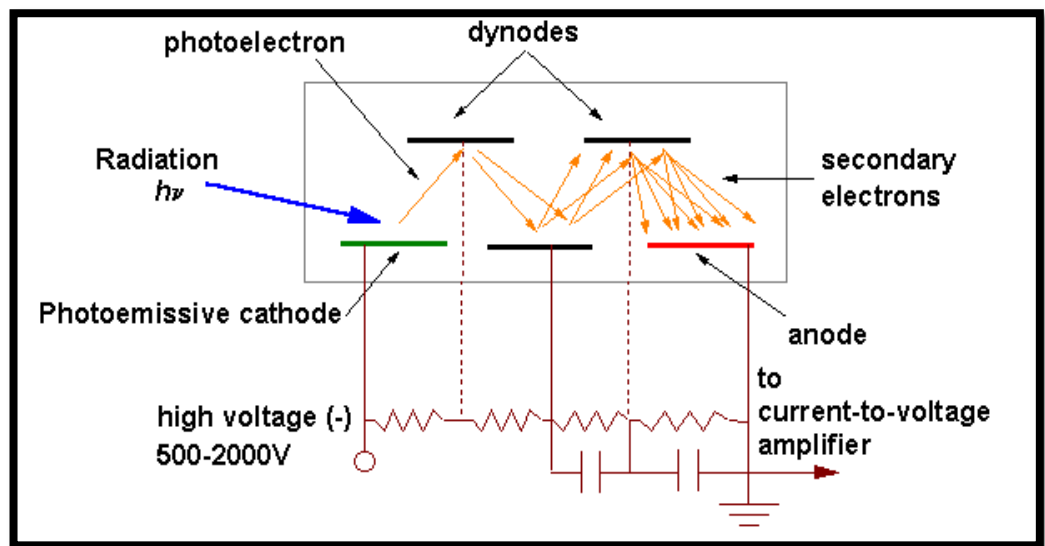


Figure 2.14: Schematic diagram of PMT

Radiant photon that collides the photoemissive cathode surface emits electrons as a result of photoelectric effect.

In practice, the photocathode is operated at a high negative potential, of -1000 to -2000 volts. The dynodes are also held at negative potential that decrease toward zero along the chain, and a photocathode and the first dynode potential is generally fixed at a constant voltage by a Zener diode, typically -50 to -200 volts. This potential difference caused an ejected photoelectron is accelerated toward the first dynode. Upon collision with the first dynode, several more electrons are set free and move toward the second dynode. The number of additional electrons depends on the number of dynodes and the accelerating voltage. This process continues down the dynode chain until the burst of electrons finally arrives at the anode, where amplified signal collected can be measured. The whole process occurs rapidly at the nanosecond time domain.

2.4 Objectives of the project

The main objective of this study is first to synthesize a series of phenoxy and naphthalenyloxy derivatives of pyrazines. The compound obtained then characterized through:

- i. ^1H Nuclear Magnetic Resonance Spectroscopy
- ii. ^{13}C Nuclear Magnetic Resonance Spectroscopy
- iii. Gas Chromatography-Mass Spectrometry
- iv. Infrared Spectroscopy

The second objective is to study the fluorescence characteristic of all compounds prepared with respect to:

- i. Solvents:
 - Ethyl acetate
 - Hexane
 - Ethanol
 - Tetrahydrofuran
- ii. Concentrations
- iii. Substituents
- iv. pH
- v. Effect of Oxygen.

Extra work was done on synthesizing 2-*N*-piperidinopyrazines (**62**) and the fluorescence characteristic was studied.

CHAPTER 3: RESULTS AND DISCUSSION

3.1 Synthesis of the compounds studied

All phenoxy compounds were synthesized through Williamson Ether Synthesis method. This method was developed by Alexander Williamson in 1850. This reaction involves the reaction of an alkoxide ion with primary alkyl halide via S_N2 reaction under basic condition to create ether. Reaction of alkoxide ion with secondary alkyl halides will produce low yields, due to competing elimination and with tertiary halides, only elimination products will produce. In general about this method, we combine R-group from alcohol and R-group from alkyl halide and we joint them to a bridging oxygen. In this study, through this method, there were two different reagents that should be considered and one of them is alcohol. Alcohols are weak acid, thus under adequate basic environment, in the presence of KOH, hydroxyl proton from phenol and naphthalenyloxy derivatives were removed creating alkoxide ions. Alkoxide ions are strong bases, they will attack electrophile side that they can get to. In this study, alkyl halide used were pyrazine derivatives, i.e, 2-chloropyrazine (**48**), 5-chloropyrazine-2-carboxylic acid methyl ester (**63**) and 3-chloro-2,5-dimethylpyrazine (**68**). All these compounds are strongly electron-poor in nature, and enable it to add nucleophilic reagent easily. Furthermore, as we have an alkyl halide, it is susceptible to nucleophilic attack, that particular reagent are prime to be attack by strong nucleophile of alkoxide ions, we can expect to make a Williamson ether product by S_N2 reaction. Whereas, 2-*N*-piperidinopyrazine (**62**) was formed when piperidine (**61**), which is a strong nucleophile attack 2-chloropyrazine (**48**) at 2-position, which is susceptible to nucleophilic attack due to the presence of the adjacent electron-withdrawing nitrogen atom.

In this chapter, the synthesis of pyrazine derivatives will be discussed. Reaction equation of 2-chloropyrazine (**48**) with phenol derivatives, naphtols and piperidine (**61**) are shown in Figure 3.1 below:

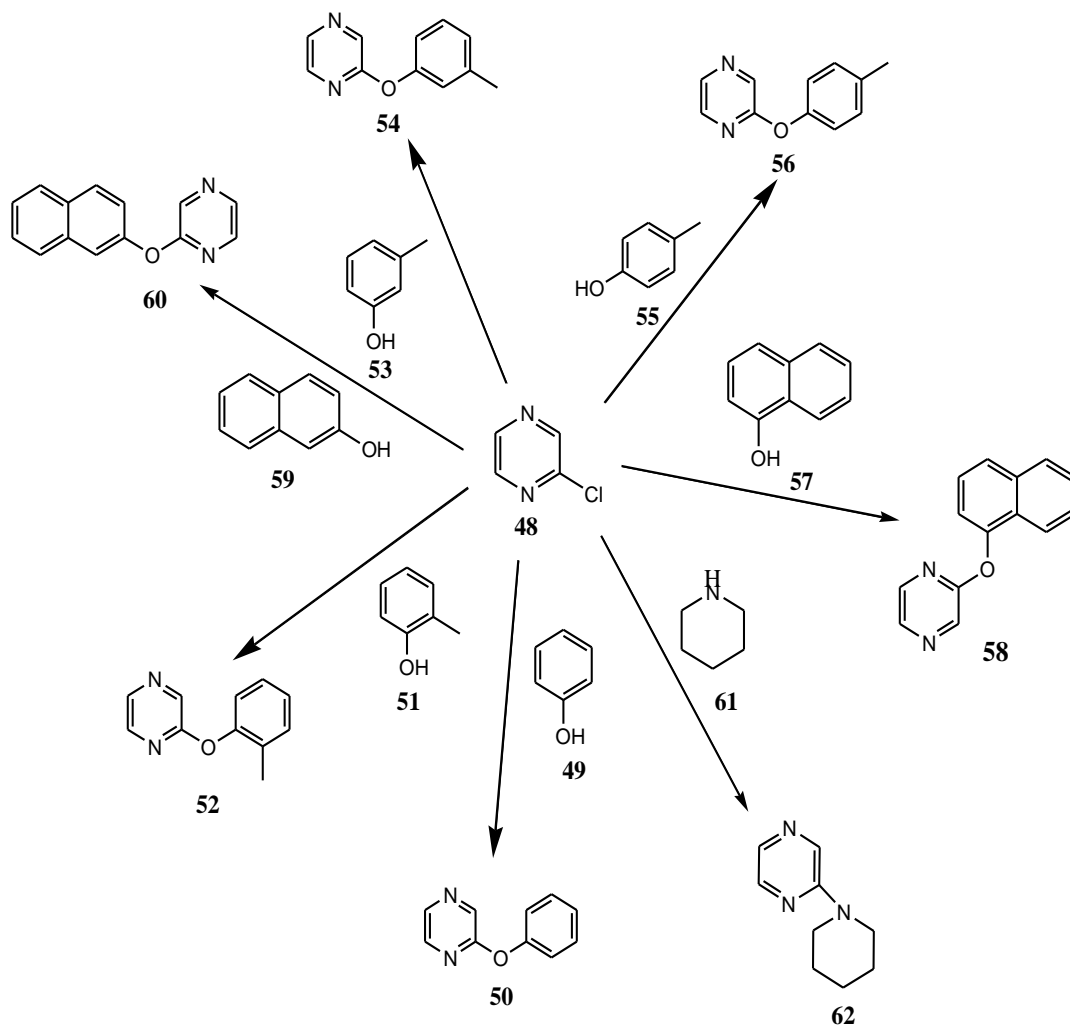


Figure 3.1: Reactions of 2-chloropyrazine (48**) with phenol derivatives, naphthols and piperidine (**61**)**

Reactions of 5-chloropyrazine-2-carboxylic acid methyl ester (**63**) with phenol (**49**), 3-nitrophenol (**64**) and 2-methylphenol (**53**) are shown in Figure 3.2 below:

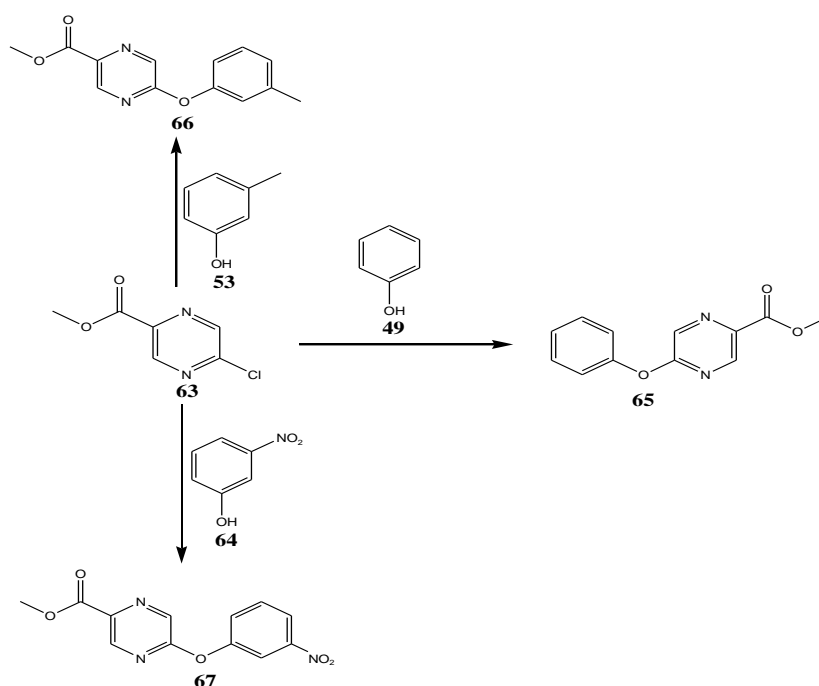


Figure 3.2: Reaction of 5-chloropyrazine-2-carboxylic acid methyl ester (63**) with phenol derivatives**

Reaction of 3-chloro-2,5-dimethylpyrazine (**68**) with phenol (**49**) is shown in Figure 3.3 below:

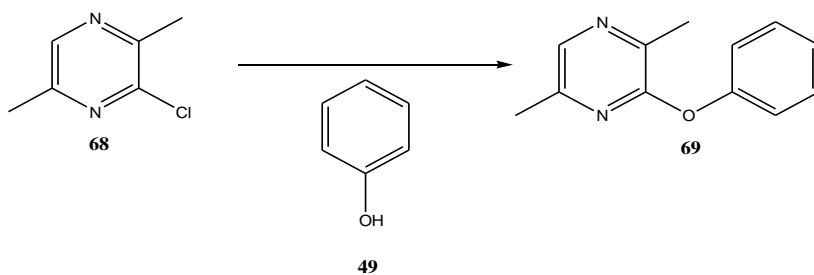


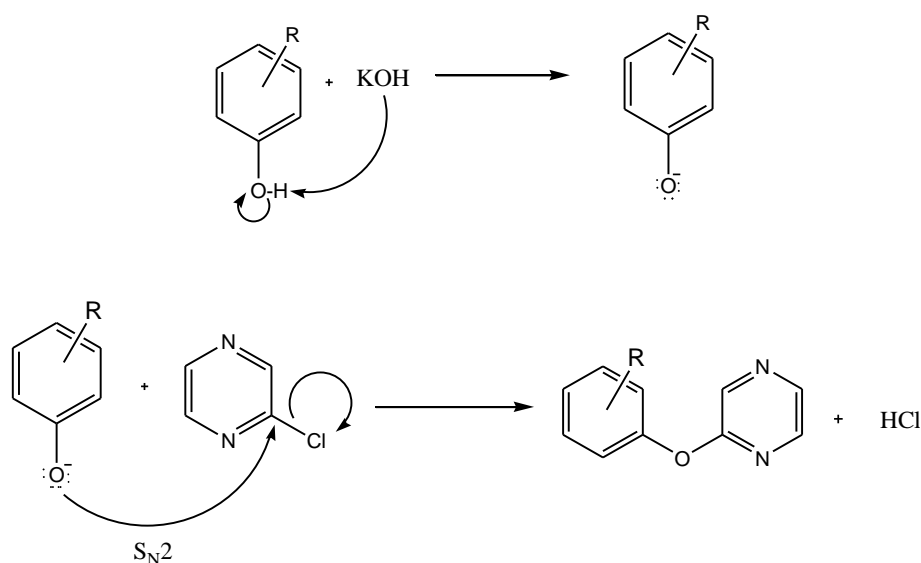
Figure 3.3: Reaction of 3-chloro-2,5-dimethylpyrazine (68**) with phenol (**49**)**

The structures of all compounds synthesized were confirmed by IR, ^1H NMR, ^{13}C NMR and GC-mass spectra. All related spectra are attached in appendix section. The details of synthesis process is described in Chapter five.

3.2 Synthesis of phenoxypyrazines

3.2.1 Reaction of 2-chloropyrazines (48) with various phenol derivatives

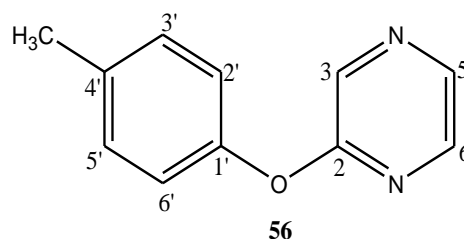
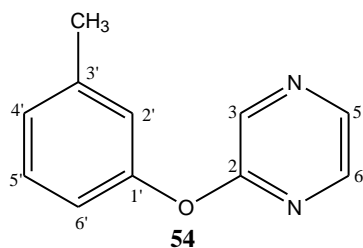
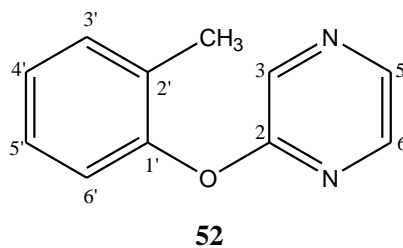
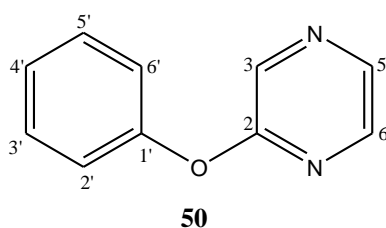
Reaction between 2-chloropyrazine (48) with phenol (49), *o*-cresol (51), *m*-cresol (53), *p*-cresol (55) and piperidine (61) gave 2-phenoxypyrazine (50), 2-*o*-toloxypyrazine (52), 2-*m*-toloxypyrazine (54), 2-*p*-toloxypyrazine (56) and 2-*N*-piperidinopyrazine (62) respectively. The reaction mechanism for formation of 2-phenoxypyrazine (50) is shown in Scheme 3.1 below:



R = phenol (49), *o*-cresol (51), *m*-cresol (53), *p*-cresol (55)

Scheme 3.1: Reaction mechanism of formation of 2-phenoxypyrazine (50)

2-Phenoxypyrazine (50) was obtained after phenol (51) was added to potassium hydroxide pellet in minimum volume of water, followed by heating until a dry white solid was formed. 2-Chloropyrazine (48) in THF was then added to the dry white solid, followed by reflux for 5 hours. The same procedure was used for the preparation of 2-(*o*-methyl)phenoxypyrazine (52), 2-(*m*-methyl)phenoxypyrazine (54), and 2-(*p*-methyl)phenoxypyrazine (56).



The infrared spectra of all compounds showed medium absorption intensity band between $1650\text{--}1550\text{ cm}^{-1}$ due to the presence of $\text{C}=\text{N}$ in pyrazine ring. Two absorption bands from weak to strong at $\sim 1600\text{ cm}^{-1}$ and between $1500\text{--}1430\text{ cm}^{-1}$ respectively, were assigned for the $\text{C}=\text{C}$ aromatic stretching vibrations in aromatic ring. Strong and sharp intensity bands observed between $1278\text{--}1281\text{ cm}^{-1}$ and $1006\text{--}1007\text{ cm}^{-1}$ were assigned to the $\text{C}\text{--}\text{O}$ stretching. Compound (**50**) showed medium and strong peaks at 696 cm^{-1} and 764 cm^{-1} respectively indicating a monosubstituted benzene ring. Whereas, compound (**52**) showed a strong absorption band at 747 cm^{-1} assigned to a benzene ring that has a substituent at *ortho* position. Besides, compound (**54**) showed two medium to strong peaks at 695 cm^{-1} and 752 cm^{-1} respectively, which represents a *meta* disubstituted benzene ring. Compound (**56**) on the other hand, showed a strong band at 841 cm^{-1} which was the characteristic of *para* disubstituted aromatic ring.

From the ^1H NMR spectra, all compounds showed similar peak in the region δ 8.41 to δ 8.01 which were attributed to H-6, H-3, and H-5 at the pyrazine ring. Compound (**50**) showed the presence of a phenyl group. A monosubstituted benzene ring showed three different kinds of protons. There were two triplet peaks detected at δ 7.42 with coupling constant of 7.6 Hz and at δ 7.24 with coupling constant of 7.12 Hz, assigned to H-3', H-5' and H-4' respectively. A doublet of doublet peak was observed at δ 7.15,

with coupling constant 1.2 Hz which was due to H-2' and H-6' of the benzene ring. For compound **(52)**, H-3' and H-4' showed multiplet at δ 7.17. Two doublet of doublet peaks were observed at δ 7.10 and δ 6.99 with coupling constant 1.2 Hz and 0.9 Hz due to H-3' and H-6' respectively. Compound **(54)** showed a triplet splitting at δ 7.30 with coupling constant 7.8 Hz representing H-5'. A peak at δ 7.06, a doublet splitting with coupling constant 7.6 Hz was observed due to H-6', a singlet peak at δ 6.97, which was assigned for H-2'. At δ 6.95, a doublet of doublet was observed with coupling constant 11 Hz which is attributed to H-4'. The ^1H NMR spectrum of **(56)** showed two doublet of doublet peaks at δ 7.08 and 6.94, with coupling constant 8.9 Hz. These two splittings were assigned to H-3', H-5' and H-2', H-6' respectively. A singlet peak was recorded for compound **(52)** at δ 2.11, **(54)** at δ 2.39 and **(56)** at δ 3.83. This was believed to be due to methyl group at benzene ring.

^{13}C NMR spectrum of compound **(50)** showed 8 peaks that indicated for 10 C atoms which consists of 2 quarternary carbons, and 8 methine carbons, which are in agreement with the corresponding molecular formula of 2-phenoxy pyrazine **(50)**. The spectrum of **(50)** showed peaks at δ 160.3 and δ 153.1 which were assigned to quarternary carbons on C-2 and C-1' of the pyrazine and the benzene ring respectively. In addition, signal at δ 141.1, δ 138.5 and δ 135.9 were assigned to C-6, C-5 and C-3 at the pyrazine ring, while, two signals at δ 129.9 and δ 121.3 were assigned to C-3'/C-5' and C-2'/C-6' respectively. The remaining signal at δ 125.5 was assigned to C-4'.

^{13}C NMR spectrum of compound **(52)**, 11 peaks were observed responded to 11 carbons in 2-*o*-phenoxy pyrazine **(52)**. At the most downfield region, there were two low intensity peaks at δ 160.2 and δ 151.2 attributed to C-2 and C-1' respectively. Another three methine carbons in pyrazine ring were observed at δ 141.3, δ 138.0, and δ 135.3 assigned to C-6, C-5, and C-3 respectively. Quarternary carbon at benzene ring

for *ortho* disubstituted methyl group was observed at δ 130.7 attributed to C-2'. All methine group at aromatic ring were detected at δ 131.6, δ 127.3, δ 125.9, and δ 121.7 corresponded to C-3', C-5', C-4', and C-6'. At the most upfield region, a peak was observed at δ 16.3 which was assigned to the carbon of methyl group of compound (**52**).

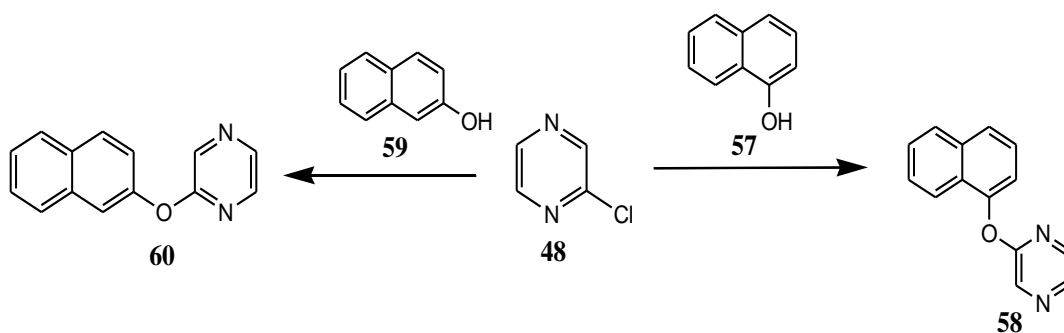
^{13}C NMR spectrum for 2-(*m*-methyl)phenoxy pyrazine (**54**) showed 11 peaks, which 3 of them are quarternary carbons, and 9 of them are methine carbons. At δ 160.4, δ 153.0, and δ 138.4 there were three quarternary carbons attributed to C-2, C-1' and C-3' respectively. All pyrazine ring carbons were observed at downfield region between δ 141.2 to δ 135.9 assigned to C-3, C-6, and C-5 due to the presence of two heteroatoms, that withdraw the electron density around the protons, thus, there is less shielding, so the chemical shift increases. All the benzene ring carbons appeared at the more upfield region, at δ 129.6, δ 126.3, δ 121.8, and δ 118.2 ascribed to C-6', C-2', C-5', and C-4' respectively. Methyl group carbon that attached at *meta* position of benzene ring was observed at δ 21.4.

^{13}C NMR spectrum of 2-*p*-tolyl oxy pyrazine (**56**) represented 9 peaks of carbons, 3 quarternary carbons and 6 methine carbon that indicated for 11 carbons in the compound (**56**). Two quarternary carbon atom that attached to the bridging oxygen between pyrazine ring and aryl group appeared in δ 160.5 and δ 154.0 due to C-2 and C-1' respectively. Methine carbon in pyrazine ring were observed at δ 141.2, δ 138.2, and δ 135.7 attributed to C-6, C-5, and C-3 respectively. Quarternary carbon substituted at para position of benzene ring was observed at δ 135.2 assigned to C-4'. There were four carbon atoms that appeared at two same chemical shifts, these were observed at δ 130.4 and δ 121.1 attributed to the C-3', C-5' and C-2', C-6' respectively, as the carbon nucleus have same electronic environment, thus it appeared at the same chemical shift. Methyl group of compound (**56**) was detected at δ 20.9.

The GC-mass spectrum of compound (**50**) displayed the $[M^+]$ peak at m/z 172 which is consistent with the molecular formula $C_{10}H_8N_2O$. On the other hand, (**52**), (**54**) and (**56**) showed a base peak at m/z 186 which corresponded to $C_{11}H_{10}N_2O$.

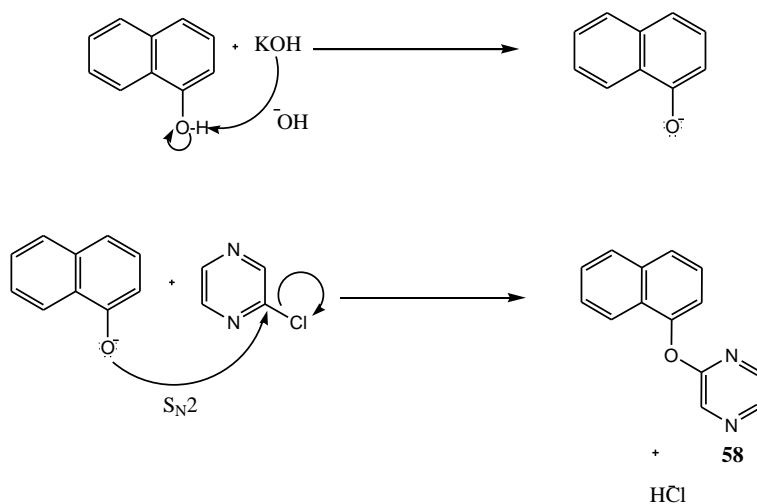
3.2.2 Reaction of 2-chloropyrazines (**48**) with 1-naphtol (**57**) and 2-naphtol (**59**)

The formation of naphthalenyloxy pyrazine derivatives for this study were shown in scheme 3.2



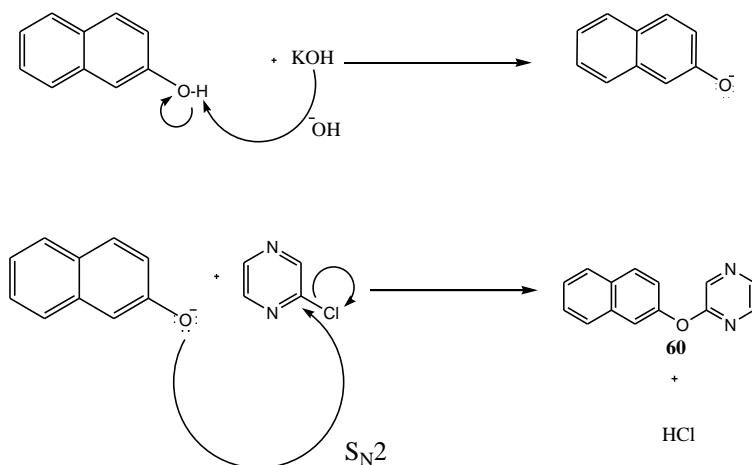
Scheme 3.2: Reaction of 2-chloropyrazine (48**) with naphthalene derivatives.**

The reaction mechanism of 2-chloropyrazine (**48**) with 1-naphtol (**57**) is shown in Scheme 3.3



Scheme 3.3: Reaction mechanism of formation of 2-(naphthalene-1-yloxy)pyrazine (58**)**

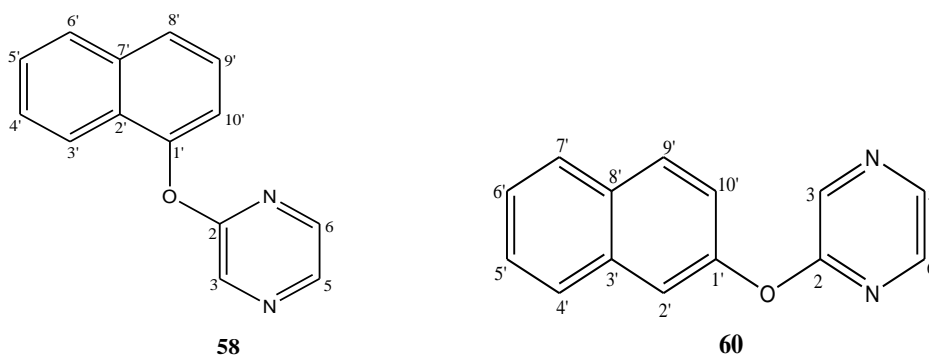
The reaction mechanism of 2-chloropyrazine (**48**) with 2-naphtol (**59**) is shown in Scheme 3.4



Scheme 3.4: Reaction mechanism of formation of 2-(naphthalene-2-yloxy)-pyrazine (60)

Reaction of 2-chloropyrazine (**48**) with 1-naphthol (**57**) yielded 66 % pure product of 2-naphthalen-1-yloxy pyrazine (**58**) after recrystallization from ethyl acetate and hexane in 1:10 ratio. While 2-chloropyrazine (**48**) react with 2-naphthol (**59**) yielded 74 % pure product of 2-naphthalen-2-yloxy pyrazine (**60**). The GC-Mass spectra of (**58**) and (**60**) gave molecular formula ion peaks at m/z 222.00 [M^+] which is agreeable with calculated mass of molecular formula $C_{14}H_{10}N_2O$.

The IR spectrum of compound (**58**) showed absorption bands similar to that of compound (**50**), (**52**), (**54**) and (**56**).



1H NMR spectra of compound (**58**) and (**60**) showed similar spectrum between the range of δ 8.56 to δ 8.09 which represent H-3, H-5, and H-6 of pyrazine ring. For compound (**58**), two doublet peaks were observed at δ 7.93 ($J=9.6$ Hz) and δ 7.80

($J=8.3$ Hz) ascribed to H-6', H-8' and H-3', respectively. A multiplet peak observed at δ 7.52 represent H-9', H-5' and H-4' of naphthalene ring. A doublet of doublet peak was observed at δ 7.29 with coupling constant 1.0 Hz due to H-10'. For compound (**60**), two doublet peaks were observed at δ 7.90 ($J=8.9$ Hz) and δ 7.62 ($J=2.3$ Hz) which are attributed to H-9' and H-2'. Furthermore, there is two doublet of doublet peaks observed at δ 7.80 ($J=7.4$ Hz) and δ 7.29 ($J=2.4$ Hz) which are attributed to H-7', H-4' and H-10' respectively. The remaining 2 H, which is H-5' and H-6' were represented by multiplet peak at δ 7.45.

^{13}C NMR spectrum of both compounds (**58**) and (**60**) showed 14 signals which are in agreement with 14 C of 2-naphthalen-1-yloxy pyrazine (**58**) and 2-naphthalen-2-yloxy pyrazine (**60**). Two peaks at relatively low intensity between the range of δ 160.8 to 149.0 which corresponded to quarternary carbon of C-2 and C-1' for (**58**) and (**60**). Besides that, both compounds showed methine carbon between the range of δ 141.4 to δ 135.0 which are assigned to C-6, C-5 and C-3 of pyrazine ring. Compound (**58**), showed two low intensity signals at δ 135.0 and δ 127.2 due to quarternary C-7' and C-2' in naphthalene ring. Signal at δ 128.1 was assigned to C-6'. There are two close signals at δ 126.6 and δ 126.5 which were assigned to C-5' and C-4' respectively. Signals δ 125.8 and δ 125.6 were attributed to C3' and C-8' respectively. Whereas, signals at δ 121.6 and δ 117.4 were due to C-9' and C-10' respectively. For compound (**60**), two quarternary carbons at naphthalene ring appeared at δ 134.2 and δ 131.4 due to C-3' and C-8' respectively. All methine carbons in naphthalene ring appeared at δ 123.0, δ 128.0, δ 127.6, δ 126.8, δ 125.7, δ 121.1, δ 118.0, which are ascribed to C-9', C-5', C-4', C-7', C-6', C-10' and C-2' respectively.

3.2.3 Reaction of 2-chloropyrazine (48) with piperidine (61)

Reaction of 2-chloropyrazine (**48**) with piperazine (**61**) produced 2-*N*-piperidinopyrazine (**62**). The reaction was shown in Figure 3.1. Mixture of piperazine

(**61**) and 2-*N*-piperidinopyrazine (**62**) in ethanol was refluxed for 2 hours. The crude product was extracted with diethyl ether and water. Evaporation of solvent, and repeatedly washed with chloroform gave the pure product of 76 %. The detailed experimental procedure was given in Chapter 5.

The GC-MS spectrum of compound (**62**) showed a $[M^+]$ peak at m/z 163 which is in agreement with the molecular formula of $C_9H_{13}N_3$. Infrared spectrum showed a weak absorption band at 1672 cm^{-1} and a medium absorption band at 1517 cm^{-1} which were assigned to the presence of C=N and C=C stretchings. A strong absorption band was observed at 2935 cm^{-1} due to C-H stretching.

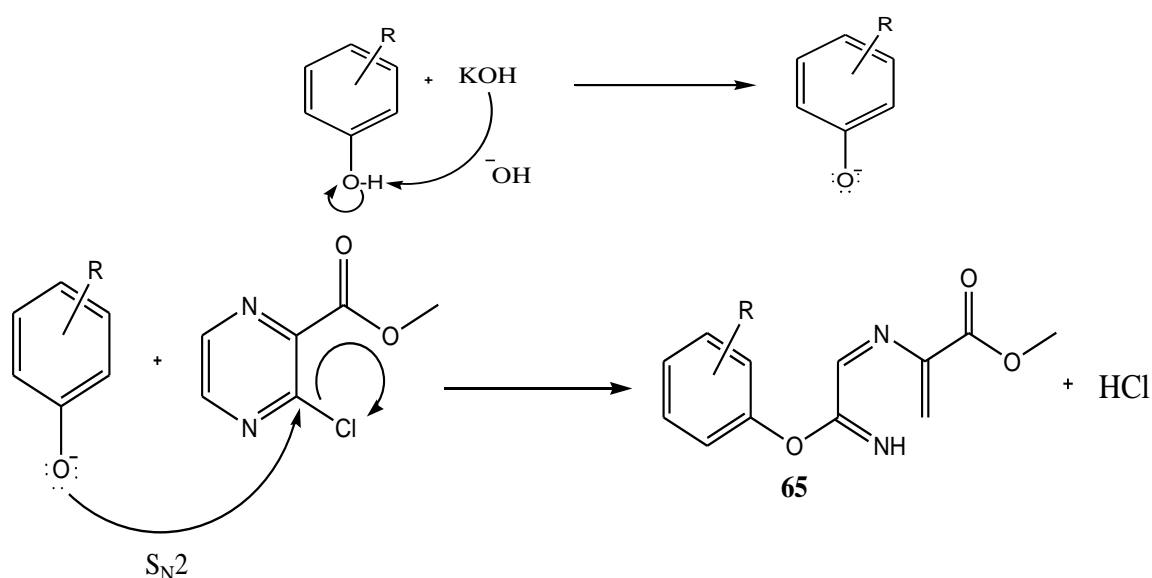
^1H -NMR spectrum showed a doublet with coupling constant of 1.4 Hz at δ 8.05 which was due to H-3. A doublet of doublet at δ 7.96 with coupling constant of 2.6 Hz and 1.4 Hz assigned to H-5. H-6 was observed as a doublet peak at δ 7.69 with coupling constant of 2.6 Hz. Two broad singlets were observed in the aliphatic region of δ 3.49 and δ 1.55, assigned to H-2', H-6' and H-3', H-4', H-5' respectively.

Nine carbon atoms were observed in ^{13}C NMR spectrum of compound (**62**), which agreed with the molecular formula of 2-*N*-piperidinopyrazine (**62**). The most deshielded quarternary carbon atom was observed at δ 155.0 which was assigned for C-2, followed by methine C-3 which was observed at δ 141.6. The remaining methane carbons at pyrazine ring were observed at δ 131.7 and δ 130.9 indicated to C-5 and C-6 respectively. The signals at δ 45.4 – δ 24.4 in the shielded region were attributed to the carbons at the piperidine ring.

3.2.4 Reaction of 2-chloropyrazine-5-carboxylic acid methyl ester (63) with phenol derivatives

The reaction of 2-chloropyrazine-5-carboxylic acid methyl ester (**63**) with phenol (**49**), phenol which attached to electron donating group, which is 3-methylphenol (**53**) and phenol which attached to electron withdrawing group, which is 3-nitrophenol (**64**) were studied. Figure 3.2 showed reaction of 2-chloropyrazine-5-carboxylic acid methyl ester (**63**) with phenol derivatives.

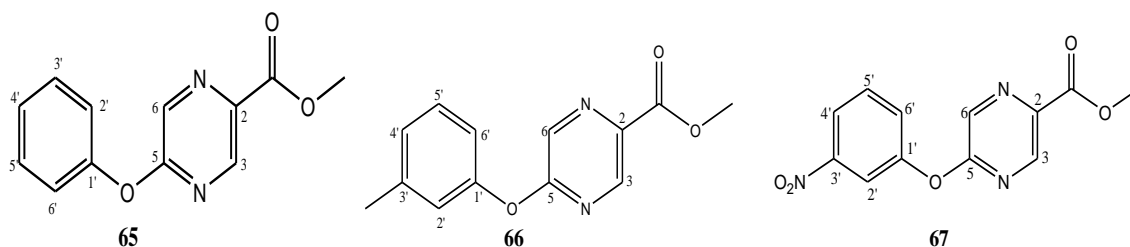
2-Chloropyrazine-5-carboxylic acid methyl ester (**63**) reacted with phenol (**49**), *m*-cresol (**53**), and 3-nitrophenol (**64**) to produce 5-phenoxy pyrazine-2-carboxylic acid methyl ester (**65**), 5-*m*-tolylloxypyrazine-2-carboxylic acid methyl ester (**66**), 5-(3-nitrophenoxy)pyrazine-2-carboxylic acid methyl ester (**67**) respectively. The mechanism of 5-chloropyrazine-2-carboxylic acid methyl ester (**63**) with phenol (**49**) is shown in Scheme 3.5.



Scheme 3.5: Reaction mechanism of formation of 5-phenoxy pyrazine-2-carboxylic acid methyl ester (65**)**

From IR spectrum of compound **(65)**, **(66)** and **(67)** showed medium intensity bands at 1347 cm^{-1} to 1576 cm^{-1} in IR spectra corresponded to C=N group in the compounds. Furthermore, a strong medium absorption band were observed at 1456 cm^{-1} to 1473 cm^{-1} and 1526 cm^{-1} to 1540 cm^{-1} respectively, due to C=C stretches in aromatic ring. Two medium bands were observed at 1001 cm^{-1} to 1194 cm^{-1} and 1271 cm^{-1} to 1279 cm^{-1} were identified, assigned to C-O bond stretches. Furthermore, a strong absorption band was observed at 1378 cm^{-1} due to C=O stretching in ester group. Compound **(67)** showed additional two strong absorption bands at 1527 cm^{-1} and 1342 cm^{-1} corresponded to nitro group in the molecule.

The GC-mass spectrum of **(65)** showed molecular ion at m/z 230 [M^+] which is consistent with the molecular formula of $C_{12}H_{10}N_2O_3$ for compound **(65)**. Whereas, **(66)** and **(67)** showed base peaks at m/z 244 [M^+] and m/z 275 [M^+] which is proportional with the molecular formula of $C_{13}H_{12}N_2O_3$ and $C_{12}H_9N_3O_5$ for **(66)** and **(67)** respectively.



The ^1H -NMR spectra of **(65)**, **(66)**, and **(67)** showed similar peaks in the region δ 8.84- δ 8.48 which were due to the H-6 and H-3 of the pyrazine ring. Compound **(65)** showed two triplet peaks at δ 7.45 and δ 7.29 with coupling constant 8.6 Hz and 7.6 Hz respectively. The phenyl group of compound **(65)** showed similar peaks to be compared with monosubstituted benzene ring of compound **(50)**. The presence of protons of the methyl group was indicated by a singlet peak at δ 4.03. The ^1H -NMR spectrum of **(66)** showed a triplet peak at δ 7.32 attributed to H-5' at benzene ring. H-6' and H-4' was

observed doublet at δ 7.11 and δ 6.96 respectively. Due to no neighbouring spin-coupled nuclei, H-2' was observed singlet at δ 6.99. At the more upfield region, singlet methoxy group and methyl group was observed at δ 4.01 and δ 2.40 respectively. On the other hand, compound (**67**) showed two doublet of doublet of doublet peaks at δ 8.17 and δ 7.55 with coupling constant 1.04 Hz and 1.0 Hz assigned for H-4' and H-6' respectively. Besides, two triplet peaks were observed at δ 8.11 and δ 7.63 with coupling constant 2.1 Hz and 8.12 Hz represent for H-2' and H-5' respectively. Whereas, a singlet peak was observed at δ 4.03 indicates for methyl proton.

The ^{13}C -NMR spectrum of compound (**65**) showed similar peaks with spectrum of compound (**50**), except additional peaks at δ 164.2 and δ 52.8 which were assigned to the carbonyl and methoxy carbons in (**65**). Furthermore, compound (**66**) carbon showed the presence of 13 carbons in the molecule with 5 quaternary carbons and 6 methine carbons which consistent with compound (**66**). Carbonyl carbon was observed at δ 164.2. Another three quaternary carbons observed at δ 161.8, δ 152.3, and δ 140.3 were assigned to C-5, C-2 and C-1'. Another two carbons at benzene ring were observed at δ 144.3 and δ 135.3 corresponded to C-3 and C-6. Four methine carbons at benzene ring, C-5', C-4', C-2' and C-6' were observed at δ 129.6, δ 127.0, δ 121.8, and δ 118.2, respectively. At the most shielded region, there were methoxy and methyl carbons observed at δ 52.8 and δ 21.4. Compound (**67**) also showed similar peaks in ^{13}C -NMR spectrum, except there were no methyl group detected and peak that assigned for C-3' in (**67**) appeared more downfield region which was at δ 138.3 compared to C-3' in (**66**).

Recrystallization of 5-phenoxy pyrazine-2-carboxylic acid methyl ester (**65**) from chloroform and acetonitrile gave colourless crystal which were analysed by X-ray diffraction method. The crystal system is monoclinic and the refinement data of (**65**) are shown in Table 3.1. While ORTEP diagram of compound (**65**) is shown in Figure 3.4.

Table 3.1: The crystal system and refinement data of compound (65)

| Phase data | |
|------------------|---|
| Formula sum | C12 H12 N2 O3 |
| Formula weight | 232.24 g/mol |
| Crystal system | monoclinic |
| Space-group | P 1 21/n 1 (14) |
| Cell parameters | a=5.7325(5) Å b=7.5297(6) Å c=24.420(2) Å $\beta=93.293(1)^\circ$ |
| Cell ratio | a/b=0.7613 b/c=0.3083 c/a=4.2599 |
| Cell volume | 1052.32(15) Å ³ |
| Z | 4 |
| Calc. density | 1.46579 g/cm ³ |
| Meas. density | |
| Melting point | |
| R _{all} | 0.0559 |
| R _{Obs} | |
| Pearson code | mP108 |
| Formula type | N2O3P10Q12 |
| Wyckoff sequence | e27 |

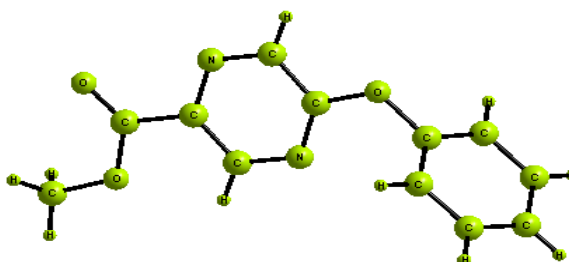
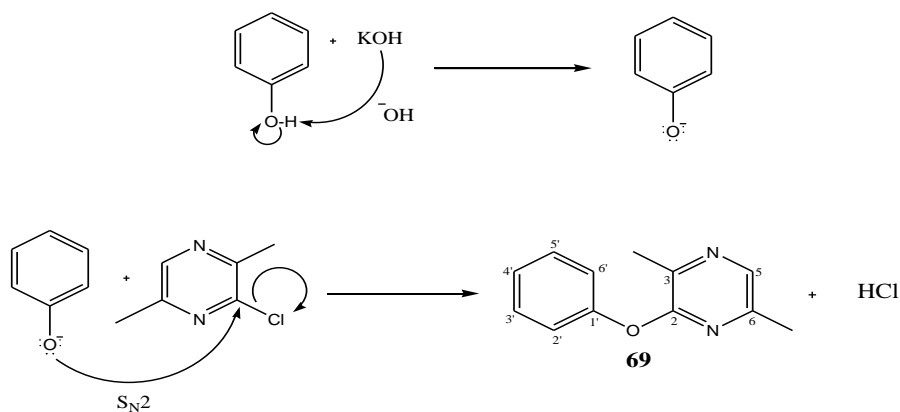


Figure 3.4: ORTEP diagram of 5-phenoxy-2-methoxypyrazine (65)

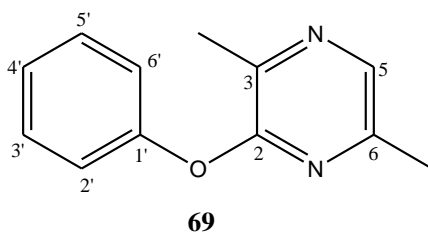
3.2.5 Reaction of 3-chloro-2,5-dimethylpyrazine (68) with phenol (49)

Phenol (**49**) was deprotonated by using potassium hydroxide in minimum amount of water. Potassium phenoxide obtained was refluxed for 5 hours with 3-chloro-2,5-dimethyl pyrazine (**68**) in tetrahydrofuran to yield 80.54 % of crude product, 2,5-dimethyl-3-phenoxy-2-methoxypyrazine (**69**). The reaction is shown in Scheme 3.6.



Scheme 3.6: Reaction mechanism of formation of 2,5-dimethyl-3-phenoxy-2-methoxypyrazine (69)

GC-mass spectrum showed molecular weight of the compound which was indicated by the molecular ion at m/z 200.00 [M^+] proportional with the molecular formula of $C_{12}H_{12}N_2O$. From IR spectrum of compound (**69**), similar characteristic of absorption bands was observed to that of compound (**50**). The presence of C=N, C=C, C-O stretching and monosubstituted benzene ring was observed for this compound.



From 1H NMR spectrum, a singlet peak of H-5 at pyrazine ring was observed at δ 8.02. Similar peaks were observed at phenyl group of compound (**69**) with phenyl group at compound (**50**) and (**65**). Two methyl groups at pyrazine ring appeared at δ 2.57 and δ 2.33, indicated for methyl substituent at C-3 and C-6 respectively.

^{13}C NMR spectrum of compound (**69**) showed the presence of 10 carbons with 4 quarternary carbons and 6 methine carbons which agree with the molecular formula of 2,5-dimethyl-3-phenoxypyrazine (**69**). The most deshielded quarternary carbon was observed at δ 157.2 which assigned for C-2, followed by quarternary C-1' which observed at δ 153.8. The remaining quarternary carbon at pyrazine ring were detected at δ 148.4 and δ 141.6 indicated for C-6 and C-3 respectively. The methine C-5 at pyrazine ring was observed at δ 137.1. Carbons at monosubstituted benzene ring at compound (**69**) showed similar peaks with spectra (**50**) and (**65**). Furthermore, two methyl carbons at C-3 and C-6 were observed at δ 20.6 and δ 18.9 respectively.

3.3 Fluorescence characteristics of synthesized compounds

Fluorescence behaviour of the synthesised compounds in various concentrations were studied, and as shown in Table 3.2, Table 3.3, Table 3.4 and Table 3.5. The

concentrations used were 3.8314×10^{-4} M, 3.8314×10^{-5} M, and 3.8314×10^{-6} M in ethyl acetate and acetonitrile.

Table 3.2: Fluorescence characteristic of 2-phenoxy pyrazine (50) in various concentrations in ethyl acetate and acetonitrile

| Solvents | Excitation wavelength (nm) | | | Fluorescence wavelength (nm) | | | Intensity | | |
|--------------------|----------------------------|-------------|-------------|------------------------------|-------------|-------------|-------------|-------------|-------------|
| | 10^{-6} M | 10^{-5} M | 10^{-4} M | 10^{-6} M | 10^{-5} M | 10^{-4} M | 10^{-6} M | 10^{-5} M | 10^{-4} M |
| EtOAc | 279 | 279 | 279 | x | 351 | 304 | x | 25.34 | 38.55 |
| CH ₃ CN | 279 | 278 | 278 | 415 | 402 | 417 | 2.78 | 17.23 | 29.91 |

Concentration = 3.8314×10^{-x} M, where 10^x M = 10^{-6} M, 10^{-5} M, 10^{-4} M

Fluorescence reading with respect to distilled water, where distilled water = 0

Table 3.3: Fluorescence characteristic of 2-*o*-tolyl oxypyrazine (52) in different concentrations in ethyl acetate and acetonitrile

| Solvents | Excitation wavelength (nm) | | | Fluorescence wavelength (nm) | | | Intensity | | |
|--------------------|----------------------------|-------------|-------------|------------------------------|-------------|-------------|-------------|-------------|-------------|
| | 10^{-6} M | 10^{-5} M | 10^{-4} M | 10^{-6} M | 10^{-5} M | 10^{-4} M | 10^{-6} M | 10^{-5} M | 10^{-4} M |
| EtOAc | 293 | 294 | 299 | 340 | 348 | 348 | 63.06 | 215.16 | 277.39 |
| CH ₃ CN | 293 | 292 | 293 | 318 | 348 | 352 | 10.68 | 15.72 | 76.78 |

Concentration = 3.8314×10^{-x} M, where 10^x M = 10^{-6} M, 10^{-5} M, 10^{-4} M

Fluorescence reading with respect to distilled water, where distilled water = 0

Table 3.4: Fluorescence characteristic of 2-*N*-piperidinopyrazine (62) in different concentrations in ethyl acetate and acetonitrile

| Solvents | Excitation wavelength (nm) | | | Fluorescence wavelength (nm) | | | Intensity | | |
|--------------------|----------------------------|-------------|-------------|------------------------------|-------------|-------------|-------------|-------------|-------------|
| | 10^{-6} M | 10^{-5} M | 10^{-4} M | 10^{-6} M | 10^{-5} M | 10^{-4} M | 10^{-6} M | 10^{-5} M | 10^{-4} M |
| EtOAc | 344 | 345 | 362 | 404 | 407 | 408 | 26.30 | 159.80 | 441.70 |
| CH ₃ CN | 348 | 348 | 371 | 411 | 415 | 419 | 51.64 | 262.40 | 460.60 |

Concentration = 3.8314×10^{-x} M, where 10^x M = 10^{-6} M, 10^{-5} M, 10^{-4} M

Fluorescence reading with respect to distilled water, where distilled water = 0

Table 3.5: Fluorescence characteristic of 2,5-dimethyl-3-phenoxy pyrazine (69) in different concentrations in ethyl acetate and acetonitrile

| Solvents | Excitation wavelength (nm) | | | Fluorescence wavelength (nm) | | | Intensity | | |
|--------------------|----------------------------|-------------|-------------|------------------------------|-------------|-------------|-------------|-------------|-------------|
| | 10^{-6} M | 10^{-5} M | 10^{-4} M | 10^{-6} M | 10^{-5} M | 10^{-4} M | 10^{-6} M | 10^{-5} M | 10^{-4} M |
| EtOAc | 293 | 293 | 294 | 340 | 344 | 346 | 47.34 | 56.72 | 100.71 |
| CH ₃ CN | 279 | 294 | 295 | 307 | 350 | 346 | 11.94 | 14.17 | 73.11 |

Concentration = 3.8314×10^{-x} M, where 10^x M = 10^{-6} M, 10^{-5} M, 10^{-4} M

Fluorescence reading with respect to distilled water, where distilled water = 0

Figure 3.5 and Figure 3.6 showed fluorescence intensities of compounds (50), (52) and (69) in acetonitrile and ethyl acetate in various concentrations.

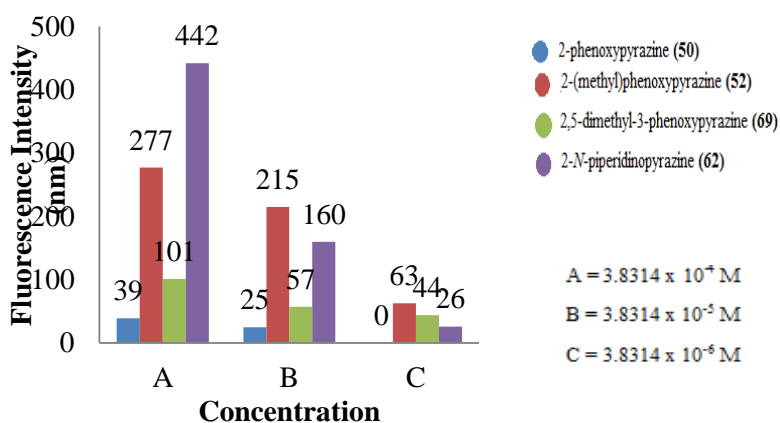


Figure 3.5: Fluorescence intensity of 2-phenoxy pyrazine (50), 2-*o*-tolyl oxy pyrazine (52), 2-*N*-piperidinopyrazine (62) and 2,5-dimethyl-3-phenoxy pyrazine (69) with three different concentrations in ethyl acetate

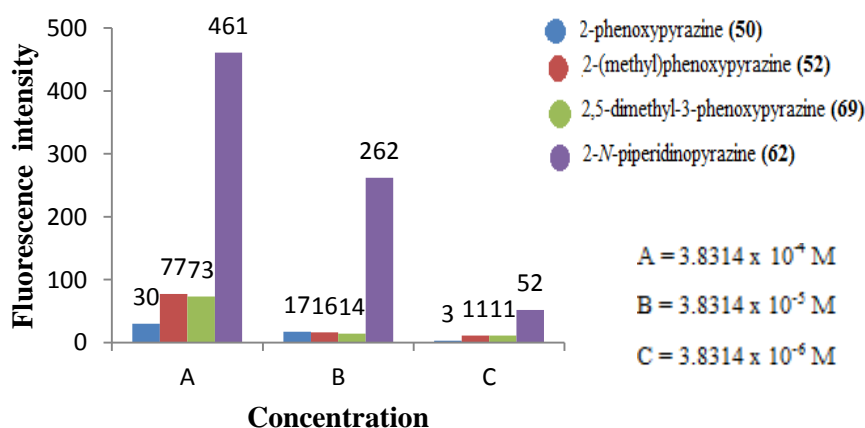


Figure 3.6: Fluorescence intensity of 2-phenoxy pyrazine (50), 2-*o*-tolyl oxy pyrazine (52), 2-*N*-piperidinopyrazine (62) and 2,5-dimethyl-3-phenoxy pyrazine (69) with three different concentrations in acetonitrile.

It can be seen from Figure 3.5 and Figure 3.6 the fluorescence intensity increases for compound (50), (52), (62) and (69) in acetonitrile and ethyl acetate with increasing concentration. It is believed that, at relatively low concentration (in the range of 10^{-4} - 10^{-6} M), concentration is proportional with intensity of fluorescence, because more light was absorbed. However, at very high concentration ($> 10^{-4}$ M), concentration quenching start to take place where the absorbance may appear to be invariant with concentration, and this phenomenon often accompanied by wavelength shift^[26].

At very high concentrations, there is so much light absorbed from the excitation source that the intensity of excitation is significantly reduced in the inner region of the specimen. It was reported that, some arise from solute-solute interactions, energy transfer, while others are derived from the optical and electronic responses of the spectrophotometric instrumentation. However, in this study, those observations were not observed because the concentrations used were in the range of 10^{-4} - 10^{-6} M.

A study covering three different compounds were made for a better understanding on the effect of oxygen on fluorescence characteristics. Table 3.6, Figure 3.7, Figure 3.8 and Figure 3.9 showed fluorescence characteristics of compounds (52), (56), and (69) in acetonitrile with the concentration of 3.8314×10^{-4} M. The measurements were taken at three different time frames, immediately, after 30 minutes and 60 minutes.

Table 3.6: Fluorescence characteristics of compounds (52), (56), and (69) in acetonitrile in 3.8314×10^{-4} M

| Compounds | Duration (min) | Excitation wavelength (nm) | Fluorescence wavelength (nm) | Fluorescence intensity (nm) |
|----------------------------------|----------------|----------------------------|------------------------------|-----------------------------|
| 2- <i>o</i> -toloxypyrazine (52) | Immediately | 292 | 351 | 81.47 |
| | 30 | 292 | 353 | 57.85 |
| | 60 | 292 | 355 | 50.78 |

Table 3.6: Continued

| | | | | |
|--------------------------------------|-------------|-----|-----|-------|
| 2- <i>p</i> -tolylloxypyrazine (56) | Immediately | 278 | 303 | 3.44 |
| | 30 | 278 | 303 | 2.64 |
| | 60 | 278 | 304 | 2.55 |
| 2, 5-dimethyl-3-phenoxypyrazine (69) | Immediately | 295 | 351 | 73.49 |
| | 30 | 295 | 345 | 69.51 |
| | 60 | 295 | 350 | 68.74 |

Fluorescence reading with respect to distilled water, where distilled water = 0

The fluorescence spectra of 2,5-dimethyl-3-phenoxypyrazine (69), 2-*o*-tolylloxypyrazine (52), and 2-*p*-tolylloxypyrazine (56) in three different times in capped condition are as shown in Figure 3.7, Figure 3.8 and Figure 3.9.

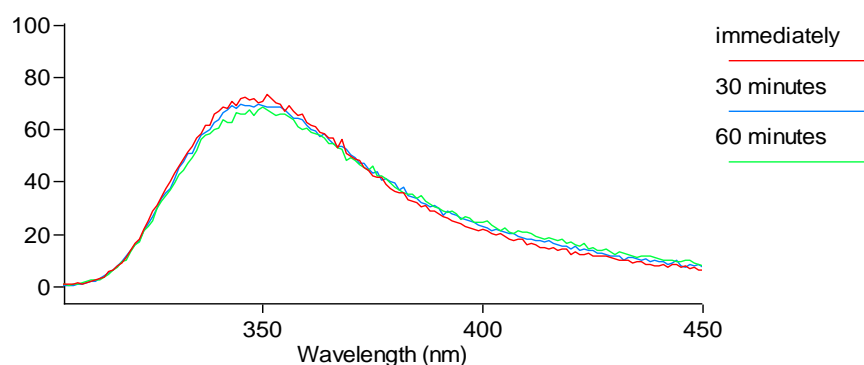


Figure 3.7: Fluorescence spectra of 2, 5-dimethyl-3-phenoxypyrazine (69) taken at different time frames in acetonitrile (concentration: 3.8314×10^{-4} M)

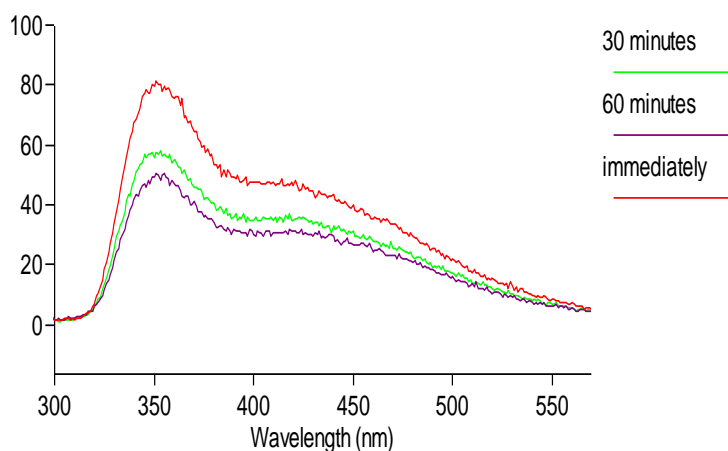


Figure 3.8: Fluorescence spectra of 2-*o*-tolylloxypyrazine (52) at different time frames in acetonitrile (concentration: 3.8314×10^{-4} M)

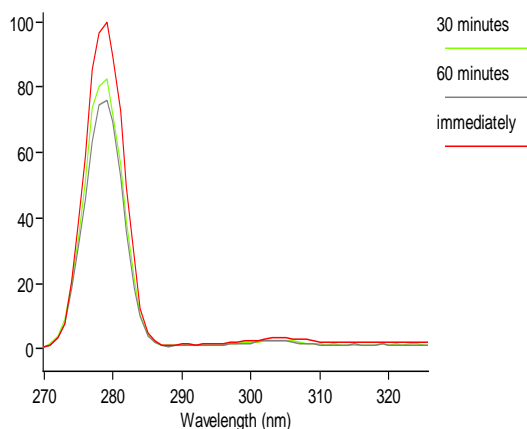


Figure 3.9: Fluorescence spectra of 2-*p*-toloxypyrazine (56**) at different time frames in acetonitrile (concentration: 3.8314×10^{-4} M)**

The fluorescence intensities of 2-*o*-toloxypyrazine (**52**), 2-*p*-toloxypyrazine (**56**) and 2, 5-dimethyl-3-phenoxy pyrazine (**69**), decreases with time while there were no any change of spectra shape and no any shift at maxima during the quenching process as shown in Figure 3.7, Figure 3.8 and Figure 3.9.

The possible explanation for this phenomenon is the quenching effect of oxygen with time. Oxygen is an efficient quencher for many organic fluorophores because of its high solubility in organic solvents and aqueous solutions. This quenching is so efficient, that most cases, the reaction rate is diffusion controlled^[34-36]. As the solution was left to stand for 30 minutes and 60 minutes, it was expected that more oxygen diffused into solution and quenched the fluorescence further.

In general, fluorescence quenching can be followed by either static or dynamic and sometimes both^[36]. In dynamic quenching mechanism, diffusive encounters between compound studied and oxygen occurred during the lifetime of the excited state. Whereas, in static quenching, fluorescence quenching occurs as a result of the formation of a non-fluorescent ground state complex between compound studied and oxygen. Since there is no work done in the literature related to the quenching mechanism of the

compound studied with molecular oxygen in solution, therefore, more work need to be carried out before a concrete conclusion can be made.

It has been reported that^[37-41], pH also influences the fluorescence intensity of the compounds studied. Fluorescence molecules have lifetimes in the lowest excited singlet state at extremely short period, (i.e 10^{-11} - 10^{-7} s). However, some chemical phenomena are fast enough to compete with the photophysical processes that deactivate the excited molecule. These include, excited basic fluorophores with acidic species and acidic fluorophores with basic species in the solution. The change of environmental pH of fluorophores also affects the fluorescence intensity of the compounds studied. A study covering five different pH values was carried out to study the effect of pH on the fluorescence characteristic of selected compounds and are summarized in Table 3.7 below.

Table 3.7: Fluorescence characteristics of 2-phenoxy pyrazine (50) and 5-(3-nitrophenoxy)pyrazine-2-carboxylic acid methyl ester (67) in various pH (concentration: 3.8314×10^{-5} M)

| Compounds | Conditions | pH | Excitation wavelength (nm) | Fluorescence wavelength (nm) | Intensity |
|--|------------|----|----------------------------|------------------------------|-----------|
| 5-(3-Nitrophenoxy)pyrazine-2-carboxylic acid methyl ester (67) | Acidic | 2 | 292 | 358 | 2.14 |
| | | 3 | 274 | 323 | 18.73 |
| | Neutral | 7 | 280 | 320 | 24.63 |
| | Basic | 11 | 276 | 318 | 27.86 |
| | | 12 | 282 | 320 | 32.02 |
| 2-Phenoxy pyrazine (50) | Acidic | 2 | 279 | 326 | 31.36 |
| | | 3 | 279 | 321 | 41.38 |
| | Neutral | 7 | 279 | 324 | 42.02 |
| | Basic | 11 | 279 | 322 | 45.37 |
| | | 12 | 279 | 323 | 48.69 |

Fluorescence reading with respect to distilled water, where distilled water = 0

The fluorescence spectra of 2-phenoxy pyrazine (50) and 5-(3-nitrophenoxy)pyrazine-2-carboxylic acid methyl ester (67) in five different pHs in capped condition are as shown in Figure 3.10 and Figure 3.11 respectively.

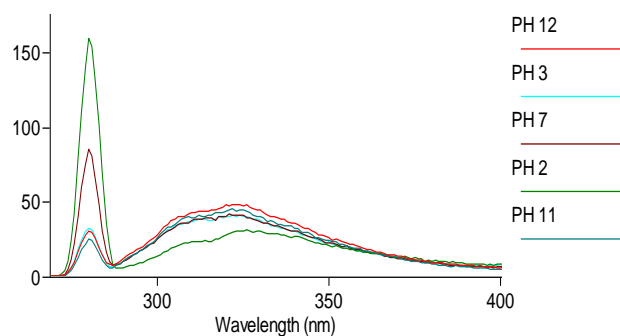


Figure 3.10: Fluorescence spectra of 2-phenoxy pyrazine (50) in various pH (concentration: 3.8314×10^{-5} M)

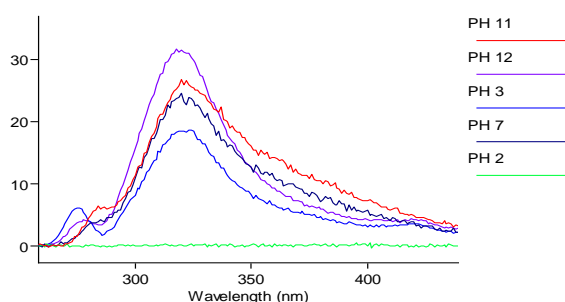


Figure 3.11: Fluorescence spectra of 5-(3-nitrophenoxy)pyrazine-2-carboxylic acid methyl ester (67) in various pH (concentration: 3.8314×10^{-5} M)

From the Table 3.8, it shows that compounds (50) and (67) are strongly emissive in basic media but is quenched in acidic media. This phenomenon is probably due to quenching of fluorescence by hydrogen ions^[42]. Transferring of electron to the phenoxy ring quenched the fluorescence intensities of compounds (50) and (67). The mechanism is demonstrated in Figure 3.12 and Figure 3.13 below.

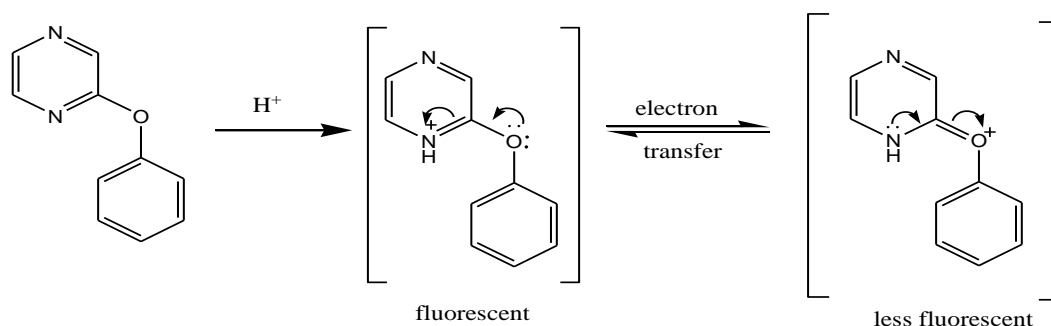


Figure 3.12: The electron transfer mechanism of (50) to the phenoxy ring

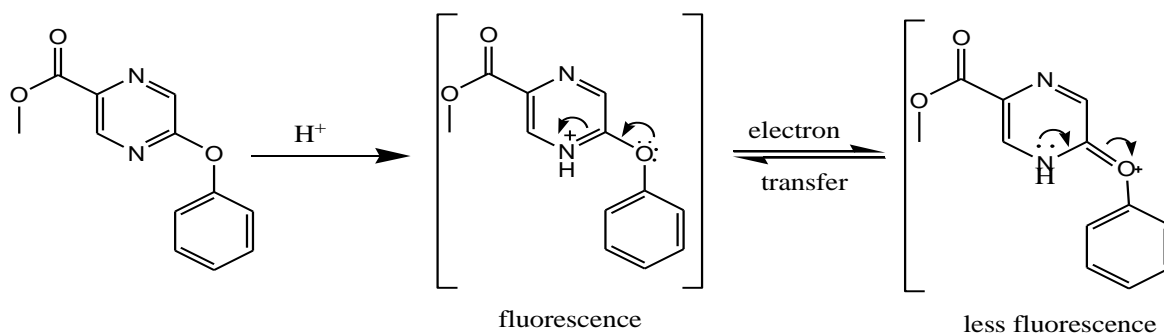


Figure 3.13: The electron transfer mechanism of 5-(3-nitrophenoxy)pyrazine-2-carboxylic acid methyl ester (67) to the phenoxy ring

Similar observation was observed on pyranine, fluorescein, tinopal^[43] and glycytyrosine, tyrosine and tyrosine methyl ester as reported by Audrey white^[44].

Amongst the goal of this study was to relate the fluorescence intensities of a few selected compounds synthesized with solvents polarity. One polar protic solvent which was ethanol, one polar aprotic solvent, tetrahydrofuran, and two non-polar solvents hexane and ethyl acetate with widely different dielectric constant were chosen. Fluorescence characteristic of 2-*o*-tolylloxypyrazine (**52**), 2-*p*-tolylloxypyrazine (**56**), and 2, 5-dimethyl-3-phenoxy pyrazine (**69**) in five different solvents are shown in Table 3.8 and Figure 3.14.

Table 3.8: Fluorescence characteristics of (52), (56) and (69) in various solvents in 3.8314 x10⁻⁴ M.

| Compounds | Solvents | Excitation wavelength (nm) | Emission wavelength (nm) | Intensity |
|--|-----------------|----------------------------|--------------------------|-----------|
| 2- <i>o</i> -tolylloxypyrazine (52) | Hexane | 293 | 343 | 335.37 |
| | Ethyl acetate | 299 | 348 | 277.39 |
| | Tetrahydrofuran | 284 | 349 | 55.83 |
| | Ethanol | 294 | 350 | 12.63 |
| 2- <i>p</i> -tolylloxypyrazine (56) | Hexane | 277 | 368 | 50.06 |
| | Ethyl acetate | 279 | 294 | 47.00 |
| | Tetrahydrofuran | 277 | 311 | 32.16 |
| | Ethanol | 278 | 323 | 12.41 |
| 2, 5-dimethyl-3-phenoxy pyrazine (69) | Hexane | 293 | 339 | 77.48 |
| | Ethyl acetate | 294 | 339 | 77.49 |
| | Tetrahydrofuran | 291 | 315 | 68.67 |
| | Ethanol | 296 | 347 | 10.10 |

Fluorescence reading with respect to distilled water, where distilled water = 0

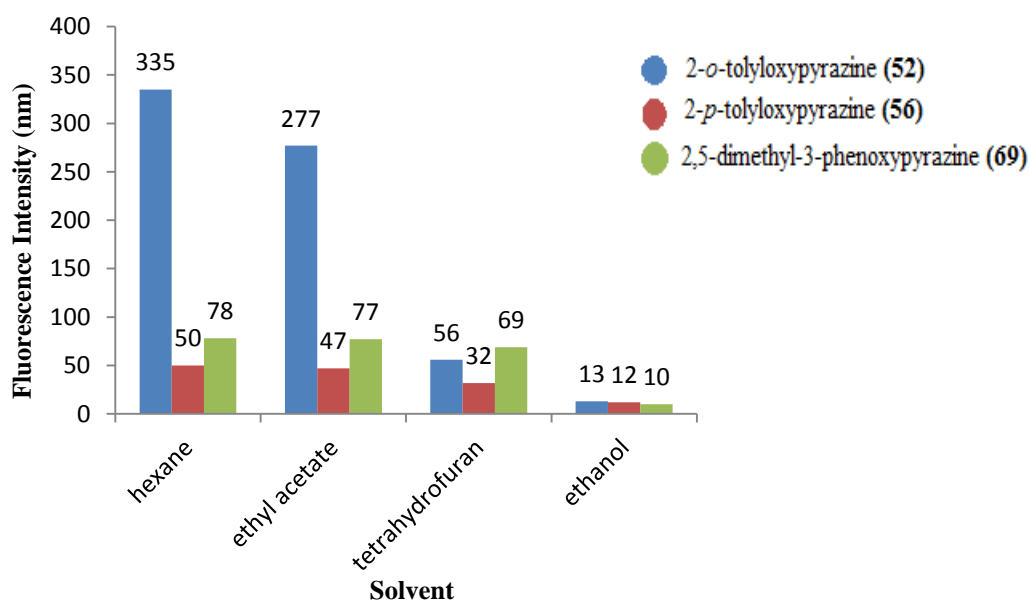


Figure 3.14: Fluorescence intensity of (52), (56) and (69) in various solvents at 3.8314×10^{-4} M.

From Table 3.8 and Figure 3.14, compound (52), (56), and (69) show highest fluorescence intensity in non-polar media. Increasing in polarity of the medium, the fluorescence intensity of the system does not change significantly as long as aprotic solvent were used. On the contrary, a drastic fall in the fluorescence intensity was observed in protic solvent. Interaction of compound (52), (56), and (69) with hexane and ethyl acetate solvents depends on the dipole-induce-dipole forces, while with tetrahydrofuran, the interaction depends on the stronger dipole-dipole forces. Hence, in ethanol, apart from dipole-dipole interaction, ethanol has hydrogen atom bonded to electronegative oxygen is a hydrogen-bond donor solvent. As all compounds (52), (56), and (69) have unshared valence electron pair at oxygen and nitrogen atoms which enable these compounds to act as proton acceptor from ethanol. These compounds can behave as a weak Bronsted acid, thus donate proton to basic site on compound (52), (56), and (69), which result in electronic charge transfer from compound (52), (56), and (69) to ethanol solvent^[45]. In this study, it was believed that formation of solute-solvent exciplexes were responsible for the higher deactivation rate of fluorescence intensity

observed. The formation of excited state complex of compound **(52)**, **(56)**, and **(69)** with ethanol were shown in Figure 3.15.

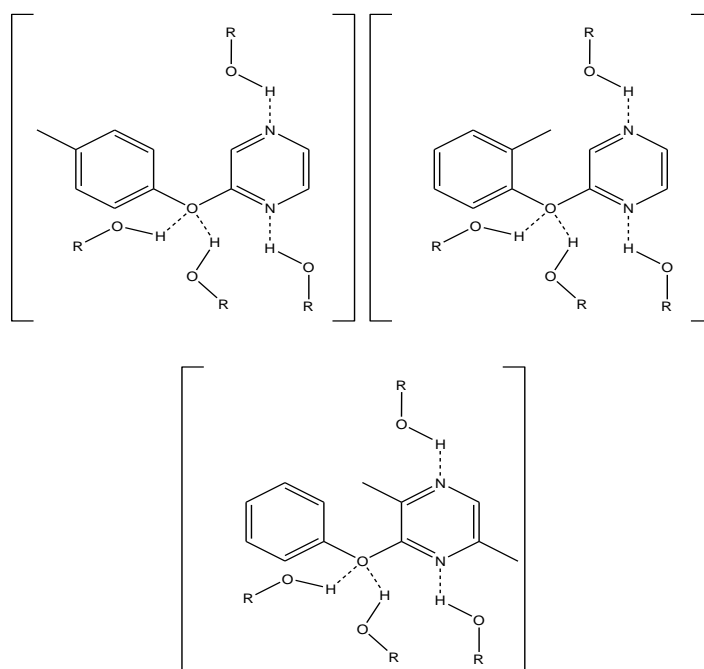


Figure 3.15: Formation of hydrogen bonded complexes of compound **(52), **(56)**, and **(69)** in ethanol**

This type of hydrogen bond presumably enhances intersystem crossing thus the emission intensity is dramatically reduced due to strong fluorescence quenching. Fluorescence characteristic of heterocyclic compounds are solvent dependent as it have low-lying $n-\pi^*$ transitions. It has been reported that inversion can occur between $\pi-\pi^*$ and $n-\pi^*$ states when the hydrogen-bonding power and the polarity of solvents increase, because $n-\pi^*$ state shifts to higher energy, while $\pi-\pi^*$ shift to lower energy $n-\pi^*$ transition are characterized by molar absorption coefficients that are at least a factor of 10^2 smaller than $\pi-\pi^*$ transitions. Furthermore, its radiative lifetime is at least 100 times longer than low-lying $\pi-\pi^*$ transitions. This extremely slow process explains the low fluorescence intensity of compound **(52)**, **(56)** and **(69)** in ethanol.

Table 3.8, also shows that all compounds showed highest fluorescence intensity in hexane. It is believed that in nonpolar solvent, there is no or very little difference in

energy between the Franck-Condon state and the equilibrium state. According to Franck-Condon principle, the charge-transfer fluorescence emission spectra are expected to show far stronger influences of the environment than the charge transfer absorption spectra^[46]. The possible explanation for this phenomenon is because in nonpolar media, the interaction between solute-solvent depends only on induced dipole-induced dipole term and dipole-induced dipole term, therefore no orientation strain occurred. Hence, in hexane solvent, the Franck-Condon and equilibrium states are approximately the same^[47]

One of the early studies relative to effect of solvent on fluorescence involving chlorophyll was reported by R. S. Becker and J. Fernandez which exhibits extremely weak fluorescence efficiency in benzene and gradually increase in fluorescence intensity by addition of hydroxylic solvents^[48]. There were many fluorescence probe which strongly fluorescent in hydrophilic environment and weakly fluorescent in hydrophobic environment^{[46][49-50]}, but there is also opposite behaviour of the some fluorophores such as acridine^[51], pyrenecarboxaldehyde^[52] and 7-methoxy-4-methylcoumarins^[53].

The molecular structure can have profound effect on the wavelengths of fluorescence emission. The effect of degree of conjugation and linearity of molecular structure system to fluorescence characteristic were studied with a series of compounds which is 2-phenoxy pyrazine (**50**), 2-naphthalen-1-yloxy pyrazine (**58**), and 2-naphthalen-2-yloxy pyrazine (**60**). Table 3.8 below show the fluorescence characteristic of compound (**50**), (**58**), (**60**) and Figure 3.16 show the fluorescence spectra of compounds (**50**), (**58**), (**60**) in acetonitrile at 3.8314×10^{-5} M.

Table 3.9: Fluorescence characteristics of compounds (50), (58), and (60) in acetonitrile at 3.8314×10^{-5} M

| Compounds | Excitation value (nm) | Fluorescence wavelength (nm) | Fluorescence Intensity |
|---|-----------------------|------------------------------|------------------------|
| 2-phenoxy pyrazine (50) | 278 | 402 | 17.23 |
| 2-naphthalen-1-yloxy pyrazine (58) | 280 | 342 | 12.10 |
| 2-naphthalen-2-yloxy pyrazine (60) | 275 | 466 | 18.53 |

Fluorescence reading with respect to distilled water, where distilled water = 0

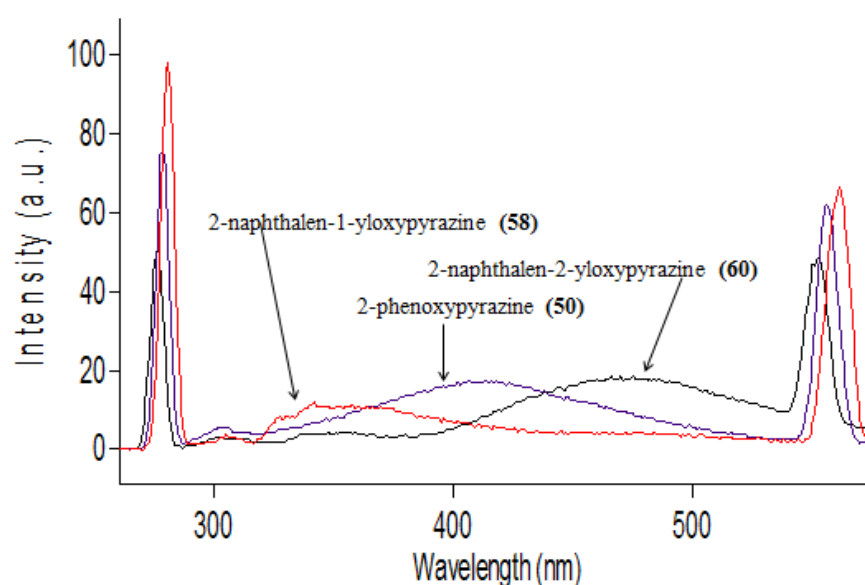
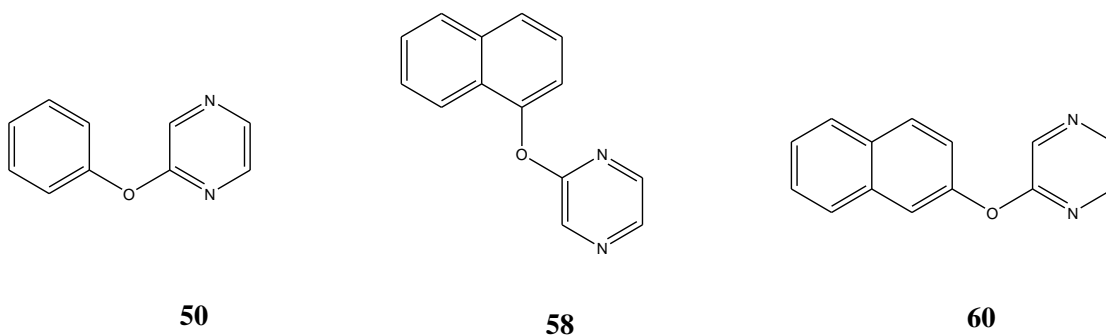


Figure 3.16: Fluorescence spectra of compound (50), (58), and (60) in acetonitrile at 3.8314×10^{-6} M

From Table 3.9 and Figure 3.16, we can see that compound (**60**) showed highest fluorescence intensity compared to compound (**48**) and (**58**). Base on Figure 3.16 above, we can see compound (**60**) experienced bathochromic shift to the higher wavelength 466 nm, compared to compound (**58**), 342 nm and (**60**), 402 nm. The explanation for this observation is probably because the highly conjugation effect of compound (**60**) allowed the π bonds to be delocalized over several carbon atoms. Consequently, compound (**60**) absorbs light at longer wavelength (lower energy) to be promoted to a higher energy level. It is known that, the smaller the gap between the ground and

lowest electronic excited state, the longer the wavelength of the fluorescence^[53]. Thus, this is probably the reason why compound **(60)** experienced a bathochromic shift. This phenomenon was also practically demonstrated by benzene, naphthalene, and anthracene, which exhibit their fluorescence emission maxima at 262 nm, 320 nm, and 379 nm respectively.^{[25][54-55]}

Furthermore, compound **(60)** also showed highest fluorescence intensity followed by compound **(50)** and **(58)**. The explanation for this observation is probably because high fluorescence yields are observed in highly conjugated “rigid” molecules^{[54][56]}. This is because as explained before, conjugate structure of compound **(60)** restricted it from rotating and vibrating freely. This ensures that the energy gap between the lowest singlet state and the ground electronic state is large enough for deactivation through internal conversion. This observation is in agreement with the work done by Takanori Ochi et. al.^[57].



Although compound **(58)** have conjugated system too, but it has a non-linear system structure compared to compound **(60)** and **(50)**, which exhibit lower fluorescence intensity and hypsochromic shift. Similar properties are also observed for non-linear structure of phenanthrene and benz[a]anthracene compared with linear structured compounds of anthracene and tetracene as reported by George G. Guilbault^[55]. In addition, low fluorescence intensity observed for compound **(58)** is attributed to its non-

rigid structure which enables it to reduce fluorescence intensity due to vibrational amplitudes during fluorescence lifetime in the excited state. Hence, energy absorbed diminished as heat. This finding is supported by the work of Nijegorodov and Downey^[58] which have demonstrated that decreasing the planarity and rigidity, increases the value of intersystem crossing rate constant (K_{st}).

A series of phenoxy pyrazine derivatives that were modified on their phenyl ring were synthesized. Typical electron-donating group, methyl and electron accepting substituents $-\text{NO}_2$ were selected owing to their easy commercial availability or preparation. The fluorescence characteristics of these compounds were investigated. Table 3.10 show the fluorescence characteristic of compounds 5-phenoxy pyrazine-2-carboxylic acid methyl ester (**65**), 5-*m*-toloxypyrazine-2-carboxylic acid methyl ester (**66**), and 5-(3-nitrophenoxy)pyrazine-2-carboxylic acid methyl ester (**67**) in hexane and tetrahydrofuran.

Table 3.10: Fluorescence characteristic of compound (65**), (**66**), and (**67**) in hexane and tetrahydrofuran in $3.8314 \times 10^{-4} \text{ M}$**

| Compounds | Solvents | Excitation wavelength (nm) | Fluorescence wavelength (nm) | Intensity |
|--|-----------------|----------------------------|------------------------------|-----------|
| 5-phenoxy pyrazine-2-carboxylic acid methyl ester (65) | Hexane | 293 | 362 | 6.36 |
| | Tetrahydrofuran | 291 | 414 | 22.61 |
| 5- <i>m</i> -toloxypyrazine-2-carboxylic acid methyl ester (66) | Hexane | 298 | 362 | 9.84 |
| | Tetrahydrofuran | 292 | 423 | 36.64 |
| 5-(3-nitrophenoxy)pyrazine-2-carboxylic acid methyl ester (67) | Hexane | 283 | 488 | 0.60 |
| | Tetrahydrofuran | 293 | 334 | 0.75 |

Fluorescence reading with respect to distilled water, where distilled water = 0

Figure 3.17 and Figure 3.18 show the fluorescence spectra of compounds (**65**), (**66**), and (**67**) in hexane and tetrahydrofuran at $3.8314 \times 10^{-4} \text{ M}$ respectively.

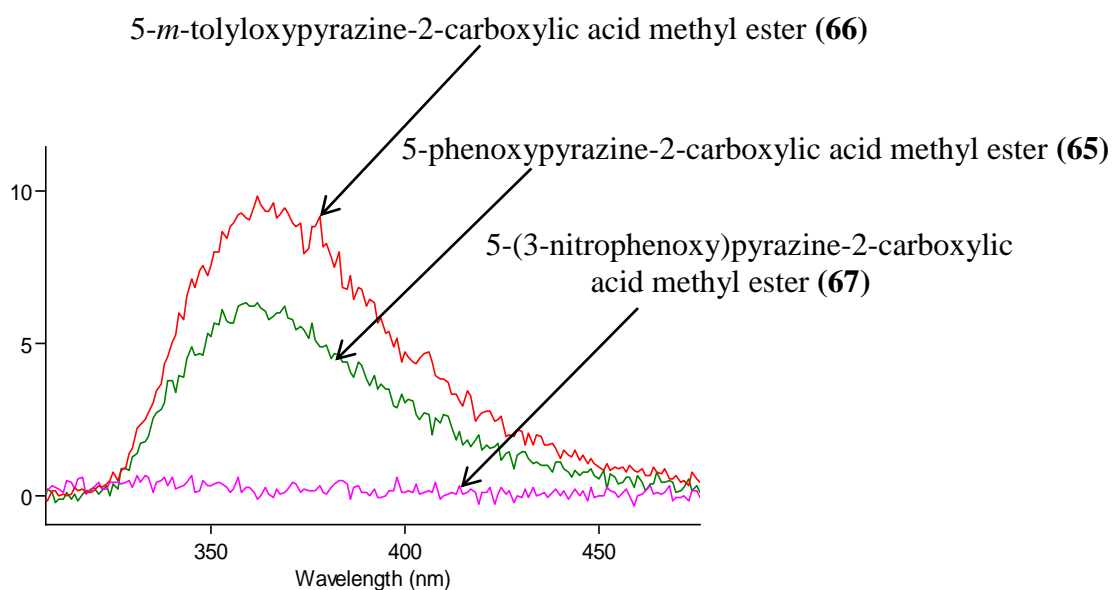


Figure 3.17: Fluorescence spectra of compound (65**), (**66**), and (**67**) in hexane in 3.8314×10^{-4} M**

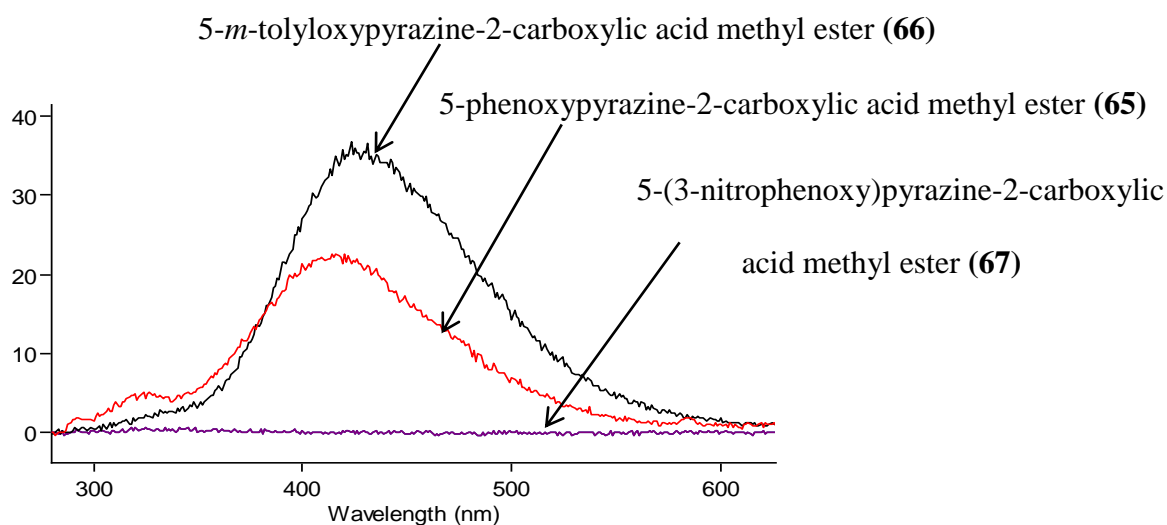


Figure 3.18: Fluorescence spectra of compound (65**), (**66**), and (**67**) in tetrahydrofuran in 3.8314×10^{-4} M**

Generally, introducing the remote substitution showed a profound effect on the fluorescence characteristic when comparing 5-phenoxy pyrazine-2-carboxylic acid methyl ester (**65**), introducing a methyl group substituent in compound (**66**) showed an increase in fluorescence intensity. On the contrary, introducing an electron-withdrawing group $-\text{NO}_2$ substituent as in compound (**67**), quenched the fluorescence intensity.

Compound **(67)** showed the lowest fluorescence intensity, compared to compounds **(65)** and **(66)**. In general, the presence of heavy atoms as substituent may result in fluorescence quenching due to increase probability of intersystem crossing process due to the existence of a low-lying $n-\pi^*$ transitions. In general, fluorescence from $n-\pi^*$ states showed weak fluorescence characteristic because of its longer excited state lifetime compared to $\pi-\pi^*$ states. Furthermore, it also exhibits faster intersystem crossing rate due to smaller singlet-triplet energy gap, $E(S-T)$ than for $S_1(\pi-\pi^*)$. This may be explained by the enhanced spin-orbit coupling between $S_1(n-\pi^*)$ and the triplet state in which intersystem coupling occur resulting from strong electron withdrawing character of $-\text{NO}_2$ group. This phenomenon is in agreement with the work done by Brian Wardle^[59] which reported the effect of $-\text{NO}_2$ group to naphthalene and its derivatives to fluorescence efficiency. The same observation was also reported by other researchers^{[25][60-61]}.

Compound **(66)** showed higher fluorescence intensity due to the presence of methyl group at the benzene ring. Even methyl is a very weak electron-donating group substituent, it was found to engender a profound shift to fluorescence spectrum of compound **(66)**, this is an evidence that even quite modest perturbations to compound **(66)** structure, sufficient to affect fluorescence efficiency. The presence of methyl group associated with conjugated aromatic molecule can enhance fluorescence intensity by increasing the reactivity and electron density in aromatic system^[60], thus increased the capability to increase the fluorescence intensity by increasing the rate of relaxation. Thus, this effect also extends fluorescence maxima further to the red as solvent polarity increase^[62-63], as can be seen from Figure 3.17 and Figure 3.18. Fluorescence peak of compounds **(65)**, **(66)**, and **(67)** shifted more to the red in tetrahydrofuran compared in hexane as tetrahydrofuran solvent is more polar than hexane^[64-65]. Besides, the presence of methyl substituent also tend to induce an increase in the molar absorption coefficient

of compound **(66)**^[66]. Hence, high fluorescence intensity observed in compound **(66)** was due to electron-donating group substituent at benzene ring. This incident also observed by HBDI anion compound as reported by Gregor Jung^[67].

The position of the methyl group at the benzene ring in **(66)** is likely to contribute to high fluorescence intensity. Although in ground state electrons tend to move to *ortho* and *para* position resulting to resonance effect. It was reported by Howard E. Zimmerman^[68] that excited state counterparts do not follow the *ortho-para* rule, but rather exhibit “*meta* effect”. This excited state phenomenon, results from selective electron transmission to *ortho* and *meta* sites in S₁ transition. As a consequence, *meta*-substituted compounds tend to exhibit high fluorescence intensity due to rapid excited-state reaction and radiationless decay rates. Thus, compound **(66)** showed highest fluorescence intensity compared to compound **(65)** and **(67)**.

To further support the previous result on the effect of electron-donating group and electron-withdrawing groups 2-phenoxy pyrazine **(50)** and 2,5-dimethyl-3-phenoxy pyrazine **(64)** were synthesized, and the fluorescence characteristic of **(50)**, **(65)** and **(69)** are shown in Table 3.11.

Table 3.11: Fluorescence characteristic of compound (50), (65), and (69) in hexane at 3.8314x10⁻⁴ M

| Compounds | Solvents | Excitation wavelength (nm) | Fluorescence wavelength (nm) | Intensity |
|---|-----------------|----------------------------|------------------------------|-----------|
| 2-phenoxy pyrazine (50) | Hexane | 278 | 343 | 19.52 |
| | Tetrahydrofuran | 289 | 321 | 23.81 |
| 5-phenoxy pyrazine-2-carboxylic acid methyl ester (65) | Hexane | 293 | 362 | 6.36 |
| | Tetrahydrofuran | 291 | 414 | 22.61 |
| 2,5-dimethyl-3-phenoxy pyrazine (69) | Hexane | 294 | 340 | 82.41 |
| | Tetrahydrofuran | 286 | 335 | 31.56 |

Fluorescence reading with respect to distilled water, where distilled water = 0

Figure 3.19 and Figure 3.20 show fluorescence spectra of compound (50), (65) and (69) in hexane and tetrahydrofuran in 3.8314×10^{-4} M respectively.

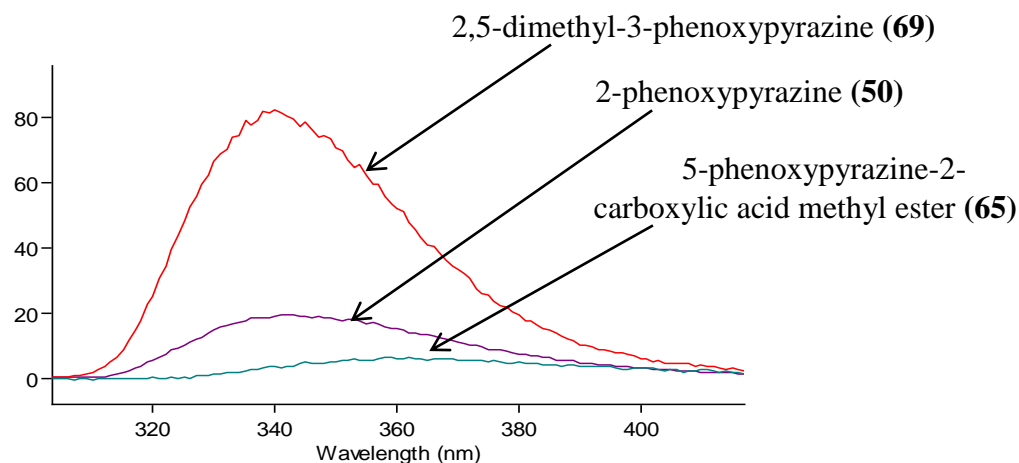


Figure 3.19: Fluorescence spectra of compound (50), (65), and (69) in hexane at 3.8314×10^{-4} M

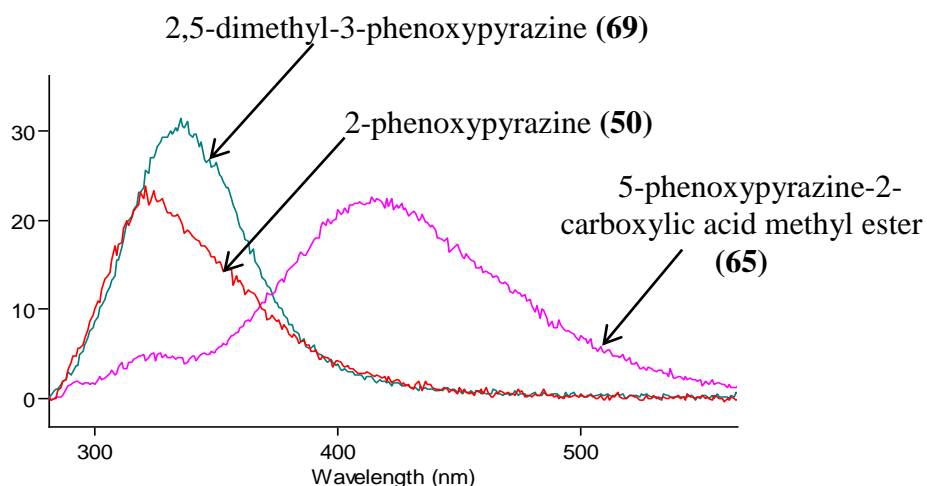


Figure 3.20: Fluorescence spectra of compound (50), (65), and (69) in tetrahydrofuran at 3.8314×10^{-4} M

Similar observations were observed with 2-phenoxy pyrazine (50), 2,5-dimethyl-3-phenoxy pyrazine (69) whereby the presence of electron-donating group gave higher fluorescence intensity, whereas 5-phenoxy pyrazine-2-carboxylic acid methyl ester (65), which has an electron-withdrawing group showed lower fluorescence intensity.

Introducing two methyl groups at π electron deficient heterocyclic pyrazine ring^[69-73] in 2-phenoxy pyrazine (50), stabilized the pyrazine ring through resonance effect by

increasing the electron density at the pyrazine ring. Thus as explained before, the presence of electron donating substituent is capable of increasing fluorescence intensity. As a result, compound (69) showed higher fluorescence intensity than compound (50) due to electron donating group effect.

On the other hand, compound (65) showed lowest fluorescence intensity probably due to the $-\text{COOCH}_3$ substituent that introduce $n-\pi^*$ transitions in the molecule, which lead to diminish fluorescence intensity by encouraging intersystem crossing from the excited singlet state to the triplet state as discussed earlier. Thus, the observation is in agreement with the previously recorded observation for compounds (66), (65), and (67).

A series of substituted *ortho*-, *meta*-, and *para*- of 2-methoxypyrazine derivatives were synthesized to investigate the effect of positions of substitution on fluorescence characteristic. Table 3.12 showed fluorescence characteristics of 2-*o*-tolylloxypyrazine (52), 2-*m*-tolylloxypyrazine (54), and 2-*p*-tolylloxypyrazine (56) in various solvents

Table 3.12: Fluorescence characteristic of 2-*o*-tolylloxypyrazine (52), 2-*m*-tolylloxypyrazine (54), and 2-*p*-tolylloxypyrazine (56) in various solvents at concentration 3.8314×10^{-4} M

| Compounds | Solvents | Excitation (nm) | Fluorescence wavelength (nm) | Fluorescence intensity |
|--|-----------------|-----------------|------------------------------|------------------------|
| 2-(<i>o</i> -methyl)phenoxy pyrazine (52) | Hexane | 293 | 343 | 335.37 |
| | Tetrahydrofuran | 281 | 343 | 44.45 |
| | Ethanol | 279 | 304 | 83.66 |
| | Ethyl acetate | 299 | 348 | 277.39 |
| 2-(<i>m</i> -methyl)phenoxy pyrazine (54) | Hexane | 288 | 341 | 4.92 |
| | Tetrahydrofuran | 303 | 363 | 9.30 |
| | Ethanol | 302 | 359 | 9.32 |
| | Ethyl acetate | 302 | 359 | 9.31 |
| 2-(<i>p</i> -methyl)phenoxy pyrazine (56) | Hexane | 277 | 368 | 50.06 |
| | Tetrahydrofuran | 277 | 311 | 32.16 |
| | Ethanol | 278 | 323 | 12.41 |
| | Ethyl acetate | 279 | 294 | 47.00 |

Fluorescence reading with respect to distilled water, where distilled water = 0

Figure 3.12 showed a histogram of the fluorescence intensity of compounds (52), (54), and (56) in hexane, tetrahydrofuran, ethanol, and ethyl acetate.

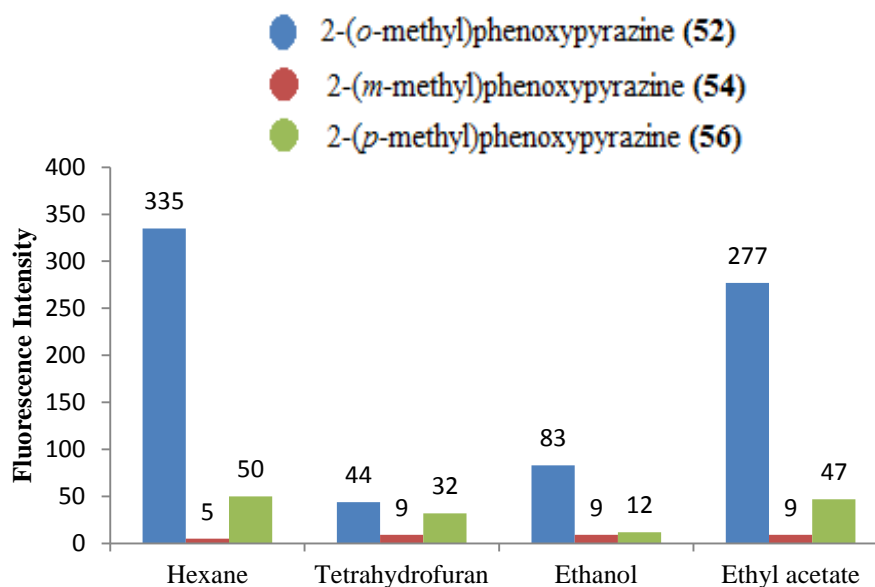


Figure 3.21: Fluorescence characteristic of 2-*o*-toloxypyrazine (52), 2-*m*-toloxypyrazine (54), and 2-*p*-toloxypyrazine (56) in various solvents at concentration 3.8314×10^{-4} M

It can be seen from Table 3.12 and Figure 3.21 above that introducing methyl group to *ortho*-, *meta*-, and *para*- position in benzene ring to 2-phenoxy pyrazine (50) caused a dramatic effect on fluorescence efficiency. Fluorescence intensity is in the order of 2-*o*-toloxypyrazine (52) > 2-*p*-toloxypyrazine (56) > 2-*m*-toloxypyrazine (54) regardless of solvent polarity. It indicates that, addition of electron-donating group substituent at *ortho* leads to more fluorescence efficiency, followed by *para* and *meta* positions. Compounds (52) and (56) with electron-donating group at *ortho* and *para* position respectively exhibit higher fluorescence intensity than compound (54) which have methyl group at *meta* position probably due to inductive and resonance effect in benzene ring. The presence of strong electronegative oxygen atom adjacent to π system, activate the aromatic ring by increasing the electron density on the ring through a resonance donating effect. Figure 3.22 below showed resonance mechanism in 2-phenoxy pyrazine (50), parent compound for compound (52), (54), and (56).

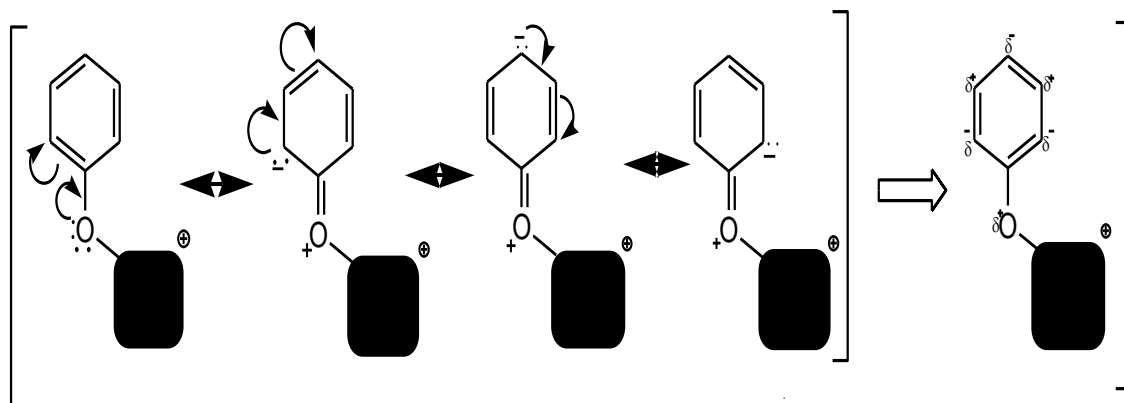


Figure 3.22: Resonance mechanism in 2-phenoxy pyrazine (50)

Hence, resonance effect in Figure 3.22 allowed electron density to be positioned at the *ortho* and *para* positions more than *meta* position^[74]. Thus, addition of methyl group at *ortho* and *meta* positions enhanced more the reactivity of aromatic structure and increasing the availability of π electrons in the ring. In addition, since the basic strength of cresols decrease in the order *o*-cresol > *p*-cresol > *m*-cresol^[75-77]. Therefore, compound (56) results in highest fluorescence intensity followed by compound (52) and (54).

CHAPTER 4: CONCLUSION

Eleven compounds were successfully synthesised and were characterized using ^1H NMR, ^{13}C NMR, GC-Mass Spectrometry, and IR spectroscopy.

Fluorescence characteristic of compounds were studied in three different concentrations (3.8314×10^{-4} M, 3.8314×10^{-5} M, and 3.8314×10^{-6} M) and the fluorescence intensity is proportional to the concentration of compounds.

Studies on the effect of fluorescence characteristic in the presence of air were carried out by measuring the fluorescence intensity of compounds **(52)**, **(56)** and **(69)** in acetonitrile with constant concentration in three different time frames. From the results obtained, all compound showed fluorescence intensity diminished with time, apart from that, there were no change in spectra shape and no shift in fluorescence maxima during quenching process. In case of pHs, different pH affect fluorescence intensity, for compounds **(50)** and **(67)** within the five different pH studied, covering acid, neutral and basic conditions. Both compounds exhibit strong emission in basic media but quenched in acidic media. Both phenomenon appeared due to quenching effect of hydrogen ions on fluorescence intensity.

Heterocyclic compounds fluorescence behaviour are solvent dependent. To understand the effect of different solvents to fluorescence spectra, compounds **(52)**, **(56)**, and **(69)** were measured in four different solvents with wide range of solvent polarity. All compounds showed highest emission in nonpolar solvents and fluorescence intensity gradually diminished with increasing solvent polarity. Drastic fall was observed by all compounds when polar aprotic solvents were used. The explanation of this phenomenon was discussed in discussion part.

Molecular structure showed profound effect in fluorescence characteristic. The molecular structure of a molecule determines the energies of the ground and excited states of fluorescing, which usually exerted in the positions (energies) of the fluorescence maxima. In this study, we focus on the effect of compound rigidity, linearity, different substitution position, electron-withdrawing group and electron-donating group to fluorescence spectra. Compound (60) showed highest fluorescence intensity and bathochromic shift compared to compounds (50) and (58) due to rigidity and planar system structures.

The effect of substituents on the fluorescence characteristics of aromatic hydrocarbons are quite complex. The nature of substituents can also alter the fluorescence characteristic tremendously. A series of phenoxy pyrazines that were modified at phenyl ring were prepared. Methyl group substituent with electron donating group properties was introduced in compound (66) and $-\text{NO}_2$ electron accepting substituents was introduced in compound (67) and their parent compound, compound (65) was synthesized in order to investigate the effect of substituents nature to fluorescence characteristics. It was believed that compound (66) showed highest fluorescence intensity engendered by the presence of electron donating group which is capable to enhance fluorescence efficiency by increasing electron density at benzene ring and through “*meta* effect”. In contrary, introducing electron withdrawing group $-\text{NO}_2$ substituent in compound (67) quenched the fluorescence intensity due to the existence of a low-lying $n-\pi^*$ transitions.

On the other hand, introducing methyl group substituent at different positions in the benzene ring in compounds synthesized showed dramatic effect to fluorescence spectra of compounds (52), (54), and (56). Compounds (52) and (56) with electron donating group at *ortho* and *para* position respectively in benzene ring exhibit high fluorescence intensity, than compound (54) with methyl group at *meta* position in compound (54)

showed nearly fluorescence quenching attributed to inductive and resonance effect in the benzene ring.

The work should be extended to synthesis using 3-chloro-2,5-dimethylpyrazine (**68**) and piperidine (**61**) as starting materials to react with phenol derivatives and pyrazine derivatives respectively. It is hoped that, this research should be extended to not only nitrogen containing heterocycles but to 'O' and 'S' containing heterocycles. Since interesting findings were observed with piperidino pyrazines, future work may be expanded in looking at various amino derivatives of pyrazines with substituents on the pyrazine ring.

CHAPTER 5: EXPERIMENTAL DETAILS

5.0 General procedures

All solvents used are AR gred and were distilled pure before using. Unless otherwise stated. All reagents and organic solvents were used as received from commercial suppliers.

Analytical Thin Layer Chromatography (TLC) was performed using aluminium sheets, silica gel 60 F₂₅₄. Spots were developed in ethyl acetate:hexane as the solvent or eluent and viewed under ultra violet light or in potassium permanganate solution.

¹H-NMR and ¹³C-NMR were recorded in CDCl₃ on the JEOL FT-NMR Lambda 400 MHz spectrometer and FT-NMR AVN 400 MHz. Chemical shifts are reported in ppm and on δ scale and the coupling constant was reported in Hz.

Mass spectra were recorded with GC-MS Hewlett-Packard HP 6890 series with mass selective indicator and GCMS QP5050a Shimadzu in hexane solvent.

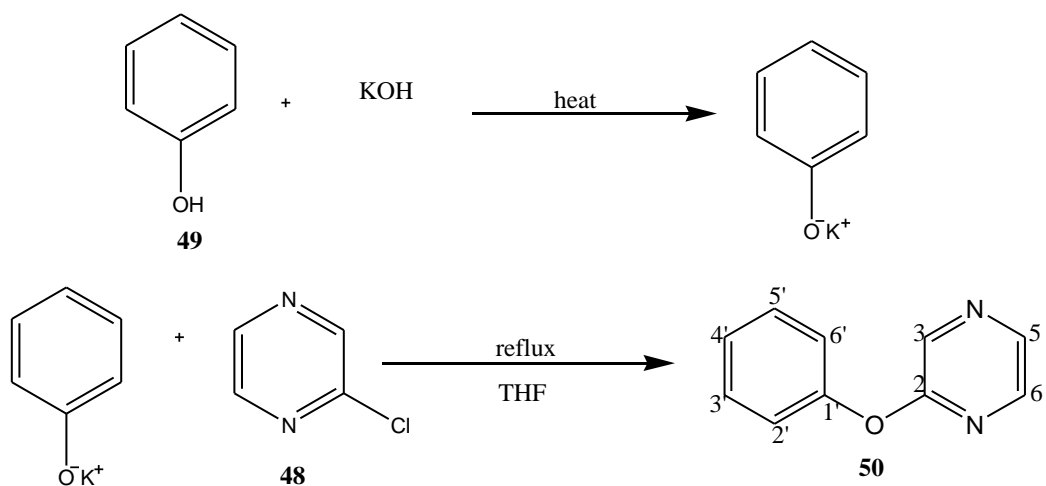
Infrared spectra were recorded using Perkin Elmer 298 in KBr for solid compounds and neat for liquid compounds.

Fluorescence spectra were recorded by Fluorescence Spectrometer, Model Cary Eclipse. The measurements were recorded at the same setting, at the room temperature and quartz cell were used.

5.1 Preparation of pyrazine and naphthalene derivatives

5.1.1 Pyrazine derivatives

5.1.1.1 Preparation of phenoxypyrazine (50)

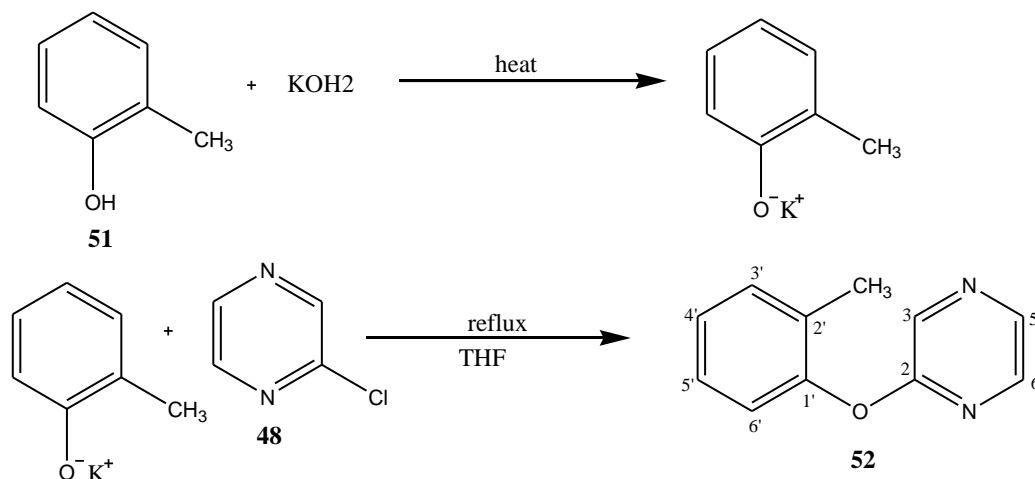


Procedure:

Phenol (**49**) (2.000 g, 0.02 moles) was added to potassium hydroxide pellet (1.430 g, 0.03 moles) in minimum volume of water (5 ml). The mixture was heated until a dry white solid was formed. 2-Chloropyrazine (**48**) (2.27 ml, 0.03 mole) in THF (5 ml) was then added to the dry white solid and refluxed for 5 hours. The mixture was cooled to room temperature and the solvent was removed. Water (10 ml) was added to the reaction mixture followed by extraction with chloroform (3×10 ml). The organic layer was washed twice with water (2×10 ml) and dried over anhydrous sodium sulphate. Filtration and evaporation of chloroform and recrystallization gave the pure product of 2-phenoxypyrazine (**50**). M.p. $48^{\circ}\text{C} - 50^{\circ}\text{C}$, (1.6613 g, 45%), IR (ν_{max} , cm^{-1}): 1578 ($\text{C}=\text{N}$), 1534 and 1406 (aromatic $\text{C}=\text{C}$), 1283 and 1007 ($\text{C}-\text{O}$); ^1H -NMR (ppm, 400 MHz, CDCl_3) δH : 8.43 (1H, d, $J=1.4$ Hz, H-3), 8.26 (1H, d, $J=2.7$ Hz, H-6), 8.10 (1H, dd, $J=1.4$ Hz, 1.4 Hz, H-5), 7.42 (2H, t, $J=7.5$ Hz, 7.6 Hz, H-3', H-5'), 7.24 (1H, t, $J=7.12$ Hz, H-4'), 7.15 (2H, dd, $J=1.2$ Hz, 0.9 Hz, H-2', H-6'); ^{13}C NMR δC ; 160.3

(C-2), 153.1 (C-1'), 141.1 (C-6), 138.5 (C-5), 135.9 (C-3), 129.9 (C-3', C-5'), 125.5 (C-4'), 121.3 (C-2', C-6'); M^+ found=172.00; $C_{10}H_8N_2O$ requires $M^+ = 172.06$.

5.1.1.2 Preparation of 2-*o*-methylphenoxy pyrazine (52)

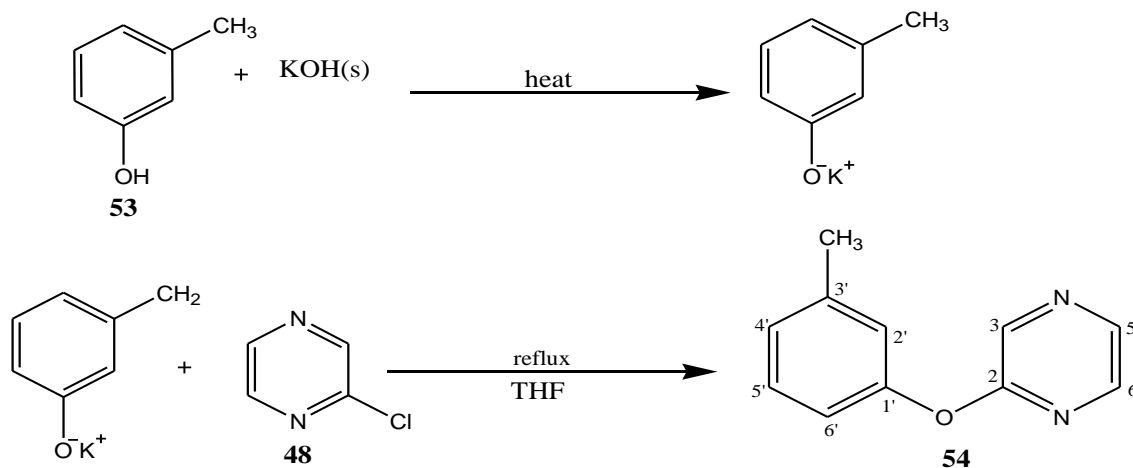


Procedure:

Minimum amount of water was added into potassium hydroxide pellet (3.660 g, 0.65 moles), all potassium hydroxide pellet were dissolved in sonicator. *o*-Cresol (51) (6.77 ml, 0.65 moles) was added into the reaction mixture and the mixture was heated until the solution mixture turn to solid form. The reaction was continued by the addition of 2-chloropyrazine (48) (2.97 ml, 0.03 moles) in THF (12 ml) to the dry white solid and the mixture was refluxed for 7 hours. The mixture was cooled to room temperature and the solvent was removed under *vacuo*. The mixture extracted with chloroform (3 × 10 ml). The organic layer was washed three times with water (3 × 10 ml) and dried over anhydrous sodium sulphate. Filtration and evaporation of chloroform and recrystallization in acetonitrile gave yellowish liquid product of 2-*o*-phenoxypyrazine (52) (4.7002 g, 57.88 %), IR (ν_{max} , cm^{-1}): 1579 (C=N), 1530 and 1399 (aromatic C=C), 1278 and 1007 (C-O); 1H -NMR (ppm, 400 MHz, $CDCl_3$) δ_H : 8.35 (1H, d, $J=1.4$ Hz, H-3), 8.16 (1H, d, $J=2.6$ Hz, H-6), 8.01 (1H, dd, $J=1.3$ Hz, 1.3 Hz, H-2), 7.17 (2H, m, H-4', H-5'), 7.10 (1H, dd, $J=1.2$ Hz, 2.7 Hz, H-3'), 6.99 (1H, dd, $J=0.9$ Hz, 0.8 Hz,

H-6'), 2.11 (3H, s, CH₃); ¹³C NMR δ_C: 160.2 (C-2), 151.2 (C-1'), 141.3 (C-6), 138.0 (C-5), 135.3 (C-3), 131.6 (C-3'), 130.7 (C-2'), 127.3 (C-5'), 125.9 (C-4'), 121.7 (C-6'), 16.3 (CH₃); MS: M⁺ found=186.00 ; C₁₁H₁₀N₂O requires M⁺=186.08.

5.1.1.3 Preparation of 2-(*m*-methyl)phenoxy pyrazine (**54**)

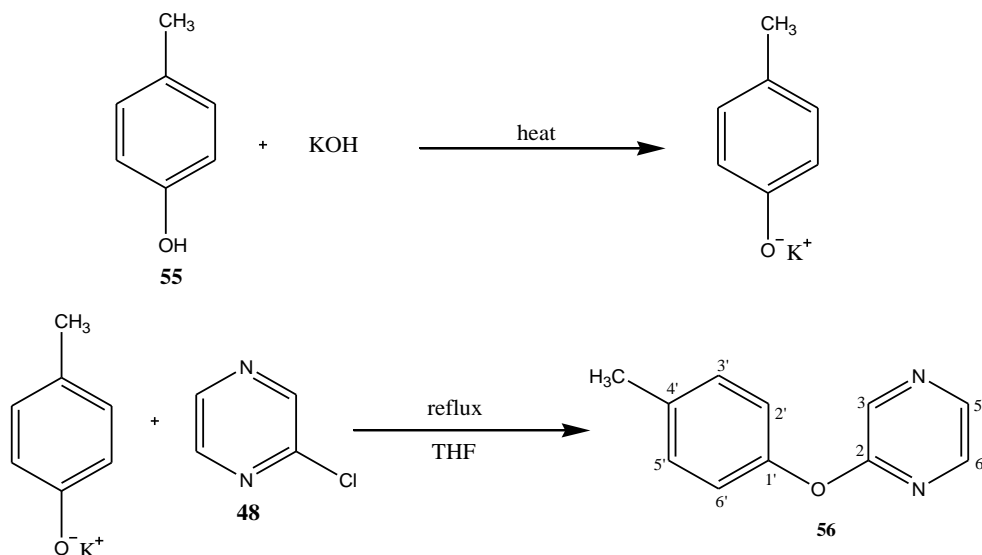


Procedure:

3-Methylphenol (**53**) (3.00 mL, 0.03 moles) was added to potassium hydroxide pellet (1.600 g, 0.03 moles) in minimum volume of water (5.00 mL). The mixture was heated until a dry white solid was formed. 2-Chloropyrazine (**48**) (3.20 mL, 0.04 moles) in 12 mL THF was then added to the dry white solid and refluxed for 7 hours and 30 minutes. The mixture was cooled to room temperature and the solvent was removed under *vacuo*. Water (10 mL) was added to reaction mixture followed by extraction with chloroform (3 x 10 mL). The organic layer was washed three times with distilled water (3 x 10 mL) and dried over anhydrous magnesium sulphate. Filtration and evaporation of chloroform solvent gave crude product which was further recrystallized from acetonitrile gave pure 2-(*m*-tolxyloxy)pyrazine (**54**). M. p. 54-56 °C, (3.3391 g, 65.55 %), IR (ν_{max} , cm⁻¹): 1613 (C=N), 1531 and 1466 (aromatic C=C), 1279 and 1007 (C-O); ¹H-NMR (ppm, 400 MHz, CDCl₃) δ_H: 8.41 (1H, d, *J*=1.2 Hz, H-3), 8.25 (1H, d, *J*=2.7 Hz, H-5), 8.11 (1H, dd, *J*=1.4 Hz, 1.4 Hz, H-6), 7.30 (1H, t, *J*=7.8 Hz, 7.7 Hz, H-5'), 7.06 (1H, d, *J*=7.6 Hz, H-6'), 6.97 (1H, s, H-2'), 6.95 (1H, dd, *J*=11.0 Hz, 7.3 Hz, H-

4'), 2.39 (3H, s, CH₃); ¹³C NMR δ_C: 160.4 (C-2), 153.0 (C-1'), 141.2 (C-3), 140.1 (C-3'), 138.4 (C-6), 135.9 (C-5), 129.6 (C-6'), 126.3 (C-2'), 121.8 (C-5'), 118.2 (C-4'), 2.39 (CH₃); MS: M⁺ found=186.00; C₁₁H₁₀N₂O requires M⁺=186.21.

5.1.1.4 Preparation of 2-*p*-methylphenoxypyrazine (56)

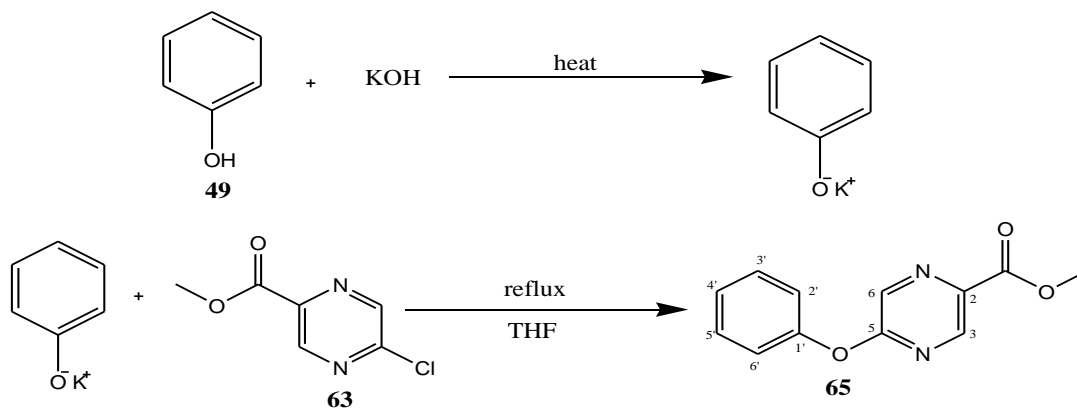


Procedure:

p-Cresol (**55**) (2.94 mL, 0.03 moles) was added to potassium hydroxide pellet (1.868 g, 0.03 moles) in (5 mL) volume of distilled water. The mixture was heated until a dry white solid was formed. 2-Chloropyrazine (**48**) (3.90 ml, 0.44 moles) in THF (5 ml) was added to the solid mixture and the mixture was refluxed for 5 hours 30 minutes. The mixture was cooled to room temperature and the solvent was removed under *vacuo*. The mixture extracted with chloroform (3 × 10 ml). The organic layer was washed three times with water (3 × 10 ml) and dried over anhydrous sodium sulphate. Filtration and evaporation of chloroform and recrystallization gave the pure product of (**56**). M.p. 44-46 °C, (0.7068 g, 93.00 %), IR (ν_{max} , cm⁻¹): 1580 (C=N), 1504 and 1404 (aromatic C=C), 1281 and 1006 (C-O); ¹H-NMR (ppm, 400 MHz, CDCl₃) δ_H: 8.41 (1H, d, *J*=1.4 Hz, H-3), 8.23 (1H, d, *J*=2.6 Hz, H-6), 8.10 (1H, dd, *J*=1.4 Hz, 1.4 Hz, H-5), 7.08 (2H, d, *J*=8.9 Hz, H-3', H-5'), 6.94 (2H, d, *J*=8.9 Hz, H-2', H-6'), 3.83 (3H, s, CH₃); ¹³C

NMR δ_C ; 160.5 (C-2), 154.0 (C-1'), 141.2 (C-6), 138.2 (C-5), 135.7 (C-3), 135.2 (C-4'), 130.4 (C-3', C-5'), 121.1 (C-2', C-6'), 20.9 (CH₃); MS: M⁺ found=186.00; C₁₁H₁₀N₂O requires M⁺=186.21 .

5.1.1.5 Preparation of 5-phenoxy pyrazine-2-carboxylic acid methyl ester (65)

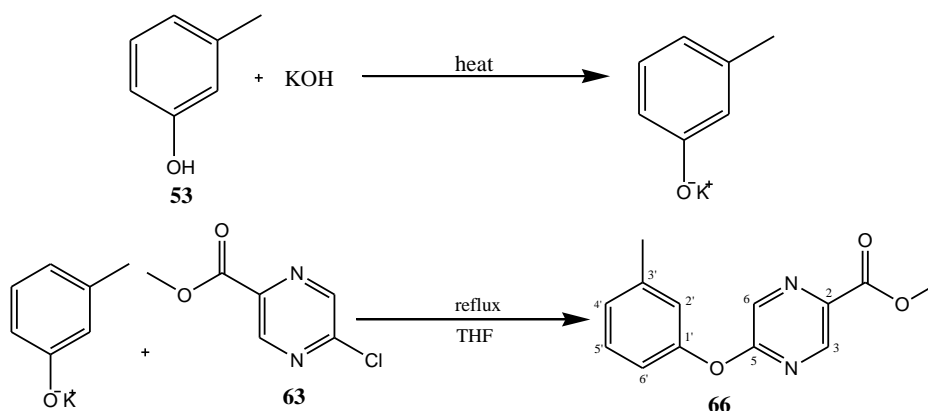


Procedure:

Phenol (**49**) (1.250 g, 0.01 moles) was added to potassium hydroxide pellet (0.7400 g, 0.01 moles) in minimum volume of distilled water (5 mL). The mixture was heated until a dry solid was formed. 5-Chloropyrazine-2-carboxylic acid methyl ester (**63**) (2.0000 g, 0.01 moles) in THF (5 mL) was then added to the dry white solid and refluxed for 7 hours. The mixture was cooled to room temperature and the solvent was removed under *vacuo*. The procedure followed by extraction of the mixture with chloroform (3 × 10 ml). The organic layer was washed twice with water (3 × 10 ml) and dried over anhydrous sodium sulphate. Filtration and evaporation of chloroform and recrystallization in acetonitrile and chloroform solvent (1:1) gave the pure product of 5-phenoxy pyrazine-2-carboxylic acid methyl ester (**65**). M. p. 96-98 °C, (1.9081 g, 75.07 %), IR (ν_{max} , cm⁻¹): 1347 (C=N), 1456 and 1540 (aromatic C=C), 1188 and 1279 (C-O), 1738 (C=O); ¹H-NMR (ppm, 400 MHz, CDCl₃) δ_H : 8.84 (1H, d, J =1.2 Hz, H-6), 8.50 (1H, d, J =1.2 Hz, H-3), 7.47 (2H, t, J =7.9 Hz, H-3', H-5'), 7.31 (1H, t, J =7.6 Hz, H-4'), 7.19 (2H, dd, J =1.0 Hz, 1.2 Hz, H-2', H-6'), 4.03 (3H, s, CH₃); ¹³C NMR δ_C : 164.2 (C=O), 161.7 (C-2), 152.3 (C-5), 144.2 (C-3), 137.3 (C-1'), 135.4 (C-6), 129.9 (C-2', C-

6'), 126.1 (C-4'), 121.3 (C-3', C-5'), 52.8 (O-CH₃); MS: M⁺ found=230.00; C₁₂H₁₀N₂O₃ requires M⁺ = 230.07.

5.1.1.6 Preparation of 5-*m*-toloxypyrazine-2-carboxylic acid methyl ester (**66**)



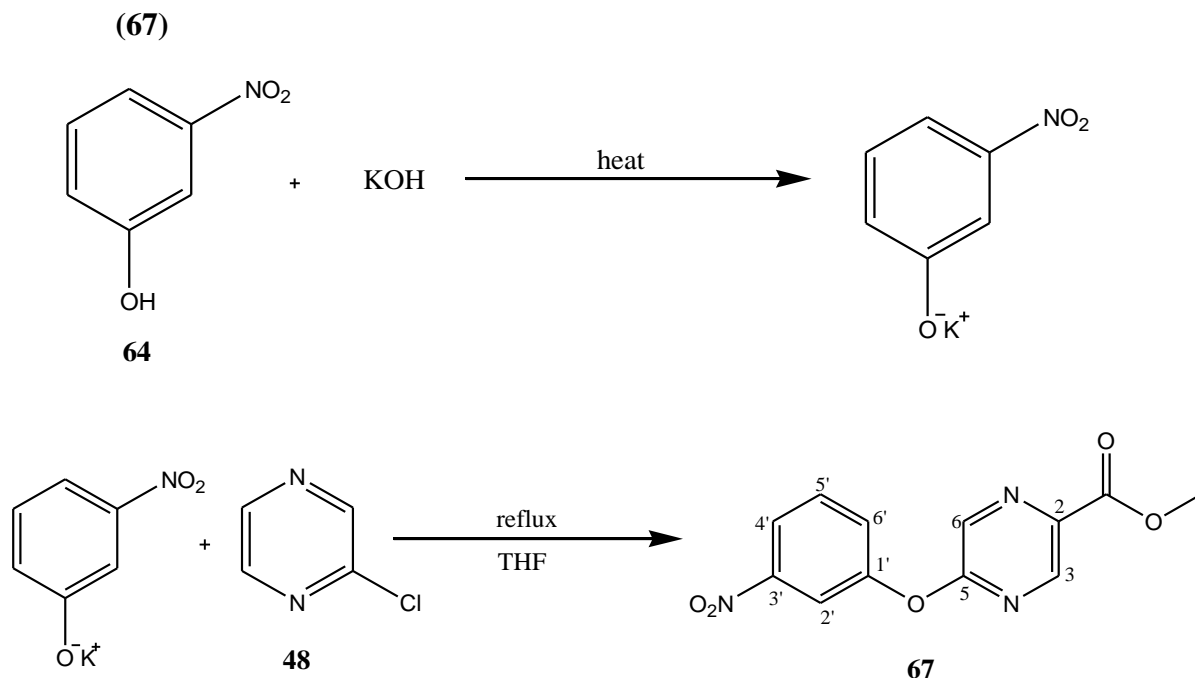
Procedure:

m-Cresol (**53**) (0.8 ml, 0.007 moles) was added to the potassium hydroxide pellet (1.0000 g, 0.018 moles) which was dissolved in minimum volume of distilled water. The mixture was heated until dark brown solid was formed. Methyl-5-chloro-2-pyrazinecarboxylate (**63**) (1.220 g, 0.007 moles) in THF (12 ml) was added to the dry dark brown solid and was refluxed for 6 hours. Then, the mixture was cooled under room temperature and THF solvent was removed under *vacuo*. Water (10 ml) was added to the mixture and the mixture was extracted with chloroform (3 x 10 ml). The organic layer then washed three times with distilled water (3 x 10 ml) and dried over anhydrous magnesium sulphate. Filtration and evaporation of chloroform solvent gave orange oil crude product which further recrystallized from acetonitrile gave pure 5-*m*-Toloxypyrazine-2-carboxylic acid methyl ester (**66**). M. p. 66-68 °C, (1.3010 g, 75.34 %), IR (ν_{max} , cm⁻¹): 1576 (C=N), 1537 and 1456 (aromatic C=C), 1274 and 1001 (C-O), 1737 (C=O); ¹H-NMR (ppm, 400 MHz, CDCl₃) δ_H : 8.84 (1H, s, H-6), 8.48 (1H, s, H-3), 7.32 (1H, t, *J*=7.7 Hz, 7.6 Hz, H-5'), 7.11 (1H, d, *J*=7.6 Hz, H-4'), 6.99 (1H, s, H-2'), 6.96 (1H, d, *J*=9.2 Hz, H-6'), 4.01 (3H, s, OCH₃), 2.40 (3H, s, CH₃); ¹³C NMR δ_C : 164.2 (C=O), 161.8 (C-5), 152.3 (C-2), 144.3 (C-3), 140.3 (C-1'), 137.1 (C-3'), 135.3

(C-6), 129.6 (C-5'), 127.0 (C-4'), 121.8 (C-2'), 118.2 (C-6'), 52.8 (O-CH₃), 21.4 (CH₃);

MS: M⁺ found=244.00 ;C₁₃H₁₂N₂O₃ requires M⁺ = 244.08.

5.1.1.7 Preparation of 5-(3-nitrophenoxy)pyrazine-2-carboxylic acid methyl ester

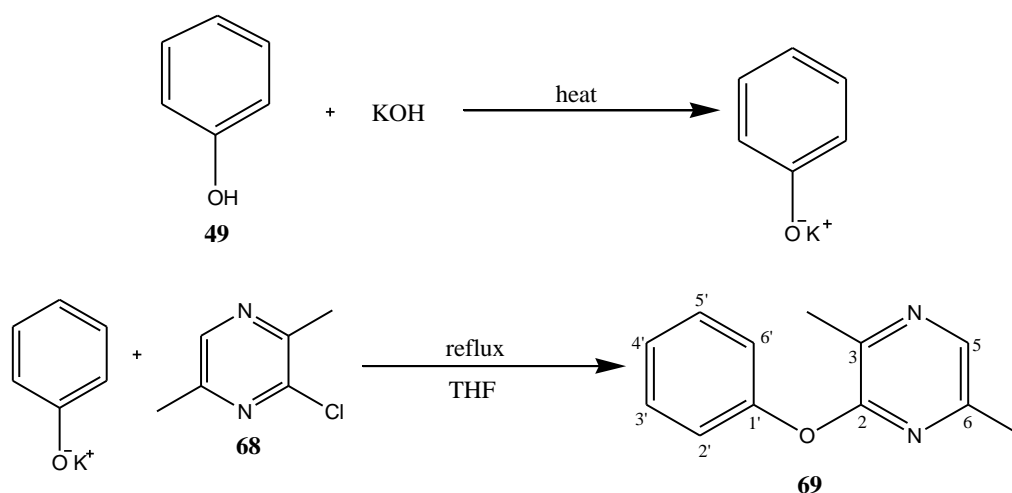


Procedure:

Potassium hydroxide pellet (0.2000 g, 0.004 moles) was dissolved in water (5 ml) and *m*-nitrophenol (**64**) (0.5000 g, 0.003 moles) was added to the solution and stirred for 10 minutes at room temperature. The mixture was then heated with heating mantle until white solid formed. Then, the mixture left at room temperature until it cools. Methyl-5-chloro-2-pyrazine carboxylate (**63**) (0.5000 g, 0.003 moles) in THF (12 ml) was added to the reaction mixture and refluxed for 6 hours 30 minutes. The mixture was cooled and the solvent was evaporated off. The mixture was then extracted three times with chloroform (3 x 10 ml). The organic layer was washed with water (3 x 10 ml) and dried over sodium sulphate. Evaporation of chloroform gave crude product with orange colour solid which was purified using column chromatography on silica using ethyl acetate-hexane mixture (1:1.5) as the solvent. Evaporation of the solvent gave 5-(3-

Nitrophenoxy)pyrazine-2-carboxylic acid methyl ester (**67**). M. p. 120-124 °C, (0.6081 g, 80.11 %), IR (ν_{max} , cm^{-1}); 1304 (C-N), 1578 (C=N), 1473 and 1526 (aromatic C=C), 1194 and 1271 (C-O), 1737 (C=O), 1737 and 1342 (N-O); $^1\text{H-NMR}$ δ_{H} : 8.83 (1H, d, $J=1.3$ Hz, H-3), 8.60 (1H, d, $J=1.3$ Hz, H-6), 8.17 (1H, ddd, $J=1.04$ Hz, H-4'), 8.11 (1H, t, $J=2.1$ Hz, H-2'), 7.63 (1H, t, $J=8.12$ Hz, H-5'), 7.55 (1H, ddd, $J=1.0$ Hz, H-6'), 4.03 (3H, s, CH_3); $^{13}\text{C NMR}$ δ_{C} : 163.9 (C=O), 160.6 (C-5), 152.5 (C-2), 149.1 (C-3'), 143.8 (C-3), 138.3 (C-1'), 135.5 (C-6), 130.5 (C-5'), 127.8 (C-4'), 120.9 (C-2'), 117.2 (C-6'), 52.8 (OCH_3); MS: M^+ found=275.00; $\text{C}_{12}\text{H}_9\text{N}_3\text{O}_5$ requires $\text{M}^+=275.22$.

5.1.1.8 Preparation of 2,5-dimethyl-3 phenoxypyrazine (**69**)

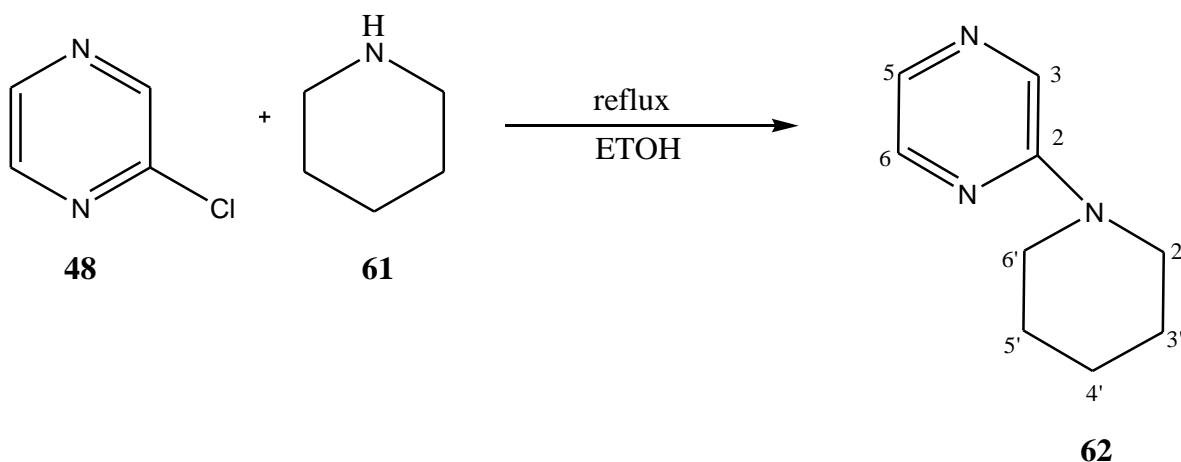


Procedure:

Minimum volume of water (5 ml) was added to potassium hydroxide pellet (2.84 g, 0.05 moles). After all potassium hydroxide was dissolved, phenol (**49**) (3.5800 g, 0.04 moles) was added. The mixture was heated until a dry white solid was formed. 3-Chloro-2,5-dimethyl pyrazine (**68**) (2.00 ml, 0.03 mol) in THF (5 ml) was then added to the dry white solid and refluxed for 5 hours. The mixture was cooled to room temperature and the solvent was removed. The mixture extracted with chloroform (3×10 ml). The organic layer was washed twice with water (2×10 ml) and dried over anhydrous sodium sulphate. Filtration and evaporation of chloroform and recrystallization gave the dark orange liquid product of 2,5-dimethyl-3-

phenoxy pyrazine (**69**). (4.0931 g, 80.54 %), (4.0931 g, 80.54 %), IR (ν_{max} , cm^{-1}): 1592 (C=N), 1539 and 1490 (aromatic C=C), 1286 and 1003 (C-O); $^1\text{H-NMR}$ δ_{H} : 8.02 (1H, s, H-2), 7.37 (2H, t, $J=8.3$ Hz, $J=7.6$ Hz, H-3', H-5'), 7.18 (1H, t, $J=7.4$ Hz, $J=7.4$ Hz, H-4'), 7.12 (2H, dd, $J=1.0$ Hz, $J=0.8$ Hz, H-2', H-6') 2.57 (3H, s, C-3-CH₃), 2.33 (3H, s, C-6-CH₃); ^{13}C NMR δ_{C} : 157.2 (C-5), 153.8 (C-1'), 148.4 (C-3), 141.6 (C-6), 137.1 (C-2), 129.4 (C-3', C-5'), 124.5 (C-4'), 120.8 (C-2', C-6'), 20.6 (C-3-CH₃), 18.9 (C-6-CH₃); MS: M^+ found=200.00; C₁₂H₁₂N₂O requires M^+ =200.09.

5.1.1.9 Preparation of 2-N-piperidinopyrazine (**62**)



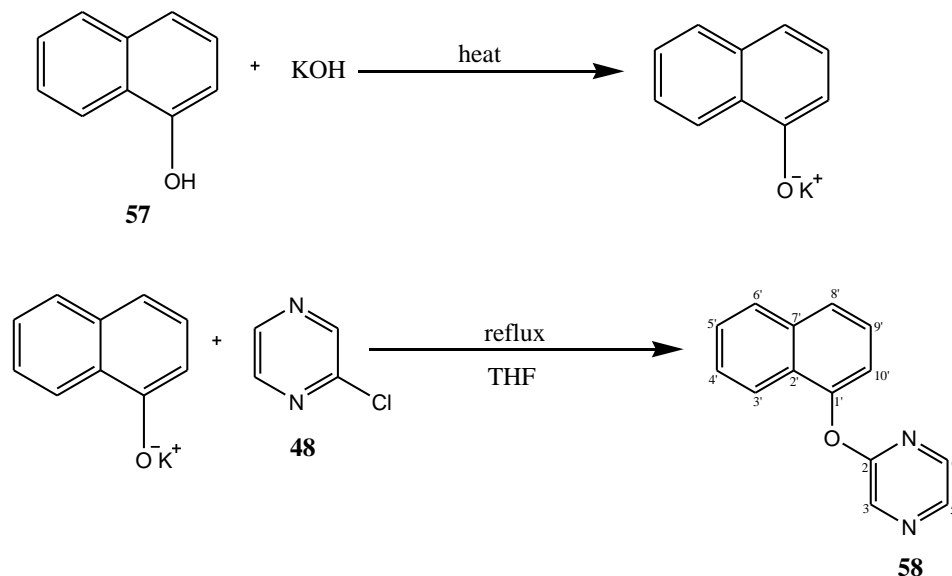
Procedure:

2-Chloropyrazine (**48**) (0.40 ml, 4.516 mmoles) was added to a solution of piperidine (**61**) (5.00 ml, 0.05 moles) in ethanol and the mixture was refluxed for 2 hours. The mixture was then cooled and the solvent was evaporated off. The residue was dissolved in water and then extracted with diethyl ether (3×10 ml). The ether extracts were washed with water (3×10 ml) and dried over anhydrous sodium sulphate. Evaporation of the solvent gave the product, a yellowish liquid which was purified by washing with several portions of diethyl ether. (0.561 g, 76%); IR (ν_{max} , cm^{-1}): 1672 (C=N), 1517 (C=C), 2935 (C-H); ^1H NMR (ppm, 400 MHz, CDCl₃) δ_{H} : 8.05 (1H, d, $J=1.4$ Hz, H-3), 7.96 (1H, dd, $J=2.6$ Hz, 1.4 Hz, H-5), 7.69 (1H, d, $J=2.6$ Hz, H-6), 3.49 (4H, s, H-2', H-6'), 1.55 (6H, s, H-3', H-4', H-5'); ^{13}C NMR (ppm, 100 MHz, CDCl₃) δ_{C} : 155.0

(C-2), 141.6 (C-3), 131.7 (C-5), 130.9 (C-6), 45.4 (C-2', C-6'), 25.0 (C-5',C-3'), 24.4 (C-4'); GCMS: Found $M^+=163.00$; $C_9H_{13}N_3$ requires $M^+=163.22$.

5.1.2 Naphthalene derivatives

5.1.2.1 Preparation of 2-naphthalen-1-yloxy pyrazine (58)

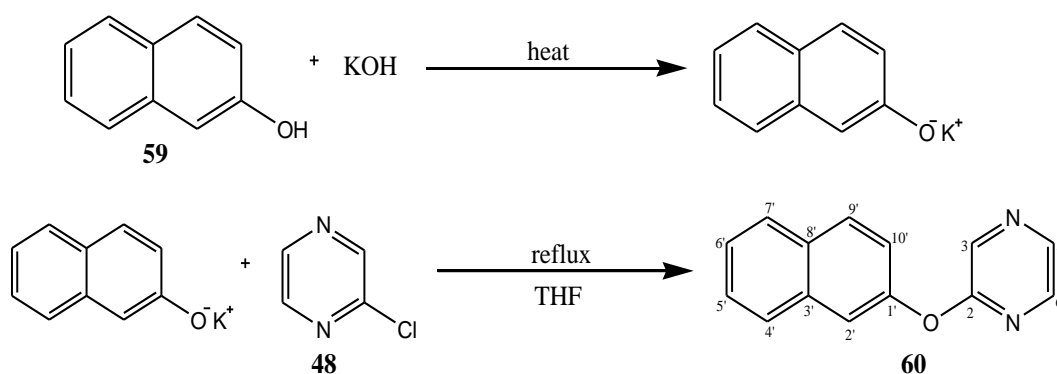


Procedure:

1-Naphthol (**57**) (0.8800 g, 0.006 moles) was added to potassium hydroxide pellet (0.6900 g, 0.006 moles) in minimum volume of water (5 mL). The mixture was heated until a dry white solid was formed. 2-Chloropyrazine (**48**) (0.5 mL, 0.006 moles) in THF (5 mL) was added to the dry brown solid and the mixture was refluxed for 6 hours and 35 minutes. The mixture was cooled to room temperature and the solvent was removed under *vacuo*. Water (10 mL) was added to reaction mixture followed by extraction with chloroform (3 x 10 mL). The organic layer was washed three times with distilled water (3 x 10 mL) and dried over anhydrous magnesium sulphate. Filtration and evaporation of chloroform solvent gave crude product which further recrystallized from ethyl acetate and hexane (1:10) gave pure product of 2-naphthalen-1-yloxy pyrazine (**58**). M. p. 98-102°C, (0.884 g, 66.30 %), IR (ν_{max} , cm^{-1}): 1580 (C=N), 1530 and 1469 (aromatic C=C), 1278 and 1005 (C-O); 1H -NMR (ppm, 400 MHz,

CDCl₃) δ_H : 8.56 (1H, d, J=1.2 Hz, H-3), 8.30 (1H, d, J=2.7 Hz, H-6), 8.09 (1H, dd, J=1.4 Hz, 1.4 Hz, H-5), 7.93 (2H, d, J=9.6 Hz, H-6', H-8'), 7.80 (1H, d, J=8.3 Hz, H-3'), 7.52 (3H, m, H-9', H-5', H-4'), 7.29 (1H, dd, J=1.0 Hz, 0.9 Hz, H-10'); ¹³C NMR δ_C : 160.8 (C-2), 149.0 (C-1'), 141.4 (C-6), 138.6 (C-5), 135.4 (C-3), 135.0 (C-7'), 128.1 (C-6'), 127.2 (C-2'), 126.6 (C-5'), 126.5 (C-4'), 125.8 (C-3'), 125.6 (C-8'), 121.6 (C-9'), 117.4 (C-10'); MS: M⁺ found=222.00; requires C₁₄H₁₀N₂O M⁺ = 222.08.

5.1.2.2 Preparation of 2-naphthalen-2-yloxypyrazine (60)



Procedure:

2-Naphtol (**59**) (4.9900 g, 0.04 moles) was added to potassium hydroxide pellet (3.0200 g, 0.05 moles) which was dissolved in 5 mL distilled water. The mixture was heated until white dry solid formed. 2-Chloropyrazine (**48**) (3.80 mL, 0.03 moles) in 5 mL THF was added to the solid mixture and refluxed for 5 hours. The mixture was cooled to room temperature and the solvent was removed. The crude product was extracted with chloroform (3 x 10 mL). The organic layer part was washed (3 x 10 mL) and dried over anhydrous sodium sulphate. Filtration and evaporation of chloroform followed by recrystallization in toluene and ethyl acetate (3:1) gave the product (5.5287 g, 74.04%). M. p. 90-92 °C, (3.339 g, 65.55 %), IR (ν_{max} , cm⁻¹): 1624 (C=N), 1530 and 1462 (aromatic C=C), 1280 and 1005 (C-O); ¹H-NMR (ppm, 400 MHz, CDCl₃) δ_H : 8.49 (1H, d, J=1.3 Hz, H-3), 8.29 (1H, d, J=2.7 Hz, H-5), 8.11 (1H, dd, J=1.4 Hz, 1.4 Hz, H-4), 7.90 (1H, d, J=8.9 Hz, H-9'), 7.80 (2H, dd, J=7.4 Hz, 1.6 Hz, H-7', H-4'), 7.62 (1H,

d, $J=2.3$ Hz, H-2'), 7.45 (2H, m, H-5', H-6'), 7.29 (1H, dd, $J=2.4$ Hz, 2.4 Hz, H-10'); ^{13}C NMR δ_{C} : 160.4 (C-2), 150.7 (C-1'), 141.3 (C-6), 138.7 (C-5), 136.0 (C-3), 134.2 (C-3'), 131.4 (C-8'), 123.0 (C-9'), 128.0 (C-5'), 127.6 (C-4'), 126.8 (C-7'), 125.7 (C-6'), 121.1 (C-10'), 118.0 (C-2'); MS: M^+ found=222.00 ; $\text{C}_{14}\text{H}_{10}\text{N}_2\text{O}$ requires M^+ =222.08

5.2 Fluorescence measurements

Fluorescence spectra of all compound studied were recorded using fluorescence spectrometer, Model Cary Eclipse using 5 mm slits. All spectra were recorded at room temperature. Sample was prepared from stock solution 3.8314×10^{-4} M of the corresponding compound in ethyl acetate, tetrahydrofuran, acetonitrile, ethanol and hexane to give concentration 3.8314×10^{-5} M, and 3.8314×10^{-6} M.

5.2.1 Fluorescence Measurement of pyrazine derivatives

2-phenoxy pyrazine (50)

2-phenoxy pyrazine (**50**) (0.6 mg) was dissolved in corresponding solvents in 10 mL volumetric flask.

Concentration = 3.8314×10^{-x} M, where $10^x=10^{-4}$, 10^{-5} and 10^{-6}

With respect to distilled water, where distilled water = 0

Excitation and emission slits = 5

2-(*o*-methyl)phenoxy pyrazine (52)

2-(*o*-methyl)phenoxy pyrazine (**50**) (0.7 mg) was dissolved in corresponding solvents in 10 mL volumetric flask.

Concentration = 3.8314×10^{-x} M, where $10^x=10^{-4}$, 10^{-5} and 10^{-6}

With respect to distilled water, where distilled water = 0

Excitation and emission slits = 5

2-(*m*-methyl)phenoxy pyrazine (54)

2-(*m*-methyl)phenoxy pyrazine (**54**) (0.7 mg) was dissolved in corresponding solvents in 10 mL volumetric flask.

Concentration = 3.8314×10^{-x} M, where $10^x = 10^{-4}$, 10^{-5} and 10^{-6}

With respect to distilled water, where distilled water = 0

Excitation and emission slits = 5

2-(*p*-methyl)phenoxy pyrazine (56)

2-(*p*-methyl)phenoxy pyrazine (**56**) (0.7 mg) was dissolved in corresponding solvents in 10 mL volumetric flask.

Concentration = 3.8314×10^{-x} M, where $10^x = 10^{-4}$, 10^{-5} and 10^{-6}

With respect to distilled water, where distilled water = 0

Excitation and emission slits = 5

2-*N*-piperidinopyrazine (62)

2-*N*-piperidinopyrazine (**62**) (0.6 mg) was dissolved in corresponding solvents in 10 mL volumetric flask.

Concentration = 3.8314×10^{-x} M, where $10^x = 10^{-4}$, 10^{-5} and 10^{-6}

With respect to distilled water, where distilled water = 0

Excitation and emission slits = 5

5-phenoxy pyrazine-2-carboxylic acid methyl ester (65)

5-phenoxy pyrazine-2-carboxylic acid methyl ester (**65**) (0.9 mg) was dissolved in corresponding solvents in 10 mL volumetric flask.

Concentration = 3.8314×10^{-x} M, where $10^x = 10^{-4}$, 10^{-5} and 10^{-6}

With respect to distilled water, where distilled water = 0

Excitation and emission slits = 5

5-*m*-toloxypyrazine-2-carboxylic acid methyl ester (66)

5-*m*-toloxypyrazine-2-carboxylic acid methyl ester (**66**) (0.9 mg) was dissolved in corresponding solvents in 10 mL volumetric flask.

Concentration = 3.8314×10^{-x} M, where $10^x = 10^{-4}$, 10^{-5} and 10^{-6}

With respect to distilled water, where distilled water = 0

Excitation and emission slits = 5

5-(3-nitrophenoxy)pyrazine-2-carboxylic acid methyl ester (67)

5-(3-nitrophenoxy)pyrazine-2-carboxylic acid methyl ester (**67**) (1.1 mg) was dissolved in corresponding solvents in 10 mL volumetric flask.

Concentration = 3.8314×10^{-x} M, where $10^x = 10^{-4}$, 10^{-5} and 10^{-6}

With respect to distilled water, where distilled water = 0

Excitation and emission slits = 5

2,5-dimethyl-3-phenoxy pyrazine (69)

2,5-dimethyl-3-phenoxy pyrazine (**69**) (0.8 mg) was dissolved in corresponding solvents in 10 mL volumetric flask.

Concentration = 3.8314×10^{-x} M, where $10^x = 10^{-4}$, 10^{-5} and 10^{-6}

With respect to distilled water, where distilled water = 0

Excitation and emission slits = 5

2-naphthalen-1-yloxy pyrazine (58)

2-naphthalen-1-yloxy pyrazine (**58**) (0.9 mg) was dissolved in corresponding solvents in 10 mL volumetric flask.

Concentration = 3.8314×10^{-x} M, where $10^x = 10^{-4}$, 10^{-5} and 10^{-6}

With respect to distilled water, where distilled water = 0

Excitation and emission slits = 5

2-naphthalen-2-yloxy pyrazine (60)

2-naphthalen-2-yloxy pyrazine (**60**) (0.9 mg) was dissolved in corresponding solvents in 10 mL volumetric flask.

Concentration = 3.8314×10^{-x} M, where $10^x = 10^{-4}$, 10^{-5} and 10^{-6}

With respect to distilled water, where distilled water = 0

Excitation and emission slits = 5

REFERENCES

- Bruice, P. Y. (2004). *Organic Chemistry: Study Guide And Solutions Manual*. (4th ed.). Pearson Prentice Hall.
- Palmer, M. H. (1967). *The structure and reactions of heterocyclic compounds*. London: Edward Arnold, 89-92.
- Wheatley, P. J. (1957). The crystal and molecular structure of pyrazine. *Acta Crystallographica*, 10(3), 182-187.
- Eicher, T., Hauptmann, S., & Speicher, A. (2013). *The Chemistry of Heterocycles: Structures, Reactions, Synthesis, and Applications 3rd*. John Wiley & Sons.
- Schomaker, V. T., & Pauling, L. (1939). The electron diffraction investigation of the structure of benzene, pyridine, pyrazine, butadiene-1, 3, cyclopentadiene, furan, pyrrole, and thiophene. *Journal of the American Chemical Society*, 61(7), 1769-1780.
- Joule J. A. and Mills, K. (2008). *Heterocyclic Chemistry: Reactivity of the Diazines Pyridazine, Pyrimidine and Pyrazine*. (5th ed.). John Wiley & Sons.
- Joule J. A., Mills K., Smith G. F. (1995). *Heterocyclic Chemistry*. (3rd ed). London : Chapman & Hall, 189-224.
- Elderfield, R. C. (1950-67). *Heterocyclic compounds*. New York: Wiley, Vol 6, 377-454.
- Albert, A., Goldacre, R. and Philips, J. (1948). "The strength of heterocyclic bases." *J. Chem. Soc.*, 2240-2249.
- Mahmood K., Hamid, A. H. A. (1988). *Kimia Heterosiklik*, Kuala Lumpur: Dewan Bahasa dan Pustaka, 139-150.

- Jia, C. and Batterman, S. (2010). "A critical review of naphthalene sources and exposures relevant to indoor and outdoor air." *International journal of environmental research and public health* 7(7), 2903-2939.
- Soghoian, S., et al. (2012). "Health risks of using mothballs in Greater Accra, Ghana." *Tropical Medicine & International Health* 17(1), 135-138.
- Gassett, J. W., Wiesler, D. P., Baker, A. G., Osborn, D. A., Miller, K. V., Marchinton, R. L., & Novotny, M. (1997). Volatile compounds from the forehead region of male white-tailed deer (*Odocoileus virginianus*). *Journal of chemical ecology*, 23(3), 569-578.
- Chen, J., Henderson, G., Grimm, C. C., Lloyd, S. W. & Laine, R. A. (1998). Termites fumigate their nests with naphthalene, *Nature* 392, 5558-559.
- Azuma, H., Toyota, M., Asakawa, Y., Kawano, S., *Phytochemistry*, 1996, Vol. 42, 999-1004 .
- Arora, R. (Ed.). (2012). *Microbial Biotechnology: Energy and environment*. India: Defence Research and Development Organization, 280.
- Goodrich, K. R. (2012). "Floral scent in Annonaceae." *Botanical Journal of the Linnean Society* 169(1), 262-279.
- Chen, J., et al. (1998). "Naphthalene in Formosan subterranean termite carton nests." *Journal of agricultural and food chemistry* 46(6), 2337-2339.
- Supaka, N., Juntongjin, K., Damronglerd, S., Delia, M. L., & Strehaiano, P. (2004). Microbial decolorization of reactive azo dyes in a sequential anaerobic-aerobic system. *Chemical Engineering Journal*, 99(2), 169-176.

- Thalacker, C., Röger, C. and Würthner, F. (2006). "Synthesis and Optical and redox properties of core-substituted naphthalene diimide dyes." *The Journal of organic chemistry* 71(21), 8098-8105.
- Clar, E. (1964). *Polycyclic Hydrocarbons*. London: Academic Press Inc. Ltd. Vol. 1, 211-220.
- Mahmood, K., Abdullah, Z., Rahman, N. A. (1993). *Kimia Hidrokarbon Aromatik: Sebatian Aromatik Polinukleus*. Kuala Lumpur: Kursus Pengajian Tinggi Fajar Bakti, 97-115.
- Hepworth, J. D., Waring, D. R. and Waring, M. J. (2002). *Aromatic Chemistry*. (Vol. 3). Thomas Graham House, Science Park, Milton Road, Cambridge CB40WF, UK: The Royal Society of Chemistry), 135-147.
- Tomlinson, M. (1971). *An Introduction to The Chemistry of Benzenoid*. Headington Hill Hall, Pergamon Press.
- Valeur, B. and Berberan-Santos, M. N. (2013). *Molecular fluorescence: principles and applications*. John Wiley & Sons.
- Rost, F. W. (1992). *Fluorescence microscopy* (Vol. 1). Cambridge University Press
- Lakowicz, J. R. (ed.). (2007). *Principles of fluorescence spectroscopy*. Springer.
- Sauer, M., Hofkens, J., and Enderlein, J. (2010). *Handbook of Fluorescence Spectroscopy and Imaging: From Ensemble to Single Molecules*. John Wiley & Sons.
- Schulman, S. G., et al. (1999). *Introduction to fluorescence spectroscopy*. J. Wiley.

- Lee, K. H., Choi, C. S. and Jeon, K. S. (2002). "Fluorescence Tuning Using Conjugated Aromatic Imine Systems." *Journal of Photoscience* 9(3), 71-74.
- Cisse, L., Tine, A., & Aaron, J. J. (1996). Effect of electron donating substituents on the electronic absorption and fluorescence spectra of coumarin derivatives. *Bulletin of the Chemical Society of Ethiopia*, 10(1).
- Crouch, S. R. and James, D. I. (1988). *Spectrochemical analysis*. Prentice Hall.
- Mitschele, J. (1996). "Beer-Lambert Law." *Journal of Chemical Education* 73(11), A260.
- Arık, M., Çelebi, N., & Onganer, Y. (2005). Fluorescence quenching of fluorescein with molecular oxygen in solution. *Journal of Photochemistry and Photobiology A: Chemistry*, 170(2), 105-111.
- Lakowicz, J. R., and Weber, G. (1973). Quenching of fluorescence by oxygen. Probe for structural fluctuations in macromolecules. *Biochemistry*, 12(21), 4161-4170.
- El-Daly, S. A., Okamoto, M., and Hirayama, S. (1995). Fluorescence quenching of N,N'-bis(2,5-di-*tert*-butylphenyl)-3,4:9,10-perylenebis(dicarboximide)(DBPI) by molecular oxygen. *Journal of Photochemistry and Photobiology A: Chemistry*, 91(2), 105-110.
- Patel-Sorrentino, N., Mounier, S., & Benaim, J. Y. (2002). Excitation–emission fluorescence matrix to study pH influence on organic matter fluorescence in the Amazon basin rivers. *Water Research*, 36(10), 2571-2581.
- Kubo, T., Kanemori, K., Kusumoto, R., Kawai, T., Sueyoshi, K., Naito, T., & Otsuka, K. (2015). Simple and Effective Label-Free Capillary Electrophoretic Analysis of Sugars by Complexation Using Quinoline Boronic Acids. *Analytical chemistry*.

- Liu, Y. Y., Wu, M., Zhu, L. N., Feng, X. Z., & Kong, D. M. (2015). Colorimetric and Fluorescent Bimodal Ratiometric Probes for pH Sensing of Living Cells. *Chemistry–An Asian Journal*.
- Joshi, S., & Pant, D. D. (2015). Interaction of quinine sulfate with anionic micelles of sodium dodecylsulfate: A time-resolved fluorescence spectroscopy at different pH. *Spectrochimica Acta Part A: Molecular and Biomolecular Spectroscopy*, 148, 49-59.
- Sun, M., Yu, H., Li, H., Xu, H., Huang, D., & Wang, S. (2015). Fluorescence Signaling of Hydrogen Sulfide in Broad pH Range Using a Copper Complex Based on BINOL–Benzimidazole Ligands. *Inorganic chemistry*.
- Malavašić, M., Poklar, N., Maček, P., & Vesnaver, G. (1996). Fluorescence studies of the effect of pH, guanidine hydrochloride and urea on equinatoxin II conformation. *Biochimica et Biophysica Acta (BBA)-Biomembranes*, 1280(1), 65-72.
- Zhu, H., Derksen, R. C., Krause, C. R., Fox, R. D., Brazee, R. D., & Ozkan, H. E. (2005). "Effect of solution pH conditions on fluorescence of spray deposition tracers." *Applied engineering in agriculture* 21(3), 325-329.
- White, A. (1959). "Effect of pH on fluorescence of tyrosine, tryptophan and related compounds." *Biochemical Journal* 71(2), 217.
- Köhler, G., and Karl R. (1993). "Solvent effects on excited state relaxation phenomena." *Pure and applied chemistry* 65(8), 1647-1652.
- Citterio, D., Minamihashi, K., Kuniyoshi, Y., Hisamoto, H., Sasaki, S. I., & Suzuki, K. (2001). Optical determination of low-level water concentrations in organic solvents using fluorescent acridinyl dyes and dye-immobilized polymer membranes. *Analytical chemistry*, 73(21), 5339-5345.
- Becker, R. S. (1969). *Theory and Interpretation of Fluorescence and Phosphorescence*. Ohio State University: Wiley Interscience a division of John Wiley & Sons, 283

J. Fernandez, J. and Becker, R. S.(1959). *J. Chem. Phys.*, 31, 467

Nakanishi, J., Nakajima, T., Sato, M., Ozawa, T., Tohda, K., & Umezawa, Y. (2001). Imaging of conformational changes of proteins with a new environment-sensitive fluorescent probe designed for site-specific labeling of recombinant proteins in live cells. *Analytical chemistry*, 73(13), 2920-2928.

Saroja, G., Soujanya, T., Ramachandram B. and Samanta A. (1998). 4-Aminophthalimide Derivatives as Environment-Sensitive Probes, *J. Fluorescence* 8, 405-410.

Homocianu, M. (2011). "Solvent effects on the electronic absorption and fluorescence spectra." *Journal of Advanced Research in Physics* 2(1).

Kalyanasundaran, K. and Thomas, J. K. (1977). Solvent-Dependent Fluorescence of Pyrene-3-Carboxaldehyde and its Applications in the Estimation of Polarity at Micelle-Water Interfaces, *J. Phys. Chem.* 81, 2176-2180

Uchiyama, S., Takehira, K., Yoshihara, T., Tobita, S., & Ohwada, T. (2006). Environment-sensitive fluorophore emitting in protic environments. *Organic letters*, 8(25), 5869-5872.

Spencer, R. G., & Coble, P. G. (2014). Sampling Design for Organic Matter Fluorescence Analysis. *Aquatic Organic Matter Fluorescence*, 125.

Guilbault, G. G. (Ed.). (1990). *Practical fluorescence* (Vol. 3). CRC Press.

Evans, J. M. (2003). *Potassium channels and their modulators: from synthesis to clinical experience*. CRC Press.

- Ochi, T., Yamaguchi, Y., Wakamiya, T., Matsubara, Y., & Yoshida, Z. I. (2008). "Block modification of rod-shaped π conjugated carbon frameworks with donor and acceptor groups toward highly fluorescent molecules: synthesis and emission characteristics." *Organic & biomolecular chemistry* 6(7), 1222-1231.
- Nijegorodov, N. I., & Downey, W. S. (1994). The influence of planarity and rigidity on the absorption and fluorescence parameters and intersystem crossing rate constant in aromatic molecules. *The Journal of Physical Chemistry*, 98(22), 5639-5643.
- Wardle, B. (2009). *Principles and applications of photochemistry*. John Wiley & Sons.
- Lawrence, J. F., & Frei, R. W. (2000). *Chemical derivatization in liquid chromatography*. Elsevier.
- Sathyanarayana, D. N. (2001). *Electronic absorption spectroscopy and related techniques*. Universities Press.
- Mittal, K. L. (Ed.). (2005). *Polyimides and other high temperature polymers: synthesis, characterization and applications* (Vol. 3). CRC Press, 22.
- Barigelletti, F., & Braig, A. (2010). *Photochemistry* (Vol. 38). A. Albini (Ed.). Royal Society of Chemistry, 77.
- Robards, K., Robards, K., Haddad, P. R., & Jackson, P. E. (1994). *Principles and practice of modern chromatographic methods*. Academic Press, 204.
- Schirmer, R. E. (1990). *Modern methods of pharmaceutical analysis* (Vol. 2). CRC press., 305.
- Raj, G. (2008). *Photochemistry*. (5th ed.) Krishna Prakashan Media. 122.

Jung, G. (2012). *Fluorescent Proteins*. Springer, 51.

Zimmerman, H. E. (1998). *Meta-Ortho* Effect in Organic Photochemistry: Mechanistic and Exploratory Organic Photochemistry 1, 2. *The Journal of Physical Chemistry A*, 102(28), 5616-5621.

Bohle, M., Boyd, G. V., Fischer, E., Friedrich, K., Grashey, R., Hurst, D. T., Huthmacher, K., Hubner, F., Kollenz, G., Neunhoeffer H., Niclas, H. J., Pfeiffer W. D., Rupp, S., Schaumann, E. and Wakefield, B. J. (2014). *Houben-Weyl Methods of Organic Chemistry Vol. E 9c, Supplement: Hetarenes III*. Georg Thieme Verlag., 923.

Dewick, P. M. (2006). *Essentials of organic chemistry: for students of pharmacy, medicinal chemistry and biological chemistry*. John Wiley & Sons.

Liu, W. (1997). *Direct and efficient convergent synthetic routes to pyrazine C-nucleosides*. University of Michigan.

Barlin, G. B.(2009).*The Chemistry of Heterocyclic Compounds: The Pyrazines*. (Vol. 41) John Wiley & Sons.

Sathyanarayana, D. N. (2001). *Electronic absorption spectroscopy and related techniques*. Universities Press.

Pillai, C. N. (2009).*Textbook of Organic Chemistry: Phenols*. India: Universities Press, 339.

Topsom, R. D.(1981). "The isolated molecule approach. Theoretical studies of the inductive effect." *Journal of the American Chemical Society* 103(1), 39-44.

Tyagi, V. P. (2009). *Essential Chemistry Xii*. Ratna Sagar, 11.29.

Carey, F. A. (1996). "*Organic chemistry*." New York: McGraw-Hill Inc. 488.

LIST OF PUBLICATION

1. Idris, A. M., Arifin, A., Johari, H. N., & Abdullah, Z. (2013). Synthesis and Fluorescence Properties 2-*N*-Piperidinopyrazines. *Asian Journal of Chemistry*, 25(14), 8121-8124.

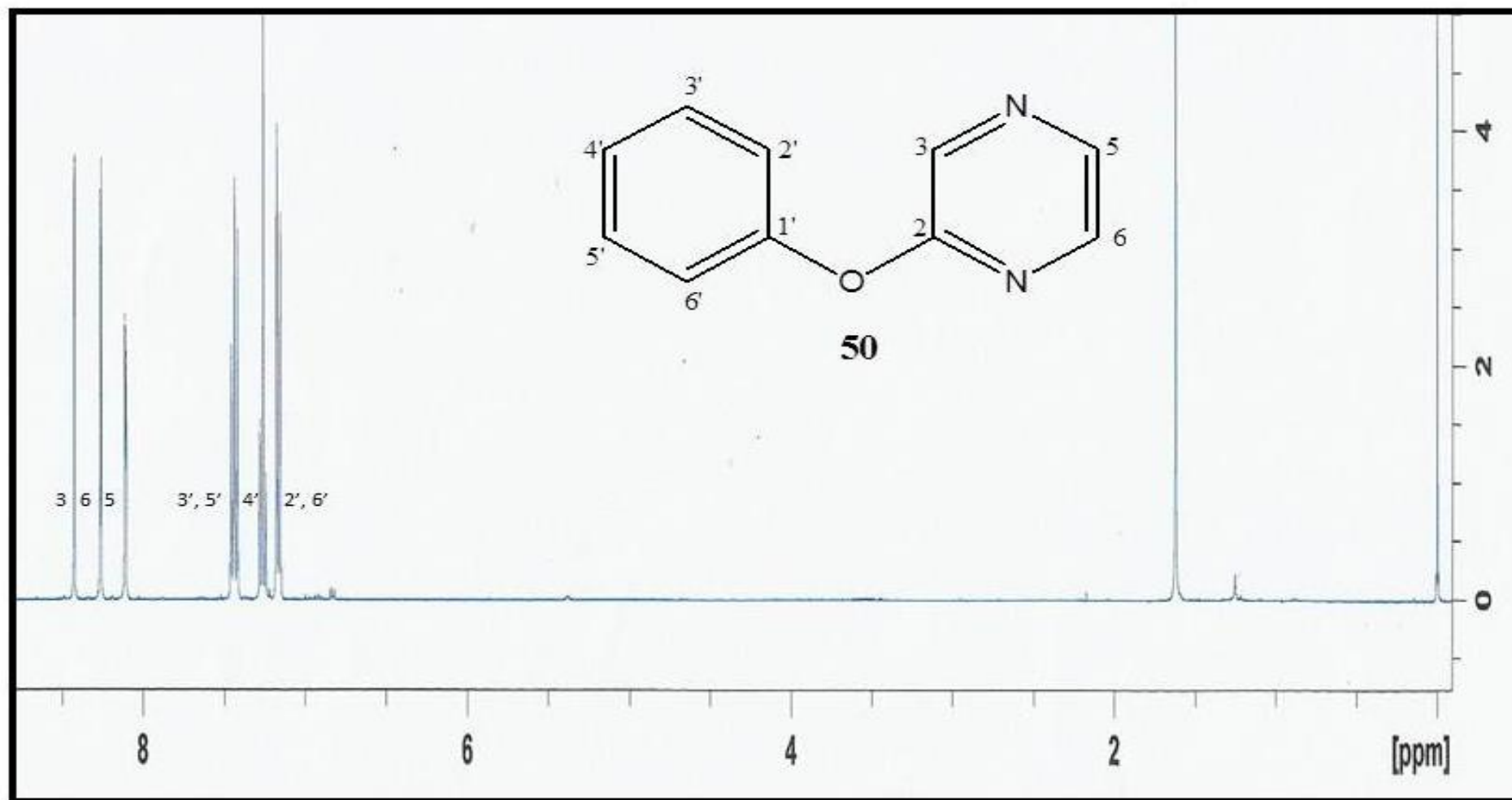
CONFERENCE PROCEEDING

1. **International Conference for Young Chemist (ICYC 2013)**-Selected Naphtalenyloxy and Phenoxy Pyrazines: Synthesis and Fluorescence Characteristic
2. **International Conference on Ionic Liquids 2013 (ICIL 13)**-Synthesis of Selected Phenoxy Pyrazines Using Williamson Ether Synthesis

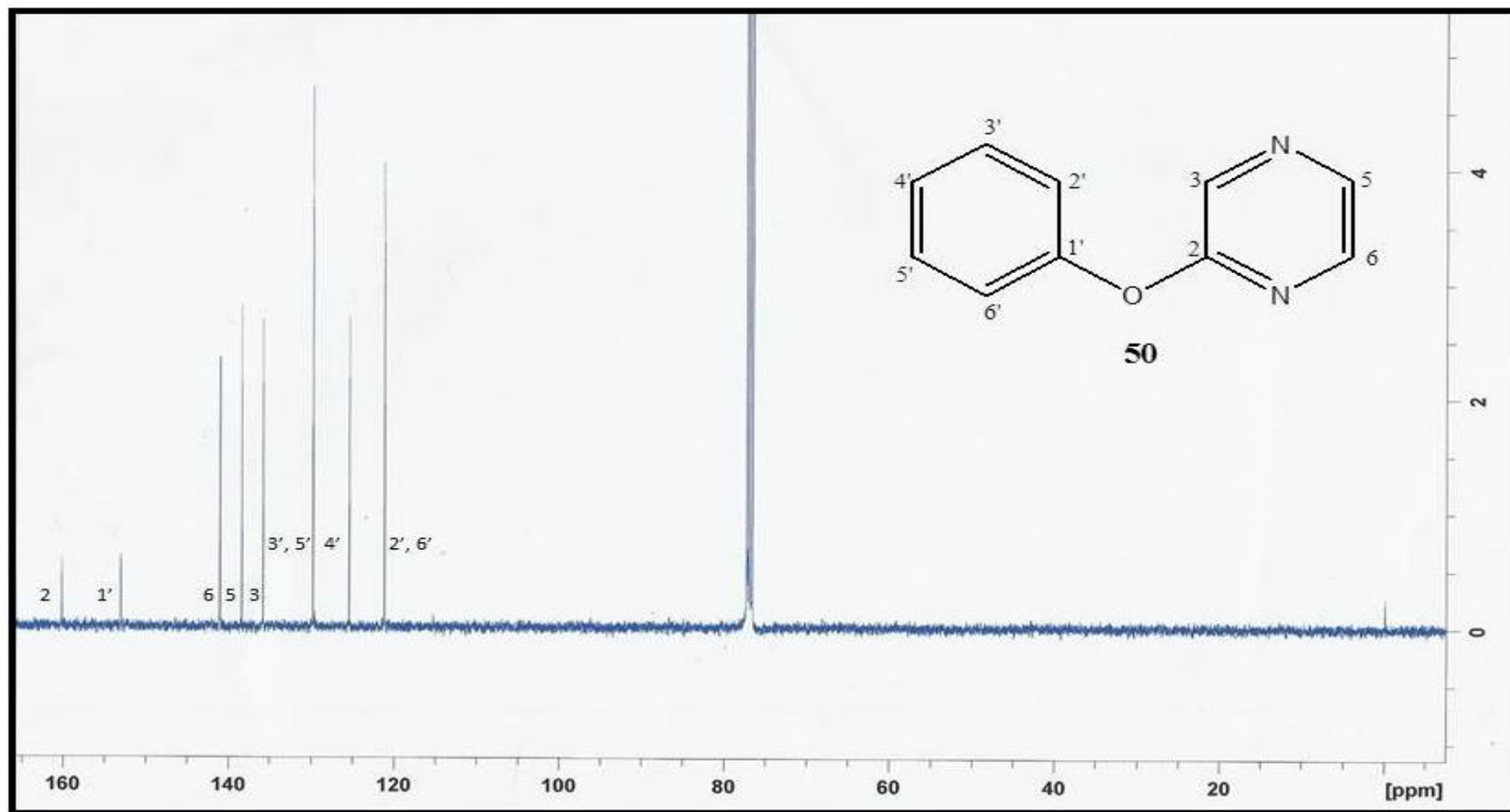
APPENDICES

Appendix 1: ^1H NMR, ^{13}C NMR, IR and GCMS Spectra

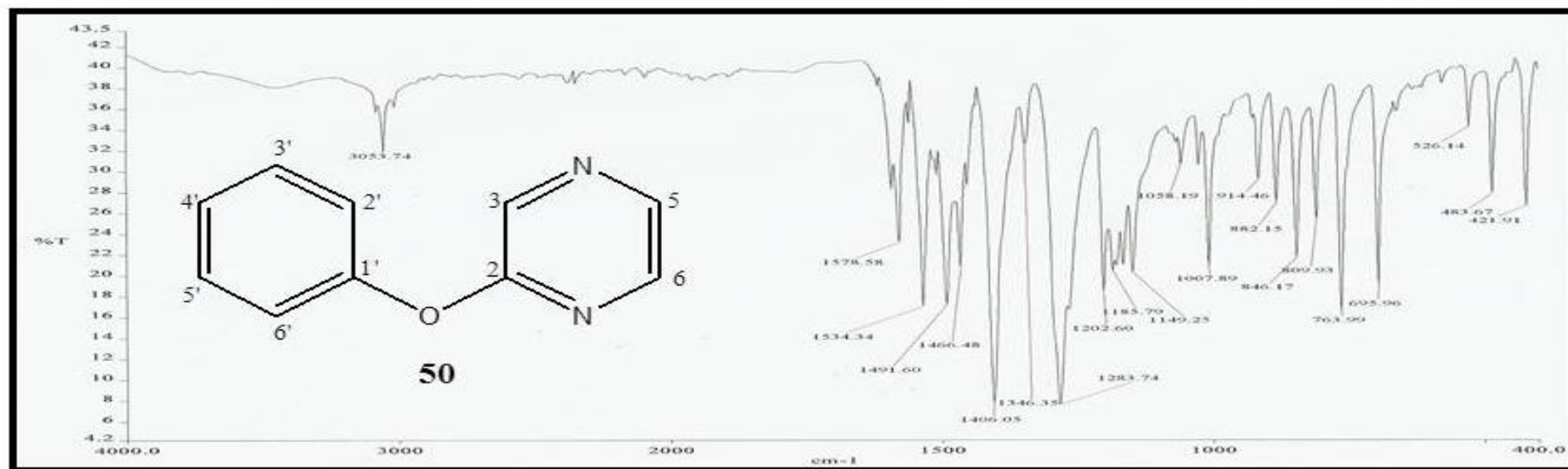
Appendix 2: Publication



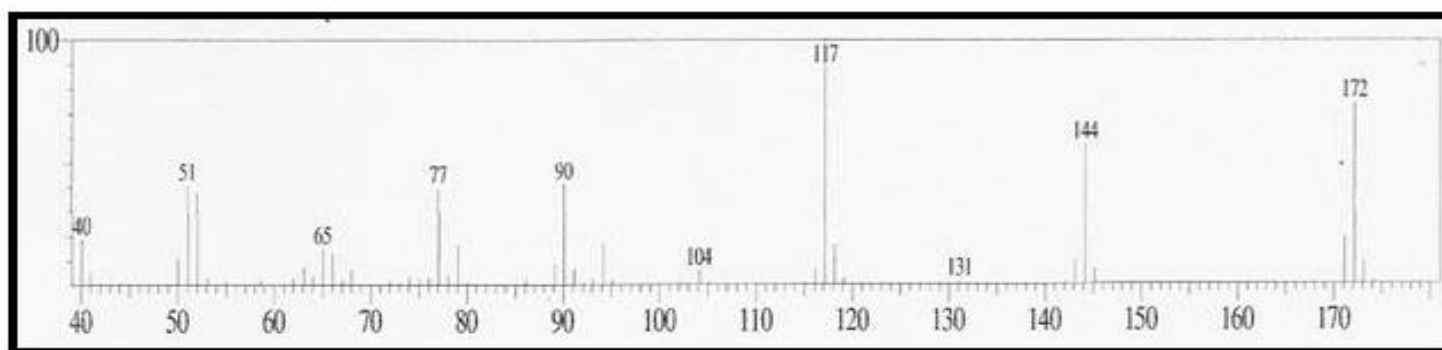
^1H NMR spectrum (CDCl_3 , 400 MHz) of 2-phenoxy pyrazine (50)



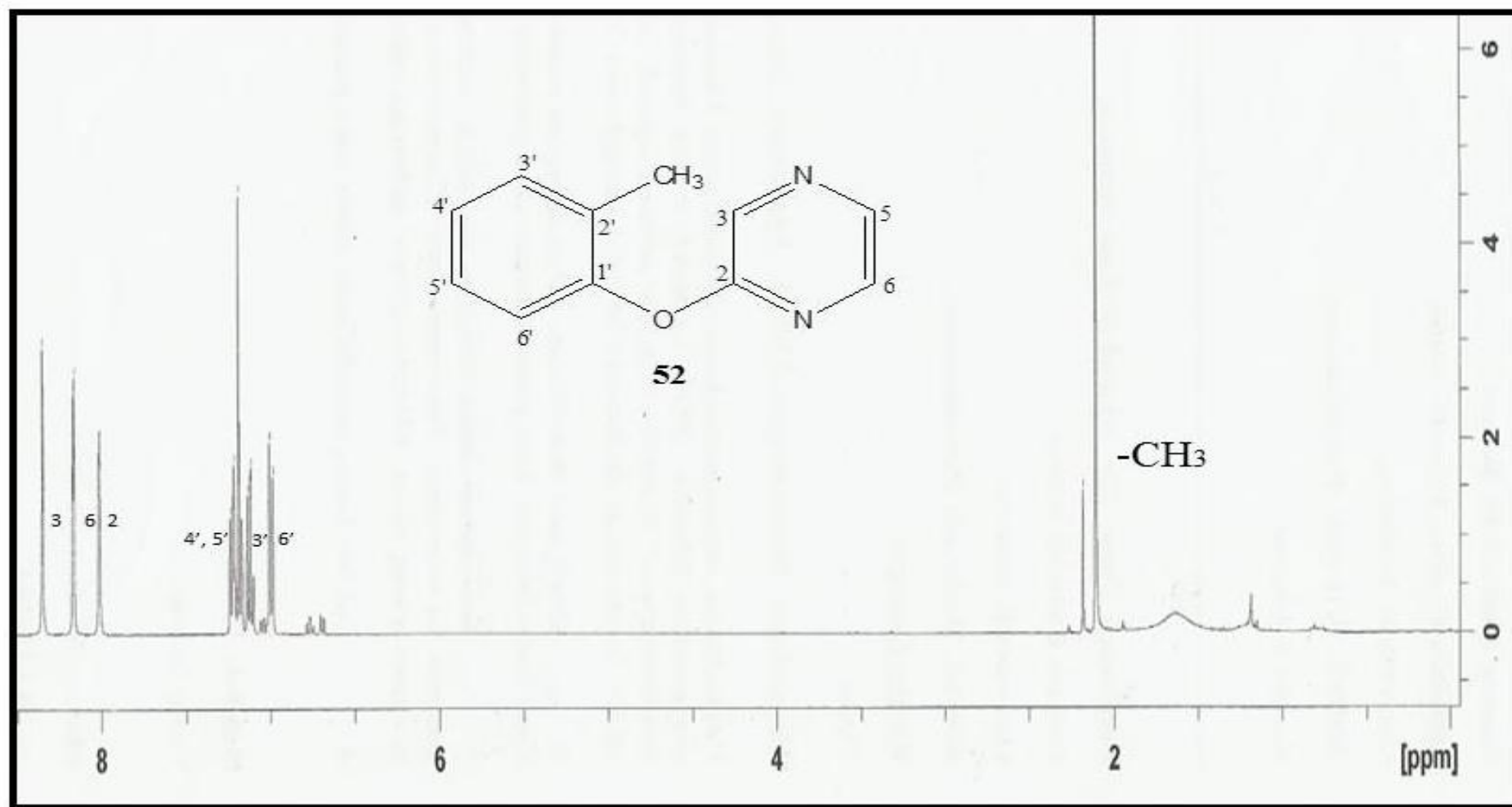
^{13}C NMR spectrum (CDCl_3 , 400 MHz) of 2-phenoxy pyrazine (50)



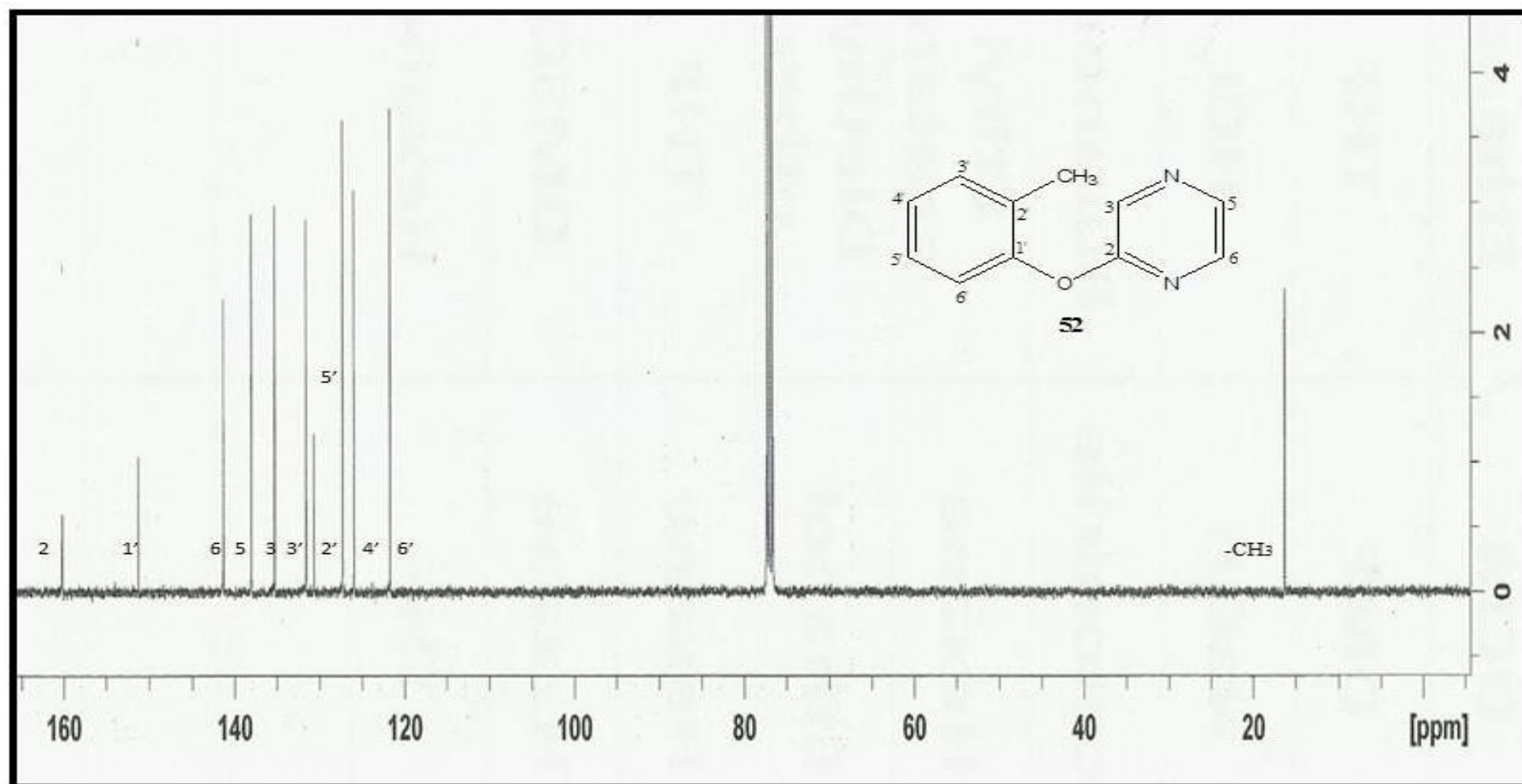
IR spectrum of 2-phenoxy pyrazine (50)



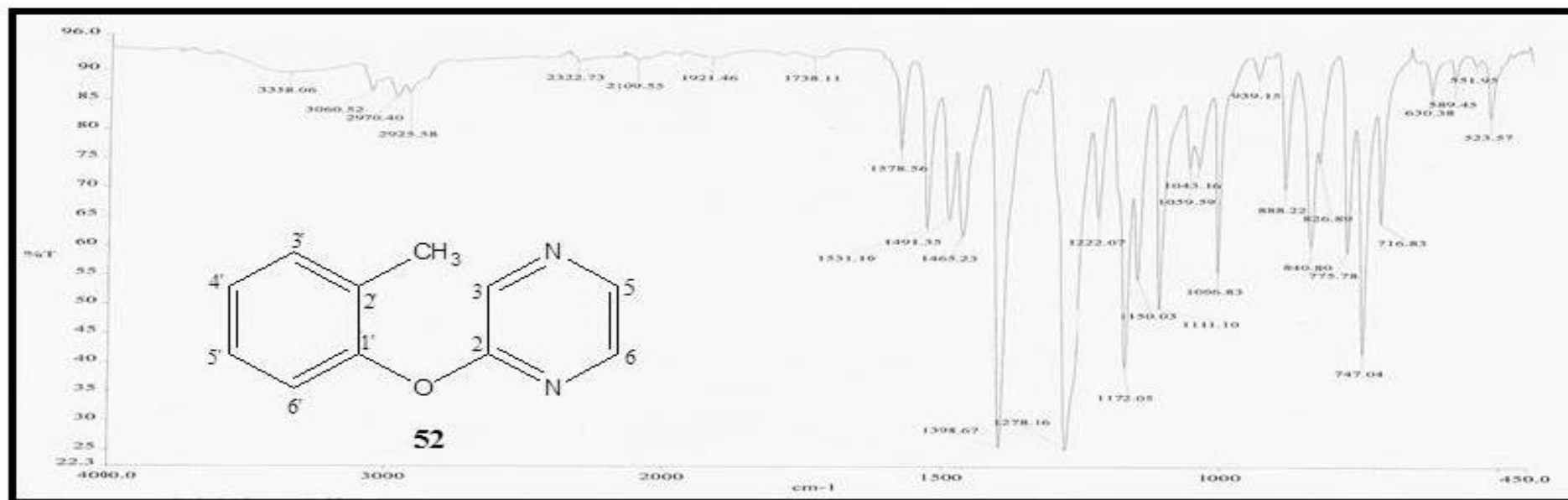
GCMS spectrum of 2-phenoxy pyrazine (50)



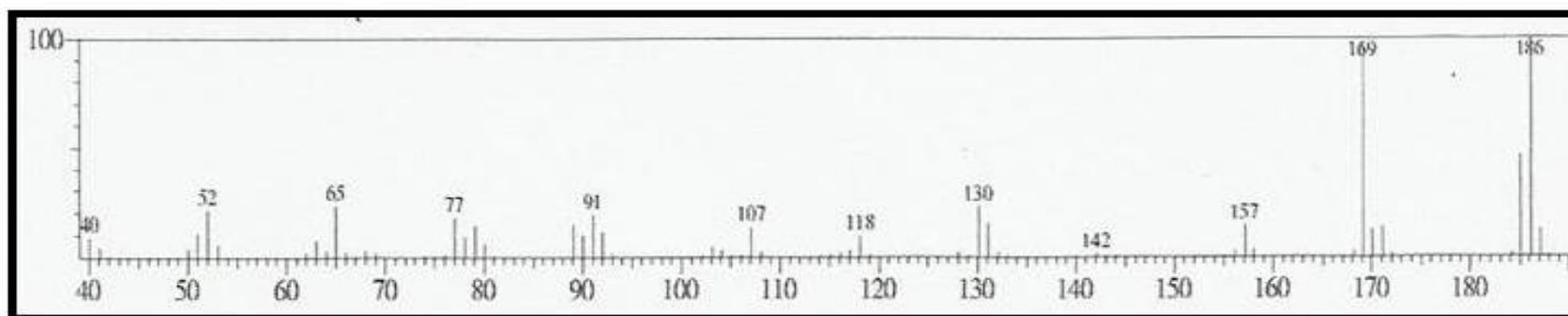
^1H -NMR spectrum (CDCl_3 , 400 MHz) of 2-*o*-phenoxy pyrazine (52)



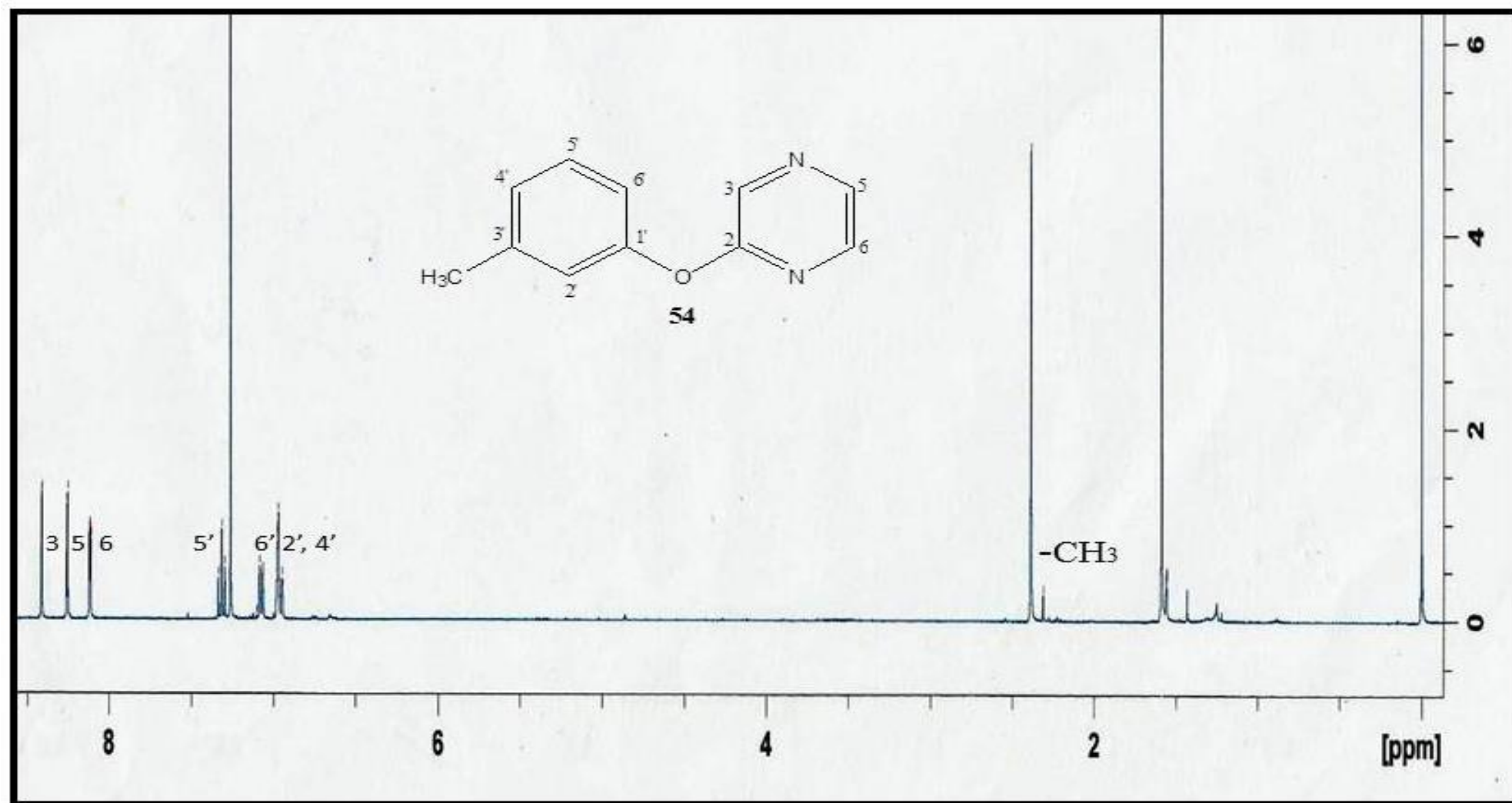
^{13}C NMR spectrum (CDCl_3 , 400 MHz) of 2-*o*-phenoxy pyrazine (52)



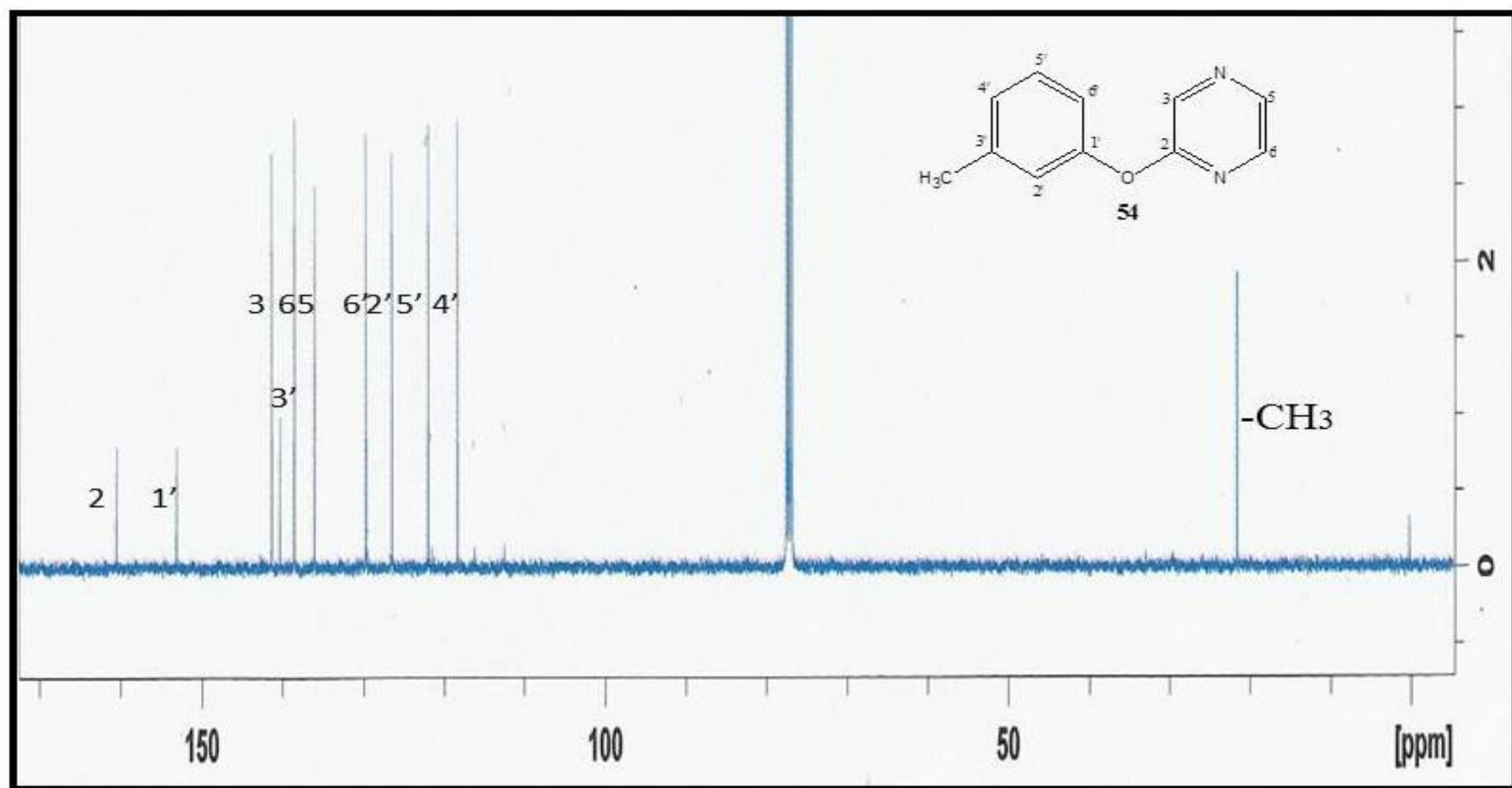
IR spectrum of 2-o-methylpyrazine (52)

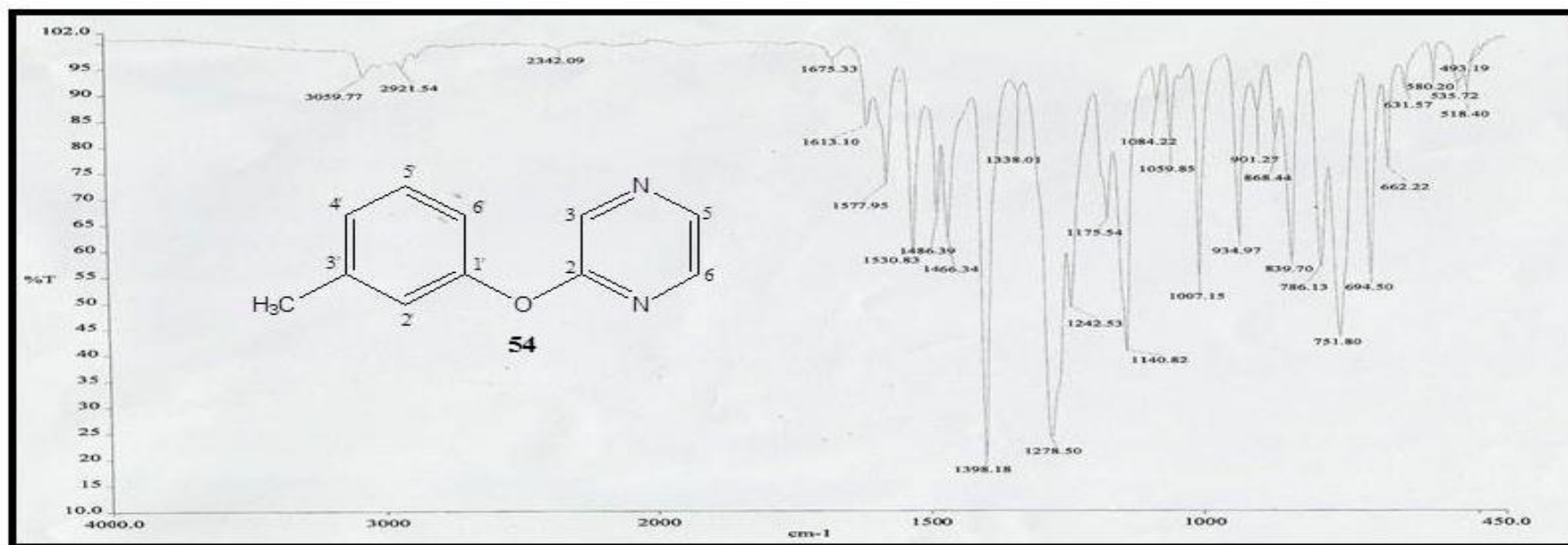


GCMS spectrum of 2-o-methylpyrazine (52)

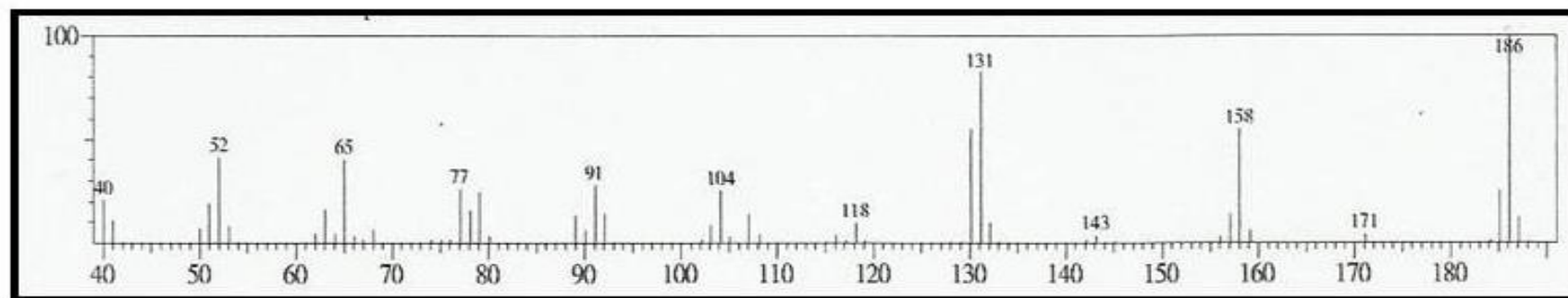


^1H NMR spectra (CDCl_3 , 400MHz) of 2-*m*-phenoxy pyrazine (54)

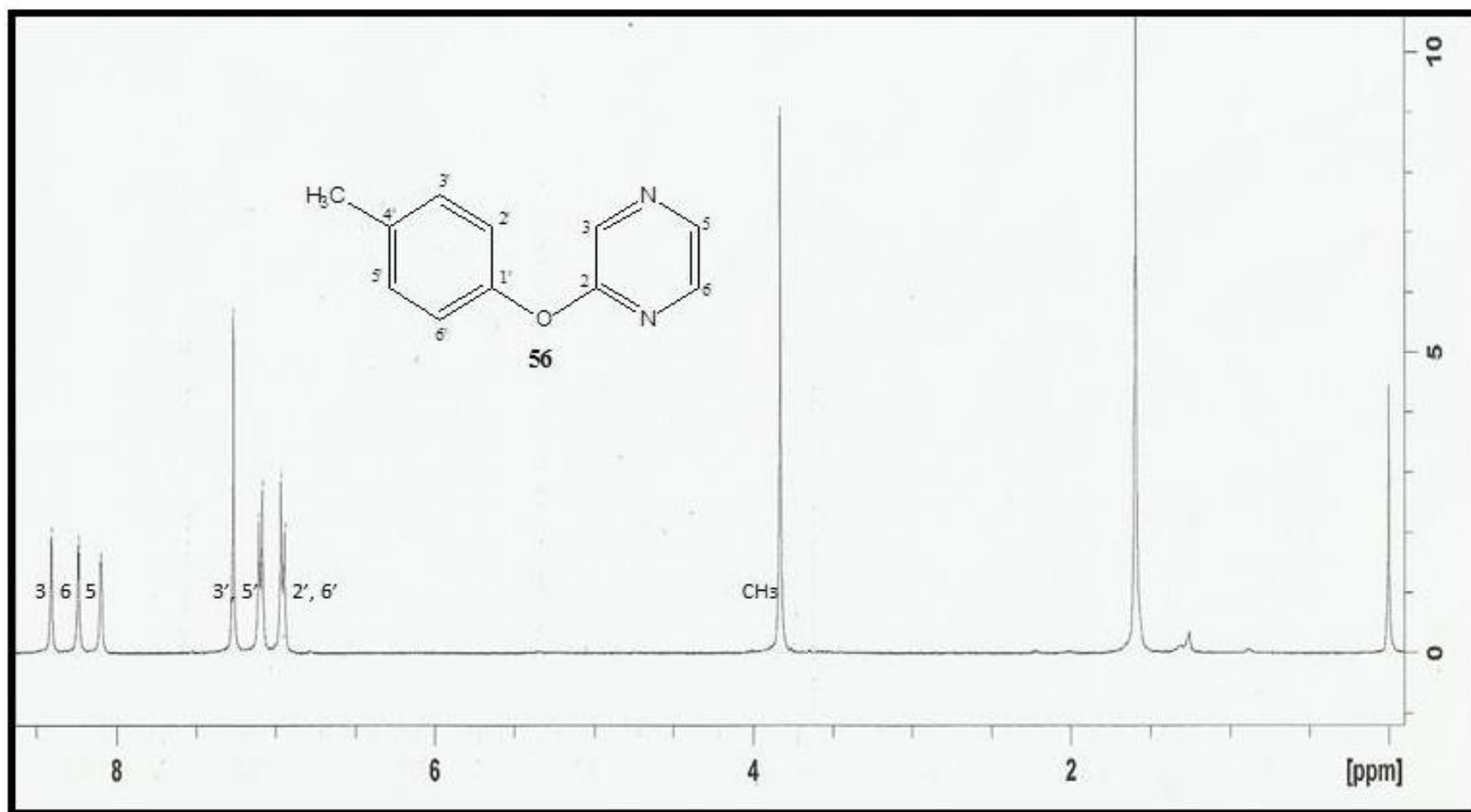




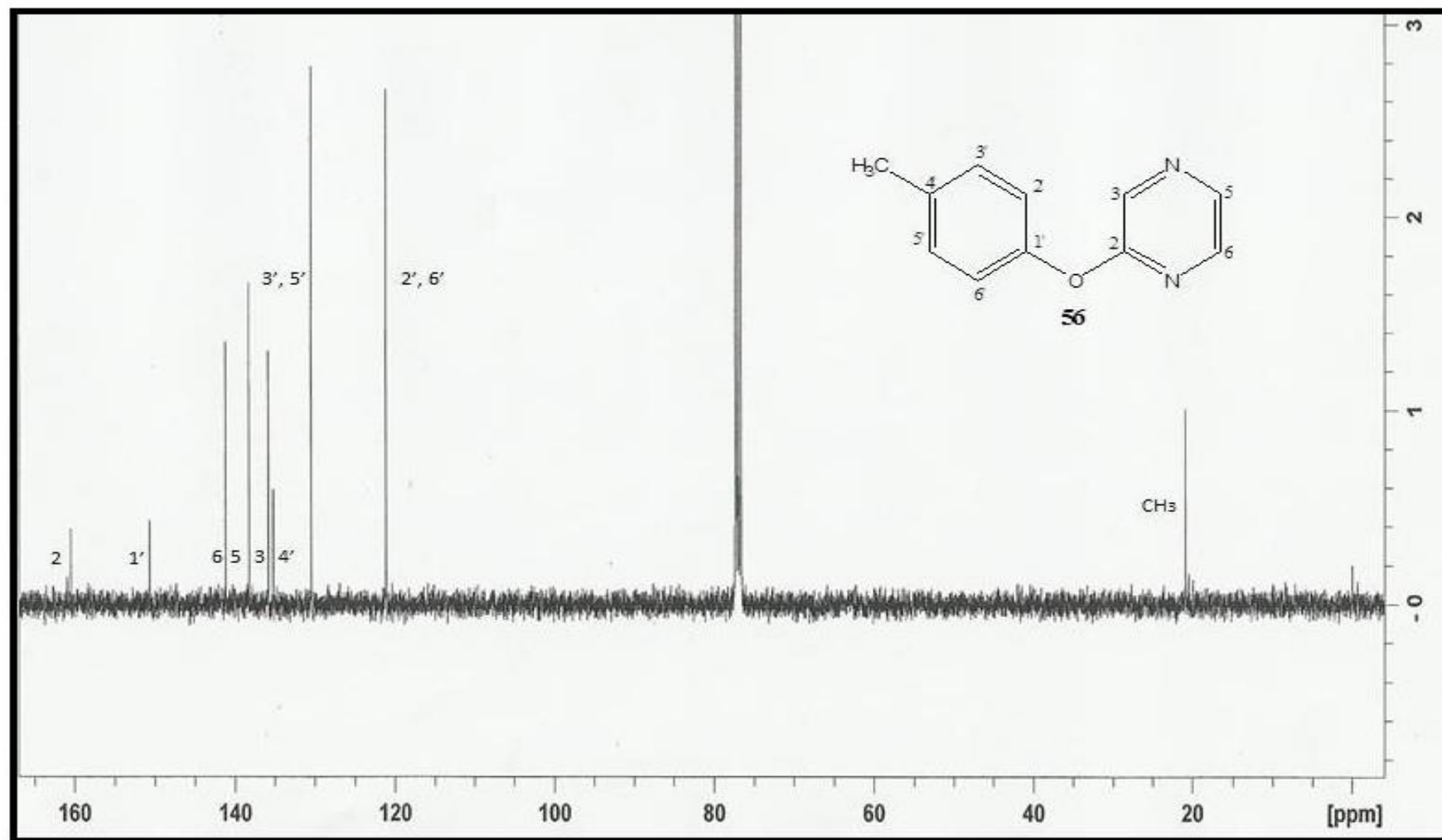
IR spectrum of 2-*m*-phenoxy pyrazine (54)



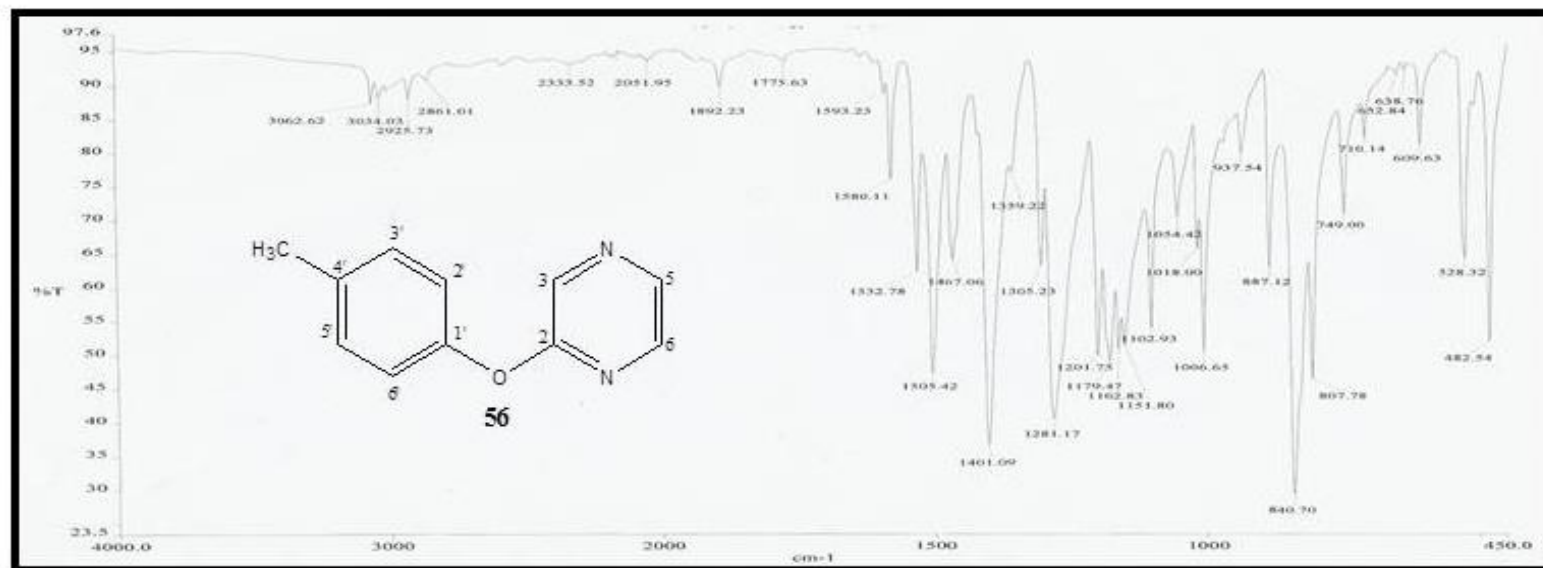
GCMS spectrum of 2-*m*-phenoxy pyrazine (54)



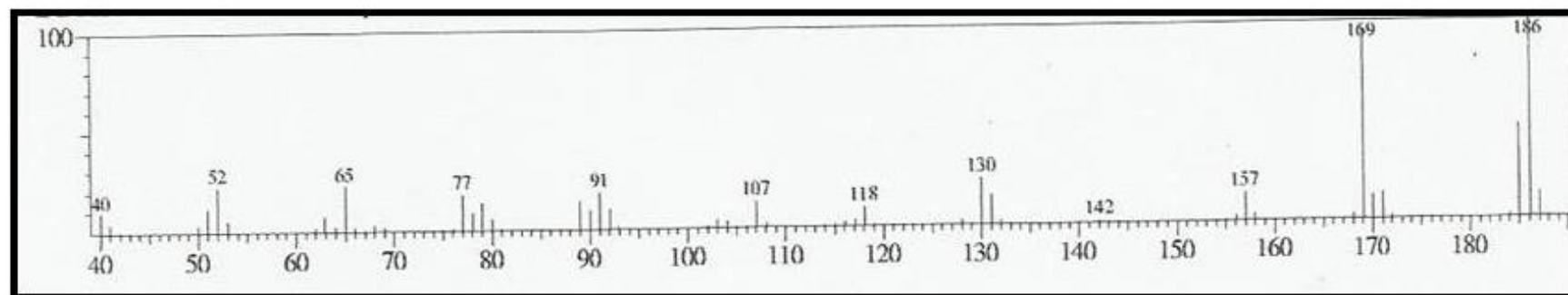
^1H NMR Spectrum (CDCl_3 , 400 MHz) of 2-*p*-toloxypyrazine (56)



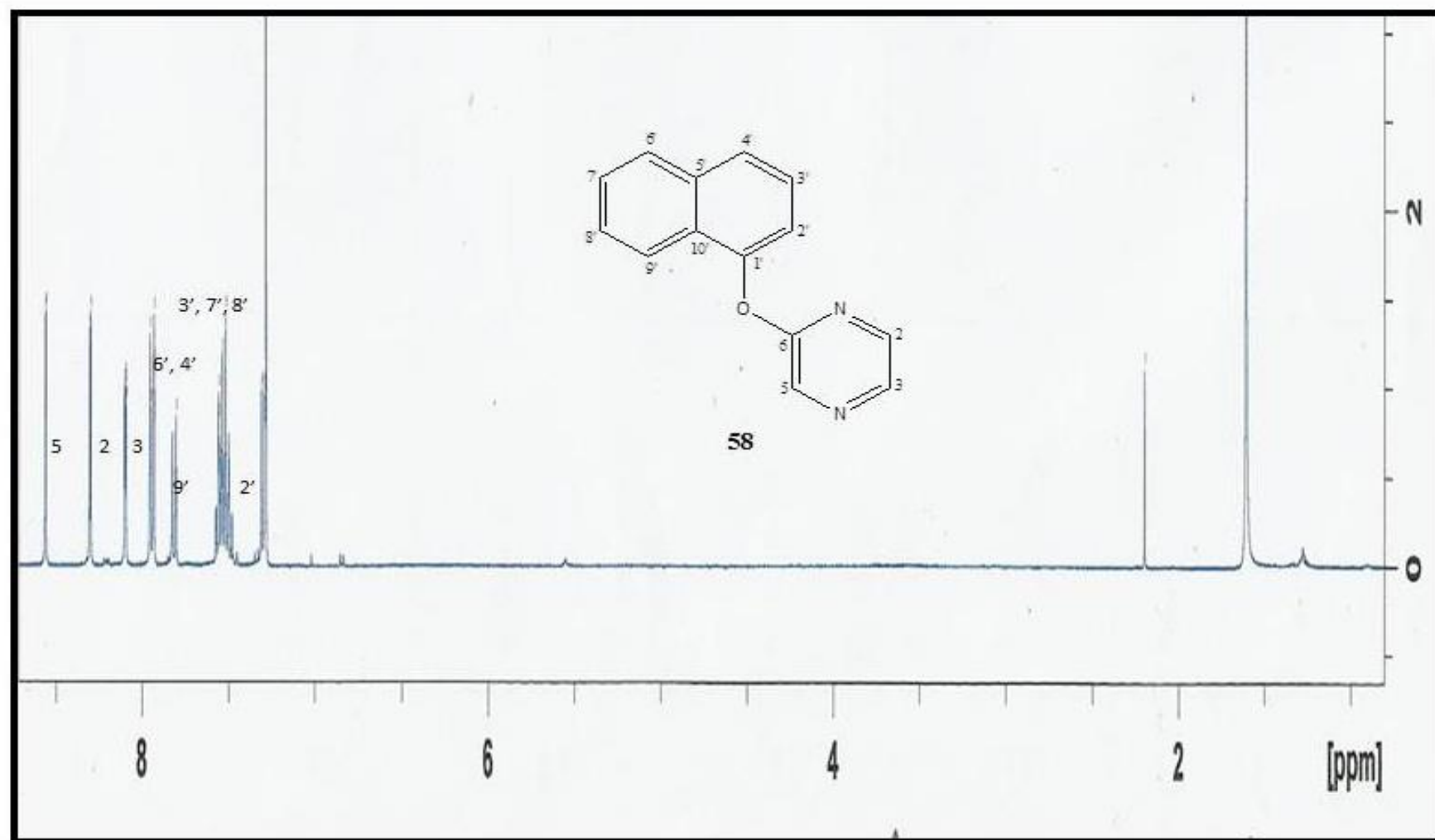
^{13}C NMR spectrum (CDCl_3 , 400 MHz) of 2-*p*-phenoxy pyrazine (56)



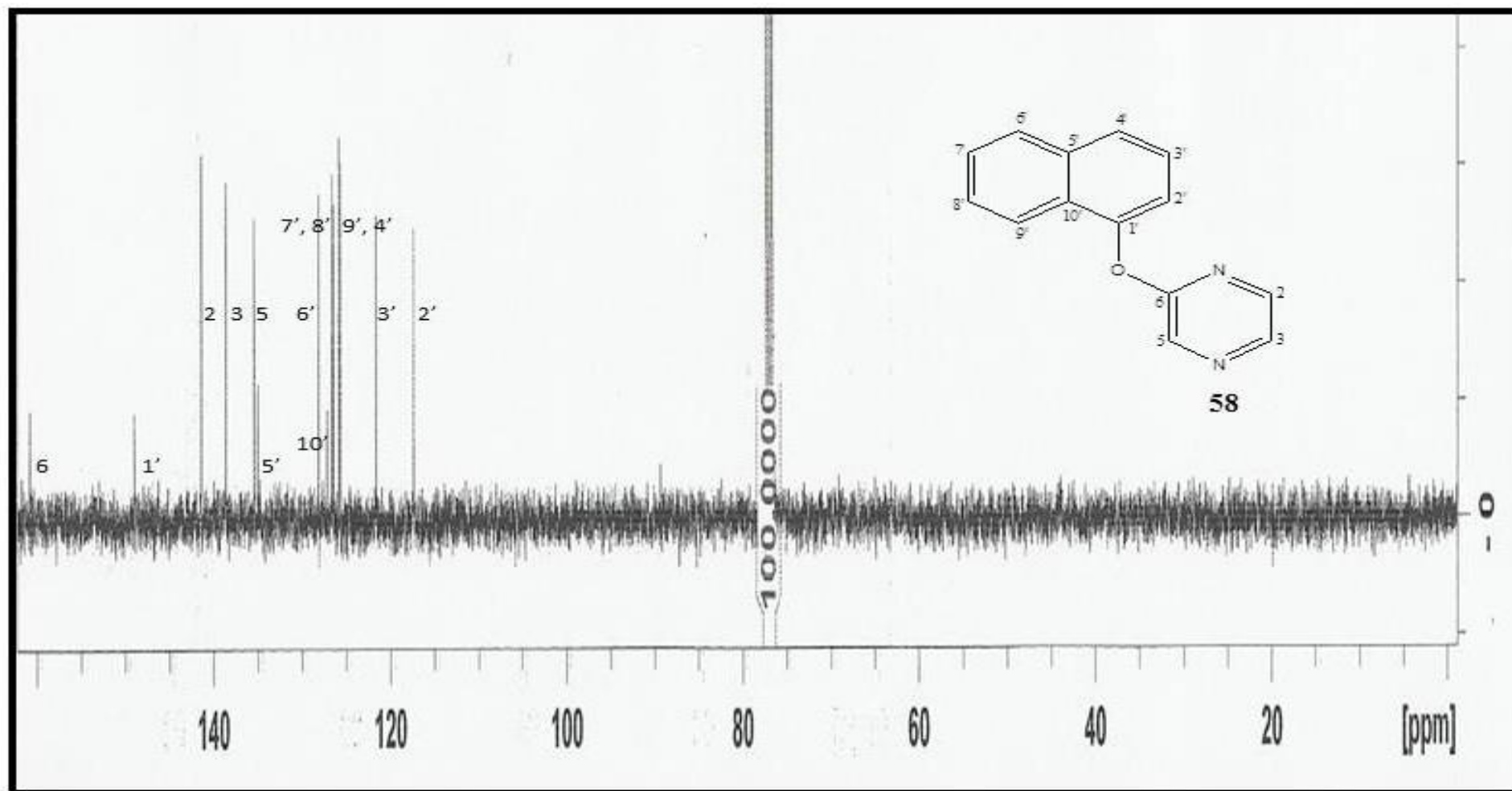
IR spectrum of 2-*p*-toloxypyrazine (56)



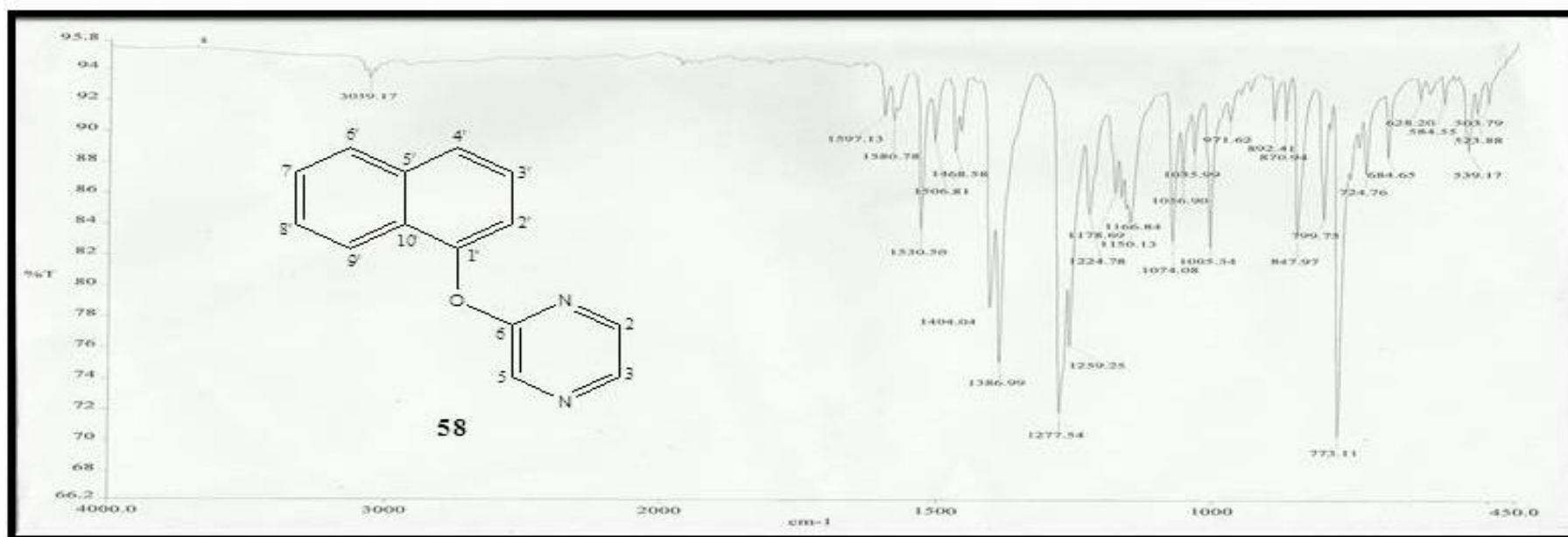
GCMS spectrum of 2-*p*-toloxypyrazine (56)



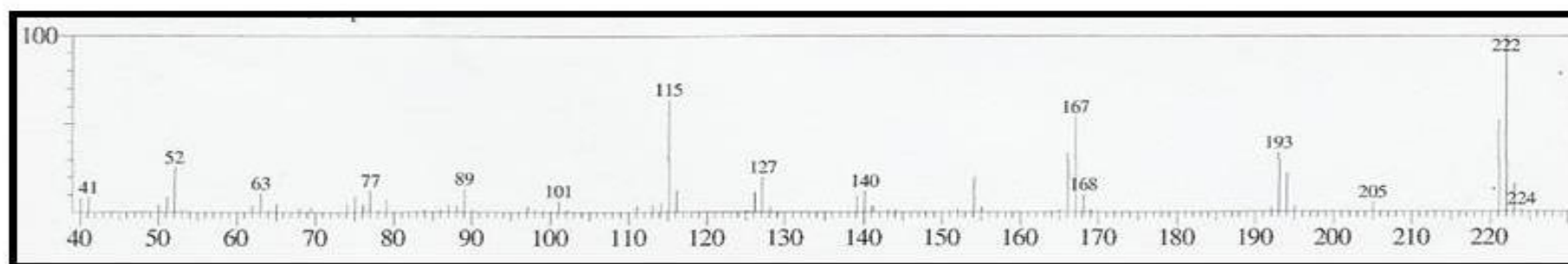
^1H NMR spectrum (CDCl_3 , 400 MHz) of 2-naphthalen-1-yloxy pyrazine (58)



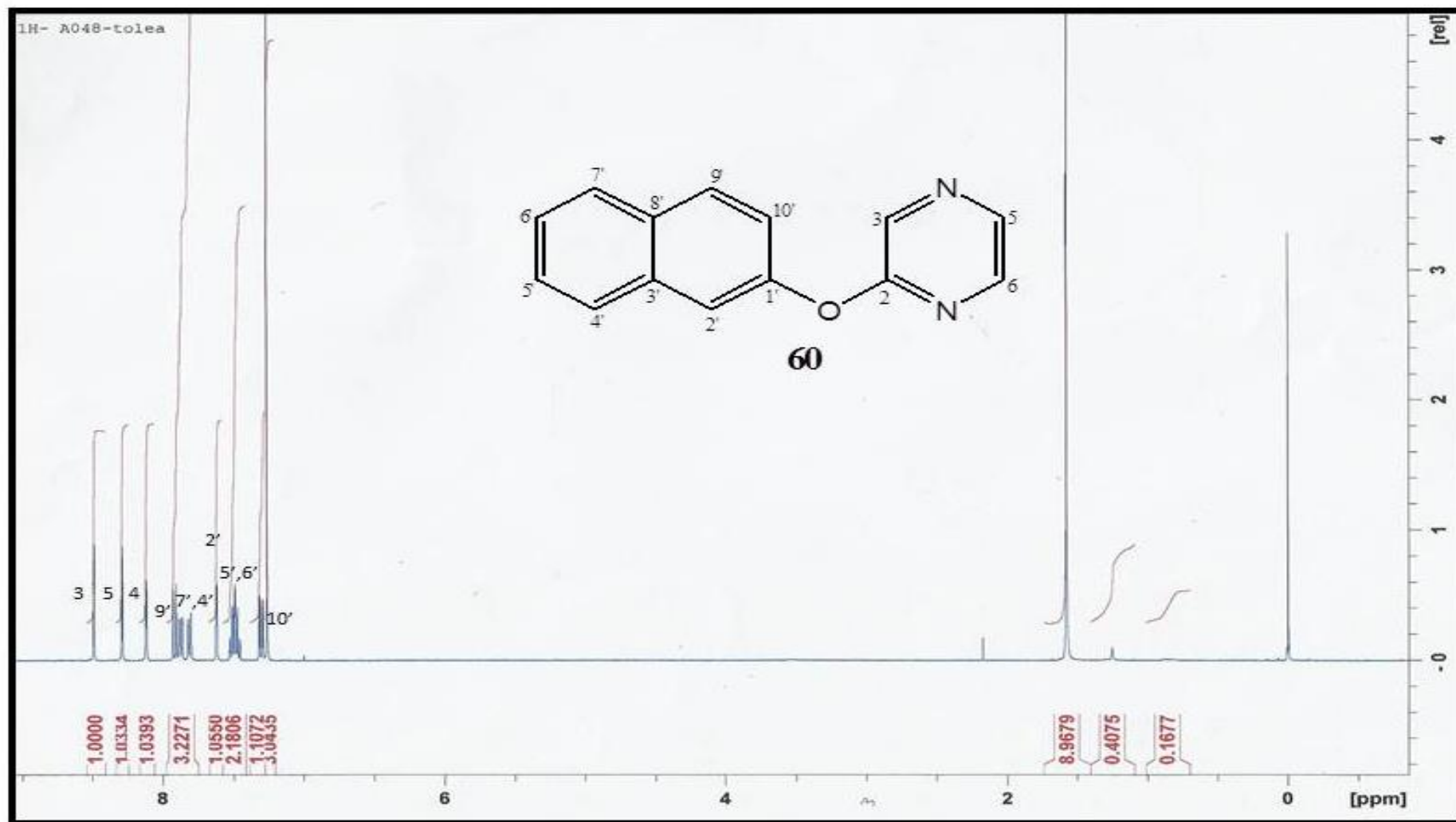
^{13}C NMR spectrum (CDCl_3 , 400 MHz) of 2-naphthalen-1-yloxypyrazine (58)



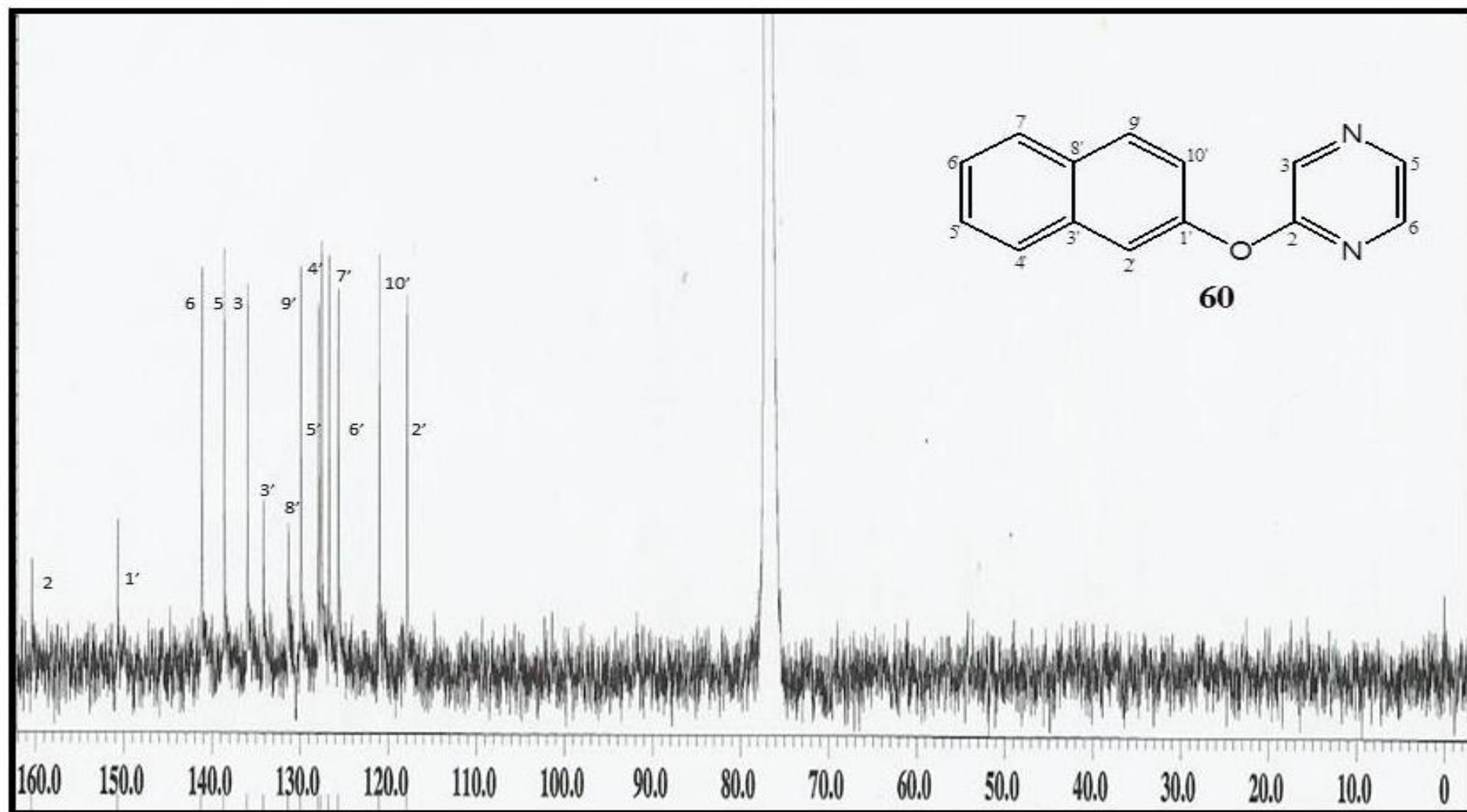
IR spectrum of 2-naphthalen-1-yloxypyrazine (58)



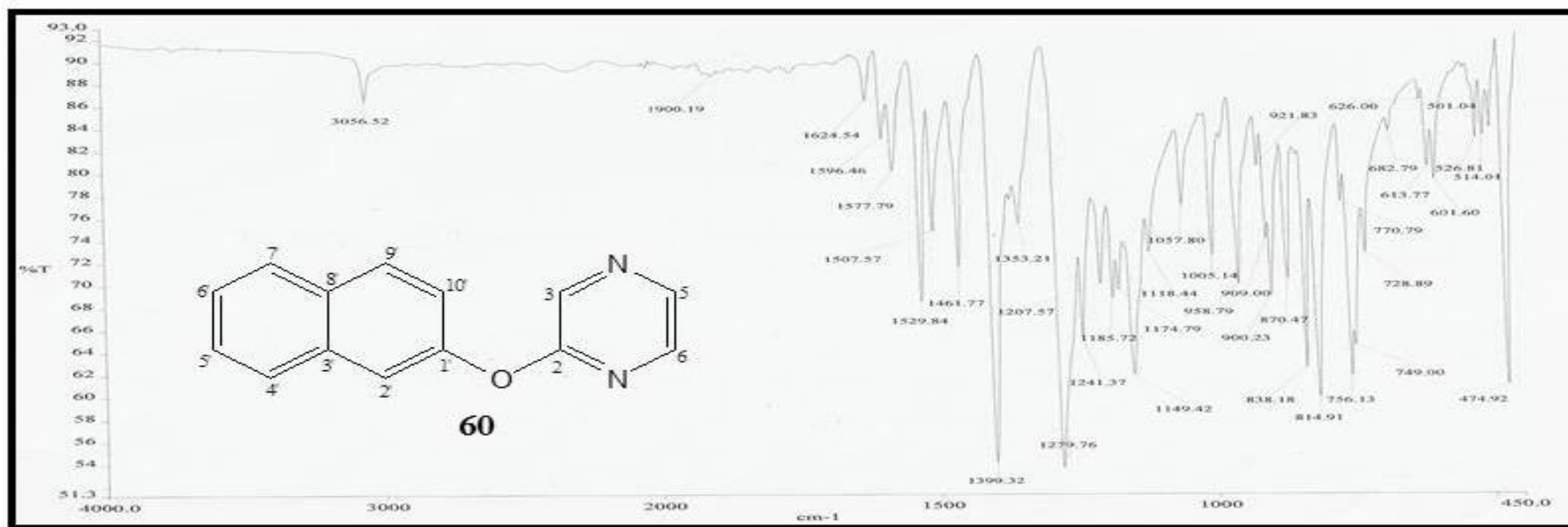
GCMS spectrum of 2-naphthalen-1-yloxypyrazine (58)



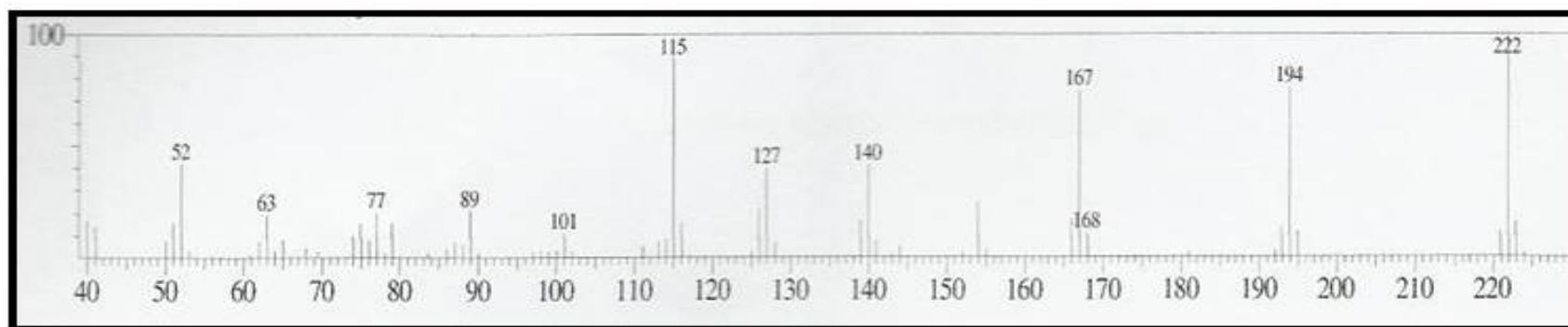
^1H NMR spectrum (CDCl_3 , 400 MHz) of 2-naphthalen-2-yloxypyrazine (60)



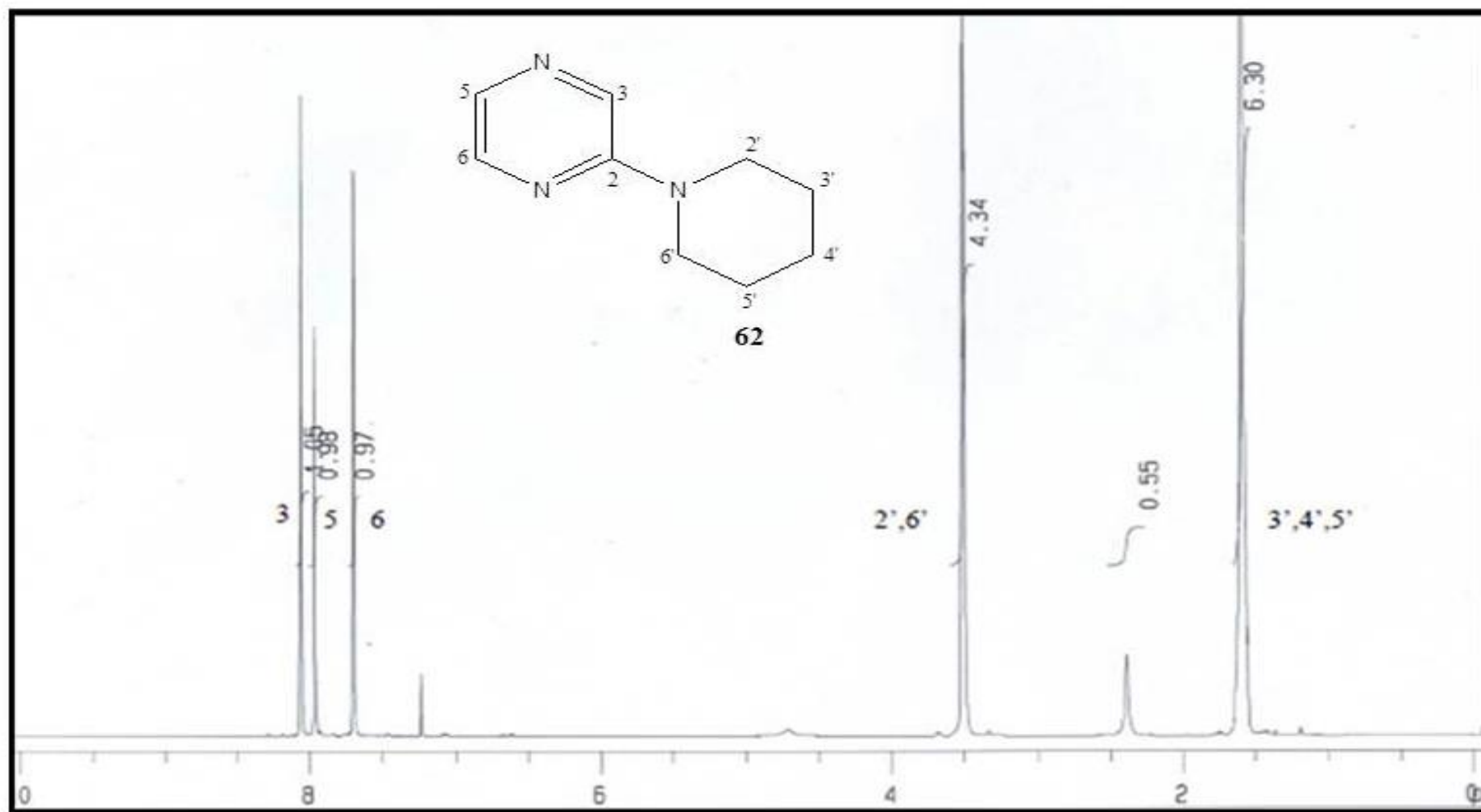
^{13}C NMR spectrum (CDCl_3 , 400 MHz) of 2-naphthalen-2-yloxypyrazine (60)



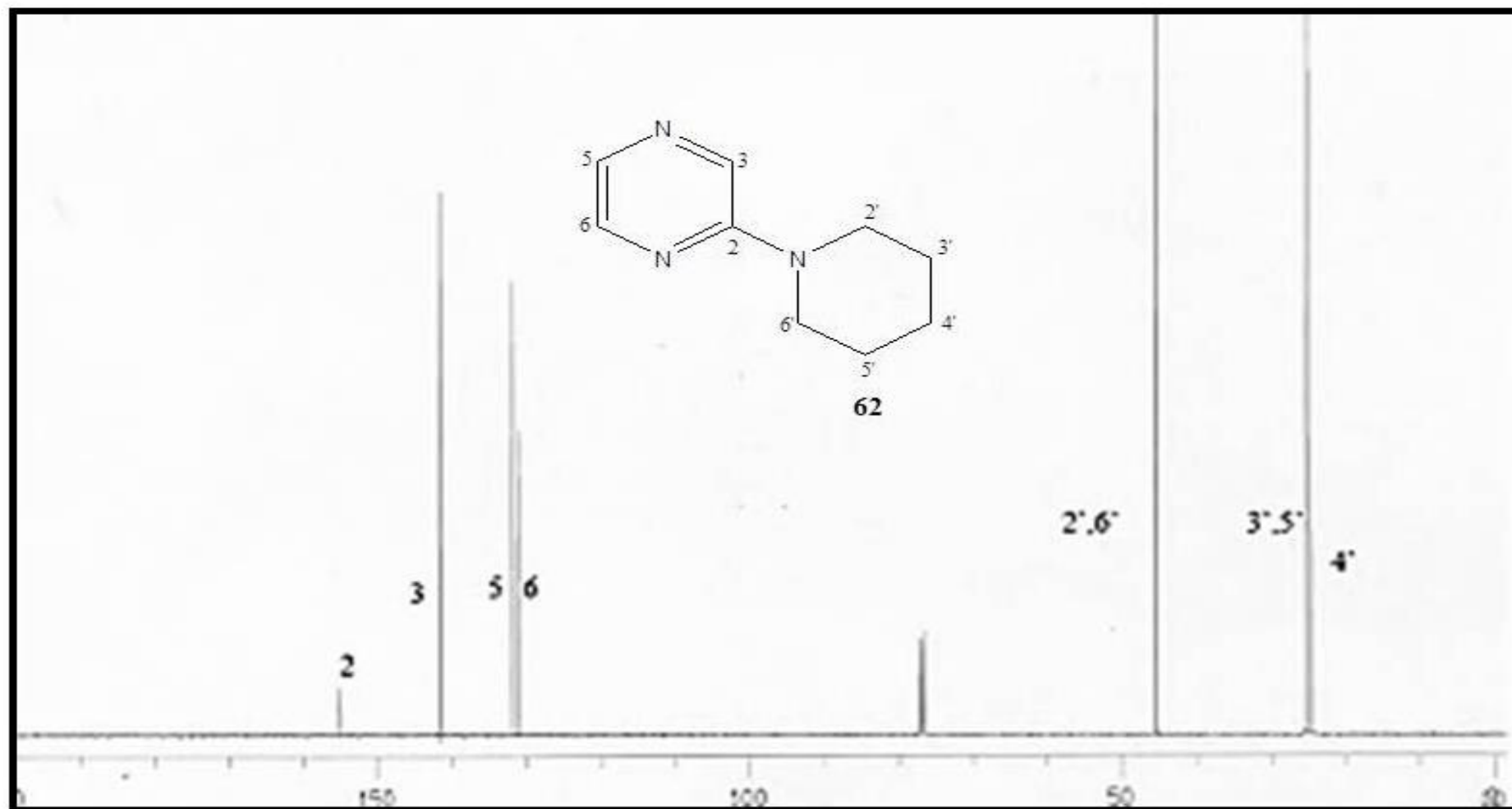
IR spectrum of 2-naphthalen-2-yloxy pyrazine (60)



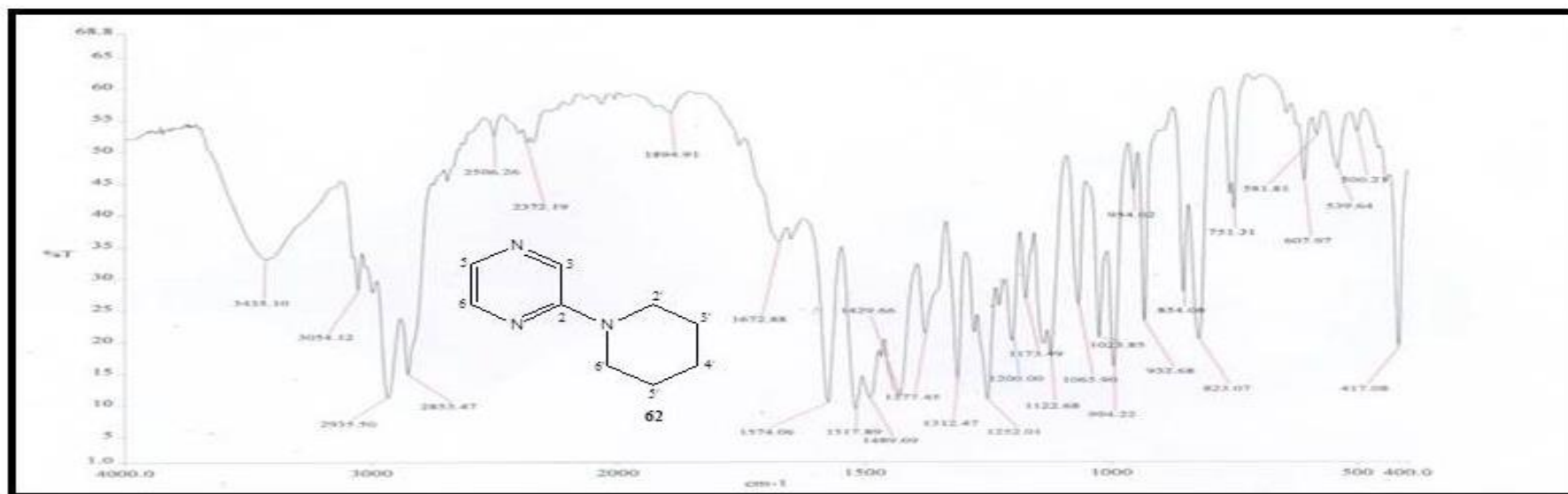
GCMS spectrum of 2-naphthalen-2-yloxy pyrazine (60)



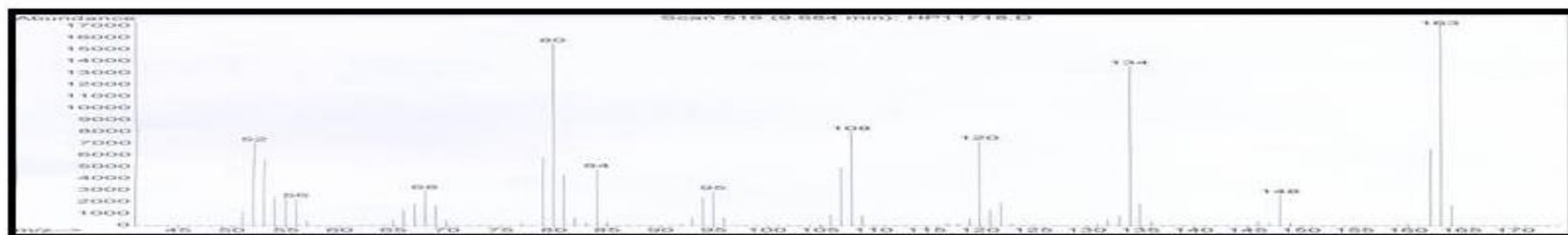
^1H NMR spectrum (CDCl_3 , 400 MHz) of 2-*N*-piperidinopyrazine (62)



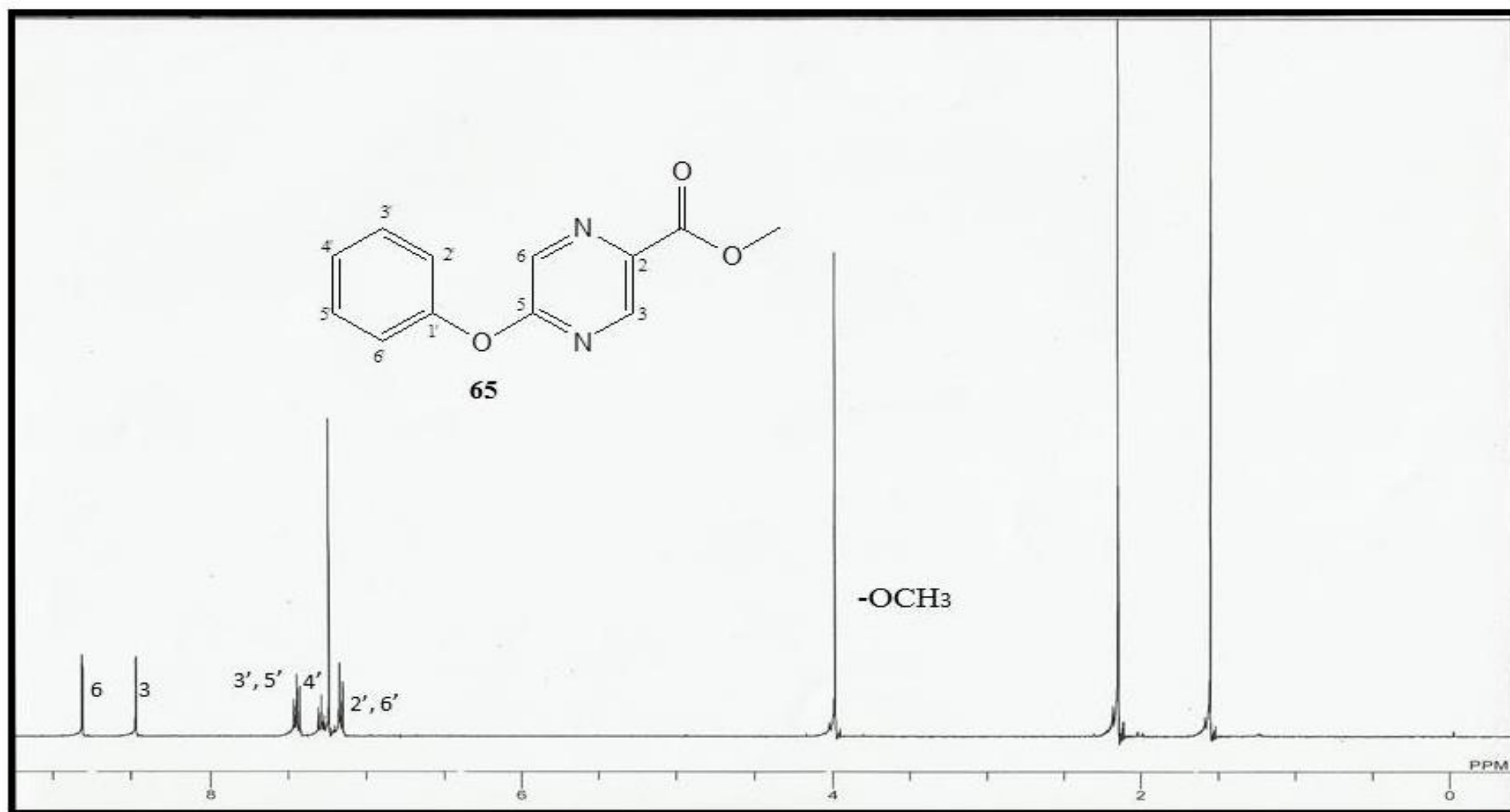
^{13}C NMR spectrum (CDCl_3 , 400 MHz) of 2-*N*-piperidinopyrazine (62)



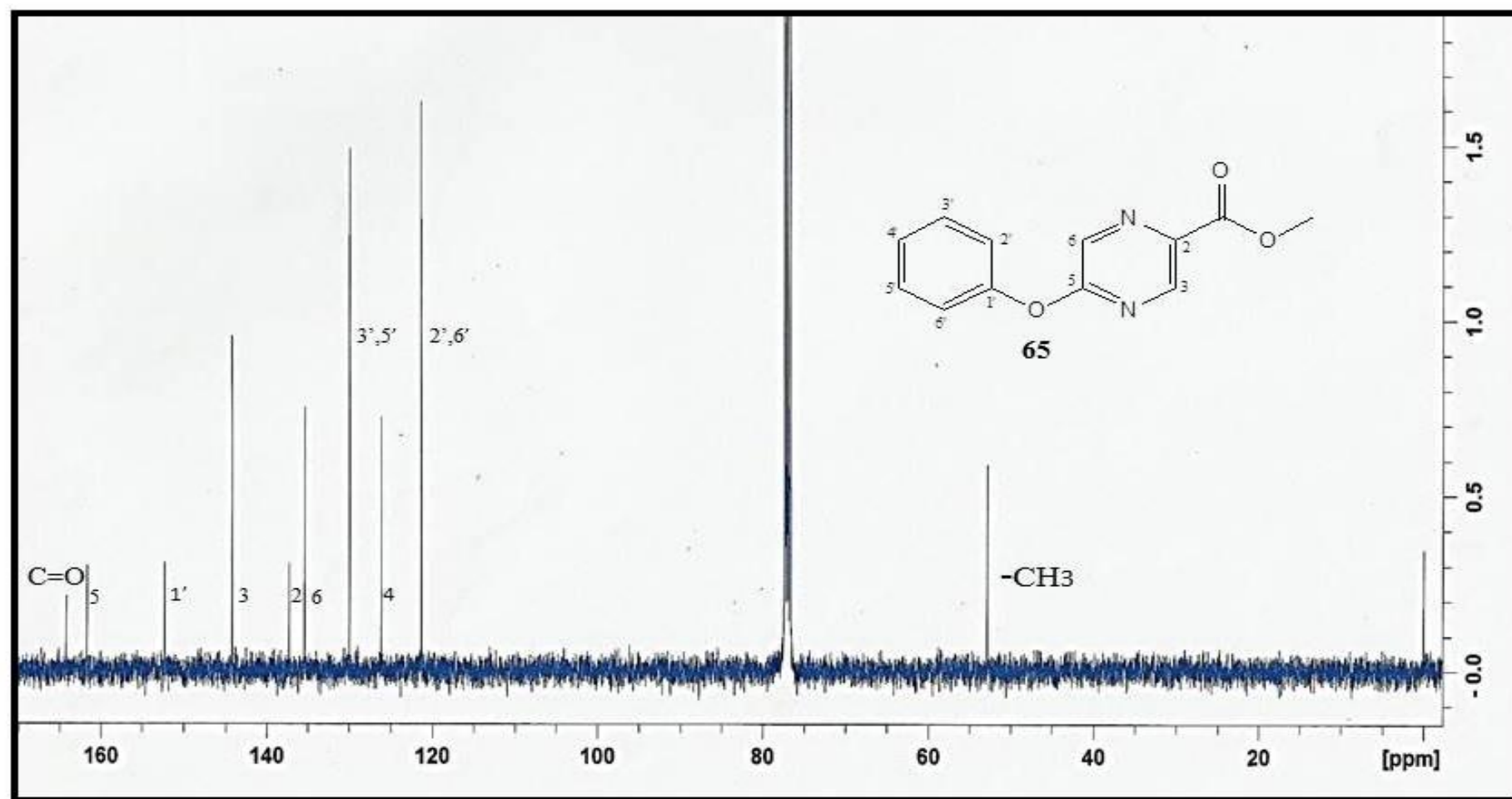
IR spectrum of 2-*N*-piperidinopyrazine (62)



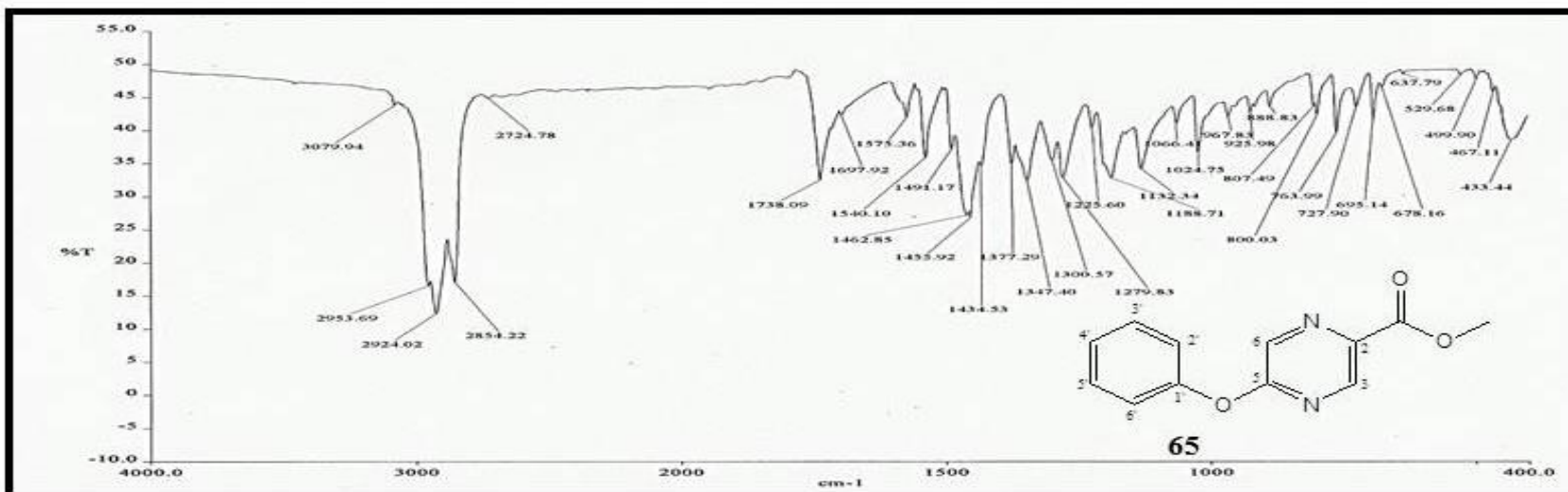
GCMS spectrum of 2-*N*-piperidinopyrazine (62)



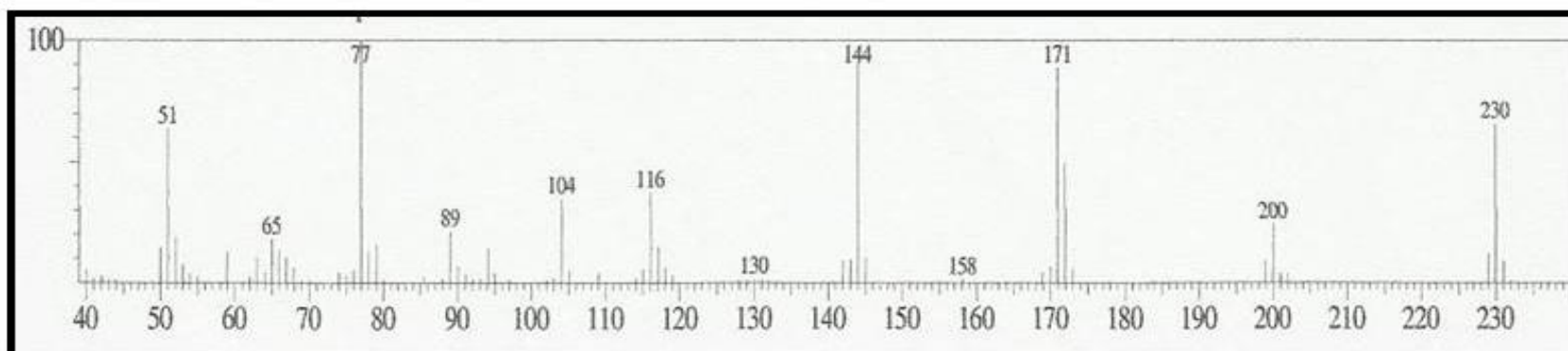
^1H NMR spectrum (CDCl_3 , 400 MHz) of 5-phenoxypryrazine-2-carboxylic acid methyl ester (65)



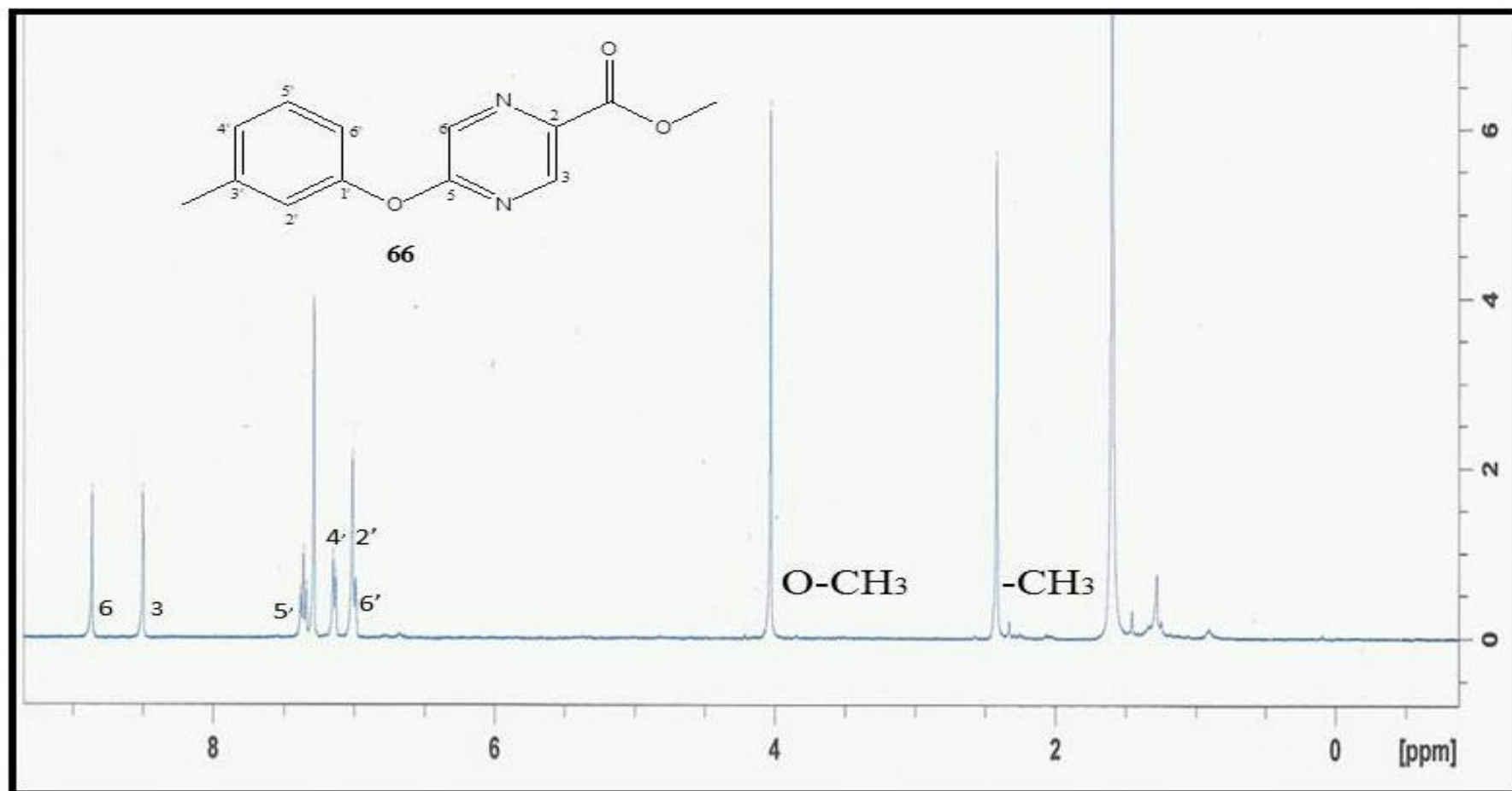
^{13}C NMR spectrum (CDCl_3 , 400 MHz) of 5-phenoxy pyrazine-2-carboxylic acid methyl ester (65)



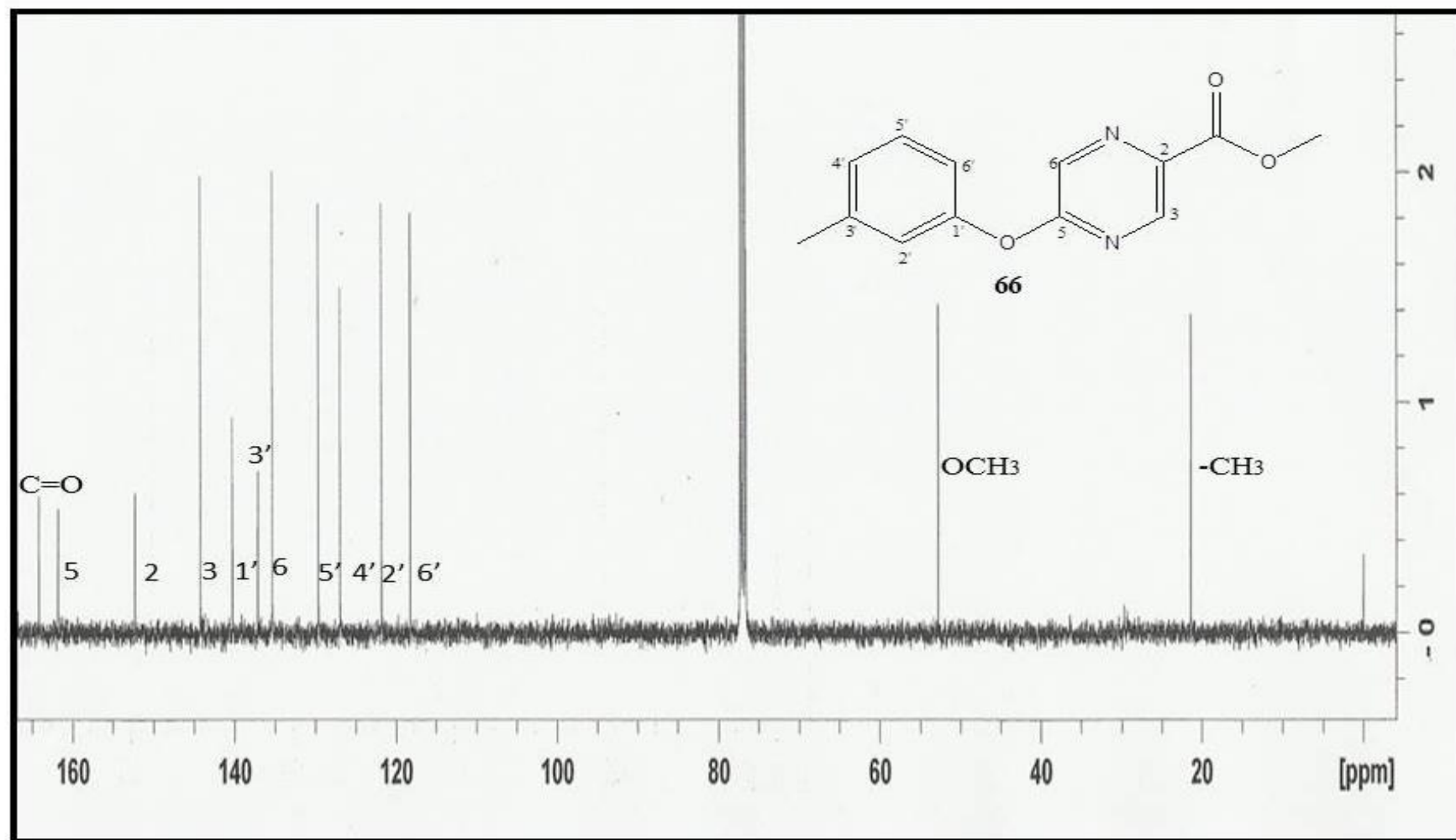
IR spectrum of 5-phenoxy pyrazine-2-carboxylic acid methyl ester (65)



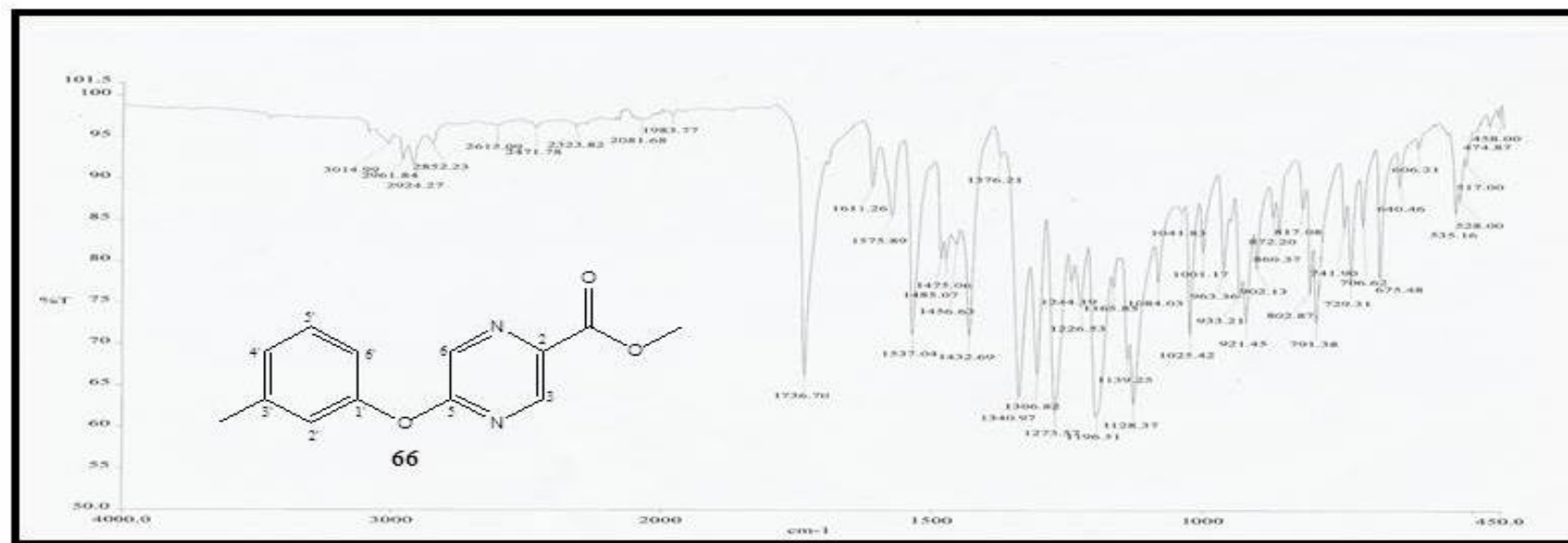
GCMS spectrum of 5-phenoxy pyrazine-2-carboxylic acid methyl ester (65)



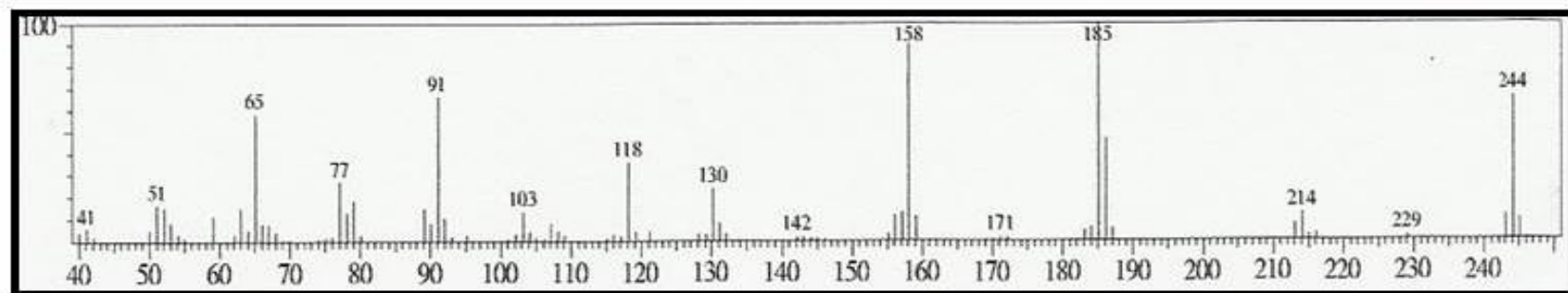
^1H NMR spectrum (CDCl_3 , 400 MHz) of 5-*m*-toloxypyrazine-2-carboxylic acid methyl ester (66)



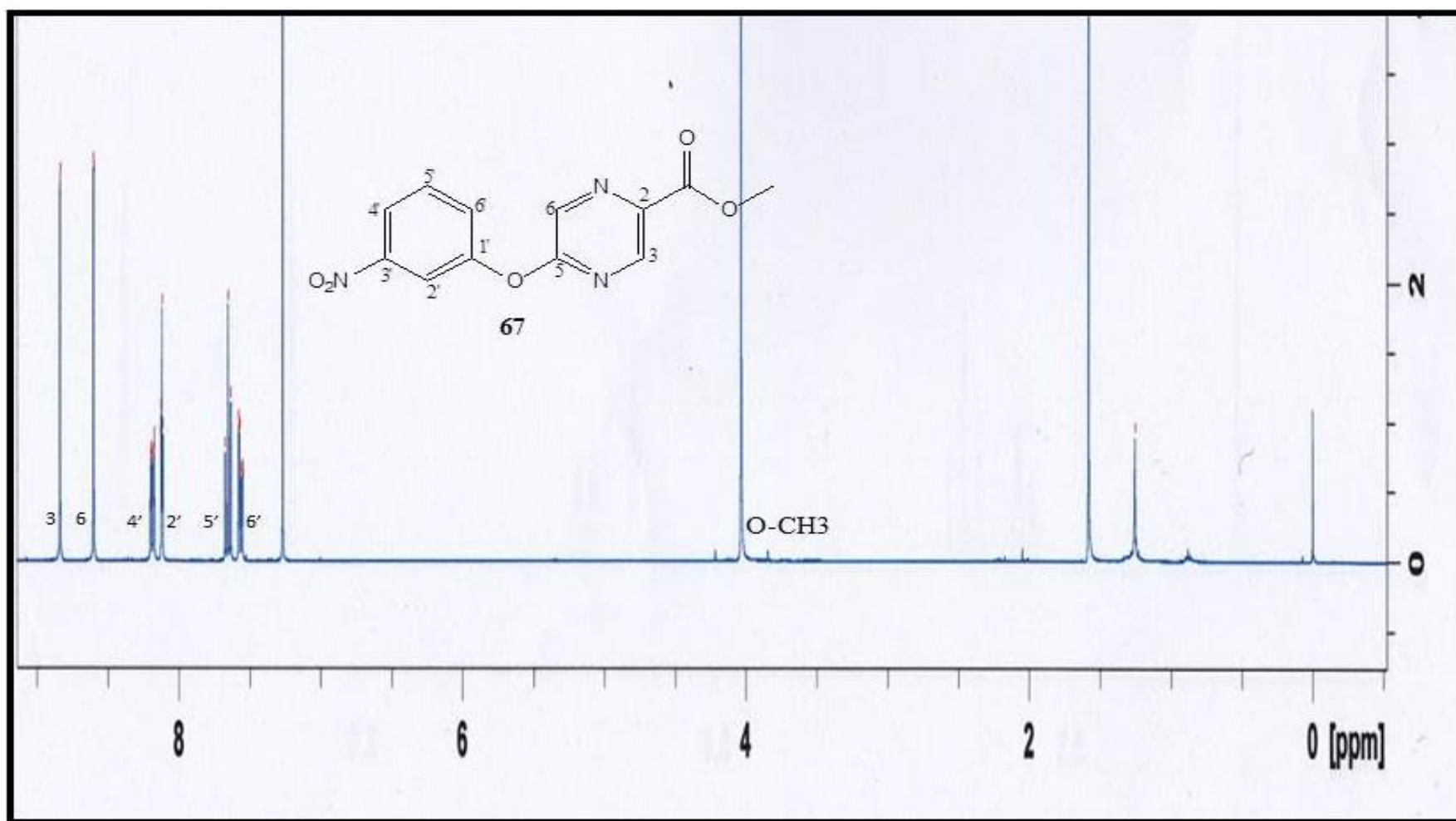
^{13}C NMR spectrum (CDCl_3 , 400 MHz) of 5-*m*-toloxypyrazine-2-carboxylic acid methyl ester (66)



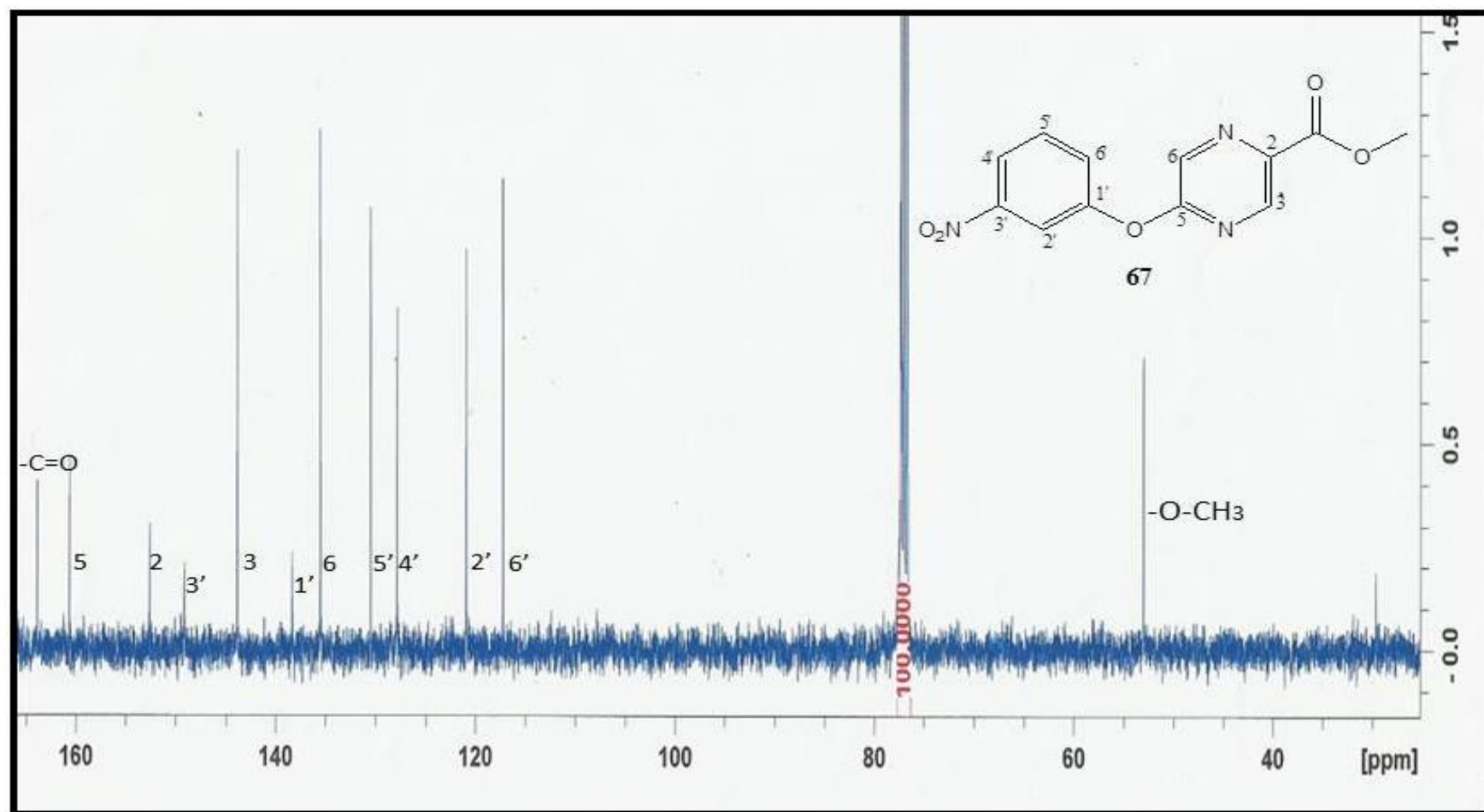
IR spectrum of 5-*m*-tolylloxypyrazine-2-carboxylic acid methyl ester (66)



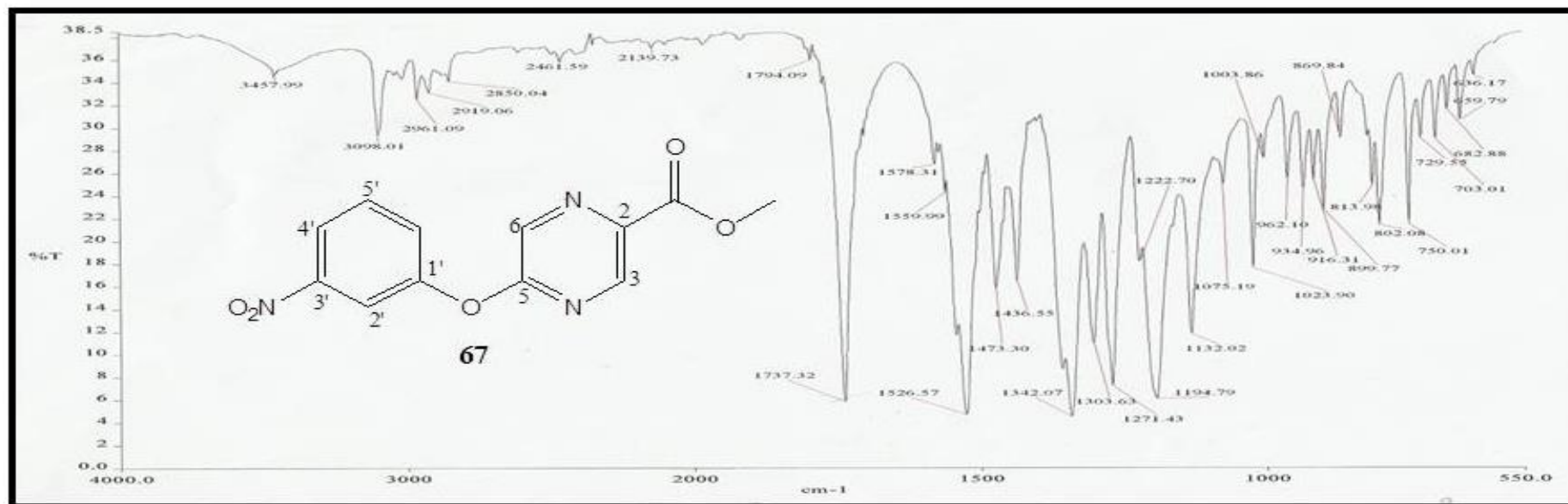
GCMS spectrum of 5-*m*-tolylloxypyrazine-2-carboxylic acid methyl ester (66)



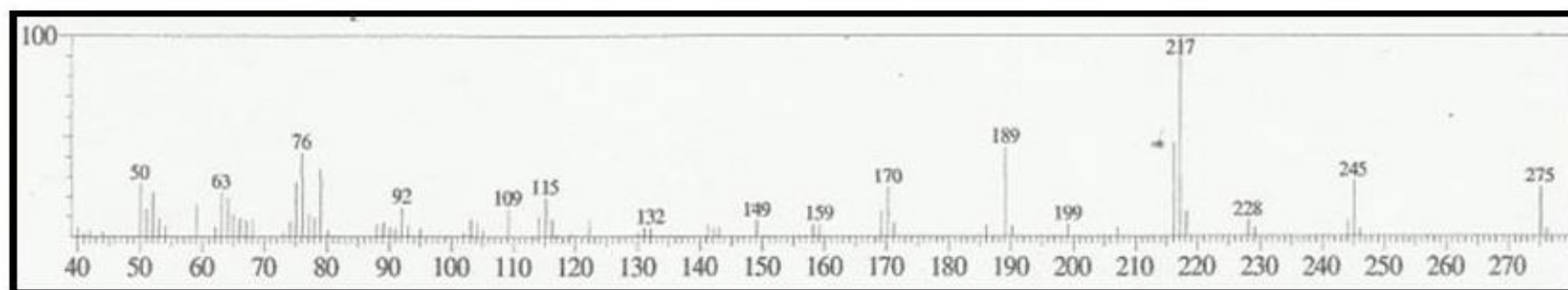
^1H -NMR spectrum (CDCl_3 , 400 MHz) of 5-(3-nitrophenoxy)pyrazine-2-carboxylic acid methyl ester (67)



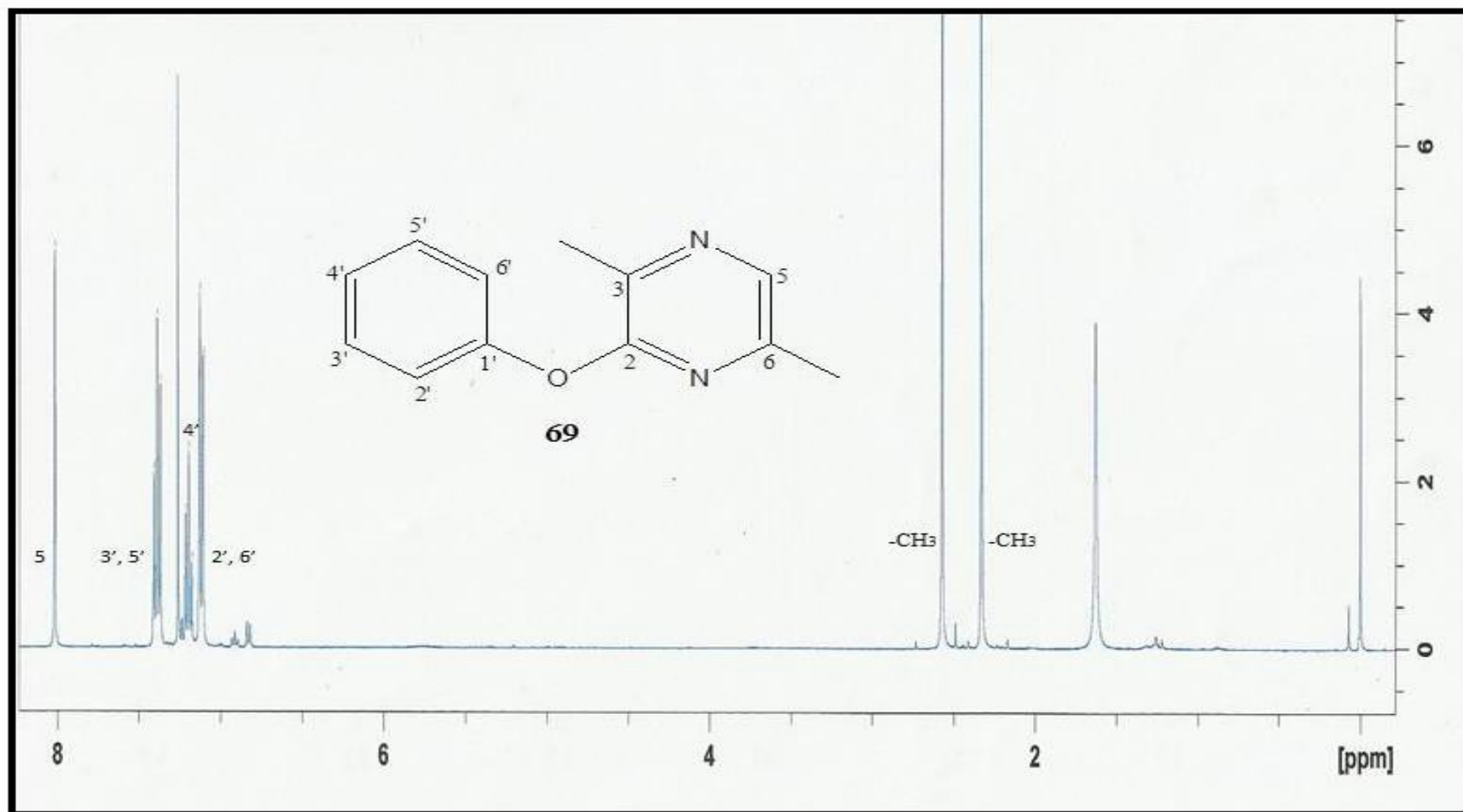
^{13}C NMR spectrum (CDCl_3 , 400 MHz) of 5-(3-nitrophenoxy)pyrazine-2-carboxylic acid methyl ester (67)



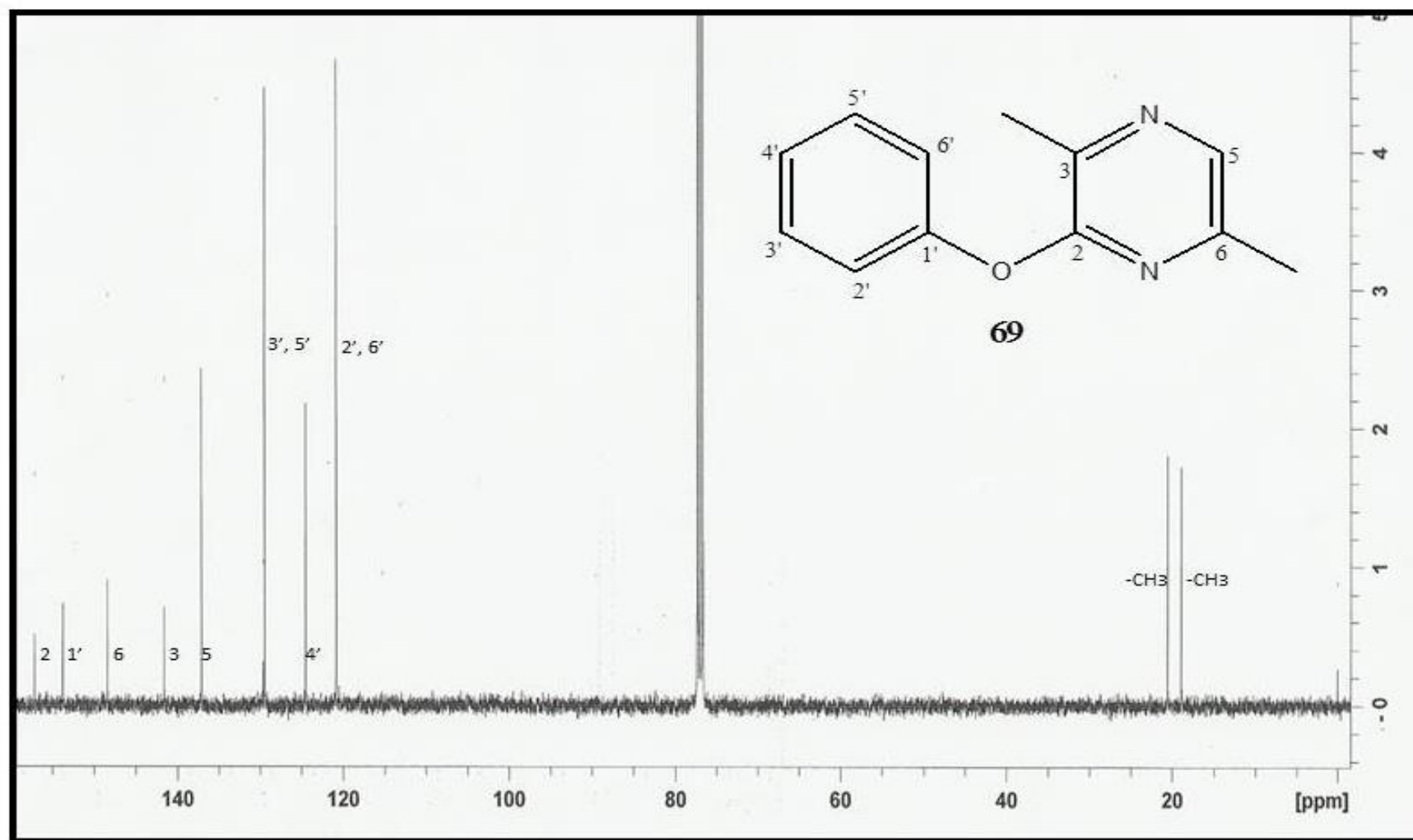
IR spectrum of 5-(3-nitrophenoxy)pyrazine-2-carboxylic acid methyl ester (67)



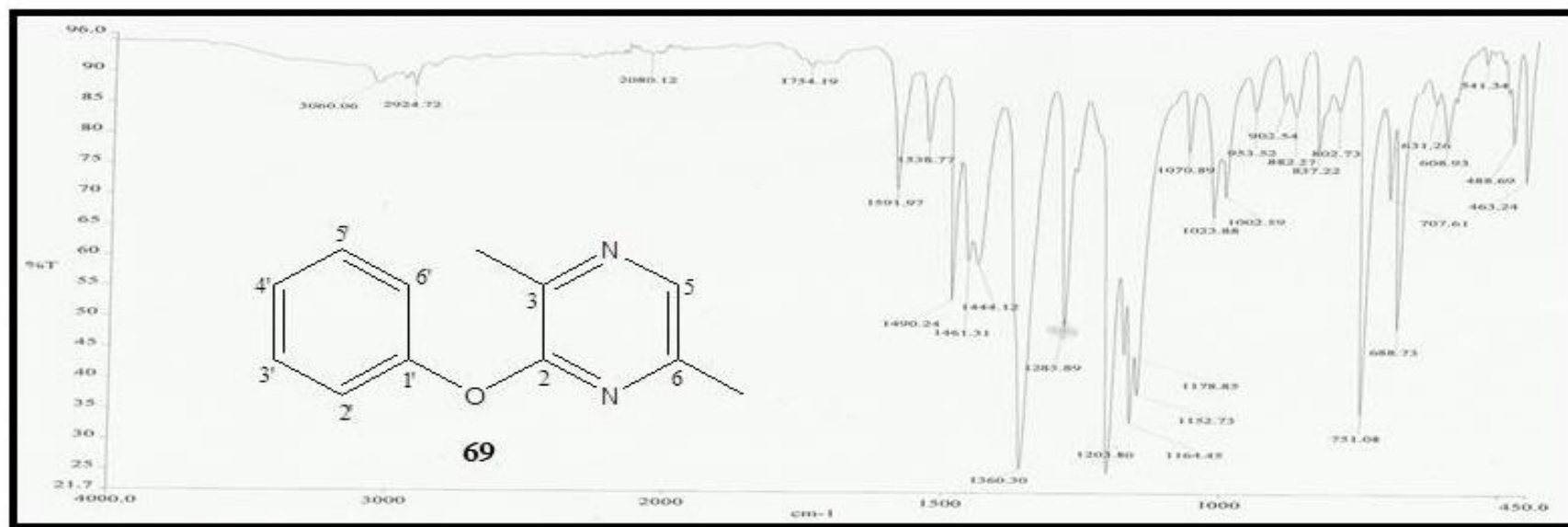
GCMS spectrum of 5-(3-nitrophenoxy)pyrazine-2-carboxylic acid methyl ester (67)



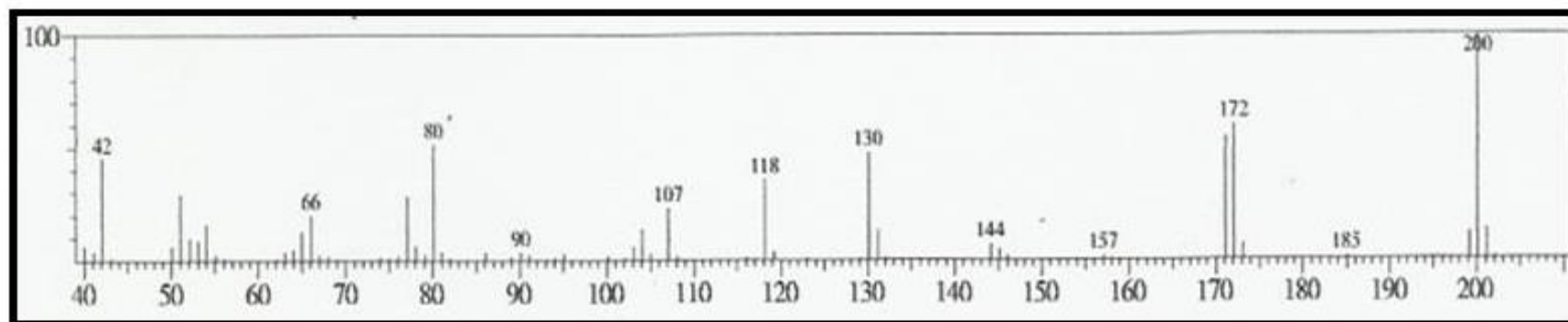
^1H NMR Spectrum (CDCl_3 , 400 MHz) of 2,5-dimethyl-3-phenoxy pyrazine (69)



^{13}C NMR spectrum (CDCl_3 , 400 MHz) of 2,5-dimethyl-3-phenoxy pyrazine (69)



IR spectrum of 2,5-dimethyl-3-phenoxy pyrazine (69)



GCMS spectrum of 2,5-dimethyl-3-phenoxy pyrazine (69)

Synthesis and Fluorescence Properties 2-*N*-Piperidinopyrazines

AZILA MOHD IDRIS¹, AZHAR ARIFIN¹, HASNA NADIAH JOHARI¹ and ZANARIAH ABDULLAH^{1,2,*}

¹Department of Chemistry, Faculty of Science, Universiti of Malaya, Kuala Lumpur, Malaysia

²Section for Co-curricular Courses, External Faculty Electives & TITAS (SKET), Universiti of Malaya, Kuala Lumpur, Malaysia

*Corresponding author: Fax: +60 3 79674193/5488; Tel: +60 3 79674240/5410; E-mail: zana@um.edu.my

(Received: 25 January 2013;

Accepted: 5 August 2013)

AJC-13886

2-*N*-Piperidinopyrazine, 2-*N*-(3-methyl)piperidinopyrazine and 2-*N*-(4-methyl)piperidinopyrazine were synthesized by reacting 2-chloropyrazine with piperidine, 3-methylpiperidine, 4-methylpiperidine respectively. The structures of these compounds were confirmed by spectroscopic methods. Fluorescence studies were carried out in tetrahydrofuran, acetonitrile, ethyl acetate and ethanol. 2-*N*-Piperidinopyrazine showed the highest fluorescence intensity in tetrahydrofuran followed by 2-*N*-(4-methyl)piperidinopyrazine. The fluorescence intensity decreases as the polarity of the solvent increases.

Key Words: 2-*N*-Piperidinopyrazine, 2-*N*-(3-Methyl)piperidinopyrazine, 2-*N*-(4-Methyl)piperidinopyrazine, Fluorescence.

INTRODUCTION

Pyrazine represents an important class of heterocyclic compounds¹⁻⁴. The structural unit is found in many natural products. They are important flavour ingredient in food^{5,6}, which also occur as flavour constituents of peas, coffee, capsicum peppers and wines⁷. Although present in very small amounts, they are extremely odorous and can be detected at concentration as low as 0.00001 ppm. Pyrazine is an aromatic heterocycles, therefore it undergoes electrophilic aromatic substitution. However, nucleophilic substitution of pyrazine has been reported^{8,9}. The nucleophilic reagents can attack at the 2, 3, 5 and 6 positions of the pyrazine ring. Studies have shown that the nucleophiles attacked the ring becomes easier in the presence of at least one powerful electron releasing group such as NH₂, OH, SH in another position on the ring.

The fluorescence characteristic of heterocyclic compounds in general and pyrazine in particular is less studied. However, our group has reported on the fluorescence characteristics of pyridines, pyrimidines and purines⁹⁻¹². In this paper, the fluorescence characteristics of 2-piperidinopyrazines will be reported.

EXPERIMENTAL

Organic solvents were distilled prior to use. Thin Layer Chromatography (TLC) was performed using MERCK 25 TLC plates 20 × 20 cm silica gel 60 F₂₅₄ precoated aluminium plate. Nuclear magnetic resonance (NMR) spectra were taken in deuterated chloroform on the JEOL FT-NMR Lambda 400

MHz and FT-NMR ECA 400 MHz spectrometers, IR spectra were recorded on a Perkin-Elmer 1600 series FT-IR or a Perkin-Elmer RX1 FT-IR spectrophotometer. Melting point was carried out in glass capillaries recorded on a melting point apparatus Fargo MP-ID and are uncorrected. Mass spectroscopic analyses were performed at a Hewlett-Packard HP 6890 Series of GC System with mass selective indicator and GCMS QP5050A Shimadzu. Fluorescence spectra were recorded using Fluorescence Spectrometer, Model F2000, Hitachi and Luminescence Spectrometer, Model LS 50B, Perkin Elmer. The measurements were recorded at room temperature at the same setting in quartz cells.

2-*N*-Piperidinopyrazine: 2-Chloropyrazine (0.40 mL) was added to a solution of piperidine (5.00 mL) in ethanol and the mixture was refluxed for 2 h. The mixture was then cooled and the solvent was evaporated off. The residue was dissolved in water and then extracted with diethyl ether (3 × 10 mL). The ether extracts were washed with water (3 × 10 mL) and dried over anhydrous sodium sulphate. Evaporation of the solvent gave the product, a yellowish liquid which was purified by washing with several portions of diethyl ether. (0.5606 g, 76 %); IR (KBr, ν_{max} , cm⁻¹): 1672 (C=N), 1517 (C=C), 2935 (C-H); ¹H NMR (ppm, 400 MHz, CDCl₃) δ _H: 8.05 (1H, d, *J* = 1.4 Hz, H-3), 7.96 (1H, dd, *J* = 2.6 Hz, 1.4 Hz, H-5), 7.69 (1H, d, *J* = 2.6 Hz, H-6), 3.49 (4H, s, H-2', H-6'), 1.55 (6H, s, H-3', H-4', H-5'); ¹³C NMR (ppm, 100 MHz, CDCl₃) δ _C: 155.0 (C-2), 141.6 (C-3), 131.7 (C-5), 130.9 (C-6), 45.4 (C-2', C-6'), 25.0 (C-5', C-3'), 24.4 (C-4'); GCMS: Found *M*⁺ = 163.00; C₉H₁₃N₃ requires *M*⁺ = 163.22.

2-*N*-(3-Methyl)piperidinopyrazine: 2-Chloropyrazine (0.20 mL) was added to 3-methylpiperidine (1.33 mL) and refluxed in oil bath at 120–140 °C. The reaction was stopped when starting material could no longer be detected on TLC. The mixture was then cooled and dissolved in 10 mL of water. The aqueous layer was extracted with ether (3 × 10 mL). The ethereal layer was washed twice with water (10 mL) and dried over anhydrous sodium sulphate. Filtration and evaporation of the solvent gave the crude mixture which was purified using preparative thin layer chromatography. Ethyl acetate-hexane mixture (1:2) was used as the solvent system. (0.1337 g, 34 %); IR (KBr, ν_{max} , cm^{-1}): 1673 (C=N), 1517 (C=C), 2927 (C-H); ^1H NMR (ppm, 400 MHz, CDCl_3) δ_{H} : 8.04 (1H, d, $J = 1.4$ Hz, H-3), 7.94 (1H, dd, $J = 2.6$ Hz, 1.4 Hz, H-5), 7.66 (1H, d, $J = 2.6$ Hz, H-6), 4.10 (2H, d, $J = 12$ Hz, H-6'), 2.73 (1H, td, $J = 12.6$ Hz, 2.9 Hz, H-2'), 2.41 (1H, t, $J = 10.9$ Hz, H-2'), 1.42 (4H, m, H-5', H-4'), 1.03 (1H, m, H-3'), 0.86 (3H, d, $J = 6.5$ Hz, CH_3); ^{13}C NMR (ppm, 100 MHz, CDCl_3) δ_{C} : 155.0 (C-2), 141.7 (C-3), 131.8 (C-5), 131.1 (C-6), 52.2 (C-6'), 45.0 (C-2'), 33.1 (C-5'), 30.6 (C-4'), 24.8 (C-3'), 19.3 (CH_3); GCMS: Found $M^+ = 177.00$; $\text{C}_{10}\text{H}_{15}\text{N}_3$ requires $M^+ = 177.25$.

2-*N*-(4-Methyl)piperidinopyrazine: 2-Chloropyrazine (0.20 mL) was added to 4-methylpiperidine (2.20 mL). The reaction mixture was refluxed in an oil bath for 2 h. The mixture was then cooled and the solvent was evaporated off. The reaction mixture was dissolved in water and then extracted with diethyl ether (3 × 10 mL). The ether extracts were washed with water and dried over anhydrous sodium sulphate. Evaporation of solvent gave 2-*N*-(4-methyl) piperidinopyrazine, a yellowish liquid. (0.3049 g, 77 %); IR (KBr, ν_{max} , cm^{-1}): 1673 (C=N), 1518 (C=C), 2924 (C-H); ^1H NMR (ppm, 400 MHz, CDCl_3) δ_{H} : 8.08 (1H, d, $J = 1.4$ Hz, H-3), 7.98 (1H, dd, $J = 2.6$ Hz, 1.4 Hz, H-5), 7.69 (1H, d, $J = 2.6$ Hz, H-6), 4.22 (2H, d, $J = 12$ Hz, H-2'), 2.79 (2H, td, $J = 12.6$ Hz, 2.4 Hz, H-6'), 2.60 (2H, d, $J = 12$ Hz, H-3'), 1.54 (1H, m, H-4'), 0.99 (2H, m, H-5'), 0.85 (3H, d, $J = 4$ Hz, CH_3); ^{13}C NMR (ppm, 100 MHz, CDCl_3) δ_{C} : 155.1 (C-2), 141.7 (C-3), 131.9 (C-5), 131.2 (C-6), 45.0 (C-2'), 33.6 (C-3'), 31.0 (C-4'), 21.9 (CH_3); GCMS: Found $M^+ = 177.00$; $\text{C}_{10}\text{H}_{15}\text{N}_3$ requires $M^+ = 177.25$.

Fluorescence studies: Fluorescence spectra were recorded using fluorescence spectrometer, Model F2000, Hitachi (with

the sensitivity is 2) and Luminescence Spectrometer, Model LS 50B, Perkin Elmer using 2.5 mm slits. Quinine sulphate (10 ppm in 0.1 N sulphuric acid) was used as the standard. All spectra were recorded at room temperature and are corrected for phototubes response and by subtraction of the solvent background. The fluorescence spectra of all the compounds were measured in tetrahydrofuran acetonitrile, ethyl acetate and ethanol of concentrations of 10^{-6} M in capped and uncapped conditions.

RESULTS AND DISCUSSION

2-*N*-Piperidinopyrazine (1), 2-*N*-(3-methyl)piperidinopyrazine (2) and 2-*N*-(4-methyl)piperidinopyrazine (3) were obtained when 2-chloropyrazine were treated with piperidine, 3-methylpiperidine and 4-methylpiperidine respectively as shown in Fig. 1.

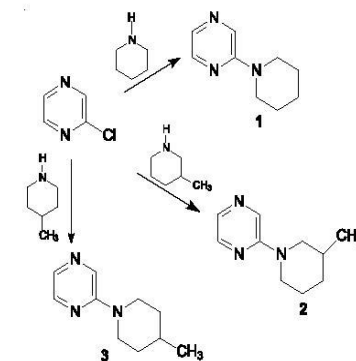


Fig. 1. Formation of 2-*N*-piperidinopyrazine (1), 2-*N*-(3-methyl)piperidinopyrazine (2) and 2-*N*-(4-methyl)piperidinopyrazine (3) from 2-chloropyrazine

The structure of 2-*N*-piperidinopyrazine (1), 2-*N*-(3-methyl)piperidinopyrazine (2) and 2-*N*-(4-methyl)piperidinopyrazine were confirmed by spectroscopic methods. In general, the presence of the adjacent electron withdrawing nitrogen atom in pyrazine makes the 2-position of pyrazine ring activated towards the nucleophilic attack. Thus, nucleophilic substitution reaction occurs at this position. The detail

| 2-Y-Pyrazine | Solvent | Excitation wavelength (nm) | Fluorescence wavelength (nm) | Intensity |
|---------------------------|-----------------|----------------------------|------------------------------|-----------|
| -N-Piperidino (1) | Tetrahydrofuran | 345 | 403 | 62.27 |
| | Acetonitrile | 348 | 411 | 51.64 |
| | Ethyl acetate | 344 | 404 | 26.3 |
| | Ethanol | 349 | 422 | 4.183 |
| -N-3-Methylpiperidino (2) | Tetrahydrofuran | 347 | 402 | 27.42 |
| | Acetonitrile | 347 | 414 | 11.31 |
| | Ethyl acetate | 345 | 401 | 15.32 |
| | Ethanol | 348 | 424 | 3.37 |
| -N-4-Methylpiperidino (3) | Tetrahydrofuran | 345 | 402 | 29.62 |
| | Acetonitrile | 347 | 411 | 17.80 |
| | Ethyl acetate | 343 | 404 | 21.88 |
| | Ethanol | 348 | 425 | 2.56 |

assignments of protons and carbons of compounds **1**, **2** and **3** are given in experimental section.

Fluorescence studies: Table-1 shows the fluorescence emission peaks of piperidinopyrazine derivatives in tetrahydrofuran, acetonitrile, ethyl acetate and ethanol respectively. It can be seen from Table-1 that all compounds showed the highest fluorescence intensity in tetrahydrofuran followed by acetonitrile, ethyl acetate and ethanol.

The fluorescence spectrum of 2-*N*-piperidinopyrazine in various solvents is as shown in Fig. 2.

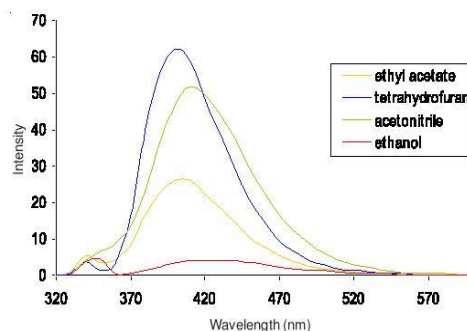


Fig. 2. Fluorescence spectra of 2-*N*-piperidinopyrazine in various solvents

Table 1 and Fig. 2 show that there is a shift in fluorescence maxima in polar solvents for all compounds. This observation is due to the fact that in most polar molecules, the excited state is more polar than the ground state. Hence, an increase in the polarity of the solvent produces a greater stabilization of the excited state than of the ground state. Consequently, a shift in fluorescence spectra to longer wavelength is observed as the polarity and dielectric constant of the solvents increases¹³. 2-*N*-Piperidinopyrazine showed a higher shifting of fluorescence peak in THF and acetonitrile which both are polar aprotic solvents and have higher dielectric constant. This observation is in the agreement with the work done by Drobnik and Augenstein^{14,15}.

2-*N*-Piperidinopyrazine showed the lowest fluorescence intensities in ethanol. The observations are believed to be due to the quenching effect from the "hydrogen bonded solvents" associated with the lone pair of electrons on the pyrazine ring and the amino group. As the result, it is not available to move

around the system, thus low fluorescence intensity was observed. It is also believed that both compounds formed complex with the solvent as shown in Fig. 3, whereby the intramolecular charge transfer transitions *via* hydrogen bonding are formed.

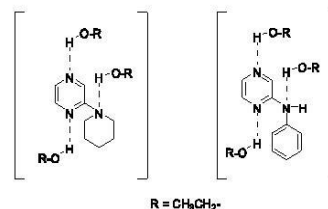


Fig. 3. Formation of hydrogen bonding with the solvent

This phenomenon is also explained by Weissstuch and Testa¹⁶ which they had reported that in some aromatic heterocyclic compounds with hydrogen bonding formation quenched the fluorescence intensity. The formation of hydrogen bond which is capable of conjugating with the π -electron system of the heterocyclic ring, results in the mobility of the π -electron been disturbed and caused the fluorescence intensity to be reduced. This phenomenon also favours the low lying $n \rightarrow \pi^*$ transitions which refers to the excitation of a non-bonding electron to an antibonding orbital. It was pointed out that $n \rightarrow \pi^*$ transitions are usually not observed in fluorescence spectra and when present are weak¹⁶. As the results, a decrease in fluorescence intensity was observed. Similar observation was recorded with 2-*N*-(3-methyl)piperidinopyrazine and 2-*N*-(4-methyl)piperidinopyrazine.

Both 2-*N*-(3-methyl)piperidinopyrazine and 2-*N*-(4-methyl)piperidinopyrazine showed lower fluorescence intensity in all solvents compared to 2-*N*-piperidinopyrazine. The reduced fluorescence intensity observed is probably due to the reduction in the rigidity of the piperidino ring. The presence of methyl group on the piperidino ring increases the vibrational amplitudes of the ring, thus energy absorbed was dissipated as heat. This phenomena was in agreement with the work done by Yang *et al.*¹⁷ and Joshi nee Pant *et al.*¹⁸.

Table-2 shows the fluorescence intensity of 2-*N*-piperidinopyrazine, 2-*N*-(3-methyl)piperidinopyrazine and 2-*N*-(4-methyl)piperidinopyrazine in tetrahydrofuran and acetonitrile at different concentrations.

| TABLE-2 FLUORESCENCE INTENSITY OF, 2- <i>N</i> -(3-METHYL)PIPERIDINOPYRAZINE AND 2- <i>N</i> -(4-METHYL)PIPERIDINOPYRAZINE IN TETRAHYDROFURAN, AND ACETONITRILE AT DIFFERENT CONCENTRATIONS | | | | | | | | | |
|---|---------------------------------|------------------|------------------|------------------------------|-----------|-----------|------------------|------------------|------------------|
| Solvent | 2- <i>N</i> -Piperidinopyrazine | | | | | | | | |
| | Concentration (M) | | | Fluorescence wavelength (nm) | | | Intensity | | |
| | $\times 10^{-4}$ | $\times 10^{-5}$ | $\times 10^{-6}$ | 10^{-4} | 10^{-5} | 10^{-6} | $\times 10^{-4}$ | $\times 10^{-5}$ | $\times 10^{-6}$ |
| THF | 6.127 | 6.127 | 6.127 | 401 | 402 | 403 | 560.0 | 382.7 | 62.27 |
| CH ₃ CN | 6.127 | 6.127 | 6.127 | 419 | 415 | 411 | 460.6 | 262.4 | 51.64 |
| 2- <i>N</i> -(3-Methyl)piperidinopyrazine | | | | | | | | | |
| THF | 5.578 | 5.578 | 5.578 | 401 | 404 | 402 | 505.4 | 235.3 | 27.42 |
| CH ₃ CN | 5.578 | 5.578 | 5.578 | 414 | 414 | 414 | 364.8 | 84.34 | 11.31 |
| 2- <i>N</i> -(4-Methyl)piperidinopyrazine | | | | | | | | | |
| THF | 5.578 | 5.578 | 5.578 | 403 | 400 | 402 | 518.5 | 208.0 | 29.62 |
| CH ₃ CN | 5.578 | 5.578 | 5.578 | 415 | 415 | 411 | 399.6 | 130.3 | 17.80 |

It can be seen that the fluorescence intensity increases with increasing concentration at relatively low concentrations. This observation was in agreement with the work reported earlier, where by at higher concentrations, the fluorescence intensity reaches its limiting value which normally results in concentration quenching and sometime accompanied by a shift in fluorescence wavelength¹⁹.

Conclusion

2-*N*-Piperidinopyrazine, 2-*N*-(3-methyl)piperidinopyrazine and 2-*N*-(4-methyl)piperidinopyrazine were successfully prepared and fluorescence characteristics of these compounds were studied in various solvents. 2-*N*-Piperidinopyrazine showed the highest fluorescence intensity amongst the piperidino derivatives and the highest fluorescence intensity was recorded in tetrahydrofuran. The fluorescence intensity of all the derivatives decreases with decreasing concentrations.

ACKNOWLEDGEMENTS

The authors thank Universiti of Malaya for the financial support for this project through RG047/2010AFR, RG233/2012AFR, PV081/2012A.

REFERENCES

1. V.M. Dembitsky, T.A. Glorizova and V.V. Poroikov, *Mini-Rev. Med. Chem.*, **5**, 319 (2005).
2. A. Gryszkiewicz-Wojtkielewicz, I. Jastrzebska, J.W. Morzycki and D.B. Romanowska, *Curr. Org. Chem.*, **7**, 1257 (2003).
3. K.J. McCullough, In ed.: M. Sainsbury, In Rodd's Chemistry of Carbon Compounds, Elsevier: Amsterdam, edn. 2, Vol. 4, pp. 99-171 (2000).
4. N. Sato, In eds.: A.R. Katritzky, C.W. Rees and A.J. Boulton, In Comprehensive Heterocyclic Chemistry II, Elsevier: Oxford, Vol. 6, p. 233 (1996).
5. J.A. Maga, *Food Rev. Int.*, **8**, 479 (1992).
6. (a) T. Shibamoto, *J. Food Sci.*, **51**, 1098 (1986); (b) G. Buchbauer, C.T. Klein, B. Wailzer and P. Wolschann, *J. Agric. Food Chem.*, **48**, 4273 (2000).
7. Y.-J. Cherng, *Tetrahedron*, **58**, 887 (2002).
8. C.W. Lindsley, Z. Zhao, W.H. Leister, R.G. Robinson, S.F. Barnett, D. Defeo-Jones, R.E. Jones, G.D. Hartman, J.R. Huff, H.E. Huber and M.E. Duggan, *Bioorg. Med. Chem. Lett.*, **13**, 761 (2005).
9. N. Mohd Salleh, Z. Abdullah, M.A.A. Bakar, A. MohdIdris and Z. Aiyub, *Int. J. Chem. Sci.*, **6**, 933 (2008).
10. Z. Abdullah, M.A.A. Bakar, Z. Aiyub and R. Yahya, *J. Sci. Technol. Tropics*, **3**, 39 (2007).
11. Z. Abdullah and M.A.A. Bakar, *Int. J. Chem. Sci.*, **4**, 241 (2006).
12. Z. Abdullah, M.A.A. Bakar and A. MohdIdris, *Afr. J. Chem. Sci.*, **1**, 1 (2008).
13. G.G. Guibault, *Molecular Fluorescence Spectroscopy in Comprehensive Analytical Chemistry*, Elsevier Scientific Publication Company, Vol. 8, Ch. 2 (1977).
14. J. Drobnik and L. Augenstein, *Photochem. Photobiol.*, **5**, 83 (1996).
15. J. Drobnik and L. Augenstein, *Photochem. Photobiol.*, **5**, 13 (1996).
16. J. Weisstuch and A.C. Testa, *J. Phys. Chem.*, **7**, 2999 (1970).
17. S. Yang, J. Liu, P. Zhou and G. He, *J. Phys. Chem. B*, **115**, 10692 (2011).
18. G.J. Pant, P. Singh, B.S. Rawat, M.S. Rawat and G.C. Joshi, *Spectrochim. Acta A*, **78**, 1075 (2011).
19. M. Nakazono, K. Saita, Y. Oshikawa, K. Tani, S. Nanbu and K. Zaitzu, *Spectrochim. Acta A*, **78**, 905 (2011).